

New *N,N* and *N,N,N* Ligands and Their Application in Catalytic Reactions

Dissertation zur Erlangung
des Doktorgrades der Naturwissenschaften (Dr. rer. nat.)

genehmigt vom Fachbereich Chemie
der Technischen Universität Kaiserslautern

(D 386)

Vorgelegt von

MSc Leila Taghizadeh Ghoochany

Betreuer der Arbeit: Prof. Dr. W. R. Thiel

Tag der wissenschaftlichen Aussprache: 06.06.2012

Vom Fachbereich Chemie der Technischen Universität Kaiserslautern 06.06.2012 als
Dissertation angenommen.

Dekan:

Prof. Dr.-Ing. Jens Hartung

Vorsitzender der Prüfungskommission:

Prof. Dr. S. Ernst

1. Berichterstatter:

Prof. Dr. W. R. Thiel

2. Berichterstatter:

Prof. Dr. H. Sitzmann

Die vorliegende Arbeit wurde im Fachbereich Chemie Technischen Universität Kaiserslautern im Arbeitskreis von Prof. Dr. W. R. Thiel in der Zeit von Dezember 2007 bis Mai 2012 angefertigt.

To my parents and Saeid

Abbreviations

Å	angstrom
Ac	acetate
Anal.	analytical
bpy	2,2'-Bipyridine
bpzm	bis(3,5-dimethylpyrazol-1-yl)methane
br.	broad
BSSE	basis set superposition error
bu	butyl
°C	degrees centigrade
calc.	calculated
CID	collision-induced dissociation
cod	1,5-cyclooctadiene
d	doublet
dbd	<i>N,N</i> -dimethyl-2-diphenylphosphinoaniline
DFT	density functional theory
diop	<i>O</i> -isopropylidene-2,3-dihydroxy-1,4-bis(diphenylphosphino)butane
DMF	<i>N,N</i> -dimethylformamide
DMF-DMA	<i>N,N</i> -dimethylformamide dimethyl acetal
DMSO	dimethyl sulfoxide
e.e.	enantiomeric excess
eq	equivalent
eq.	equation
ESI	electrospray ionisation
ESI-MS	electrospray mass spectrometry
Et	ethyl
Et ₂ O	diethyl ether
EtOH	ethanol
FT-IR	fourier transform infrared spectroscopy
g	gram
GC	gas chromatography
H	H ₂ -hydrogenation
h	hour

Hz	hertz
IMes	1,3-bis(2,4,6-trimethylphenyl)imidazol-2-ylidene
<i>i</i> Pr	isopropanol
IR	infrared
<i>J</i>	couplings constant
kcal	kilocalorie
M	molar
m	multiplet
Me	methyl
MeCN	acetonitrile
mg	milligram
min	minute
mL	millilitre
mm	millimetre
mw	microwave
NMR	nuclear magnetic resonance
<i>n</i> -Pr	<i>n</i> -propyl
OTf	trifluoromethanesulfonate
PCy ₃	tricyclohexylphosphine
pdpm	2-amino-4-(2-pyridinyl)pyrimidine
Ph	phenyl
por	porphyrin
ppm	parts per million
ref.	reference
refl.	reflux
RNA	ribonucleic acid
RT	room temperatur
s	singlet
T	transfer hydrogenation
T	temperature in Kelvin
t	triplet
TBD	triazabicyclodecene
<i>t</i> Bu	<i>tert</i> -Butyl

temp.	temperature in °C
Tf	triflate group (CF ₃ SO ₂ ⁻)
TH	transfer hydrogenation
THF	tetrahydrofuran
TOF	turn over frequency
TON	turn over number
Tp	trispyrazolylborate
Tp [*]	hydridotris(3,5-dimethylpyrazolyl)borate
TS	transition state
Tsdpen	<i>N</i> -tosylated 1,2-diphenyl-1,2-ethylenediamine
$\tilde{\nu}$	wave number in cm ⁻¹
ZPE	zero-point energy
δ	chemical shift in ppm
ΔG	Gibbs energy
ΔH_f	standard enthalpy of formation of a chemical compound
λ	wavelength in Å
ρ	density in g cm ⁻³

Contents

Contents

Abbreviations	
1 Introduction	1
1.1 Catalysis	1
1.2 Catalysts	2
1.3 Hydrogenation of Ketones	2
1.3.1 Transfer Hydrogenation	4
1.4 Mechanisms of the Hydrogenation.....	5
1.4.1 Classification of Catalytic Cycles According to the Hydride Transfer Mechanism	6
1.4.2 Homogeneous Transfer Hydrogenation of Substrates with Polar Bonds (T Mechanism)	9
1.5 C-H Bond Activation	21
1.5.1 Classification of C-H Activation Reactions	22
1.6 Coupling Reactions	25
2 Motivation	28
3 Results and Discussion.....	30
3.1 Ligand Synthesis	30
3.1.1 Synthesis of <i>NNN</i> Ligands	30
3.1.2 Synthesis of <i>NN</i> Ligands	46
3.1.3 Synthesis of 4,4'-Bipyrimidine-2,2'-diamine.....	58
3.1.4 Synthesis of <i>NNC</i> Ligands	58
3.1.5 Synthesis of Multidendate Ligands	59
3.2 Synthesis of Transition Metal Complexes.....	67
3.2.1 Ruthenium Complexes	67
3.2.2 Palladium Complexes.....	95
3.3 Catalytic Experiments	103
3.3.1 Catalytic Activities	103
4 Conclusion and Outlook.....	132
5 Experimental	139
5.1 General Performance.....	139
5.2 Used Devices.....	139
5.3 Ligand Synthesis	140
5.3.1. Synthesis of the <i>NNN</i> Ligands.....	140

5.3.2	Synthesis of NN Ligands	146
5.3.3	Synthesis of NNC Ligands	156
5.3.4	Synthesis of Multidentate Ligands	160
5.4	Synthesis of Transitional Metal Complexes	166
5.4.1	Ruthenium Complexes.....	166
5.4.2	Palladium Complexes	190
6	References	197
7	Index	215
7.1	Crystal Structure Data	215
7.1.1	Crystal Data and Structure Refinement for 9	215
7.1.2	Crystal Data and Structure Refinement for 16	216
7.1.3	Crystal Data and Structure Refinement for Guanidinium Salt	218
7.1.4	Crystal Data and Structure Refinement for 17d	220
7.1.5	Crystal Data and Structure Refinement for 17f	221
7.1.6	Crystal Data and Structure Refinement for 17h	223
7.1.7	Crystal Data and Structure Refinement for 33b	225
7.1.8	Crystal Data and Structure Refinement for 33a.....	227
7.1.9	Crystal Data and Structure Refinement for 33e.....	228
7.1.10	Crystal Data and Structure Refinement for 35	230
7.1.11	Crystal Data and Structure Refinement for 36a.....	232
7.1.12	Crystal Data and Structure Refinement for 36b	234
7.1.13	Crystal Data and Structure Refinement for 36f	235
7.1.14	Crystal Data and Structure Refinement for 36g	237
7.1.15	Crystal Data and Structure Refinement for 36h	239
7.1.16	Crystal Data and Structure Refinement for 36j	241
7.1.17	Crystal Data and Structure Refinement for 36k	242
7.1.18	Crystal Data and Structure Refinement for 36l	244
7.1.19	Crystal Data and Structure Refinement for 38	246
7.1.20	Crystal Data and Structure Refinement for 40a.....	247
7.1.21	Crystal Data and Structure Refinement for 40b	249
7.2	DFT calculations	252
7.2.1	Calculation of HCl.....	252
7.2.2	Calculations of cation 36a ⁺	254
7.2.3	Calculations of cation 36j ⁺	259

Contents

7.2.4	Calculations of cation $36g^+$	264
7.2.5	Heats of formation.....	269
7.3	Statutory Explanation.....	272
7.4	Acknowledgement.....	273
7.5	Curriculum Vitae.....	275

Introduction

1 Introduction

1.1 Catalysis

Catalysis is the science of accelerating and directing chemical transformations.¹ In general, more complex molecules are produced from readily attainable starting materials for versatile applications. These conversions allow the creation of a large range of products which are further required in industry or are directly commercialized for the consumer. Catalysts ensure that these reactions proceed in a highly efficient manner, giving optimum yields and avoiding unwanted by-products. Significantly, they allow a much more economical production compared to classical stoichiometric procedures and have opened up an access to yet unknown transformations.

More than 80% of all chemical products come into contact with catalysts during their synthesis, thus catalysts are necessary for the needs of today's society and so, they are a key factor for profitability and sustainability of chemical production processes. As Beller mentioned in his article on catalysis, 15-20% of the economies of the developed western nations depend directly or indirectly on catalytic processes, according to the North American Catalysis Society.¹ Therefore, it is not surprising that without catalysis lots of things which we take for granted in everyday's life – petrol or plastics, dyes and clothing, automobiles or airplanes, mobile phones or computers, medicines or cosmetics – would either not be possible or suffer in quality.

Even now, classical organic reactions that are more than 100 years old are used for syntheses of chemical products. These include nitrations, Friedel-Crafts reactions, and halogenations. One of the main disadvantage of many of them is the occurrence of stoichiometric – frequently even overstoichiometric – quantities of side products (e. g. salts) which must be separated as waste. Additionally complicated protective group techniques, are frequently required for the specific activation of a function moiety being in presence of other

functional groups. This is why often several metric tonnes of waste per metric tonne of target product are produced by conventional production processes for fine chemicals. Given these facts, there is no doubt about the necessity of inventive and versatile catalytic methods for new environmentally benign chemical processes.

1.2 Catalysts

Wilhelm Ostwald, who was awarded the Nobel prize for chemistry in 1909 has introduced the following definition for a catalyst:

"A catalyst is a compound which increases the rate of a chemical reaction without being consumed by itself and without changing the thermodynamic equilibrium of the reaction".

Up to now different kinds of catalysts have been improved and applied in all fields of chemistry. Since the 1950ies almost all of the important base chemicals are produced by using catalytic procedures. The importance of catalysis in the modern chemistry is highlighted by awarding the Noble Prize for catalytic investigations to:

- Noyori, Knowles and Sharpless , 2001 for asymmetric catalysts
- Chauvin, Grubbs and Schrock, 2005 for olefin-metatheses
- Ertl, 2007 for investigations in surface catalysis
- Heck, Negishi and Suzucki, 2010 for palladium catalyzed cross coupling reactions

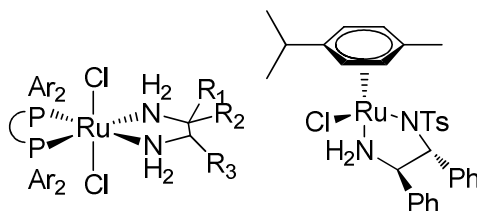
to name just the laureates of the last decade.

1.3 Hydrogenation of Ketones

Reduction of ketones to secondary alcohols is a core reaction for the synthesis of alcohols including chiral ones. A number of homogeneous catalytic systems based on Ru, Rh, Ir, and more recently Os complexes have been developed for ketone hydrogenation² and transfer hydrogenation (TH)³ reactions. One of the most significant breakthroughs in this field was done by Noyori and co-workers, leading to systems such as *trans*-[RuCl₂(PP)(1,2-diamine)] (PP = diphosphine) and [(η⁶-arene)RuCl(Tsdpen)] for efficient ketone hydrogenation

Introduction

and TH reactions, respectively (Scheme 1).⁴ They discovered, that both, activities and selectivities can be improved by the presence of a N-H functionality in the ligand being in close proximity to the metal site and named this effect "bifunctional catalysis".⁵ According to this improvement, others have investigated ligands containing amino alcohol,⁶ aminoamide,⁷ and aminocarboxylate groups⁸ with at least one hydrogen atom bound to nitrogen for the bifunctional ruthenium catalyzed hydrogenation and transfer hydrogenation. The in-situ generation of metal hydrido species was proposed for the hydrogenation mechanism (see below for mechanistic details).⁹



Scheme 1. Noyori's catalysts.

Baratta et al.^{10,11} have developed an access to arene-free catalysts which turned out to be extremely active in the transfer hydrogenation of acetophenone with NaOH as the base.¹⁰ From a mechanistic point of view, the main difference between the Baratta and the Noyori systems is, that in the former ones the alcohol and the ketone coordinate to the metal center during the catalytic process (so-called "inner-sphere" mechanism), for more details see the mechanism section, whereas in Noyori's system the substrate does not coordinate to the metal site but interacts with the ligands (so-called "outer-sphere mechanism").¹¹ In contrast to direct hydrogenation, the hydrogen in the transfer hydrogenation is from a source other than gaseous H₂. Transfer hydrogenation of ketones is the main topic of this work and will be discussed in the next sections.

1.3.1 Transfer Hydrogenation

Transfer hydrogenation (TH) is the addition of hydrogen (H_2 ; dihydrogen in inorganic and organometallic chemistry) to a molecule from a source other than gaseous H_2 . In the catalytic transfer hydrogenation of ketones the substrates are reduced to alcohols mainly with 2-propanol or formic acid as the hydrogen source.^{3,12} Highly active catalytic systems make this approach attractive for the preparation of alcohols since the direct hydrogenation process often requires handling of dangerous dihydrogen under elevated pressure. The most active systems are based on Ru, Rh, and Ir and the catalytically active metal site is coordinated by nitrogen and/or phosphorus ligands. Especially ruthenium complexes containing suitable combinations of *P*- and *N*- or mixed *P,N*-ligands turned out to be efficient catalysts for the hydrogenation and transfer hydrogenation of carbonyl compounds. Thus, bi-, tri-, and tetradentate achiral and chiral ligands have successfully been used for the preparation of these catalysts. A few general types should be mentioned here: $(P)_2(NN)RuCl_2$ and $(PP)(NN)RuCl_2$ (*P* = phosphine ligand; *PP* = diphosphine ligand; *NN* = diamine, dipyridine ligand),¹³ $(P)_2(PN)RuCl_2$ (*PN* = amino- or iminophosphine ligands, oxazolinylderrocenylphosphine),¹⁴ $(PN)_2RuCl_2$,^{14a,15} $[(\eta^6\text{-}p\text{-cymene})(PN)RuCl][BF_4]$ (*PN* = phosphole-pyridine),¹⁶ $[(\eta^6\text{-}p\text{-cymene})(NN)RuCl][BF_4]$,¹⁷ $(P)(NPN)RuCl_2$,¹⁸ $(NPN)RuCl_2$,¹⁹ $(P)(NNN)RuCl_2$ (*NPN* and *NNN* = oxazoline based ligands),²⁰ $[RuCl(CNN)(PP)]$ (*PP* = Josiphos diphosphine and *CNN* = amin/aryl/pyridine based ligands)²¹ and $(PNNP)RuCl_2$ systems (*PNNP* = diphosphine/diamine ligands).²²

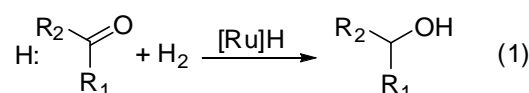
Introduction

Aliphatic and aromatic nitrogen donors have emerged as important ligands in homogeneous and heterogeneous catalysis.^{23,24} Among them tridentate aromatic nitrogen donors have been used for nickel-catalyzed asymmetric Negishi cross couplings²⁵ or for iron/cobalt catalyzed ethylene polymerization.²⁶ Furthermore polydentate imino and amino ligands have provided a considerable improvement on the catalyst performance in the catalytic transfer hydrogenation of ketones.²⁷

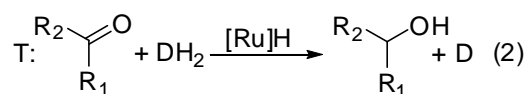
1.4 Mechanisms of the Hydrogenation

Catalytic hydrogenation of polar bonds and their asymmetric variant are key reactions in fine chemical and pharmaceutical synthesis. Homogeneous hydrogenation catalysts based on ruthenium have been known nearly for 40 years²⁸ and became the most useful catalysts for these reactions. Ruthenium complexes exhibit promising reactivity and selectivity, especially in the catalytic reduction of polar bonds, that often transcend those of the common stars of hydrogenation, complexes of rhodium and iridium.²⁹ In a series of review articles the role of some ruthenium hydrido³⁰ and dihydrogen complexes³¹ as precatalysts or intermediates in catalytic cycles was discussed.

In this section the proposed mechanisms for the H₂-hydrogenation (H) and the transfer hydrogenation (T) of carbonyl bonds will be discussed in details according to Morris classification^{12d} with a focus on ruthenium hydrido complexes which are engaged as catalysts or precatalysts (equation 1).



Equation 1. Direct hydrogenation of a carbonyl group (H).



Equation 2. Transfer hydrogenation of a carbonyl group (T).

Catalytically active species containing ruthenium hydrido units are marked as [Ru]H, where in [Ru] indicates the ruthenium center with its other ligands. The hydrogen sources DH₂ in equation 2 are generally secondary alcohols, especially 2-propanol, or formic acid, often applied as ammoniumformate, [NEt₃H][CO₂H].

Generally the catalytic cycles include two main steps. In the first step the hydride will react with the unsaturated compound, and in the second step the hydride will be regenerated from H₂ (in H) or a hydrogen donor (in T). The classification of the catalytic cycles discussed in the next sections mechanism is according to the proposed pathway for the first step as Morris has done it in his article.^{9e,12d}

1.4.1 Classification of Catalytic Cycles According to the Hydride Transfer Mechanism

The classical mechanisms of transition metal homogeneous catalysis include the reactants being bound to the central metal. Therefore, it is usually supposed that in the hydrogenation of polar bonds by ruthenium hydrides, the ketone will coordinate to ruthenium(II) at a vacant site that is opened-up by dissociation of a ligand or a solvent molecule. The carbon atom of the carbonyl group will be electrophilically activated by coordination in the inner (I) or primary coordination sphere of ruthenium (Lewis-acid) so that a *cis* coordinated hydrido ligand is able to migrate to this carbon atom (Figure 1).

Introduction

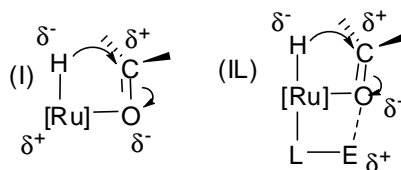


Figure 1. Attack of a hydrido ligand to the coordinated unsaturated carbonyl group in the primary coordination sphere. This is supposed to be part of the HI or TI mechanism. The [Ru] notation indicates the ruthenium ion (normally Ru(II)) and its ancillary ligands. The IL (right) notation shows additional activation by an electrophile ($E = H^+, M^+$) on an ancillary ligand. This is a part of the HIL or TIL catalytic cycles.

Mechanisms with these features will be named as HI or TI mechanisms. They are usually characterized by the dissociation of an ancillary ligand providing a vacant site for coordination of the carbonyl group. Often this vacant site is attainable by dissociation of a weakly coordinating solvent molecule. Noyori and Ohkuma^{30a} have shown that a drastic geometric change of ground state structures is necessary to obtain the essential interactions between the Ru–H bond and the π face of the carbonyl group in the inner sphere mechanism which can lead to a high activation barrier. Additional activation of the carbonyl group towards hydride attack can be provided by a coordinated ancillary ligand, L, which contains an acidic group as shown in Figure 1. Following Morris' notation,^{12d} an L is added to the end of the abbreviation in this case. For instance, HIL would refer to the hydrogenation of an unsaturated substrate with ligand assistance in the inner sphere.

The catalysts that work by an inner sphere hydride transfer have the disadvantage that they are not very selective for C=O bonds over C=C bonds, e.g. in the reduction of α,β -unsaturated ketones and aldehydes.³² This can be caused by a competition of C=C and C=O bonds for the vacant site *cis* to the hydrido ligand. Additionally monohydrides are known to accelerate the isomerization of olefins³³ and imines,³⁴ which is another unwanted side reaction.

Recently Noyori's group has introduced a non-classical mechanism for the reduction of polar bonds by ruthenium complexes which is proposed to work by the transfer of a hydride to the substrate in the second, or outer coordination sphere of the ruthenium complex. Therefore, this mechanism is called outer sphere (O) hydrogenation mechanism (Figure 2). An electrophilic activation is required either by an external electrophile (HO or TO) or by an internal electrophile bounded to an ancillary ligand (HOL or TOL) for the carbon atom of carbonyl group with a low hydride affinity.

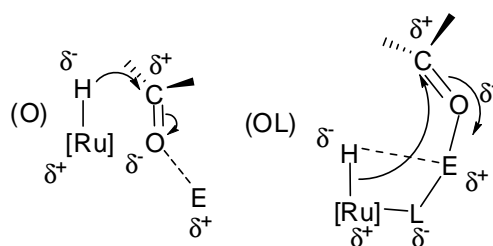


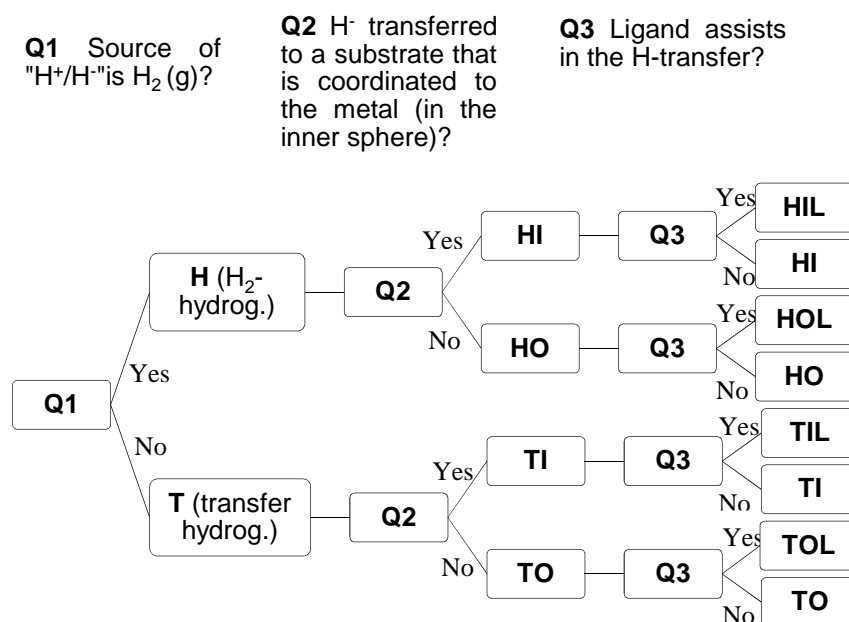
Figure 2. The outer sphere (O) attack of hydride on the unsaturated aldehyde or ketone. Usually, an electrophile (E) assists in these reactions and usually also an ancillary ligand (OL mechanism) is involved. This is part of the HO, HOL, TO or TOL catalytic cycles.

The term “metal–ligand bifunctional catalysis”^{4b} was created by Noyori to refer to the catalytic systems that are involving the HOL or TIL mechanisms. In these cases usually the ancillary ligand contains a proton (E = H in Figure 2) that can be transferred to the oxygen atom simultaneously with the hydride transfer to the carbon atom. This results in a preferred reaction of the polar C=O bond over the unpolar C=C bonds. Having a primary amine as the ancillary ligand, the “N–H effect”, the ligand geometry and a hydridic–protonic attraction arrange the Ru–H and N–H bonds precisely.

The existence of an ancillary ligand *cis* to the hydrido ligand with an NH or OH group or an electrophile, like a K⁺ ion is required for catalysts following the ligand-assisted

Introduction

mechanism. The flowchart shown in scheme 2 summarizes the classification of hydrogenation catalysts.



Scheme 2. Classification of the mechanisms related to the reduction of polar bonds; H = hydrogenation; T = transfer hydrogenation; I = inner sphere; O = outer sphere; L = ligand assisted.

Since this work is focused on the transfer hydrogenation, the mechanism of this reaction will be discussed in details in the next sections.

1.4.2 Homogeneous Transfer Hydrogenation of Substrates with Polar Bonds (T Mechanism)

The transfer hydrogenation and asymmetric hydrogenation of ketones is a useful method in organic synthesis.^{29c,30e-h,35} Among all metals, ruthenium complexes have shown the best activities in these reactions (Table 1). Naota et al. have reviewed the general catalytic chemistry of ruthenium including ruthenium hydrides and their application in catalytic hydrogenation and transfer hydrogenation in 1998.^{30f} A chapter of a book is also dedicated to transfer hydrogenations.³⁶

Different mechanisms have been proposed for these reactions but in many cases they can be divided to two types: (1) The TI mechanism in which a hydride is transferred to the coordinated substrate and (2) the TO mechanism in which a hydride is transferred in the second coordination sphere. In Table 1 typical conditions for the hydrogenation of C=O bonds by some of the TI and TO catalysts are listed.

Introduction

Table 1. Typical conditions for the transfer hydrogenation of aldehydes and ketones.^{12d}

	precatalyst (Ru)	substrate (S)	H donor (DH ₂)	additives (A)	Ru: DH ₂ :A	solvent	conversion		temp. (°C)	TOF (h ⁻¹)	cycle	ref.
							(%)	(h)				
1	Ru(H) ₂ (H ₂)(PPh ₃) ₃	4-methylcyclohexanone	iPrOH		1:100:300	iPrOH	91	1	25	91	TI	[37a]
2	RuH ₂ (PPh ₃) ₄	4-methylcyclohexanone	iPrOH		1:100:300	iPrOH	33	24	25	1	TI	[37a]
3	RuH ₂ (PPh ₃) ₄	PhMeC = O	iPrOH		1:200:neat	iPrOH	93	3	85	62	TI	[39b]
4	RuH ₂ (PPh ₃) ₄	hexanal	PhCH ₂ OH			C ₆ H ₅ Br			80	30	TI	[37b]
5	RuCl ₂ (PPh ₃) ₃	PhMeC = O	iPrOH		1:200:neat	iPrOH	0	3	85	0	TI	[39b]
6	RuCl ₂ (PPh ₃) ₃	cyclohexanone	iPrOH	NaOH	1:1000:neat:24	iPrOH	89	1	82	1800	TI	[37c]
7	RuHCl(PPh ₃) ₃	PhMeC = O	HCOOH			PhMeC = O/HCOOH	46	3	125		TI	[37d]
8	[RuH(H ₂){P(CH ₂ CH ₂ PPh ₂) ₃ }]BPh ₄	PhMeC = O	iPrOH		1:250:12000	THF	96	5	60	50	TI	[37e]
9	[RuH(H ₂){P(CH ₂ CH ₂ PPh ₂) ₃ }]BPh ₄	cyclohexanone	iPrOH		1:250:12000	THF	100	1	60	250	TI	[37e]
10	RuH ₂ (CO)(PPh ₃) ₃	PhMeC = O	HCOOH			PhMeC = O/HCOOH	28	3	125		TI	[37d]
11	RuHCl(CO)(PPh ₃) ₃	PhHC = O	HCOOH		1:760:1760	PhHC = O/HCOOH	47	3	Reflux	280	TI	[37f]
12	RuHCl(CO)(PPh ₃) ₃	PhHC = O	HCOOH		1:760:1760	PhHC = O/HCOOH	23	0.27	mw ^a	860	TI	[37f]
13	Ru ₄ H ₄ (CO) ₈ ((-)-diop) ₂	PhMeC = O	iPrOH		Ru:1:2 [Ru] 1 mM	PhMeC = O/iPrOH	37	111	120		TI	[37g]
14	Ru ₄ H ₄ (CO) ₈ ((-)-diop) ₂	PhMeC = O	iPrOH	NaOiPr	Ru:1:2 [Ru] 1 mM	PhMeC = O/iPrOH	67	24	120		TI	[37g]
15	[Ru ₄ H ₃ (CO) ₁₂] ⁻	EtMeC = O	iPrOH		1:100 [Ru] 1 mM	iPrOH	95	6	82	16	TI	[45]
16	RuH(OTf)(bpzm)(cod)	cyclohexanone	iPrOH	NaOH	1:2100:neat:10	iPrOH		3	80	880	TI	[41]
17	RuH(Tp [*])(cod)	PhMeC = O	iPrOH	NaOH	1:500:neat:500	iPrOH			70	30	TI	[42]
18	RuH(Tp [*])(cod)	cyclohexanone	iPrOH	NaOH	1:500:neat:500	iPrOH	95	1.7	70	400	TI	[42]
19	RuH(Tp [*])(H ₂) ₂	cyclohexanone	iPrOH	NaOH	1:500:neat:500	iPrOH	95	3.7	70	200	TI	[42]
20	Ru(pcp)(OTf)(PPh ₃)	cyclohexanone	iPrOH	KOH	1:1000:neat:20	iPrOH			82	27000	TI	[37h]
21	RuCl ₂ (PPh ₃)(oxferphos)	PhMeC = O	iPrOH	NaOiPr	1:200:neat:4	iPrOH	94 (>99% e.e.)	2	20	100	TI	[37i]
22	[Ru(C ₅ H ₅)(NCMe)(pn)]CF ₃ SO ₃	PhMeC = O	iPrOH	NaOiPr	1:200:neat:2	iPrOH	99	24	25	8	TI	[40]
23	[Ru(C ₅ H ₅)(NCMe)((R)-ppfa)]CF ₃ SO ₃	PhMeC = O	iPrOH	NaOiPr	1:200:neat:2	iPrOH	<5 (0 e.e.)	2.5	82	80	TI	[40]
24	RuCl ₂ (Lpr)(PPh ₃)	PhMeC = O	iPrOH	KOH	1:100:neat:1.5	iPrOH	85	72	83	1.2	TI	[44]
25	RuCl ₂ {PPh ₂ (C ₆ H ₄ SO ₃ Na)} ₂	PhHC = O	NaO ₂ CH	PPh ₂ (C ₆ H ₄ SO ₃ Na)	1:100:excess:10	H ₂ O/aldehyde	99.5	1.5	80	67	TI	[37j]
26	RuH(NHCOMe)(OHiPr)(PCy ₃) ₂ (CO)	PhMeC = O	iPrOH		1:200	iPrOH	>95	6	80	32	TIL	[46]
27	[Ru(C ₆ Me ₆)(bpy)(OH ₂)](PF ₆) ₂	cyclohexanone	NaO ₂ CH		1:200:6000	H ₂ O pH 4	99	4	70	98	TO	[47]
28	[Ru(C ₆ Me ₆)(bpy)(OH ₂)](PF ₆) ₂	(NaSO ₃ -4-C ₆ H ₄)MeC = O	NaO ₂ CH		1:200:6000	H ₂ O pH 4	98	3	70	103	TO	[47]
29	[RuCl ₂ (C ₆ H ₆) ₂]	PhMeC = O	iPrOH	NH ₂ CH ₂ CH ₂ OH/KOH	1:200:neat:5	iPrOH			28	227	TOL	[30e]
30	[RuCl ₂ (C ₆ H ₆) ₂]	PhMeC = O	iPrOH	NH ₂ CH ₂ CH ₂ NHTs/KOH	1:200:neat:5	iPrOH			28	86	TOL	[30e]
31	RuCl((S,S)-NH ₂ CHPhCHPhNTs)(mesitylene)	PhMeC = O	HCOOH/NEt ₃		1:200:neat	HCOOH:NEt ₃ = 5:2	99 (98% S)	20	28	10	TOL	[30e]
32	[RuCl ₂ (C ₆ H ₆) ₂]	<i>t</i> BuOOCCH ₂ COMe	iPrOH/KOH	(1S,2R)-OCHPhCHMeNHCH ₂ C ₆ H ₄ Ph	1:100:neat:2	iPrOH	99 (67% e.e. S)	2.5	20	46	TOL	[37k]
33	[RuCl ₂ (p-cymene)] ₂	PhMeC = O	iPrOH/KOH	(1R,2S)-aminoindanol	1:400:neat:4	iPrOH	72 (91%)	4	20	72	TOL	[37l]

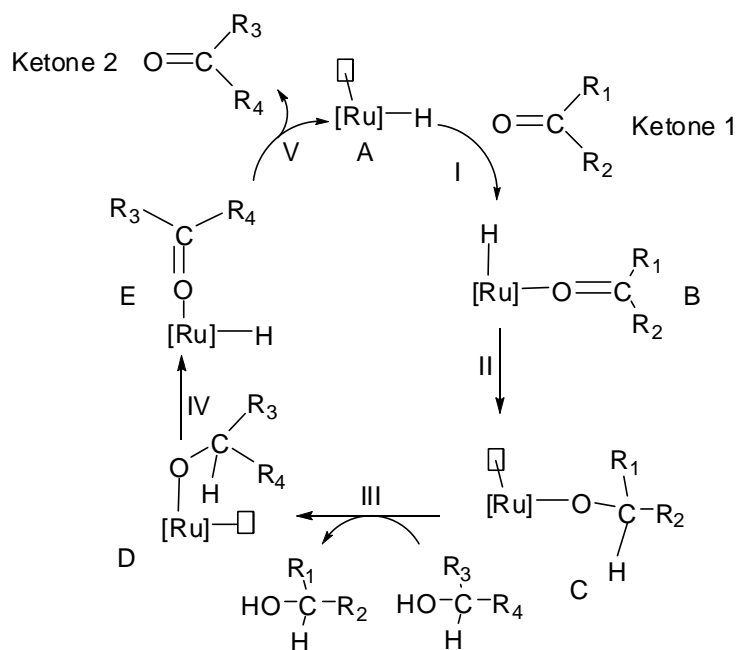
34	RuCl ₂ ((R R)-P-NH-cy-NH-P)	PhMeC = O	iPrOH	KOiPr	1:200:neat:0.5	iPrOH	e.e.) 91 (97% e.e. S)	25	23	7	TOL	[37m]
35	RuHCl(PPh ₃) ₃	PhiPrC = O	HCOOH/NEt ₃	Amine	1:100:neat:5	HCOOH/NEt ₃	100 (86% e.e. S)	120	60	0.8	TOL	[37n]
36	Ru ₂ (μ-H)(μ ₅ - Ph ₂ (C ₆ H ₄ OMe) ₂ OH···OC ₃ Ph ₂ (C ₆ H ₄ OMe) ₂)(CO) ₄	cyclohexanone	HCOOH	NaO ₂ CH	1:7200:7200:1400	HCOOH/H ₂ O/ketone	100	3	100	3800	TOL	[49]

^amw: microwave heating.

Introduction

1.4.2.1 Hydride Transfer to the Substrate in the Primary or Inner Coordination Sphere (TI)

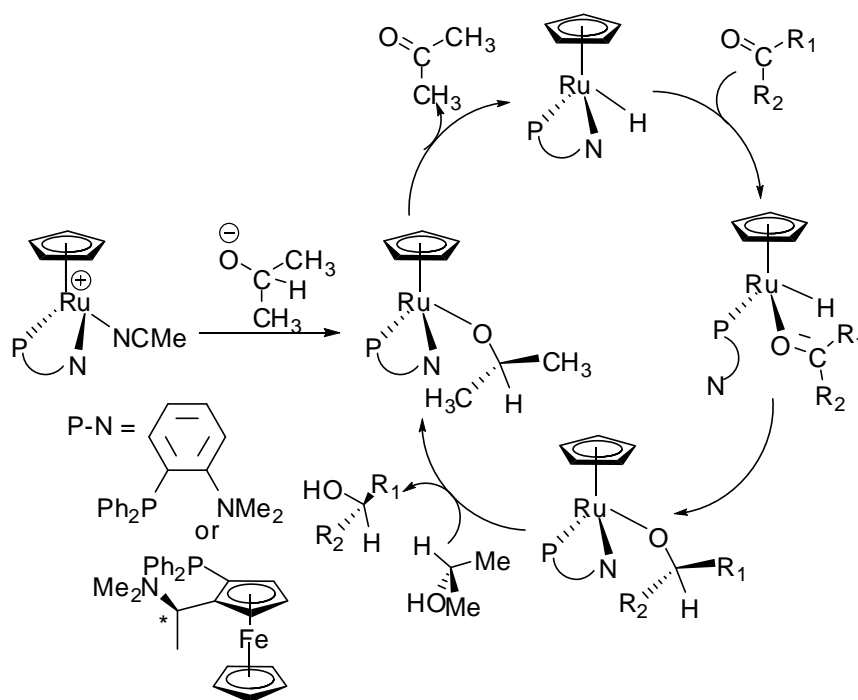
The mechanism shown in Scheme 3 is a commonly accepted one for transition metal TI catalysts.^{35b,38} In the first step ketone 1 adds to the coordinatively unsaturated Ru(II) hydrido species (A) giving the complex (B). Normally the hydride species (A), which is not isolated, is formed from a catalyst precursor. In the second step a hydride migrates to the carbon atom and the new unsaturated ruthenium species (C) will be formed. The hydrogen transfer agent cleaves the coordinated alkoxide by protonation in the third step and subsequently transfers a hydride to the metal by a β -hydride elimination. In the last step the oxidized hydrogen donor will be eliminated. A ruthenium hydrido species could only be detected in some cases.^{30h,34,39}



Scheme 3. The inner sphere transfer hydrogenation mechanism (TI).

Allowing the TI mechanism, ruthenium complexes with bidentate ligands containing phosphorus and nitrogen donors (P–N) have shown high activities in transfer hydrogenation. Complexes of the type $[\text{Ru}(\text{C}_5\text{H}_5)(\text{NCMe})(\text{P}-\text{N})](\text{CF}_3\text{SO}_3)$ shown in Scheme 4 catalyze the TI of acetophenone in 2-propanol (Table 1, entries 22, 23).⁴⁰ Although chiral ligands were used no e.e. was observed. This proves that the nitrogen end of the chelating ligand is hemilabile and

will dissociate from the metal center during the hydride transfer to the ketone (Scheme 4). The dbd ligand (dbd = *N,N*-dimethyl-2-diphenylphosphinoaniline) has a rigid structure and is not able to dissociate. Therefore the ruthenium complex has a low activity. A much more active precatalyst is realized with $[\text{Ru}(\text{C}_5\text{H}_5)(\text{PPh}_3)(\text{NCMe})_2]\text{CF}_3\text{SO}_3$ which possesses more vacant coordination sites.⁴⁰



Scheme 4. TI of ketones catalyzed by complexes $\text{RuH}(\text{C}_5\text{H}_5)(\text{P-N})$.

Chelating nitrogen ligands also have shown activity in the transfer hydrogenation of ketones in the presence of a base, e. g. NaOH. For instance $\text{RuH}(\text{OTf})(\text{bpzm})(\text{cod})$ (bpzm = bis(pyrazol-1-yl)methane, cod = cycloocta-1,5-diene, Figure 3), was reported to catalyze the transfer hydrogenation of cyclohexanone by propan-2-ol at 80 °C (Table 1, entry 16).⁴¹ The complex $\text{RuH}(\text{Tp}^*)(\text{cod})$ with a tridentate nitrogen-donor ligand (Tp^* = hydridotris(3,5-dimethylpyrazolyl)borate) was found to be active for the transfer hydrogenation of cyclohexanone and acetophenone in 2-propanol (Table 4, entries 17 and 18).⁴² $\text{RuH}(\text{Tp}^*)(\text{cod})$

Introduction

is formed from $\text{RuH}(\text{Tp}^*)(\text{H}_2)_2$ in the presence of NaOH and COD (Table 1, entry 19) and catalyzes the transfer hydrogenation of cyclohexanone.

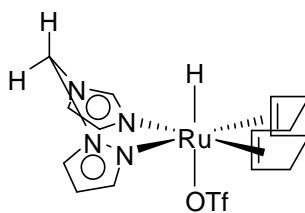
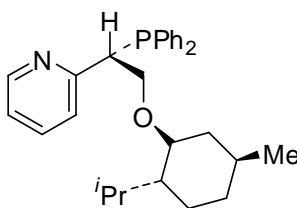


Figure 3. Structure of $\text{RuH}(\text{OTf})(\text{bpzm})$.

The complex $\text{RuCl}_2(\text{PPh}_3)\text{L}$ with a tridentate ligand L containing P, N and O donor sites (Scheme 5) is another activate catalyst for the transfer hydrogenation of cyclic ketones and acetophenone (TOF: 118800 h^{-1}) in basic media.⁴³ In this case no ruthenium(II) hydrides have been observed.



Scheme 5. Tridentate ligand containing P, N and O donor sites.

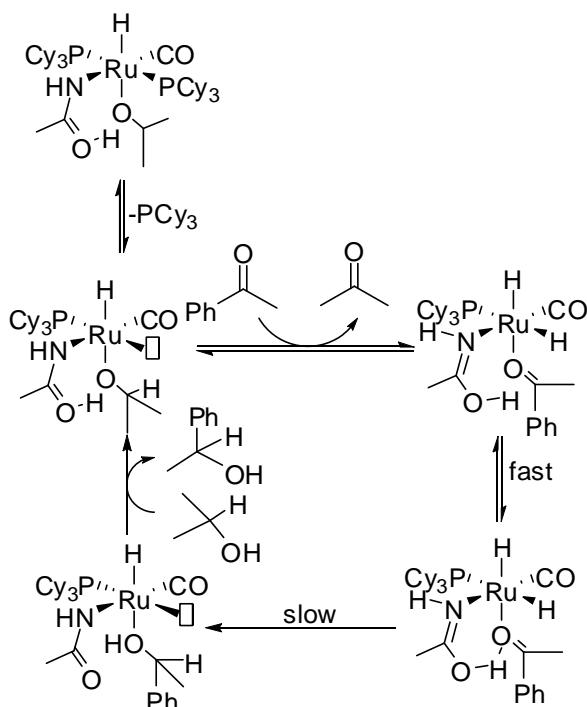
However the *trans*- $\text{RuCl}_2\text{L}(\text{PPh}_3)$ complexes of the tridentate PNP ligands $\text{PPh}_2\text{CH}_2\text{CH}_2\text{NRCH}_2\text{CH}_2\text{PPh}_2$ (R = *n*-Pr (Lpr), *n*-Bu (Lbu), *n*-Hex (Lhex), CH_2Ph (Lbz)) were poor transfer hydrogenation catalysts (Table 1, entry 24) and their activities decreased as the size of the R group on L increases.⁴⁴ In this reaction also no ruthenium(II) hydrides were detected.

Bhaduir et al.⁴⁵ have reported that the anionic hydrido carbonyl cluster $[\text{Ru}_4\text{H}_3(\text{CO})_{12}]^-$ can catalyze the transfer of hydrogen from 2-propanol to methylethylketone (Table 1, entry 15) or 2-cyclohexenone at 82 °C but this reaction suffers from poor selectivity of C=O over C=C

bond hydrogenation which was explained by a radical mechanism for the hydrogen transfer. Transfer hydrogenation of ketones ceased by using precisely purified isopropanol as the hydrogen donor. Adding hydroperoxide HOOtBu, the reaction started. The authors believe that the ruthenium cluster fragmentates and thus can initiate a radical chain propagating by 2-propoxy radicals and cyclohexenone-derived radicals.

1.4.2.1.1 *Hydride Transfer to the Substrate in the Inner Coordination Sphere with Ancillary Ligand Assistance (TIL)*

The ruthenium - acetamido complex $\text{RuH}(\text{NHCOMe})(\text{HO}^i\text{Pr})(\text{PCy}_3)_2(\text{CO})$ is an efficient precatalyst for the TIL of both aryl- and alkyl-substituted ketones and imines (Table 1, entry 26).⁴⁶ Following the proposed mechanism (Scheme 6), a PCy_3 ligand will dissociate from the precatalyst which activates it to the catalyst, $\text{RuH}(\text{NHCOMe})(\text{HO}^i\text{Pr})(\text{PCy}_3)(\text{CO})$. Addition of phosphine inhibited the reaction which is a strong evidence for the dissociation equilibrium.



Scheme 6. The TIL hydrogenation of acetophenone by $\text{RuH}(\text{NHCOMe})(\text{HO}^i\text{Pr})(\text{PCy}_3)_2(\text{CO})$ in $i\text{PrOH}$.

Introduction

1.4.2.2 Hydride Transfer to the Substrate in the Outer Coordination Sphere (TO)

The 2,2'-bipyridine ligand (bpy) in the complex $[\text{Ru}(\text{C}_6\text{Me}_6)(\text{bpy})(\text{OH}_2)](\text{PF}_6)_2$ was found to promote TO catalysis in water or water/organic biphasic systems.⁴⁷ For the hydrogenation of water-soluble as well as water insoluble ketones, TOFs range from 20 to 150 h^{-1} at 70 °C for the hydrogen transfer from sodium formate (e.g. entries 27–28 in Table 1) and the reaction reaches its maximum rate at pH 4. The formate complex $[\text{Ru}(\text{O}_2\text{CH})(\text{C}_6\text{Me}_6)(\text{bpy})]^+$ and the hydrido complex $[\text{RuH}(\text{C}_6\text{Me}_6)(\text{bpy})]^+$ are two observed intermediates in the catalytic cycle. The later complex could be identified by a resonance at -7.45 (s) in its ^1H NMR spectrum. Although the hydride is stable within the pH range of 5 to 9 at temperatures greater than 40 °C, the maximum rate of the hydrogenation occurred at pH 4 which was explained in terms of acid assistance in the hydride transfer step (see Figure 4). The narrow pH range for this catalysis can be explained as follows: Since the pK_a of HCOOH is 3.6, the rate maximum occurs in the presence of the formate ligand HCOO^- . The pK_a of the aqua complex $[\text{Ru}(\text{C}_6\text{Me}_6)(\text{bpy})(\text{OH}_2)]^{2+}/[\text{Ru}(\text{C}_6\text{Me}_6)(\text{bpy})(\text{OH})]^+$ is 7.3 which means that below pH 7.3, the aqua ligand can be displaced by formate while the hydroxide complex is present above pH 7.3 which it is not reactive towards formate.

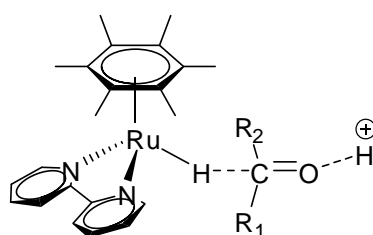
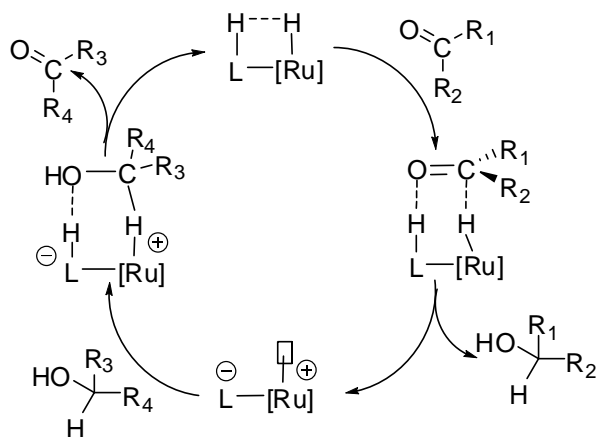


Figure 4. Acid assisted hydride transfer to ketones from $[\text{RuH}(\text{bpy})(\text{C}_6\text{Me}_6)]^+$.

1.4.2.2.1 *Hydride Transfer to the Substrate in the Outer Coordination Sphere with Ancillary Ligand Assistance (TOL)*

The discovery of Noyori and coworkers that the ligand can play a critical role in the hydrogen transfer to unsaturated compounds strongly influenced the strategies for catalyst design. Morris^{12d} described the role of the ligand as follows (Scheme 7): (1) activation of the carbon atom of the unsaturated substrate for a nucleophilic hydride attack via performing a hydrogen bond to the oxygen or nitrogen atom of the substrate, (2) allowing a cyclic transition state for H⁺/H⁻ transfer *via* a correct hyperconjugation with the metal, (3) serving as a source of the proton to be transferred along with the hydride from the metal, and (4) providing a point of interaction for enantioselective recognition of a prochiral substrate. Usually, the substrate does not coordinate to the metal and is located within the second coordination sphere of the catalyst complex.



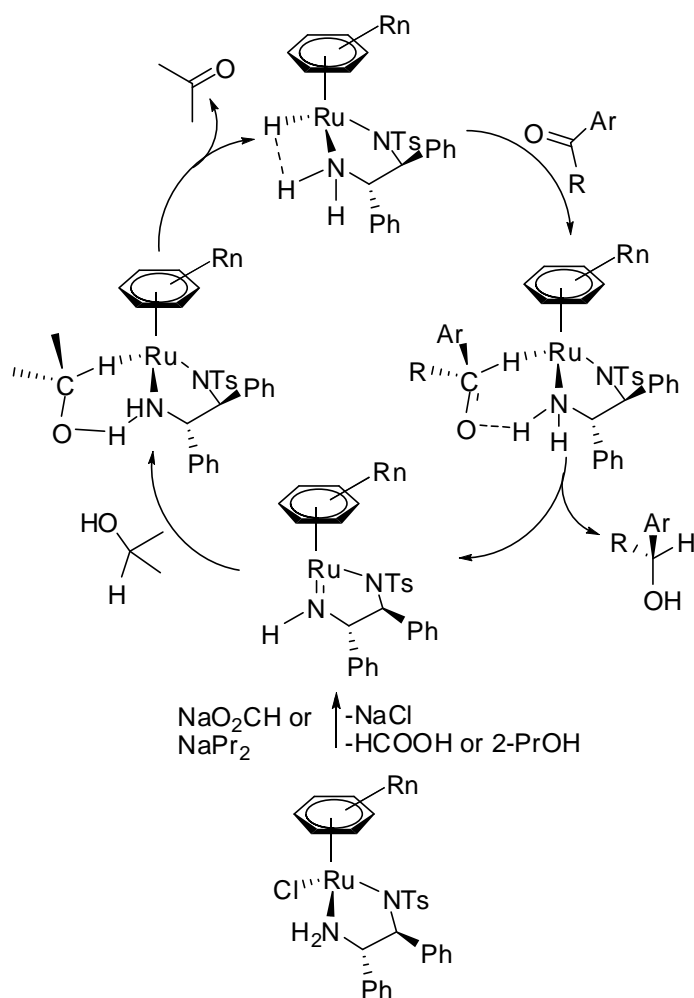
Scheme 7. TOL mechanism involving a hydrogen on a co-ligand.

Noyori's discovery of the NH effect was a revolution in transfer hydrogenation catalysis.^{30e,4b,38,48} A highly efficient catalyst system is produced by mixing chelating ligands with NH₂ groups, such as 2-aminoethanol or the mono-*N*-tosylated diamine TsNHCH₂CH₂NH₂ with a base and [RuCl₂(benzene)]₂ in 2-propanol (Table 1, entries 29–30). Using *N,N*-

Introduction

dimethylated compounds, totally inactive ruthenium complexes were synthesized. This was the first evidence for the “NH effect” in the hydrogenation of polar bonds.

The mechanism shown in Scheme 8 is proposed for the action of these catalysts in the hydrogenation of ketones providing an example for the TOL mechanism shown in Scheme 7.^{30e,4b,38,48a} Forming a hydrogen bond with the NH hydrogen atom on the axial tosylated diamine ligand, the ketone orients in the second coordination sphere. The hydride (δ^-) to substrate sp^2 -carbon (δ^+) contact and a substrate aromatic ring to η^6 -ring interaction are two chiral points to cause enantioselectivity.^{48a} An alcohol in the (*S*)-configuration is produced via a concerted H^-/H^+ transfer and then the hydrido-amine complex is regenerated by reaction with 2-propanol or formic acid.



Scheme 8. TOL of arylketones catalyzed by $\text{RuH}(\text{NH}_2\text{CHPhCHPhNTs})(\eta^6\text{-arene})$ and $\text{Ru}(\text{NHCHPhCHPhNTs})(\eta^6\text{-arene})$ (arene = C_6H_6 , $\text{MeC}_6\text{H}_4^i\text{Pr}$, $\text{C}_6\text{H}_3\text{Me}_3$, Ts = $\text{SO}_2\text{C}_6\text{H}_4\text{Me}$).

Shlov's catalyst benefits from a hydroxyl group on the ligand and catalyzes the ketone or aldehyde transfer hydrogenation using formic acid (Figure 5).⁴⁹

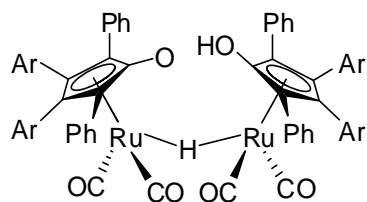


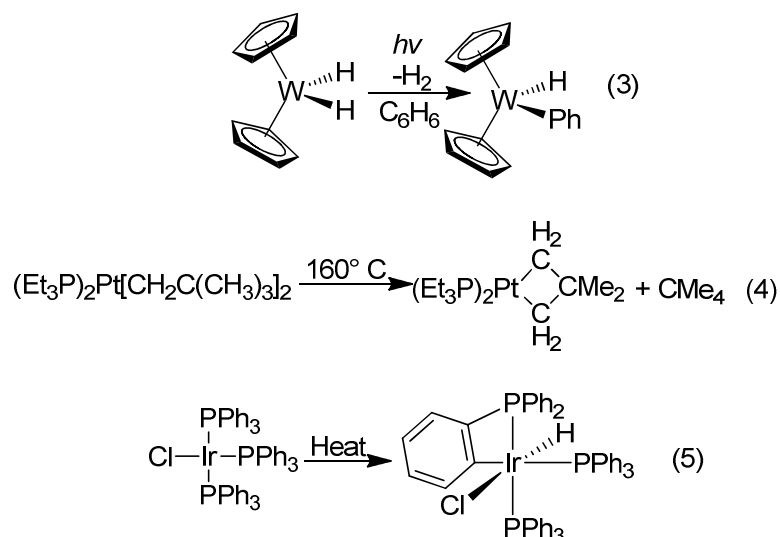
Figure 5. Shlov's catalyst.

Introduction

1.5 C-H Bond Activation

A prevalent topic in transition metal chemistry is the controlled activation of small and relatively inert molecules. Its development began in the late 1950s.⁵⁰ A yet unsolved problem in this area which is usually referred is the activation of alkanes. Until now, the reactivity of a variety of molecules has been changed by binding them to metal centers due to changes in the relative energies of their orbitals or their polarity. For instance, upon coordination to a metal centre olefins and carbon monoxide are more prone to a nucleophilic attack,⁵¹ while coordinated dioxygen often reacts with electrophiles.⁵² Even classic inert small molecules like dinitrogen participate in chemical transformations when coordinated to a transition metal.⁵³ Principally, activating inert C–H bonds should be possible in the same way, but it should not be forgotten that the small molecules mentioned above all possess lone electron pairs and/or π orbitals to interact with empty orbitals of the metals. Alkanes have none of them.

In fact, before 1980s, most of the reactions of C–H bonds coordinated to transition-metal centers ran successfully only through the participation of the π orbitals of aromatic C–H units (Scheme 9, equation (3)⁵⁴) and/or engagement of an intramolecular reaction, wherein the moiety with the C–H bond to be activated is attached to the metal (Scheme 9, equation (4)⁵⁵ & equation (5)⁵⁶).



Scheme 9. Assisted C–H bond activation at transition-metal centers.

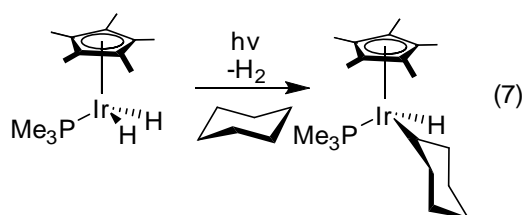
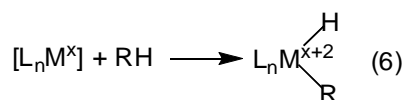
1.5.1 Classification of C-H Activation Reactions

In this section the C–H activation at metal centers leading to bond formation between a metal and an alkane carbon atom will be discussed. Bercaw⁵⁰ has classified these reactions according to their overall stoichiometry into five classes. In four classes, stable organometallic species are formed but usually just two of these happen. In the fifth class, transient organometallic species are considered to be reaction intermediates.

1.5.1.1 Oxidative addition

Low valent complexes of ‘late’ transition elements such as Re, Fe, Ru, Os, Rh, Ir, Pt are electron-rich and can undergo oxidative addition reactions (equation (6)). In some cases the reactive coordinatively unsaturated species $[L_nM^x]$ is generated from a suitable precursor by thermal or photochemical decomposition. For instance, $(\eta^5\text{-C}_5\text{Me}_5)(\text{PMe}_3)\text{Ir}^{\text{III}}\text{H}_2$ loses H_2 under photoirradiation to give the (unobserved) intermediate $(\eta^5\text{-C}_5\text{Me}_5)(\text{PMe}_3)\text{Ir}^{\text{I}}$ (equation (7)).⁵⁷

Introduction



Scheme 10. CH bond activation *via* oxidative-addition.

1.5.1.2 Sigma-bond metathesis

Alkyl or hydrido complexes of ‘early’ transition metals from group 3 of the periodic table (sometimes also metals of groups 4 and 5⁵⁸) with d^0 electron configurations may undergo a reversible reaction according to equation (8a).⁵⁹



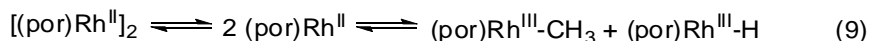
Scheme 11. Sigma-bond metathesis.

Mainly R and R' are both alkyl groups and instead of a total alkane activation, an interchange of alkyl fragments will occur. Although interconversions of dihydrogen and metal alkyl with alkane and metal hydride (equation (8c)) are observed⁶⁰, C–C single bonds formation through the alternative exchange shown in equation (8b) is not known yet.

1.5.1.3 Metalloradical activation

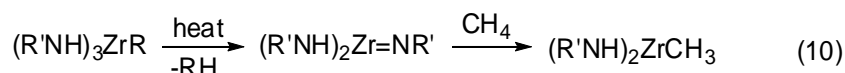
Alkane C–H bonds can be broken reversibly by rhodium(II) porphyrin complexes which exist in a monomer–dimer equilibrium (equation (9)). The most reactive hydrocarbon for this class of reaction is methane. According to the fact that the Rh–H bond strength is low (around 60 kcal mol^{-1} compared to the $105 \text{ kcal mol}^{-1}$ C–H bond of methane) the generation of

the free alkyl radicals through the abstraction of a hydrogen atom from methane by the Rh centre is prohibitively endothermic. This excludes the mechanism involving free alkyl radicals in agreement with inferences from experimental observations.⁶¹



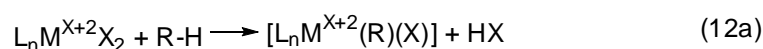
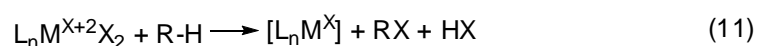
1.5.1.4 1,2-Addition

The addition of an alkane to a metal-nonmetal double bond is a 1,2-addition reaction. For instance methane is added to a Zr–N double bond (equation (10)),⁶² however just benzene is activated by a similar system and not methane.⁶³ Despite the unclear scope of alkane additions across M = N and M = C double bonds, this type of reaction is reported for other early and middle transition-metal centers.⁶⁴



1.5.1.5 Electrophilic activation

Although organometallic species are not observed as intermediates in certain reactions with functionalized alkanes as the product, these types of reactions (equation (11)) are classified as electrophilic activation reactions. Usually, this occurs in strongly polar media for late- or a post-transition metals (Pd^{2+} , Pt^{2+} and/or Pt^{4+} , Hg^{2+} , Tl^{3+}).⁶⁵ The assumed organometallic species $[\text{L}_n\text{M}^{\text{X}+2}(\text{R})(\text{X})]$ is formed by electrophilic activation *via* substitution of a metal by a proton as shown in equation (12a). A possible route leading to the product is shown in equation (12b).



Scheme 12. Electrophilic activation.

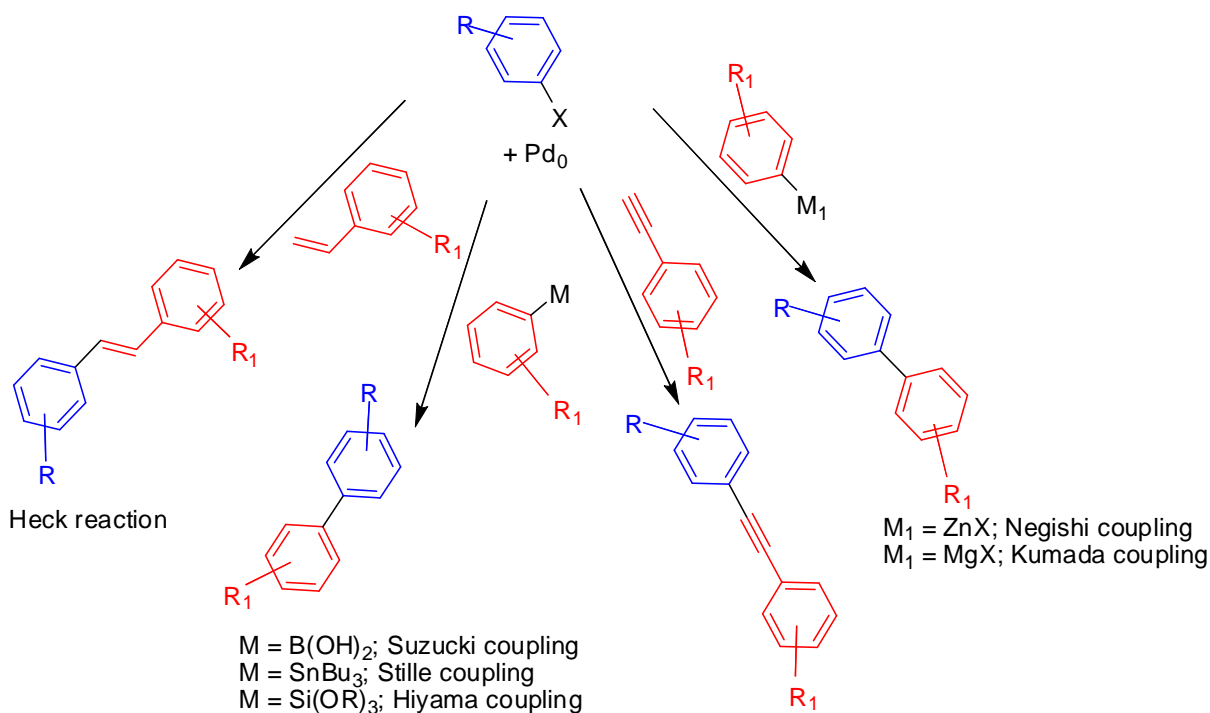
Introduction

1.6 Coupling Reactions

The usefulness of palladium-based catalysts is certainly revealed by the number of articles published in any recent organic chemistry journal.⁶⁶ Cross-coupling reactions catalyzed by palladium seem to be the most powerful methods for C-C bonds formation. Generally palladium assists the C-C bond formation between less-reactive organic electrophiles e. g. aryl halides, and different carbon nucleophiles.

Stoichiometric reactions of reactive nucleophiles with electrophiles or pericyclic reactions were the common methods for C-C bond formation about 50 years ago. Actually, today's carbon-carbon bond-forming methods were started by oxidation catalysis: An important revelation was the application of palladium(II) catalysts in the oxidation of olefins to carbonyl compounds. The Wacker process⁶⁷ is the master example. In the late 1960s, coupling reactions of arylmercury compounds in the presence of either stoichiometric or catalytic amounts of palladium(II) were developed by Richard Heck.⁶⁸ In 1972, the well-known "Heck reaction"⁶⁹ was established by him based on the reaction of phenylmercuric acetate and lithium tetrachloropalladate under an atmosphere of ethylene.^{68a} Tsutomu Mizoroki had described a similar reaction in 1971.⁷⁰

Using organometallic catalysis for the coupling between aryl halides and olefins was a breakthrough in organic synthesis which made further applications possible. Therefore, during the 1970s palladium-catalyzed coupling reactions were investigated incessantly (Scheme 13). Sonogashira coupling of aryl halides with alkynes is an example in which catalytic amounts of palladium and copper salts are used.⁷¹



Scheme 13. Some examples of palladium-catalyzed C-C coupling reactions.

Arylzinc and arylmagnesium were used by Negishi⁷² and Murahashi⁷³, respectively in palladium-catalyzed coupling reactions instead of alkenes or alkynes. Recently, the famous Negishi and Kumada coupling reactions have found extensive applications. Despite the fact that nickel can catalyze similar cross-coupling reactions concerning reactivity, selectivity, and functional-group tolerance palladium has found wider application. Palladium-catalyzed coupling of arylboronic acids and esters with aryl halides were discovered by Suzuki and Miyaura⁷⁴ for the synthesis of symmetric and unsymmetric biaryls. The use of air-stable and readily accessible arylboronic acids is the main advantage of the Suzuki-Miyaura coupling. In the same way, the palladium-catalyzed coupling of aryltin and arylsilanes were investigated by Stille⁷⁵ and Hiyama⁷⁶. Nowadays, highly efficient C-O and C-N bond formations are also known. The Buchwald–Hartwig amination is the most remarkable one.⁷⁷

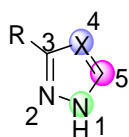
After their discovery, palladium-catalyzed cross-coupling reactions became rapidly popular. There are several reasons for their success: The tolerance of the methods to a wide

Introduction

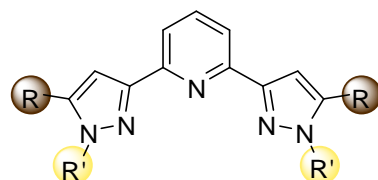
range of functional groups on both coupling partners is their noticeable feature. This allows the efficient construction of the complex organic building blocks in few steps. Additionally, a fine-tuning of the reactivity is possible by the development of ligands and co-catalysts. In the last two decades there has been no other organometallic method that has a broader investigation in academic laboratories and application in industry.⁷⁸ Their significance and superiority in organic chemistry is highlighted by awarding the Noble prize to the Heck, Negishi and Suzuki in 2010.

2 Motivation

The good results of the previous studies on the catalytic activity of ruthenium complexes in transfer hydrogenation done in Prof. Werner R. Thiel's group^{79,80} were our motivation to optimize the structure of these complexes to obtain better catalysts working under milder conditions. These studies have shown that bidentate or tridentate pyrazole-based ligands such as bispyrazole and bispyrazolypyridine are suitable for the ruthenium catalyzed hydrogenation and transfer hydrogenation of ketones. Changing the substituent on the 1-, 4- or 5 position of the pyrazole ring, the steric and electronic characteristics of the pyrazole containing ligands can be controlled (Scheme 14). This makes these ligands potentially suitable for applications in catalysis.



Scheme 14. Different possibilities for modifications at the pyrazole ring.

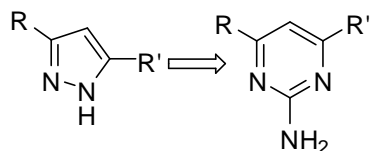


Scheme 15. The desired bispyrazolypyridine with different substituents at the pyrazole rings.

The discovery of Noyori and coworkers that activities and selectivities can be improved by the presence of a N-H functionality in the ligand being in close proximity to the metal site (bifunctional catalysis)⁵ was a significant breakthrough in hydrogenation catalysis and later on strongly influenced the strategies for catalyst design. Previous studies in Prof. Thiel's group have shown that the NH group of the pyrazole ring act in this way.^{79,80} Another aim of this work was to find methods to substitute the pyrazole against a 2-aminopyrimidine ring hoping

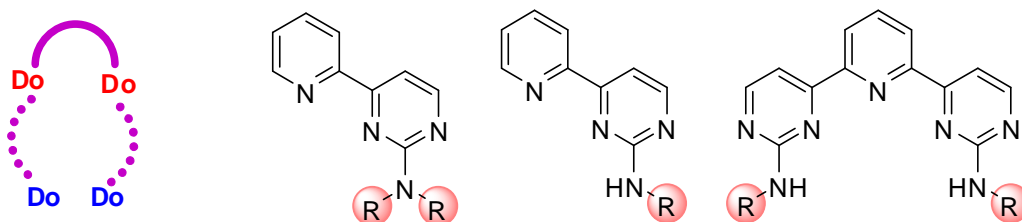
Motivation

that with the NH_2 group of this new ligands a bifunctional mechanism might be realizable (Scheme 16). The ruthenium complexes of these ligands had to be examined for transfer hydrogenation of ketones. Also, the mechanism of the reaction had to be investigated.



Scheme 16. Replacing the pyrazole against a 2-aminopyrimidine.

The NH_2 group of the new ligands is a potential site for the introduction of new substituents leading to multidentate ligands. Multidentate ligands, having pyrimidine groups as relatively soft donors for late transition metals and possessing simultaneously a binding position for a hard Lewis-acid are matter of interest in the SFB/TRR-88 (3MET) at the TU Kaiserslautern. Synthesis and characterization of such ligands were another aim of this work (Scheme 17).



Scheme 17. Introducing substituents on the amino group to obtain soft and hard donor sites.

3 Results and Discussion

3.1 Ligand Synthesis

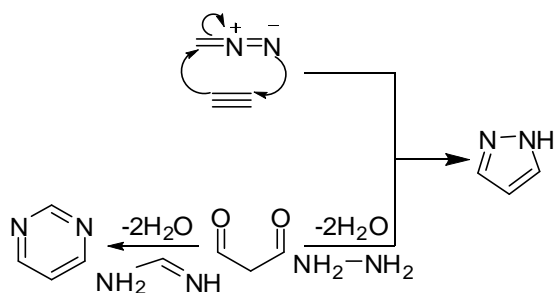
The development of new ligands bearing donor atoms other than phosphorus has aroused increasing interest in coordination chemistry, homogeneous catalysis, and organic synthesis. Mixed-donor ligands have been widely used as a result of the versatility arising from the different stereoelectronic properties of the multiple coordination sites, providing a unique reactivity of their metal complexes.⁸¹ Ligand lability is an important feature of many efficient catalysts since ligand dissociation steps are often involved in catalytic cycles. However, too much lability may lead to catalyst decomposition. Thus, at least one strongly coordinating donor is certainly required for a ligand to be used for the preparation of a transition-metal catalyst, especially when other labile sites are present. In general, a balance between the stability of the organometallic catalysts and the need to incorporate dissociable ligands is desirable for highly efficient catalysts relying on ligand dissociation in their catalytic reaction. Bidentate pyridine-derived ligands are commonly present in coordination chemistry and homogeneous catalysis, while recently symmetric tridentate planar N₃ ligands with pyridine backbones such as 2,2':6',2''-terpyridines⁸², 2,6-bis(imino)pyridines⁸³, and 2,6-bis(oxazolonyl)pyridines⁸⁴ have been investigated.

3.1.1 Synthesis of NNN Ligands

The chemistry of pyrazole, pyrimidine and their derivatives has been studied for more than 100 years.⁸⁵⁻⁸⁸ A wide bunch of synthetic routes leading to these structures have been worked out, since some members of the pyrazole and pyrimidine family play economically prominent roles in pharmacy and agrochemistry.⁸³ However, there are only two routes of general importance:^{81,89} the five-membered pyrazole ring system can either be formed by combining a diazomethane derivative and an acetylene in a 1,3-dipolar cycloaddition or by ring closure using hydrazine and a β -diketone or a derivative of similar reactivity (Scheme 18). The

Results and Discussion

latter strategy also allows the access to pyrimidines when formamidines, ureas, thioureas or guanidines are applied for the ring closure instead of hydrazine. This method is obviously favorable since the substitution pattern of the resulting 1*H*-pyrazole/pyrimidine can readily be determined by the starting materials. A large number of syntheses of pyrimidines⁸² and bispyrimidines⁸³ have been described in the literature but there are just a few reports on pyridylpyrimidines.⁸⁴



Scheme 18. Formation of five/six-membered ring systems.

3.1.1.1 Synthesis of Ligands with a Bispyrazolypyridine Backbone

Symmetrical tridentate planar bispyrazolypyridines ligands have been synthesized and investigated in the recent years in Thiel's group⁹⁰, but further modifying of these ligand was requested to get optimized ligands suitable for the ruthenium catalyzed transfer hydrogenation.

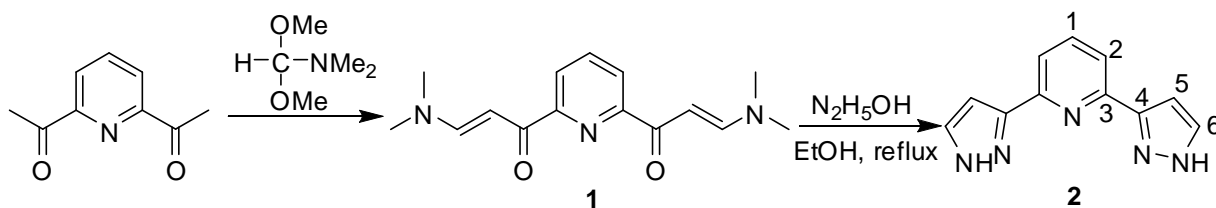
3.1.1.1.1 Synthesis of the Precursors

Bispyrazolypyridine are used as the backbone of the new ligands and synthesized as follows:

3.1.1.1.1.1 Synthesis of 2,6-di(1*H*-pyrazol-3-yl)pyridine

Starting from 1,1'-(pyridine-2,6-diyl)diethanone, 2,6-di(1*H*-pyrazol-3-yl)pyridine can be synthesized easily in two steps according to the literature.^{26h} In the first step 1,1'-(pyridine-2,6-diyl)diethanone is refluxed with 1,1-dimethoxy-*N,N*-dimethylmethanamine. The product is (2*E*,2'*E*)-1,1'-(pyridine-2,6-diyl)bis(3-(dimethylamino)prop-2-en-1-one) which will condense

in the second step with hydrazinhydrate under reflux conditions in ethanol as the solvent to obtain 2,6-di(1H-pyrazol-3-yl)pyridine (Scheme 19).

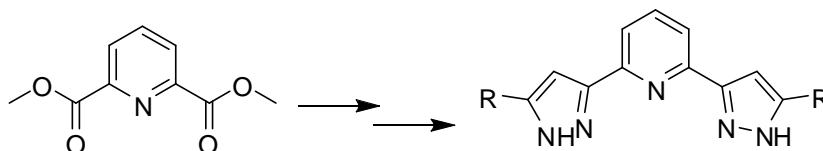


Scheme 19. Synthesis of 2,6-di(1H-pyrazol-3-yl)pyridine.

In addition to the resonance of the AB₂-system of the pyridine ring, two characteristic doublets at about 6.08 ppm and 6.86 ppm assigned to the protons in the 4- and 5-position of the pyrazol rings are observed in the ¹H NMR spectra of **2**.

3.1.1.1.2 Synthesis of the Bispyrazolylpyridine Backbone with Substituted Pyrazol Rings

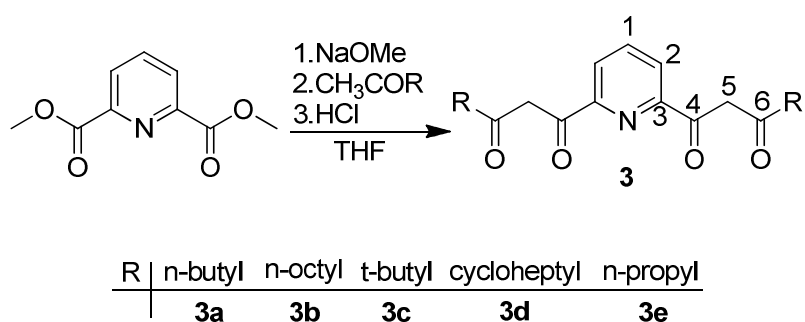
To synthesize 2,6-di(pyrazol-3-yl)pyridine having alkyl or aryl groups as substituents a two step method known from the literature (Scheme 20) was applied.⁹¹



Scheme 20. Synthesis of 2,6-di(pyrazol-3-yl)pyridine from dimethyl pyridine-2,6-dicarboxylate.

Results and Discussion

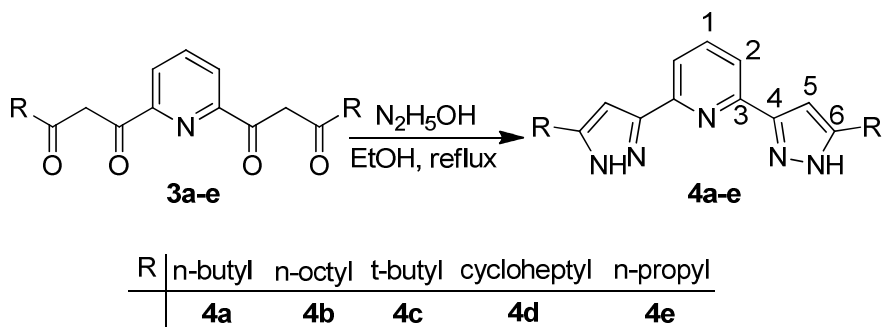
Here dimethylpyridine-2,6-dicarboxylate is reacted with the proper methylalkyl- or methylarylketone. Methylketones are favorably deprotonated regioselectively at the methyl group using sodiummethanolate as the base (Schema 21). The best solvent for this reaction is tetrahydrofuran (THF). It is required that the solution of the methylketone in THF is added dropwise to a suspension of sodiummethanolate and dimethyl pyridine-2,6-dicarboxylate. Finally the mixture is refluxed for four hours leading to the sodium salt of the tetraketone which can be converted to product by acidifying the reaction medium at the end.



Scheme 21. Synthesis of the tetraketones **3a-e**.

According to the structure of the tetraketones a series of tautomers can be formed via keto-enol tautomerization.⁹² They can be detected in the ¹H NMR spectra of these compounds. The protons of the hydroxyl group of the enol form of a 1,3-diketone appears at lower field between 15 and 16 ppm. In the IR spectrum, intensive absorptions at about 1600 cm⁻¹ and 3100 cm⁻¹ can be assigned to carbonyl and hydroxyl groups, respectively.

The pyrazol rings of the 2,6-di(pyrazol-3-yl)pyridines **4a-e** were formed via a condensation reaction between the 1,3-diketones (**3a-e**) and hydrazine (Scheme 22).⁹³ Using this method, 2,6-di(pyrazol-3-yl)pyridines with different substituents can be synthesized easily and in good yields.



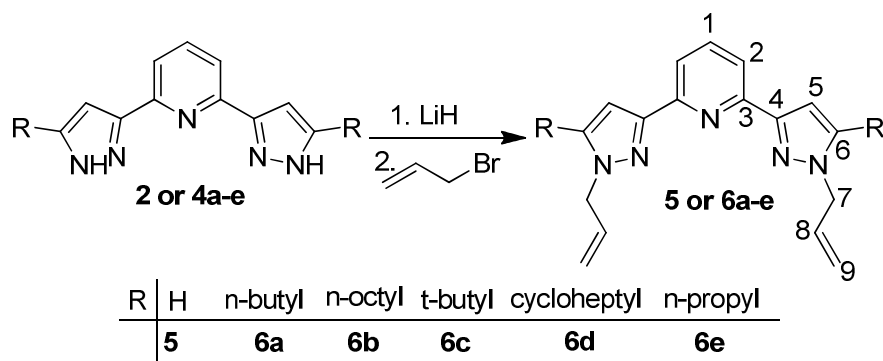
Scheme 22. Synthesis of the 2,6-di(pyrazol-3-yl)pyridines **4a-e**.

The solubility of the 2,6-di(pyrazol-3-yl)pyridines without any substituent is poor in most organic solvents. By introducing long chain alkyl or aryl groups, the solubility can be controlled.⁸² In the ¹H NMR spectra of the compounds **4a-e** a characteristic singlet for the proton in the 4-position of the pyrazol ring can be observed at about 6.5 ppm in addition to the AB₂-system of pyridine ring. In the ¹³C NMR spectra a resonance appearing at about 101 ppm can be assigned to the corresponding carbon atom.

3.1.1.1.2 Synthesis of Allylated Bispyrazolylpyridine Ligands

By introducing allylic side chains in the 1- and 1'-positions of the pyrazole rings, the 2,6-di(pyrazol-3-yl)pyridine is functionalized with substituents of moderate bulkyness. Furthermore one could expect the allylic side chains offering chelating π -donating elements, that could stabilize a 16VE ruthenium(II) intermediate in a hemilabile manner, but will not be hydrogenated itself under the given reaction conditions of the transfer hydrogenation. Deprotonation of the pyrazole units with LiH in THF and subsequent allylation with allylicbromide gives the 2,6-bis(1-allyl-5-alkyl/aryl-1H-pyrazol-3-yl)pyridines **5** and **6a-e** (Scheme 23). It should be noted here, that the use of NaH for the deprotonation of **2** or **4a-e** leads to the formation of quite stable six coordinate sodium complexes, which hamper the isolation of the target ligands.

Results and Discussion



Scheme 23. Synthesis of the 2,6-bis(1-allyl-5-alkyl/aryl-1H-pyrazol-3-yl)pyridines **5** and **6a-e**.

By functionalization of the pyrazole ring with an alkyl group (as is shown in Table 2), the resonance of H5 on the pyrazole ring changes from a doublet to a singlet and shifts by about 1 ppm towards higher field. Also H2 shifts by about 0.5 ppm towards higher field compared to **5**, indicating an increased electron density in the pyrazol ring, which is also reflected in the ^{13}C NMR resonances of these compounds. For the cycloheptyl annulated ligand **6d**, there is no pyrazole proton resonance anymore and the ^{13}C resonance of C5 is shifted to lower field, too. (Figure 6 & 7). The methylene protons at the allylic side chains of these compounds show doublets between 4.62 and 4.91 ppm indicating that these hydrogen atoms are magnetically equivalent. As expected, the two protons H9 which are not magnetically equivalent give two doublets slightly shifted upfield when the pyrazole ring is functionalized with an alkyl group.

Table 2. ^1H and ^{13}C NMR shifts of the ligands **5** and **6a-e**.

	R	H1 C1	H2 C2	H3 C3	H4 C4	H5 C5	H6 C6	H7 C7	H8 C8	H9 C9
5	H	7.86 143.3	8.22 121.4	---- 147.9	---- 144.8	7.75 108.9	---- 131.7	4.85 55.4	6.08- 5.98 132.0	5.31-5.24 119.7
6a	<i>n</i> butyl	7.59 144.4	7.79 117.9	---- 151.8	---- 150.7	6.76 103.1	---- 136.5	4.62 51.6	5.95- 5.82 133.1	5.05 & 4.88 116.5
6b	<i>t</i> butyl	7.62 150.5	7.85 118.5	---- 152.8	---- 152.2	6.81 ---	---- 136.9	4.91 53.7	6.00- 5.90 134.7	5.19 & 5.01 116.9
6c	<i>n</i> octyl	7.65 144.6	7.83 118.2	---- 152.2	---- 151.1	6.81 103.5	---- 136.6	4.72 51.9	5.99- 5.92 133.5	5.15 & 4.98 116.8
6d	cycloheptyl	7.66 143.6	7.74 119.8	---- 153.5	---- 147.5	---- 120.7	---- 136.4	4.72 52.2	5.99- 5.90 133.8	5.15 & 5.00 116.6
6e	<i>n</i> propyl	7.68 143.4	7.83 118.2	---- 152.2	---- 151.2	6.81 103.6	---- 136.7	4.73 52.0	6.01- 5.91 133.5	5.16 & 4.98 116.8

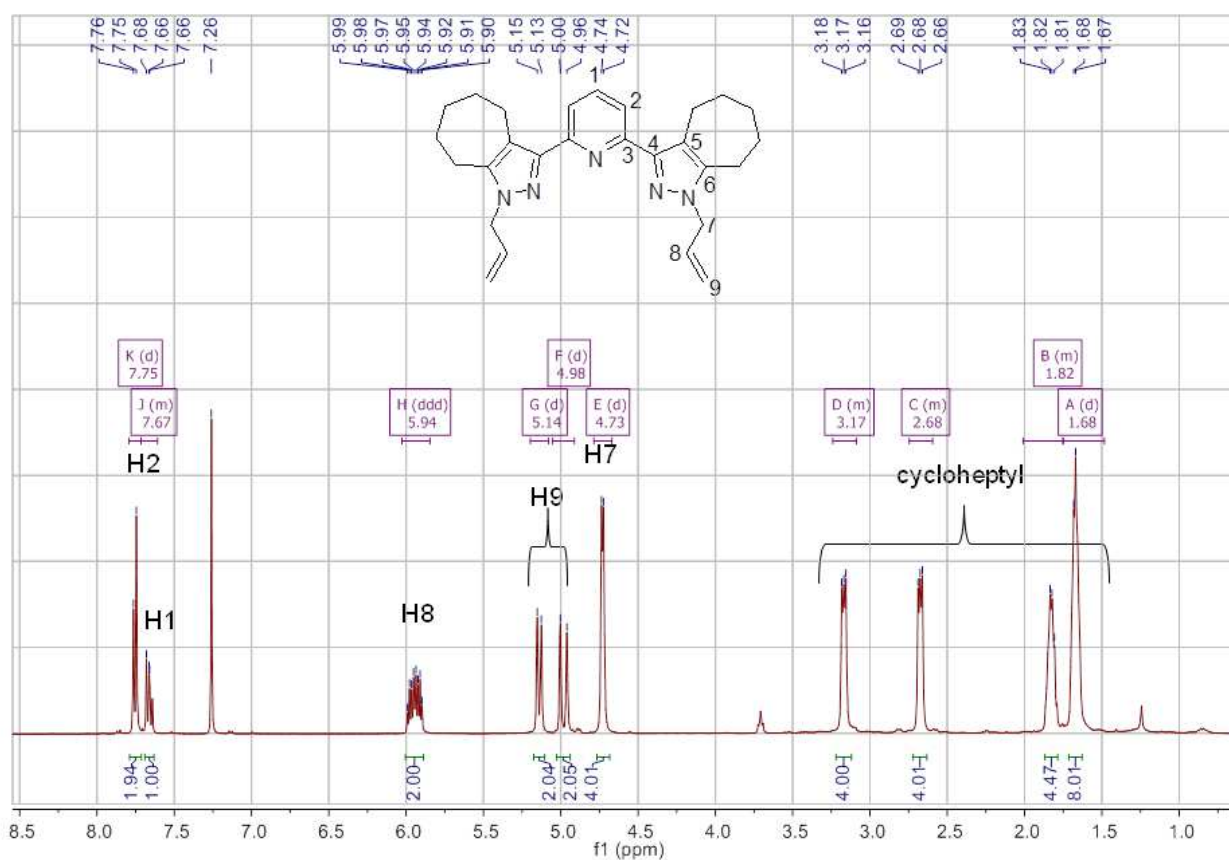


Figure 6. ^1H NMR spectrum of ligand **6d**.

Results and Discussion

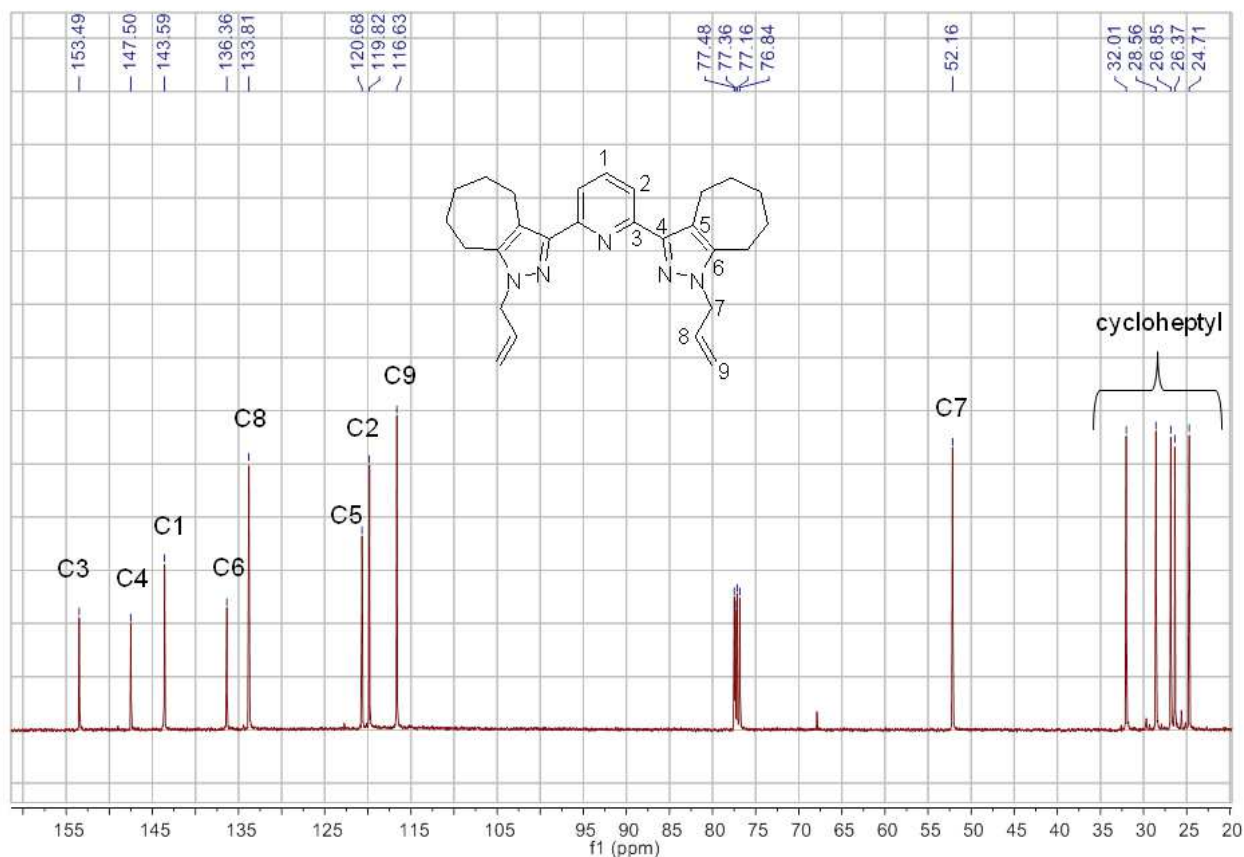
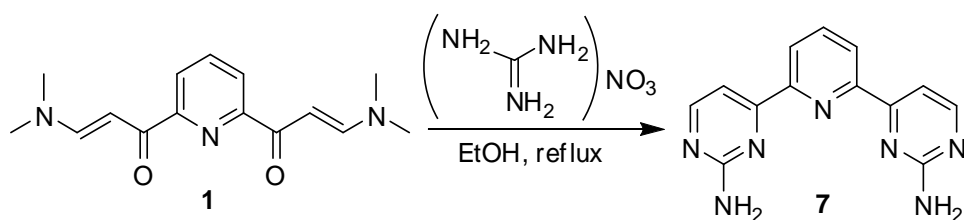


Figure 7. ^{13}C NMR spectrum of the ligand **6d**.

3.1.1.2 Synthesis of Ligands with a Bispyrimidylpyridine Backbone

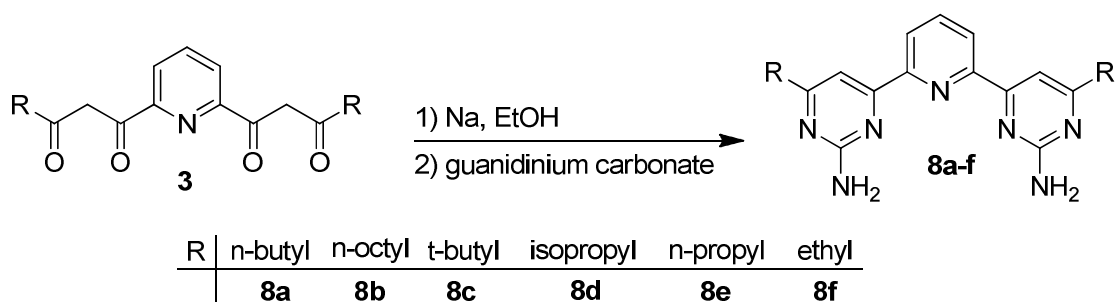
In proceeding with Thiel's group studies concerning the synthesis of *N*-alkylated 2-(3-pyrazolyl)pyridines as ligands for homogeneous catalysis,^{91c,94-100} I sought a mild and efficient method to prepare substituted 2-amino-4-(2-pyridyl)pyrimidines and 2,6-bis(2-amino-4-pyrimidyl)pyridines to use them as building blocks for new multidentate ligands. Apart from Balavoine et al. who were able to synthesize 2-amino-4-(2-pyridyl)pyrimidine and 2,6-bis(2-amino-4-pyrimidyl)pyridine by ring closure with guanidinium nitrate and 1-(2-pyridinyl)-3-dimethylaminoprop-2-enone and [2,6-bis(3-dimethylamino-1-oxoprop-2-en-yl)pyridine]

(Scheme 24),⁹³ there is no report on an efficient syntheses of such ligands from a β -diketone or a derivative of comparable reactivity.



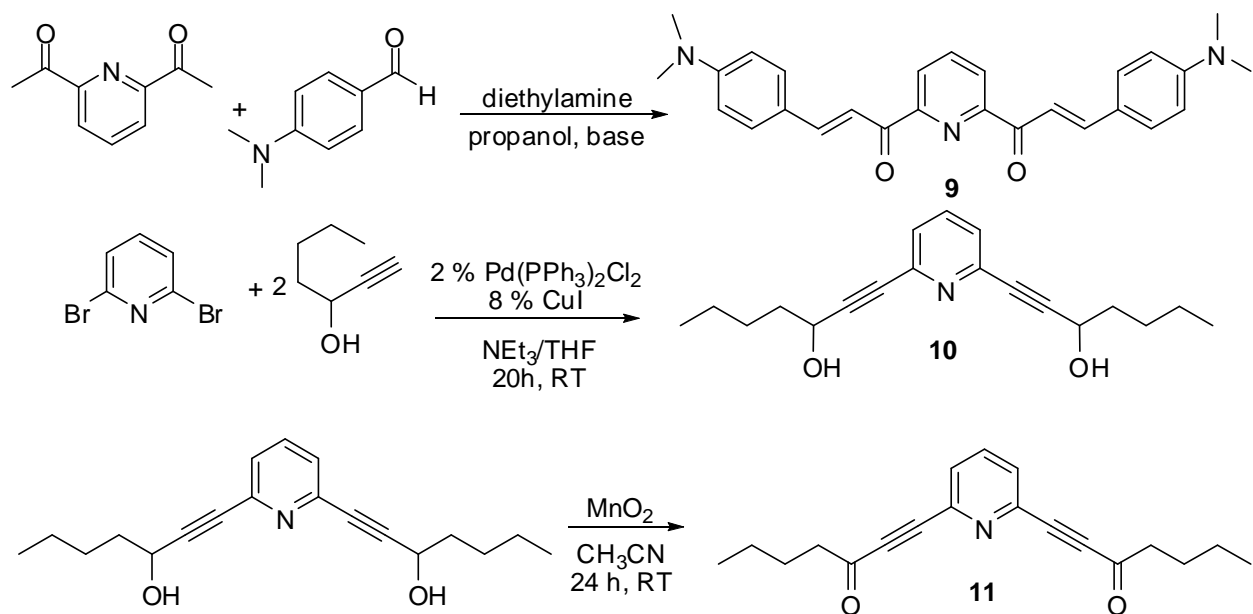
Scheme 24. Synthesis of 2,6-bis(2-amino-4-pyrimidinyl)pyridine.

The tetraketones **3** are simply accessible by the condensation of methylalkylketones and diethyl pyridine-2,6-dicarboxylate in the presence of a base^{26h} as described in section 3.1.1.1.1.2 (Scheme 21). The ring closure of **3c** with an excess of guanidinium carbonate is carried out under conventional reflux conditions in presence of NaOMe with ethanol as the solvent. After removal of the solvent and recrystallisation, **8c** is obtained as a yellow solid but in just about 9% yields (Scheme 25). Using other solvents such as butanol and DMF¹⁰¹, allowing to do the reaction at higher temperatures, did not improve the yields. Moreover different type of guanidinium salts such as carbonate, nitrate and chloride have been tested, but no product was gained. Application of microwave heating also failed.



Scheme 25. Synthesis of the 6,6'-(pyridine-2,6-diyl)bis(4-alkylpyrimidin-2-amine) in a polar solvent.

Results and Discussion



Scheme 26. Different starting materials tested for synthesizing pyrimidine based *N,N,N* ligands.

Changing the starting material to compounds **9** or **11** was expected to provide a solution to this problem. Compound **9** was synthesized according to published procedures *via* aldol condensation (Scheme 26).¹⁰² 2,6-Diacetylpyridine and two equivalents of a substituted arylaldehyde and diethylamine as the catalyst were refluxed overnight in propanol. The orange to yellow crystalline precipitate was filtered off and washed with ice-cold methanol. Suitable yellow needle like crystals of **9** for X-ray crystallography were obtained from dichloromethane. The structure is shown in Figure 8. The bond lengths C(4)-O(1), C(4)-C(5), C(5)-C(6), C(6)-C(7) are 1.2284, 1.4591, 1.3419, 1.4506 Å, respectively, showing that C(4)-C(5) and C(6)-C(7) have more single bond characteristics and C(4)-O(1) and C(5)-C(6) are almost double bonds.

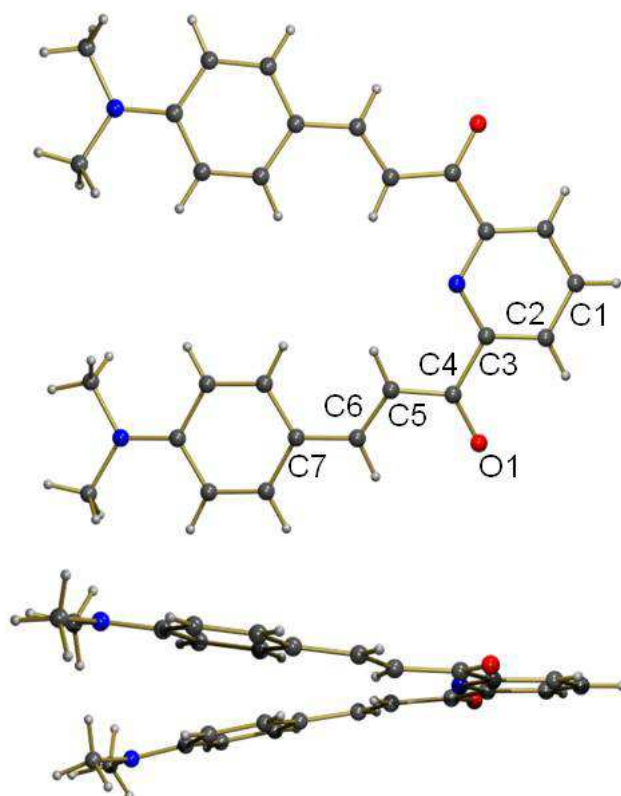
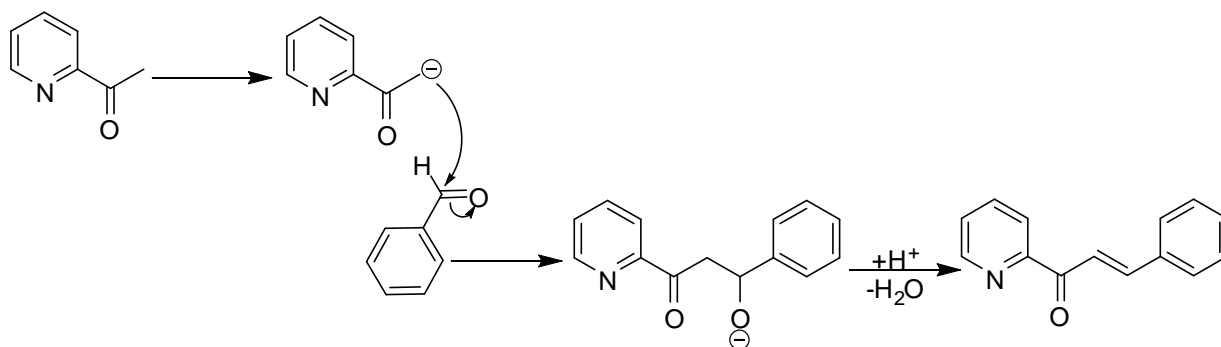


Figure 8. Molecular structure of **9** in the solid state.

According to the mechanism of the aldol condensation (Scheme 27) this method is limited to the usage of arylaldehydes.

Results and Discussion



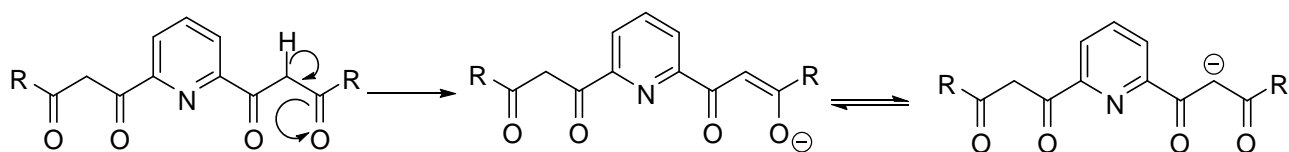
Scheme 27. Aldol condensation mechanism.

Reacting **9** with different guanidinium salts in refluxing ethanol in the presence of a base such as NaOH or NaOEt results in an oily brown substance which was not the product according to its ^1H NMR spectrum.

To obtain **10**, hept-1-yn-3-ol was synthesized first according to published methods¹⁰³ as follows: Pentanal was added slowly to a solution of ethynylmagnesium bromide at $-78\text{ }^\circ\text{C}$. The mixture was stirred for 45 min at $-78\text{ }^\circ\text{C}$ and then quenched with a saturated solution of ammonium chloride. The aqueous layer was separated and extracted with diethyl ether. The organic layer was washed with water and then brine, dried over anhydrous magnesium sulfate, and filtered. Evaporation of the solvent was followed by a Kugelrohr distillation and yielded hept-1-yn-3-ol as a colorless oil. To couple 2,6-dibromopyridine with hept-1-yn-3-ol 2.5 equivalents of triethylamine were added to a solution of 2 mol % of $\text{Pd}(\text{PPh}_3)\text{Cl}_2$, 8 mol % of CuI, 2,6-dibromopyridine in dry THF.¹⁰⁴ A color change from yellow to orange was observed. Then a solution of 2.2 equivalents hept-1-yn-3-ol 2.5 in dry THF was added dropwise, which resulted in a color change to brown. In this stage the reaction mixture became warm and if needed (depending on the amount) the mixture should be cooled. The reaction mixture was stirred at room temperature over night. Evaporating the solvent gave a brown oil, which contained **11** and some impurities according to its ^1H NMR spectrum. Column chromatography on silica gel eluting with ethylacetate did not give a pure product. Attempts to purify the

product by sublimation or crystallization also failed. So the reaction was continued with this raw product hoping that the final product can be purified. To the solution of **11** in dried CH_2Cl_2 , 20 equivalents of activated MnO_2 were added. The reaction mixture was stirred for 24 h at room temperature and then filtered through MgSO_4 . Evaporating the solvent gives a brown solid which was applied to the column chromatography on silica gel eluting with hexane:ethylacetate 1:1. The solvent was evaporated leading to a brown oil. In its ^1H NMR spectrum, the peaks of the product were not detected. According to these results it seems that the β -diketone **3** is the only reactant with which the desired product can be obtained.

Looking at the reaction mechanism it becomes obvious that the base used to activate the guanidinium salt will deactivate the β -diketone (Scheme 28). Moreover there are some reports¹⁰⁵ showing that using a polar solvent such as ethanol is not suitable for this type of reactions. However, non-polar solvents cannot be used since they are not able to dissolve the guanidinium carbonate.

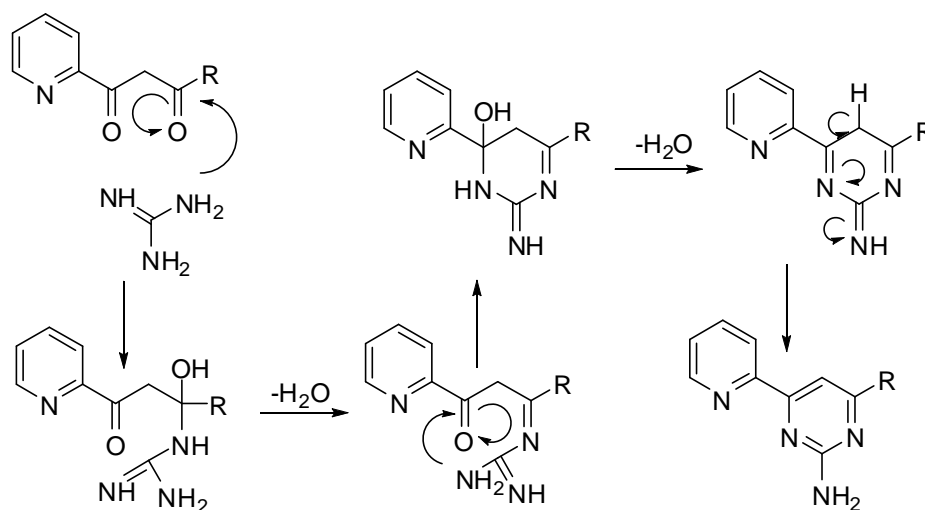


Scheme 28. Deactivation of the diketone by the base.

Fusing just the guanidinium salt and the diketone will result in the product but in low yield¹⁰⁶ (12%). Searching for a base which can activate the guanidinium carbonate but will not deactivate the β -diketone, I came up with the idea to use silica or alumina. Silica or alumina, guanidinium carbonate and **3** were mixed and ground and the reaction was carried out at different temperatures with different ratios of silica and alumina to reactants. The optimized conditions were found as follows: the reaction proceeded with two mass equivalents of silica at 200 °C for 4 h. Using two mass equivalents of silica are essential because the silica is not only

Results and Discussion

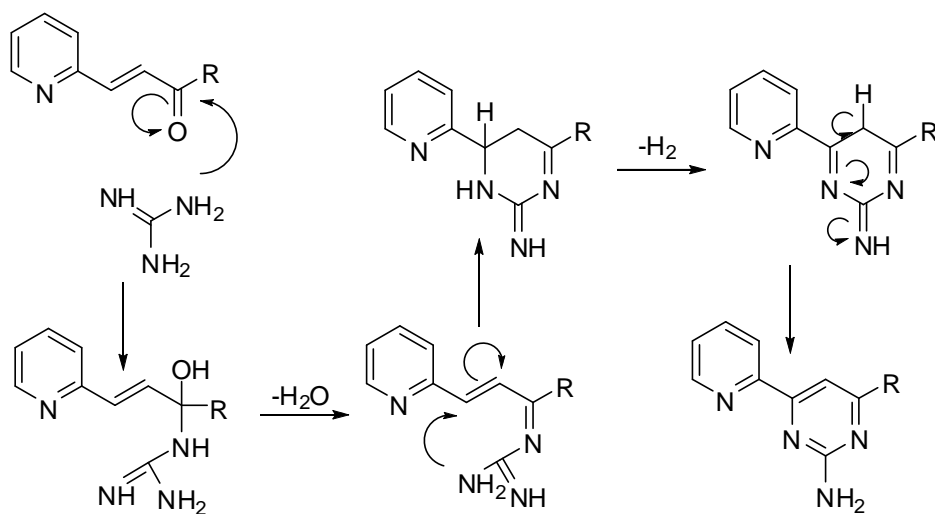
the base but also it will absorb the water being released during the reaction (Scheme 29). It is noteworthy to mention that using guanidinium nitrate did not result in product formation. It seems that releasing the CO₂ gas is necessary as a driving force for the reaction. The resulting ligands are too soluble and could not be purified by crystallization. Unfortunately all attempts to find a suitable mixture of solvents for column chromatography also failed. Acidifying with HCl and trying to precipitate the hexafluorophosphate salt was as well unsuccessful. Only the ligand with the *t*-butyl substituent was pure enough to be applied in the syntheses of multidentate ligands (see section 3.1.5).



Scheme 29. Mechanism of ring closure and water releasing.

This method is limited to compounds bearing alkyl groups on the pyrimidine ring and all efforts failed to do the reaction with reactants which are functionalized by aryl groups. The most visible difference between reactants with alkyl and aryl group is that the alkyl derivatives are waxy or oily and can be ground with the other reactants more efficiently than the powdery reactants with an aryl group. Even changing the reactant to **9** did not work probably for two reasons: first this powdery reactant cannot be ground and mixed well with the other reactants. Second, according to the ring closure mechanism (Scheme 30) elimination of H₂ is required in

the last step which is just possible in the presence of a strong base or an efficient oxidizing agent.



Scheme 30. Mechanism of ring closure with reactant **9**.

As it is shown in Table 3, functionalizing the pyrimidine ring with different alkyl group has no significance effect on the ^1H NMR and ^{13}C NMR shifts of ligands **8a-f** as it was expected. The ^1H NMR and ^{13}C NMR spectra of ligand **8b** are shown in Figures 9 and 10 as an example.

Table 3. ^1H NMR and ^{13}C NMR data of ligands **8a-f** in CDCl_3 .

	R	H1 C1	H2 C2	H3 C3	H4 C4	H5 C5	H6 C6	H7 C7	NH ₂
8a	ⁿ butyl	7.92 137.9	8.36 122.8	---- 154.5	---- 163.8	7.60 107.1	---- 173.6	---- 163.5	5.63
8b	octyl	7.94	8.42	----	----	7.67	----	----	5.12
8c	^t butyl	7.96- 7.91 138.0	8.40 122.5	---- 154.5	---- 163.9	7.96-7.91 103.8	---- 180.5	---- 163.2	5.12
8d	isopropyl	7.94 138.0	8.41 122.8	---- 154.5	---- 164.0	7.71 105.1	---- 178.4	---- 163.4	5.15
8e	ⁿ propyl	7.94 138.0	8.42 122.9	---- 154.5	---- 163.8	7.66 107.3	---- 173.4	---- 163.4	5.14
8f	ethyl	7.95 138.0	8.43 122.9	---- 154.5	---- 163.9	7.70 106.6	---- 174.6	---- 163.3	5.12

Results and Discussion

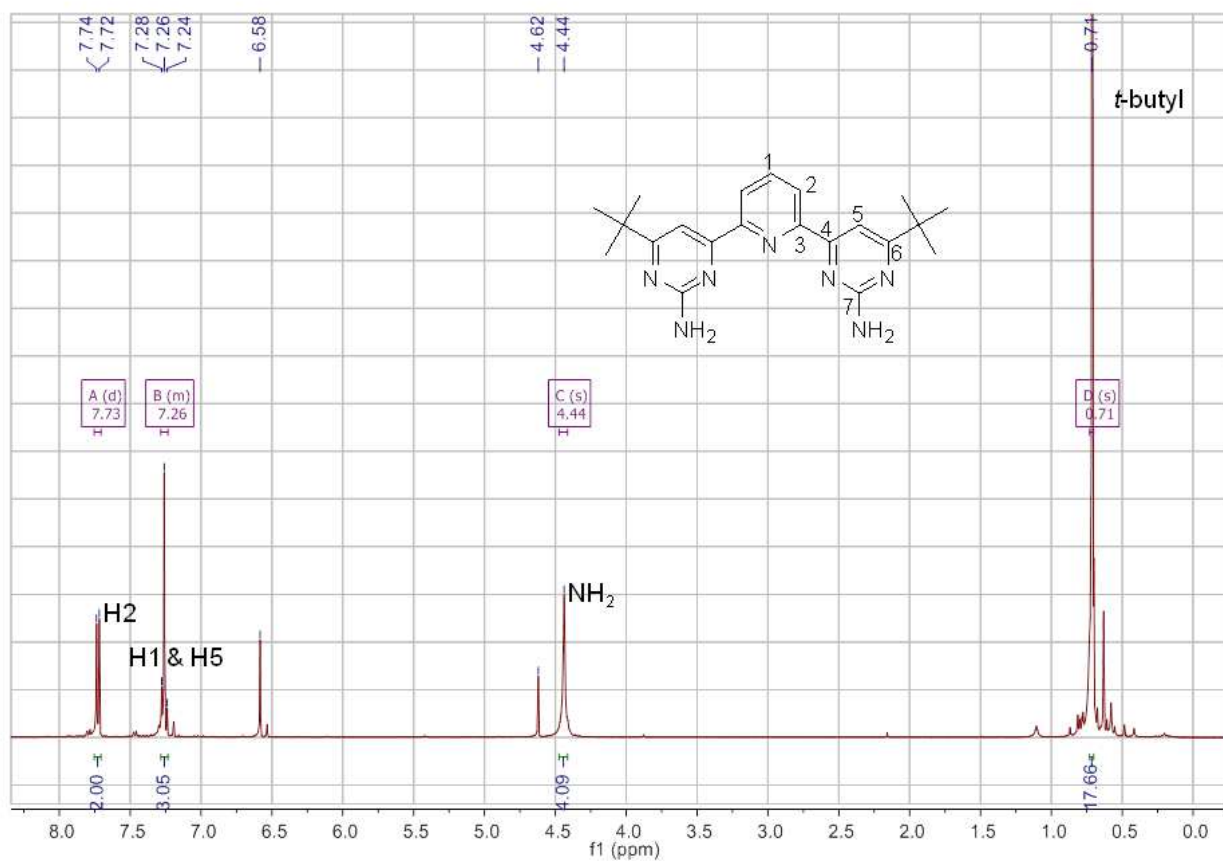


Figure 9. ^1H NMR spectrum of ligand **8b**.

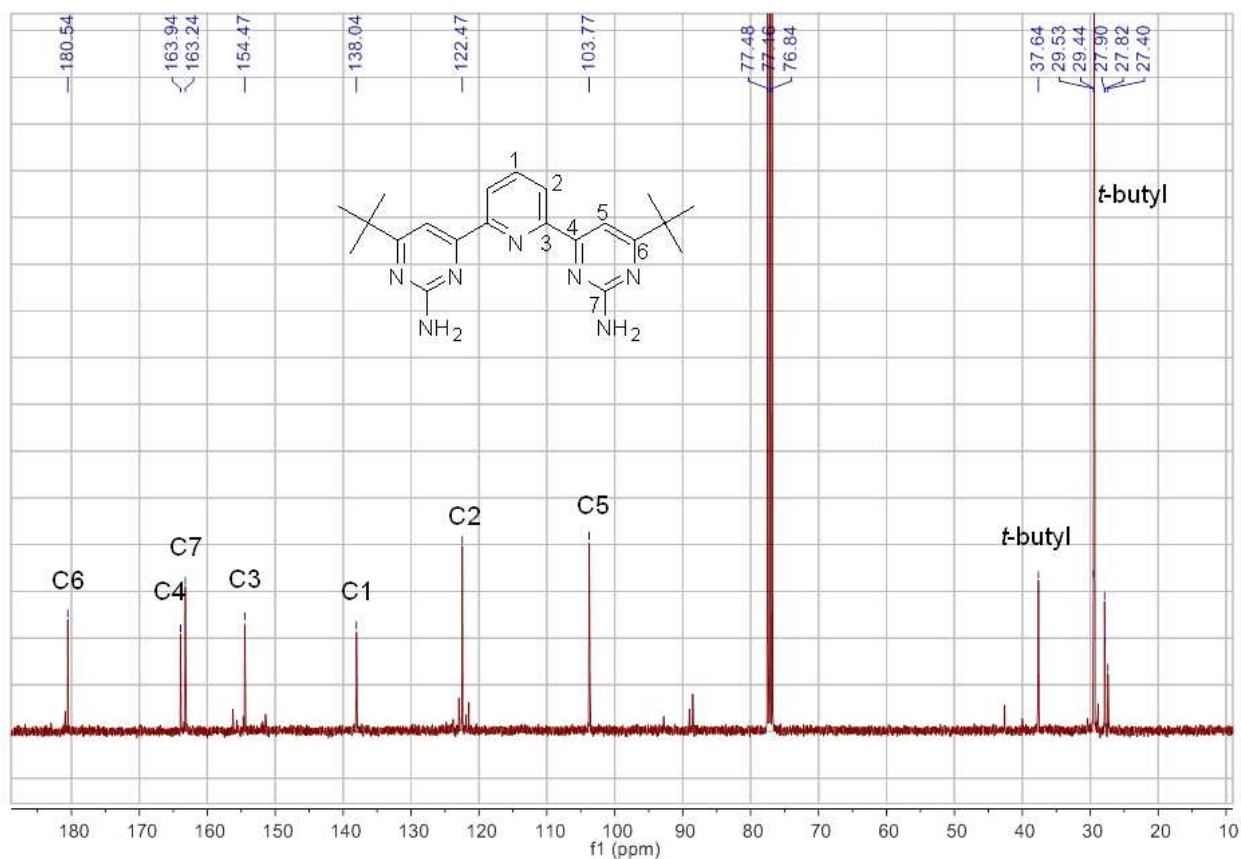


Figure 10. ^{13}C NMR spectrum of ligand **8b**.

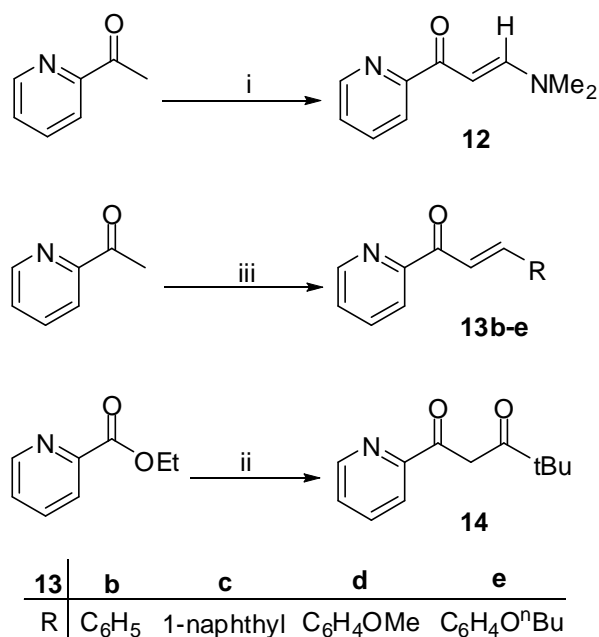
3.1.2 Synthesis of *NN* Ligands

2,2-Bipyridyl is probably the most often used aromatic *N,N*-chelating ligand in coordination chemistry.¹⁰⁷ However, pyridine chemistry makes it difficult to efficiently introduce a broad variety of substituents into this system. Since Thiel's group was looking for a *N,N'*-donor bearing an amino group in close proximity to the coordinating nitrogen atom in combination with other functions to elucidate the influence of these groups on the bifunctional catalytic transfer hydrogenation, I became interested in the 2-amino-4-(2-pyridinyl)pyrimidine motif. The chemistry of pyrimidine and its derivatives is well established.¹⁰⁸

3.1.2.1 Synthesis of the Precursors

2-Amino-4-(2-pyridinyl)pyrimidines can be obtained in a straightforward synthesis starting from versatile 2-acetylpyridine or pyridine-2-carboxylic acid ester (Scheme 31).

Results and Discussion



Scheme 31. Synthesis of **12**, **13b-e** and **14**; i) HC(NMe₂)(OMe)₂, 4 h, refl.; ii) THF, NaH, tBuC(O)Me, 12 h, refl.; iii) propanol, NH(Et)₂, arylaldehyde, 12 h, refl..

As it was mentioned earlier in section 3.1.1.2 I had to choose different types of starting materials in order to have different substituents on the pyrimidine ring. **12**, **13b-e** and **14** were synthesized using the methods which are described in sections 3.1.1.1.1, 3.1.1.1.2 and 3.1.1.2 for **12**, **14** and **13b-e**, respectively. Trying to obtain proper crystals of **13e** for X-ray crystallography I was able to crystallize **15** which is the byproduct of **13e**. The crystal structure is shown in Figure 11.

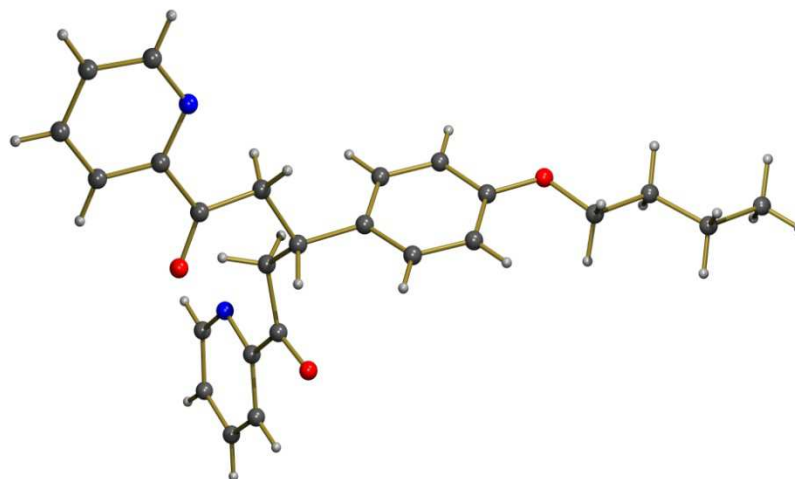
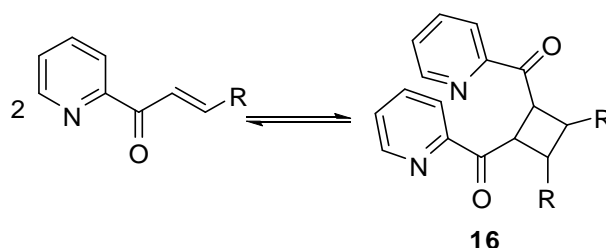


Figure 11. Molecular structure of byproduct **15** in the solid state.

Here **13b-e** can be used without problems of polymerization as it was discussed in section 3.1.1.2. In this case there is just an equilibrium between the monomer and the dimer as it is shown in Scheme 32. As the monomer is consumed it will be regenerated according to the equilibrium and this will continue until the reaction is completed.



Scheme 32. Dimerization equilibrium of **13b-e** in solution.

It is noteworthy to express at this point that the dimerization occurs in the presence of light and a color change from yellow to deep green is observed. This process is accelerated in solution which is apparent in the ^1H NMR spectra of **13d** after and before being exposed to the sunlight (Figure 12).

Results and Discussion

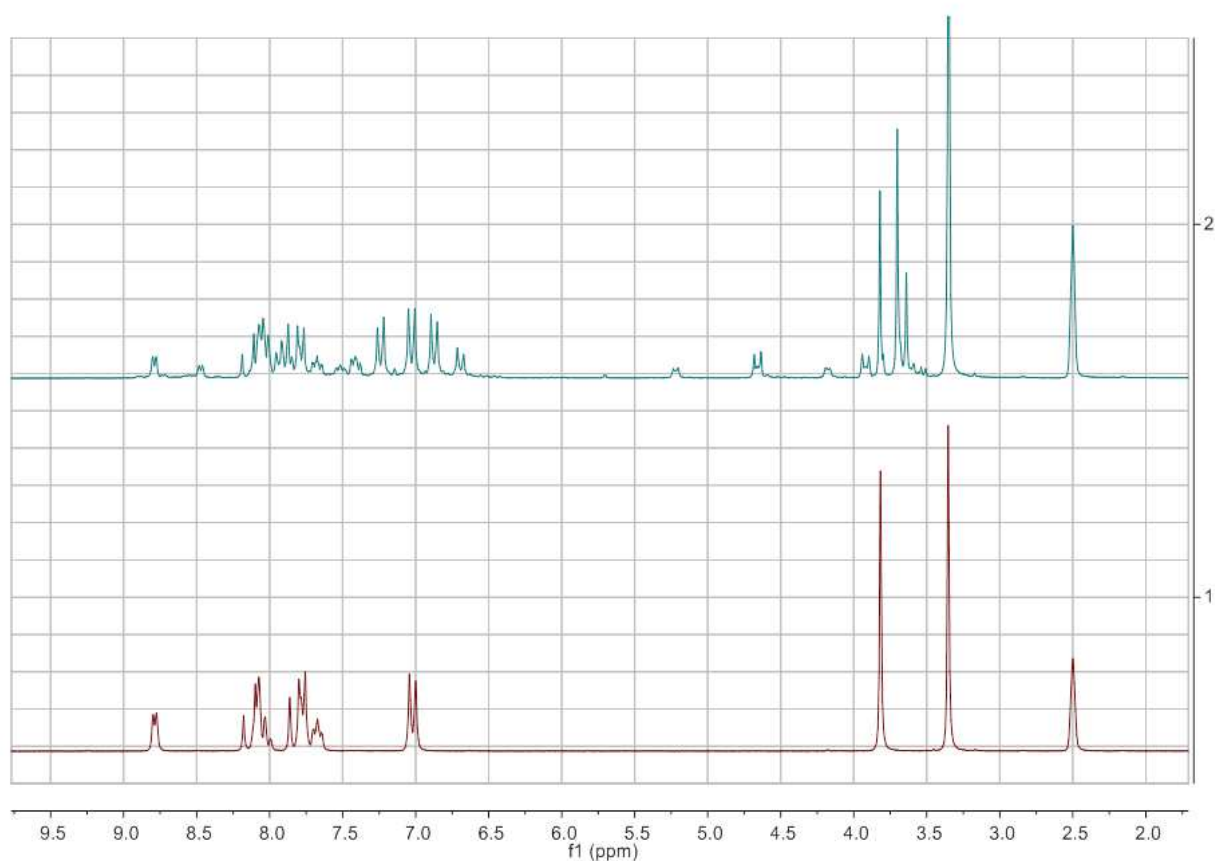


Figure 12. ^1H NMR spectrum of **13d** before (bottom) and after (above) being exposed to sunlight.

It was not possible to gain suitable crystals of **13c** for X-ray crystallography, however I was able to separate crystals of dimer **16**. Its crystal structure is shown in Figure 13. The X-ray structure analysis of **16** shows the *syn* head-to-head product while generally the major product of solid-state photodimerizations of 4-azachalcones is the *syn* head-to-tail isomer.¹⁰⁹

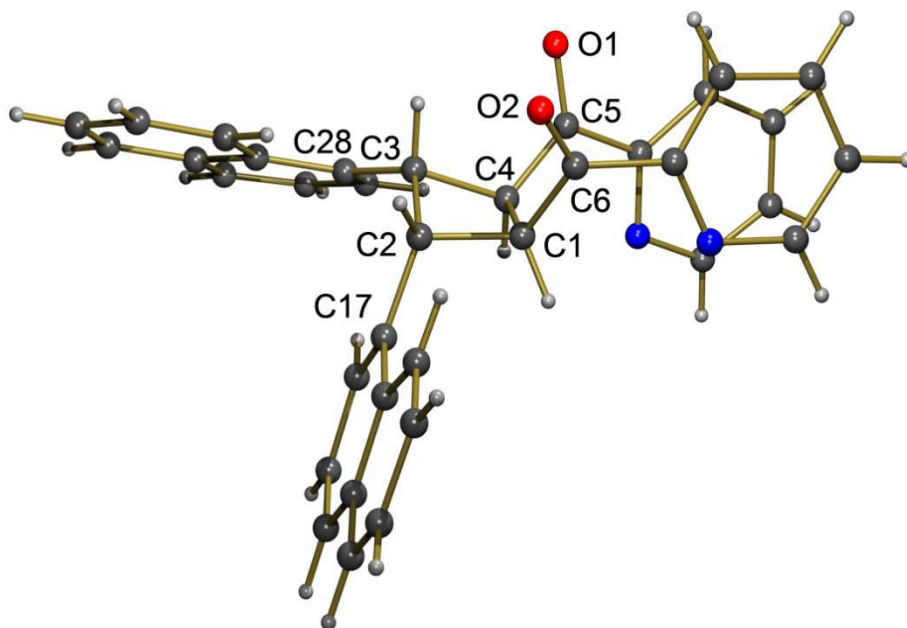
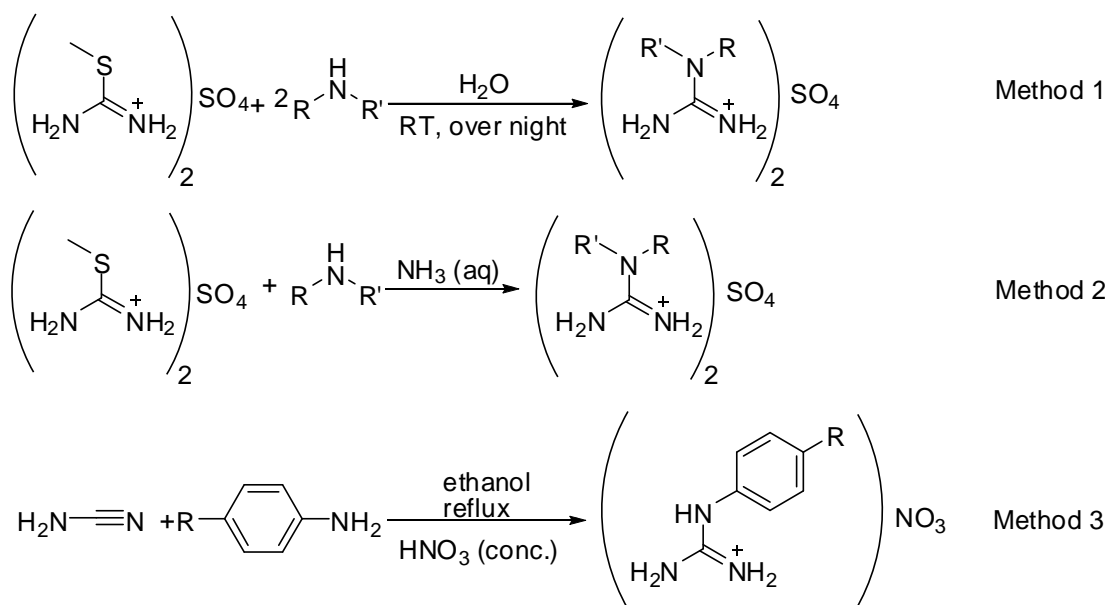


Figure 13. Molecular structure of dimer **16** in the solid state. Selected bond lengths [\AA] and dihedral angles [$^\circ$]: O1-C5 1.2208(19), O2-C6 1.212(2), C1-C2 1.5556(19), C1-C4 1.578(2), C2-C3 1.567(2), C3-C4 1.541(2), C4-C1-C2-C17 104.75(13), C2-C1-C4-C3 18.36(10), C4-C1-C2-C3 18.04(10), C2-C1-C4-C5 138.91(13), C6-C1-C4-C5 20.69(18), C6-C1-C4-C3 99.86(13), C6-C1-C2-C3 96.39(14), C6-C1-C2-C17 140.82(14), C17-C2-C3-C28 31.6(2), C6-C1-C2-C3 96.39(14), C6-C1-C2-C17 140.82(14), C17-C2-C3-C28 31.6(2), C17-C2-C3-C4 94.62(14), C1-C2-C3-C28 144.70(14), C1-C2-C3-C4 18.48(11), C2-C3-C4-C1 18.21(10), C2-C3-C4-C5 137.83(13).

3.1.2.2 Synthesis of the Guanidinium Salts

Several guanidinium salts could be synthesized by different methods, which are known from the literature, depending on the nature of the guanidinium moiety. Generally three methods were used for this purpose (Scheme 33). For salts bearing an alkyl group either method 1¹¹⁰ or method 2¹¹¹ were applied. For salts containing aryl groups, method 3¹¹² found out to be the best.

Results and Discussion



Scheme 33. Three different methods used to synthesize guanidinium salts.

Method 1: This method was used for liquid amines. Two equivalents of an alkylamine were stirred with 2-methyl-2-thiopseudourea hemisulfate in a little amount of water at room temperature over night. The release of methanethiol is a sign that the reaction is occurring. After evaporating the water, residual amine can be washed out by ethanol. If there is need to change the sulfate to the nitrate ion, the product can be treated with a hot solution of $\text{Ba}(\text{NO}_3)_2$.

Method 2: Ammonium hydroxide 30% was added to the alkylamine, followed by the addition of 2-methyl-2-thiopseudourea hemisulfate. The mixture was heated to 70 °C and stirred vigorously until the reactants dissolved. There was a vigorous evolution of methylmercaptane. The mixture was stirred at 70 °C until no effervescence of methylmercaptane was detected anymore. The mixture was then cooled to room temperature and was evaporated to dryness under reduced pressure in a rotary evaporator. The product can be crystallized from water.

Method 3: Concentrated nitric acid was added to a solution of an arylamine in ethanol followed by a 50% aqueous solution of 1.5 equivalents of cyanamide. The reaction mixture

was then heated under reflux for 16 h. The reaction was cooled to 0 °C followed by the addition of ether. The contents were then refrigerated overnight, and the resulting solid was filtered, affording the product in good yield.

The guanidinium salts can be purified by crystallization from water or ethanol. For one of them, single crystals suitable for X-ray diffraction studies were obtained, and its molecular structures in the solid state are presented in Figure 14.

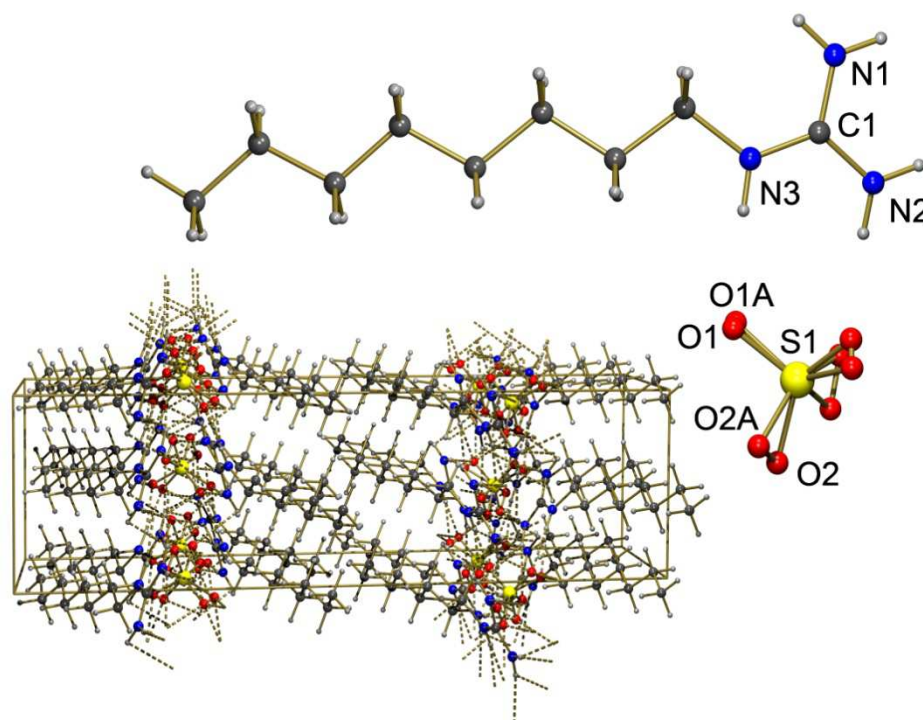


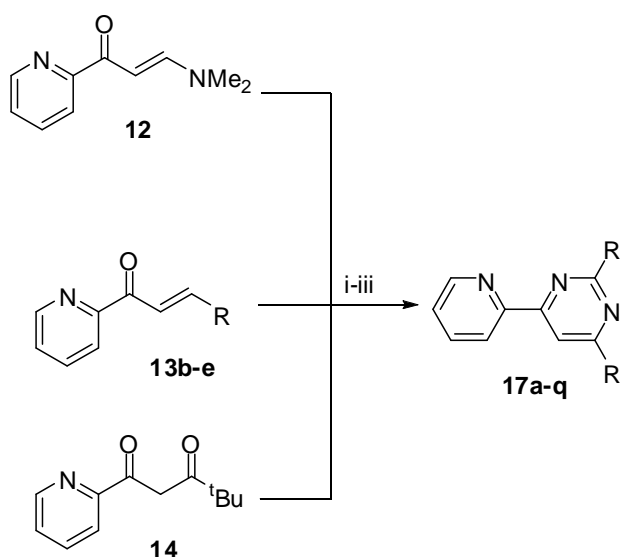
Figure 14. Molecular structure of one of the guanidinium salt in the solid state possessing a sulfate counter anion. Selected bond lengths [Å]: N1-C1 1.3284(19), N2-C1 1.3279(19), N3-C2 1.464(2), N3-C1 1.3239(18).

3.1.2.3 Synthesis of 2-Amino-4-(2-pyridinyl)pyrimidines

The desired ligands **17a-q** were obtained in good yields (Scheme 34) either by treating the intermediates **12** or **13b-e**^{113,102b} with guanidinium salts in the presence of a NaOEt in

Results and Discussion

refluxing ethanol or by grinding with guanidinium carbonate and silica as it was described in section 3.1.1.2.



17	a	b	c	d	e	f	17	g	h	i	j	k
R	H	C ₆ H ₅	1-naphthyl	C ₆ H ₄ OMe	C ₆ H ₄ O ⁿ Bu	^t Bu	R	H	^t Bu	C ₆ H ₄ OMe	H	H
R'	NH ₂	NH ₂	NH ₂	NH ₂	NH ₂	NH ₂	R'	N(CH ₂) ₄	NMe ₂	N(CH ₂) ₄	NMe ₂	N(CH ₂) ₅
17	l	m	n	o	p	q						
R	H	H	H	H	H	H						
R'	HN(CH ₂) ₂ CH ₃	HN(CH ₂) ₃ CH ₃	HN(CH ₂) ₇ CH ₃	S-HN(CH)(CH ₃)(C ₆ H ₅)	R-HN(CH)(CH ₃)(C ₆ H ₅)	HN(CH)(CH ₃) ₂						

Scheme 34. i) Synthesis of the chelate ligands; for **17a-e**: [C(NH₂)₃]₂(CO₃), EtOH, refl. 24 h; ii) for **17g-q**: [XC(NH₂)₂]₂(SO₄), EtOH, refl. 24 h; iii) for **17f**: [C(NH₂)₃]₂(CO₃), SiO₂, 200 °C, 2 h.

The ¹H NMR data of **17a-q** are summarized in Table 4. Comparing the chemical shifts, it is obvious that functionalizing the pyrimidine ring does not have a big electronic influence. Just replacing one hydrogen atom of the NH₂ group by an alkyl group causes a down field shift for the remaining amino hydrogen atom (see ligands **17l-q** in comparison to ligands **17a-f**).

Table 4. ¹H NMR data of ligands **17a-q**.

Ligand	H1	H2	H3	H4	H7	H8	NH
17a	8.68	7.49-7.45	7.93	8.32	7.49-7.45	8.41	6.79
17b	8.75	8.16-8.13	7.95	8.39	8.06	----	6.92
17c	8.70	7.73-7.51	8.05-7.99	8.42	7.74	----	6.97
17d	8.74	7.50	8.01-7.95	8.36	8.01-7.95	----	6.77
17e	8.74	7.50	8.01-7.95	8.36	8.01-7.95	----	6.76
17f	8.70	7.47	7.93	8.30	7.56	----	6.60
17g	8.67	7.50-7.45	7.92	8.36	7.50-7.45	8.44	----
17h	8.70	7.50	7.96	8.40	7.55	----	----
17i	8.74	7.52	7.99	8.45	7.99	----	----
17j	8.67	7.5-7.45	7.93	8.38	7.5-7.45	8.47	----
17k	8.65	7.42	7.87	8.31	7.46	8.44	----
17l	8.67	7.49	7.95	8.33	7.43	8.40	7.24
17m	8.69	7.50	7.97	8.34	7.44	8.41	7.25
17n	8.66	7.46	7.90	8.34	7.44	8.40	7.23
17o	8.66	7.43	7.89-7.92	8.33	7.48-7.51	8.42	7.89-7.92
17p	8.76	7.43	7.87	8.36	7.66	8.48	7.87
17q	8.68	7.48	7.95	8.34	7.44	8.41	7.08

Three members of the 2-amino-4-(2-pyridinyl)pyrimidine series (**17d**, **17f** and **17h**) could additionally be characterized structurally by single crystal X-ray diffraction (Figures 15, 16 and 17, respectively). The asymmetric units of **17d** and **17h** are built up from one molecule but for **17f** it is built up from two independent molecules. There are no hydrogen bonds in the case of **17f** and **17h** but each NH₂ group of **17d** is connected through NH---N hydrogen interactions with the pyrimidine nitrogen atom of a neighboring molecule. In all cases, the nitrogen atoms of the pyridine ring are in the *trans* position with respect to the nitrogen atoms of the pyrimidine rings in order to minimize electronic repulsion between the lone pairs of the nitrogen atoms. In **17h** and **17d**, the pyridine and pyrimidine rings are planar but in the case of **17f** they are twisted along the C(5)-C(6) and C(18)-C(19) bonds resulting in dihedral angles 163.72° and 150.06°, respectively.

Results and Discussion

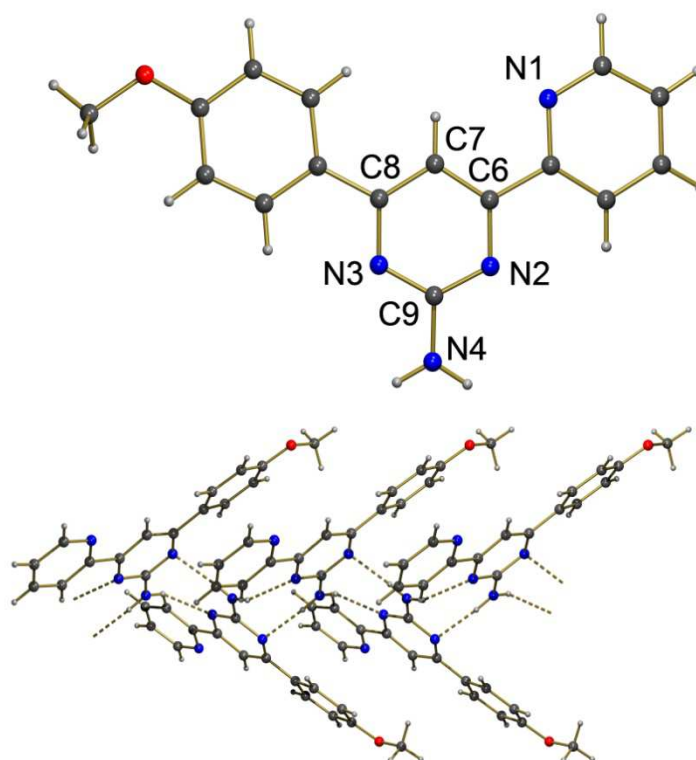


Figure 15. Molecular structure of **17d** in the solid state. Selected bond lengths [\AA] and bond angles [$^\circ$] including hydrogen bonding: N2-C6 1.3482(16), N2-C9 1.3491(16), N3-C8 1.3428(16), N3-C9 1.3474(16), N4-C9 1.3468(17), N4-H4A 0.88, H4A \cdots N 2 2.35, N4 \cdots N2 3.1510(16), N4-H4B 0.8800, H4B \cdots N3 2.1200, N4 \cdots N3 2.9847(15), N4-H4A \cdots N2 152.00, N4-H4B \cdots N3 167.00.

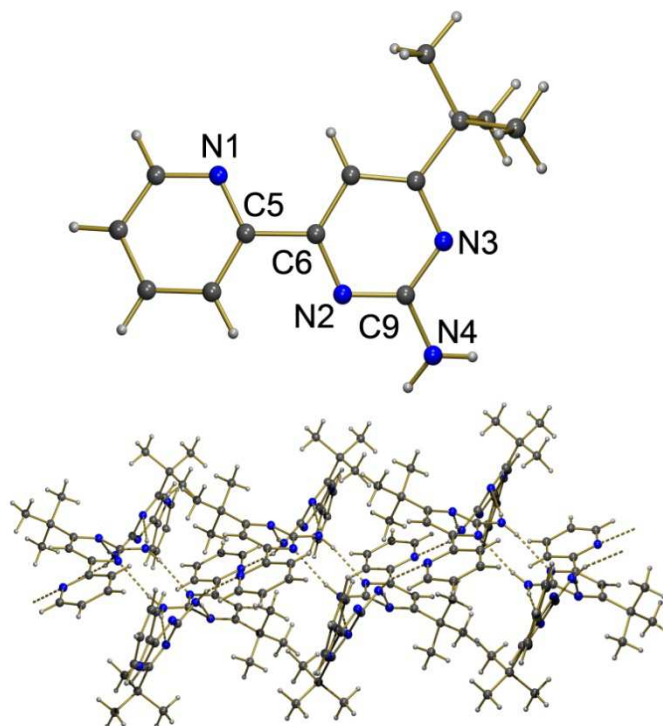


Figure 16. Molecular structure of **17f** in the solid state. Selected bond lengths [\AA], bond angles and dihedral angles [$^\circ$] including hydrogen bonding: N2-C9 1.3474(19), N3-C8 1.3425(19), N3-C9 1.3476(19), N4-C9 1.351(2), N4-H4A 0.875(17), H4A \cdots N7 2.238(17), N4 \cdots N7 3.1043(18), N4-H4B 0.879(17), H4B \cdots N5 2.277(17), N4 \cdots N5 3.1336(19), N8-H8A 0.870(15), H8A \cdots N3 2.360(16), N8 \cdots N3 3.2155(18), N8-H8B 0.882(16), H8B \cdots N6 2.251(17), N8 \cdots N6 3.1245(18), N4-H4A \cdots N7 170.7(16), N4-H4B \cdots N5 164.8(15), N8-H8A \cdots N3 167.9(16), N8-H8B \cdots N6 170.5(15), N1-C5-C6-N2 -163.72(13).

Results and Discussion

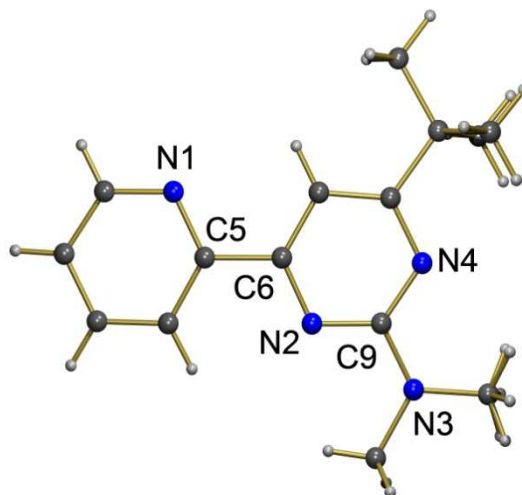


Figure 17. Molecular structure of **17h** in solid state. One of the methyl groups at the NMe₂ moiety is disordered. Selected bond lengths [Å] and dihedral angles [°]: N2-C9 1.346(2), N3-C8 1.336(2), N3-C9 1.351(2), N4-C9 1.361(2), N1-C5-C6-N2 180.00.

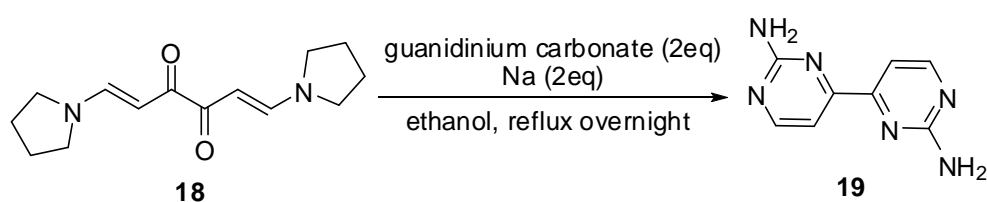
The nitrogen atoms of the amino groups are planar in all cases, and the short C-N distances (1.361(2) Å for **17h**, 1.3511(19) Å for **17f** and 1.3469(16) Å for **17d**) are within the range observed for a carbon-nitrogen double bond and are slightly longer than the other carbon-nitrogen bonds of these compounds (C-N : 1.395 Å and C=N : 1.355 Å).¹¹⁴ This is indicative for C=N *p*-bonding with a delocalization of the nitrogen lone pair into the pyrimidine ring. The carbon-nitrogen bond lengths of **17d**, **17f** and **17h** are listed in Table 5.

Table 5. Bond lengths [Å] for **17d**, **17f** and **17h**.

	17d	17f	17h
C1-N1	1.3369(18)	1.339(2)	1.339(2)
C5-N1	1.3440(16)	1.341(2)	1.340(2)
C9-N2	1.3491(16)	1.3474(19)	1.347(2)
C9-N3	1.3473(17)	1.348(2)	1.350(2)
C9-N4	1.3469(16)	1.3511(19)	1.361(2)

3.1.3 Synthesis of 4,4'-Bipyrimidine-2,2'-diamine

Precursor **18** was synthesized according to a method published in the literature.¹¹⁵ Sodium was added to the ethanol under a nitrogen atmosphere. When the reaction of sodium and ethanol was completed the guanidinium carbonate was added to the solution which was refluxed for 1 h. At the end, precursor **18** was added and the reaction mixture was refluxed overnight. After evaporating the solvent, the product was extracted using dichloromethane. The product was purified by recrystallization from ethanol.



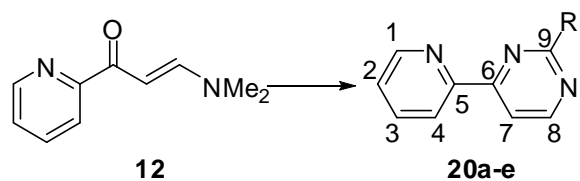
Scheme 35. Synthesis of 4,4'-bipyrimidine-2,2'-diamine.

In the ¹H NMR spectrum two doublets at 8.42 and 7.37 ppm with a coupling constant $J_{\text{HH}} = 5.0$ Hz were assigned to the pyrimidine hydrogen atoms and a singlet at 6.46 ppm was assigned to the hydrogen atoms of the NH₂ group. In ¹³C NMR spectrum four distinguished signals at 163.4, 161.8, 159.1 and 106.0 were observed.

3.1.4 Synthesis of NNC Ligands

The desired ligands **20a-e** were obtained in good yields (Scheme 36) by treating the intermediate **12** with the proper guanidinium nitrates (section 3.1.2.2) in the presence of a NaOEt in refluxing ethanol as described in section 3.1.2.3.

Results and Discussion



20	a	b	c	d	e
R'	NHC ₆ H ₅	<i>p</i> -NHC ₆ H ₄ F	<i>p</i> -NHC ₆ H ₄ Cl	<i>p</i> -NHC ₆ H ₄ OMe	<i>p</i> -NHC ₆ H ₄ CN

Scheme 36. Synthesis of the chelating *N,N,C* ligands.

As shown in Table 6, functionalization of the phenyl ring in the *para* position has almost no effect on the ¹H NMR shifts of the hydrogen atoms in the pyridine ring. However, H7 and H8 have shifted to higher field for **20d** which is functionalized by an electron donating methoxy group and to lower field for **20e** with an electron withdrawing cyanide group. In the same manner, the protons of the amino group appear at 9.56 ppm for **20d** and at 10.34 ppm for **20e**.

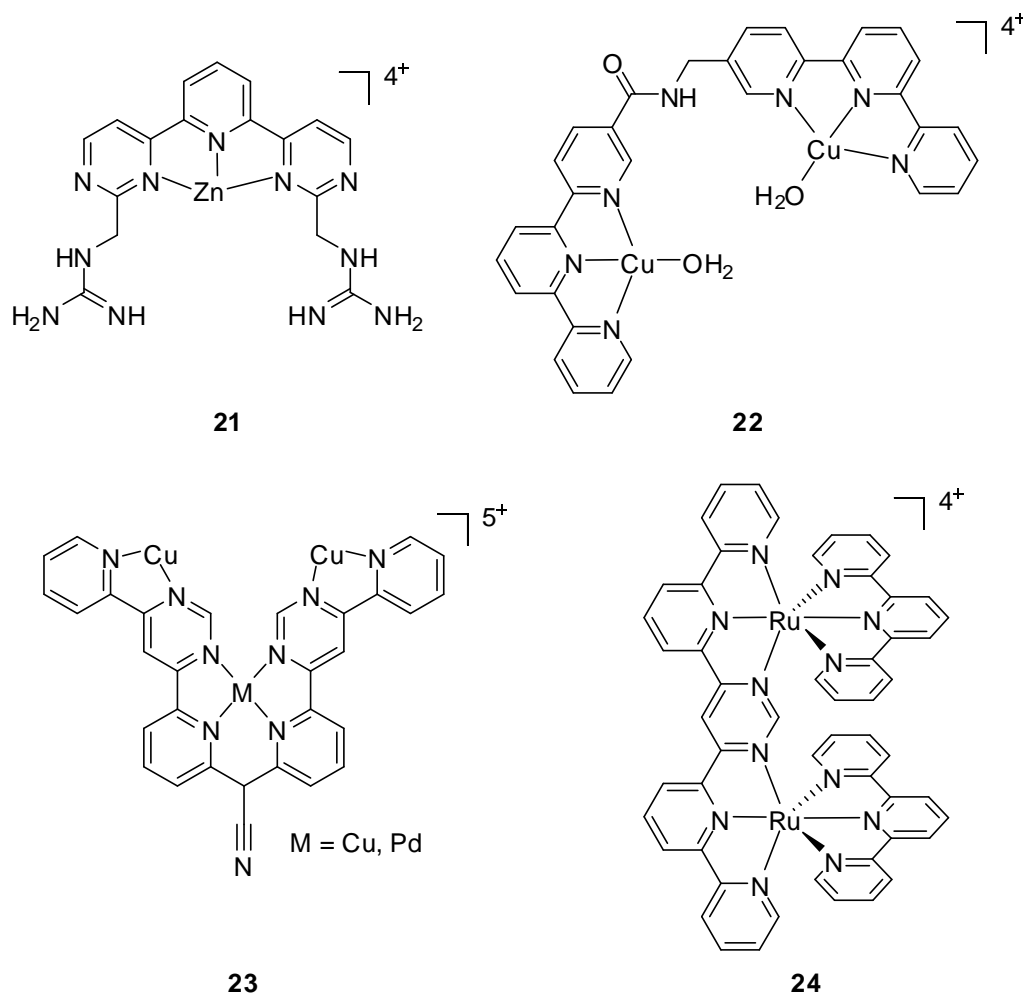
Table 6. ¹H NMR data for ligand **20a-e**.

	NH	H1	H2	H3	H4	H7	H8
20a	9.76	8.75	7.57	8.05	8.41	7.73	8.65
20b	9.79	8.74	7.56	8.03	8.39	7.81	8.63
20c	9.92	8.75	7.57	8.04	8.40	7.75	8.66
20d	9.56	8.74	7.56	8.02	8.38	7.66	8.59
20e	10.34	8.77	7.58	8.06	8.42	7.85	8.74

3.1.5 Synthesis of Multidendate Ligands

The combination of pyridine and pyrimidine can be used for designing helical complexes of multidendate ligands¹¹⁶, but there are just few examples of terpyridine analogue, tridentate ligands and their complexes.¹¹⁷ Anslyn and et al. had synthesized complex **21** (Scheme 37) and used it as a catalyst for RNA hydrolysis.^{118a} It was also applied as a selective molecular sensor for aspartate.^{118b} Another hydrolysis catalyst, which was introduced by

Hamilton et al., is a binuclear copper complex (complex **22**, Scheme 37). It shows high activity and selectivity for the cleavage of cyclic ribonucleosid-2',3'-monophosphate.¹¹⁹ The trinuclear complex **23** is as a model for an allosteric enzyme inhibitor.¹²⁰ There are also some reports on the application of multidentate ligands in supramolecular chemistry. One example of this type is complex **24** (Scheme 37) which was synthesized by Lehn et al.¹²¹



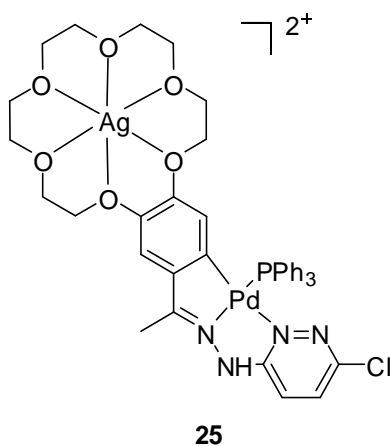
Scheme 37. Examples for complexes with multidentate pyridine/pyrimidine ligands.

Multidentate systems with crown ether units as part of the ligand structure had been attended in the recent years. Mainly alkaline metals or alkaline earth metals can be coordinated in this type of multidentate ligands according to the size of the ring. Beside the ring size, the stability of these complexes depends on the charge of the metal and the solvent which is used.

Results and Discussion

Some ligands of this type and their complexes have been synthesized by Fernández et al.^{122a,b}

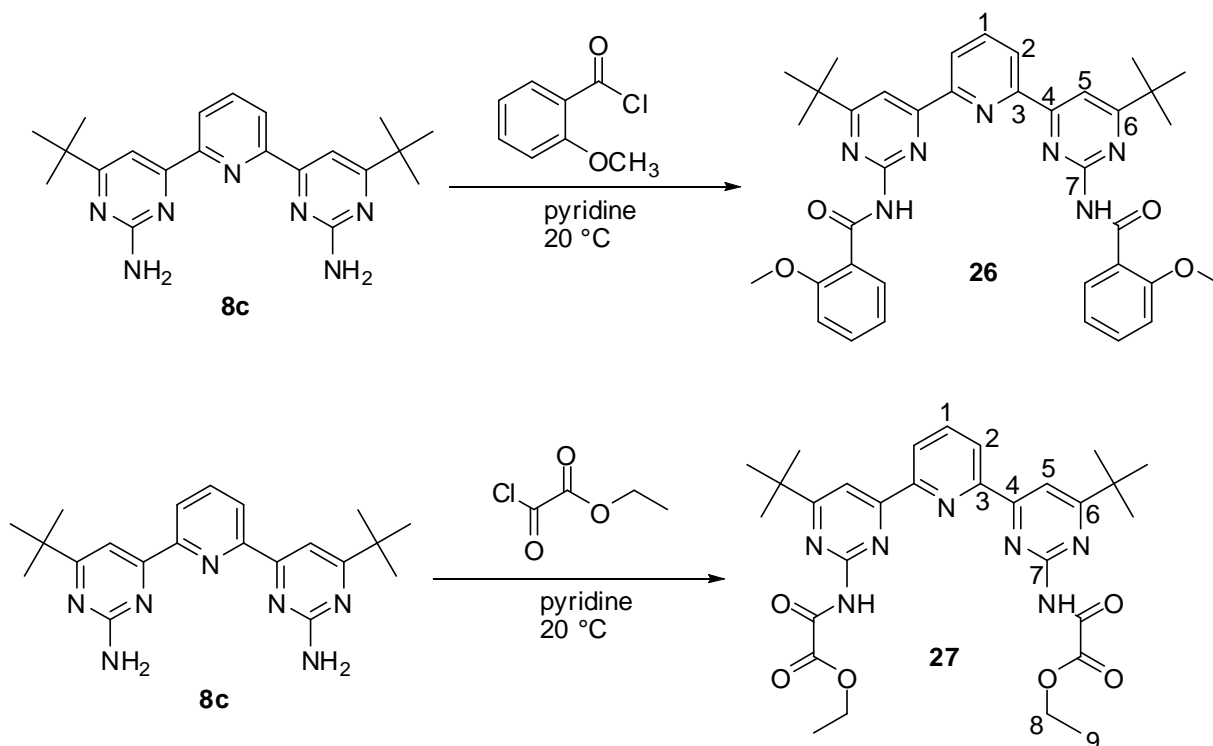
Recently the crystal structure of complex **25** (Scheme 38) was reported by this group.^{122c}



Scheme 38. A bimetallic complex in which a crown ether is a part of ligand.

Till now, multidentate ligands, having pyrimidine groups as relatively soft donors for late transition metals possessing simultaneously a binding position for a hard Lewis-acid, are not known. Such systems are matter of interest in the SFB/TRR-88 (3MET) at the TU Kaiserslautern.

Since the nitrogen atoms of pyrimidine rings are electron withdrawing, the nucleophilicity and the activity of the amino groups of **8c** are decreased, so that amidation reactions have to be done with acylhalides, which were synthesized according to procedures in literature. We here followed a protocol introduced by Reddy¹²³ in which the amine and the acyl halide are stirred at 20 °C in pyridine for 16 h. After distillation of the pyridine the multidentate ligands **26** and **27** can be crystallized from ethanol.



Scheme 39. Synthesis of multidentate ligands starting from diamines.

As expected, the resonance of the amide group in the ^1H NMR spectrum of **26** has shifted to lower field, the resonance appears at about 10.83 ppm. The resonance of the carbonyl group appears at about 165.74 ppm in the ^{13}C NMR spectrum. In IR spectrum the strong absorption at about 1697 cm^{-1} can be assigned to the carbonyl group (Figure 18).

Results and Discussion

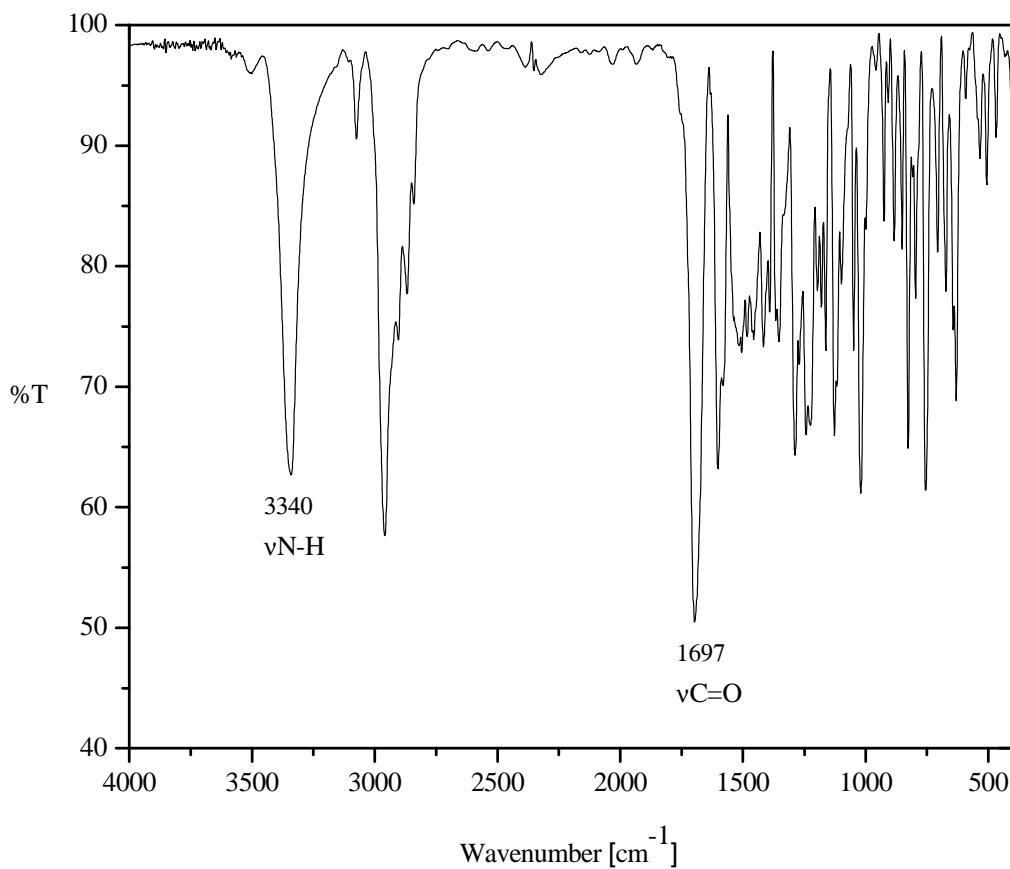


Figure 18. IR spectrum of **26**.

For **27** the resonance of the amide proton in the ¹H NMR spectrum shifted to even much lower field, the resonance appears at about 11.70 ppm (Figure 20). Two resonances at about 160.3 and 158.3 ppm in ¹³C NMR spectrum can be assigned to the two different carbonyl groups in the molecule. In the IR spectrum, three strong absorptions at about 1769, 1744 and 1727 cm⁻¹ can be assigned to the carbonyl moieties (Figure 19).

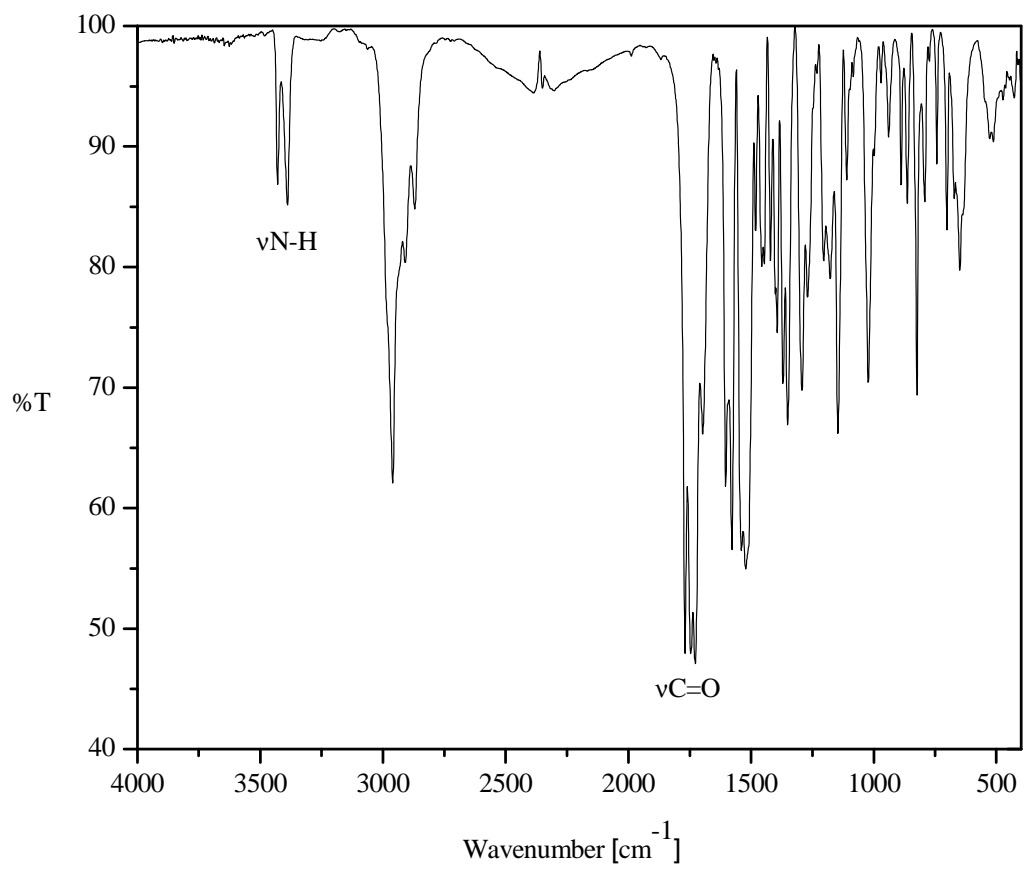


Figure 19. IR spectrum of **27**.

Results and Discussion

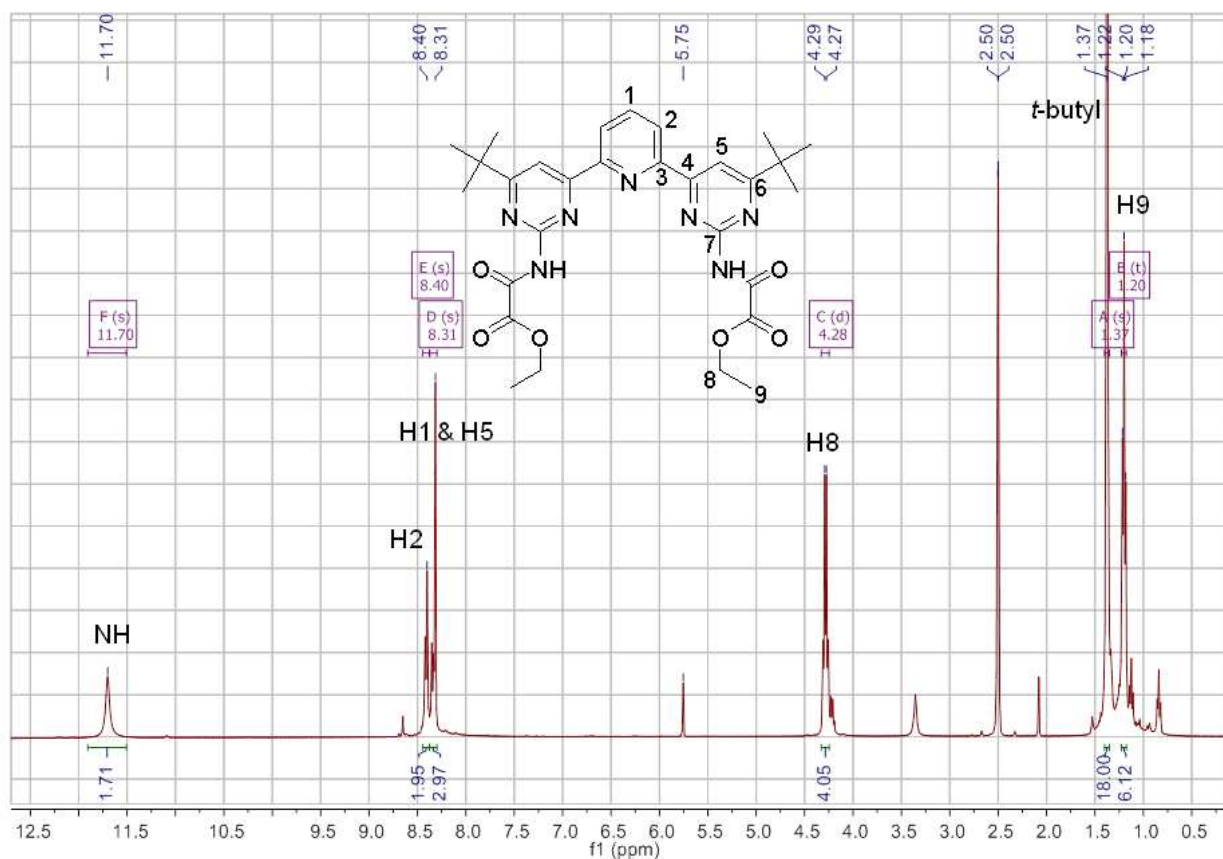
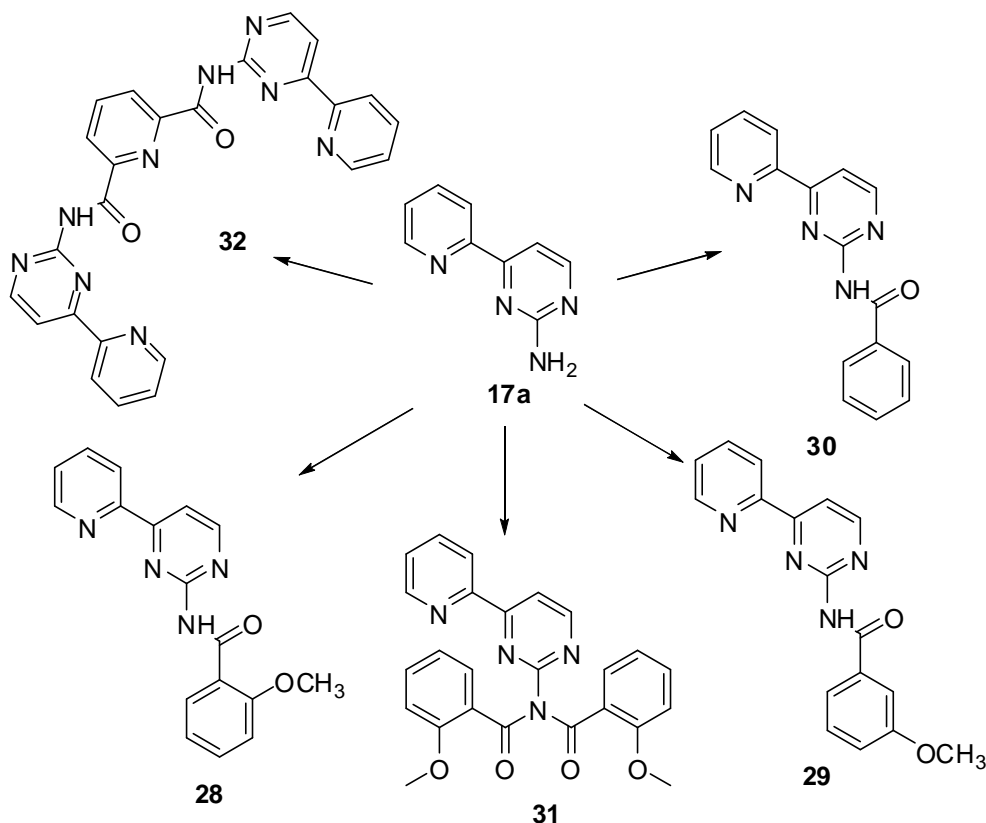


Figure 20. ¹H NMR spectrum of **27**.

Another way to gain multidentate ligands is to start from the mono amine **17a** and a diacyl halide or one or two equivalents of a proper acyl halide as shown in Scheme 40. To synthesize compounds **28**, **29** and **30** the corresponding acid was dissolved in thionylchloride and refluxed. After distillation of the excess of thionylchloride, the residue was dissolved in pyridine, the amine is added and stirred over night at room temperature. Then pyridine was evaporated and the residue was dissolved in dichloromethane, treated with NaHCO₃ and dried over MgSO₄. Evaporating the solvent results in the products. As expected, the ¹H NMR resonance of the hydrogen atom of the amide group shifted to lower field for **28**, **29** and **30** in comparison to the starting amine **17a** (10.85, 11.12 and 11.12 ppm, respectively). As predicted, the carbonyl absorption of **28** (with an electron donating methoxy group in the ortho-position)

appears at a lower energy (about 1658 cm^{-1}) than the corresponding bands of **29** and **30** (1690 and 1699 cm^{-1} , respectively).



Scheme 40. Synthesis of multidentate ligands starting from the monoamine **17a**.

Ligand **31** was synthesized as **28**, just here two equivalents of the corresponding acid were used. In the ^1H NMR spectrum, the peak which was assigned to the NH_2 group has disappeared. Instead, a peak at about 3.72 ppm appears, belonging to the six hydrogen atoms of the two methoxy groups. The two intense bands at about 1725 and 1668 cm^{-1} in the IR spectrum can be assigned to the carbonyl groups.

As mentioned before, reacting a mono amine **17a** and a diacyl halide is another way to obtain multidentate ligands. Ligand **32** was synthesized this way by applying pyridine-2,6-dicarbonyl dichloride being prepared from pyridine-2,6-dicarboxylic acid. In comparison to amine **17a** the proton resonance of amide group of **32** has shifted extremely to lower field (6.79

Results and Discussion

ppm for **17a** vs. 12.06 ppm for **32**). In the same manner the resonances of the other hydrogen and carbon atoms of **32** are shifted a little bit to lower field (8.68, 8.32, 149.41 and 120.75 ppm for **17a** vs. 8.79, 8.57, 149.84 and 121.69 ppm for **32**, respectively). The sharp and strong absorption at about 1723 cm^{-1} in IR spectrum is assigned to the carbonyl bond.

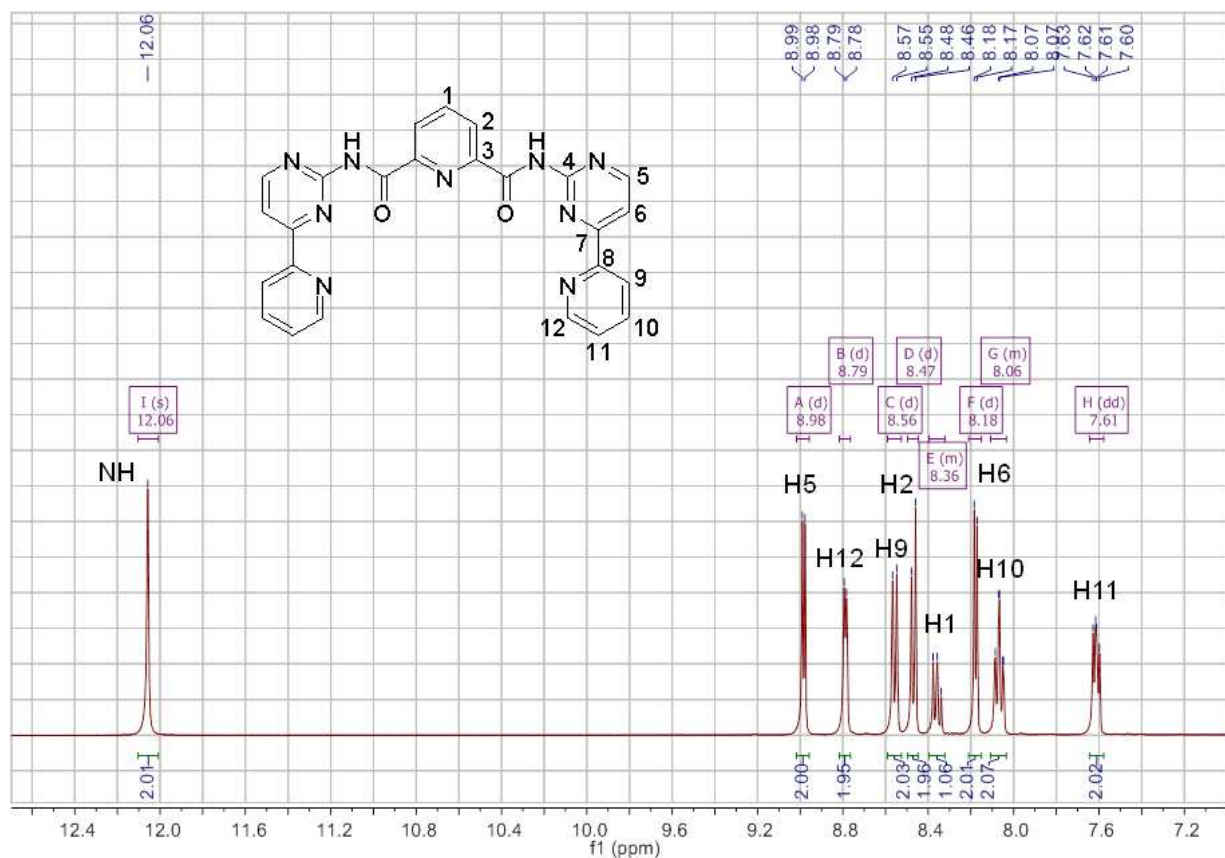


Figure 21. ^1H NMR spectrum of **32**.

3.2 Synthesis of Transition Metal Complexes

The nitrogen containing ligands, which were synthesized before, have been used to obtain ruthenium and palladium complexes.

3.2.1 Ruthenium Complexes

It is well known that catalytic transfer hydrogenation of ketons makes accessible a wide range of alcohols - including chiral ones - which are important in pharmaceutical,

agrochemical, flavor, fragrance, materials, and fine chemical industries.^{4a, 30a-e, 124} Under basic conditions and mainly in *i*PrOH as the solvent, ruthenium(II) complexes turned out to be the most active systems. Thus, a broad variety of different ruthenium complexes bearing *PP*, *NN*, *NO*, *NNN* and *NPN* ligands have been investigated for transfer hydrogenation reactions and provided a considerable improvement on the catalyst performance in the catalytic transfer hydrogenation of ketones.^{3e, 18, 27a, 35b, 47, 125}

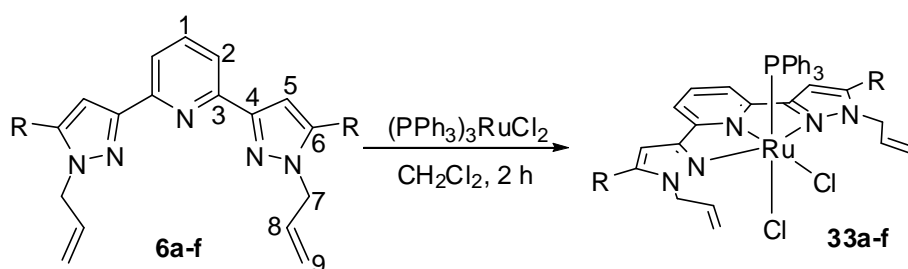
3.2.1.1 Ruthenium Complexes with Tridentate Ligands

Ruthenium complexes containing suitable combinations of *P*- and *N*- or mixed *P,N*-ligands turned out to be efficient catalysts for the hydrogenation and transfer hydrogenation of carbonyl compounds. Thus, some tridentate achiral and chiral ligands have successfully been used for the preparation of these catalysts. A few general types should be mentioned here: (P)(NPN)RuCl₂,¹⁸ (NPN)RuCl₂,¹⁹ (P)(NNN)RuCl₂ (NPN and NNN = oxazoline based ligands),²⁰ [RuCl(CNN)(PP)] [PP = (*R,S*)-1-{2-[bis(4-methoxy-3,5-dimethylphenyl)phosphanyl]ferrocenyl}ethylidicyclohexyl phosphane (Josiphos-type diphosphane) and CNN = amin/aryl/pyridine based ligands).²¹ In this chapter, the synthesis and characterization of ruthenium complexes of the type (L)(*NNN*)RuCl₂ (L = PPh₃ or CO), bearing tridentate dipyrazolpyridines as *N,N,N*-ligands will be discussed.

Treatment of **6a-f** with one equivalent of the ruthenium(II) precursor (PPh₃)₃RuCl₂ in dichloromethane at room temperature leads to the formation of the corresponding red colored ruthenium(II) complexes **33a-f** in almost quantitative yields (Scheme 41). Just **33a,b** could be purified and their structure will be discussed here. Typically for octahedral ruthenium(II) monophosphine complexes, the ³¹P NMR resonances of **33a,b** are observed at 44.20 and 42.71 ppm.¹²⁶ Recently the reaction of the *N,N,N*-ligand **4b**, having a N-H instead of a N-allyl functions, with (PPh₃)₃RuCl₂ was published by Thiel's group.¹²⁷ This variation leads to a cationic ruthenium(II) complex of the type [(PPh₃)₂(**4b**)RuCl]Cl with the two phosphine

Results and Discussion

ligands *trans* to each other (^{31}P NMR: 25.5 ppm). The ionic structure of this compound is stabilized by $\text{H}\cdots\text{Cl}$ interactions between the acidic N-H units at the two pyrazole rings and both, the coordinated chloro ligand and the free chloride counter anion. In contrast to **33a,b** (see catalytic investigations part), $[(\text{PPh}_3)_2(\mathbf{4b})\text{RuCl}]\text{Cl}$ shows just moderate transfer hydrogenation activities, which was assigned to the cationic nature of the active site and to the steric hindrance of the two triphenylphosphine ligands.



Scheme 41. Formation of the ruthenium(II) complexes **33a-f**.

In the ^1H NMR spectra of **33a,b** the resonances of the allylic methylene protons, which become diastereotopic due to the coordination of the ruthenium centre, are now split into two doublets of doublets at 5.80 and 4.76 ppm for **33a** and at 6.20 and 4.21 ppm for **33b**, which requires a *cis*-coordination of the two chloro ligands. Recrystallization of **33a**, **33b** and **33e** from $\text{CH}_2\text{Cl}_2/\text{Et}_2\text{O}$ resulted in the formation of single crystals suitable for X-ray analysis. Selected geometric parameters are presented in Table 7. As already indicated by the NMR spectra, the ruthenium centres are found in a distorted octahedral coordination environment with the tridentate *N,N,N* ligand adopting a meridional geometry and the two chloro ligands in a *cis*-arrangement (Figures 22-24). In contrast to **33b** and **33e** which crystallize with one crystallographically unit, compound **33a** crystallizes with two crystallographically independent

units in the solid state. The structural parameters of these two units are almost identical (see Index), therefore just one of the two units was taken for the discussion of the geometry. In the case of **33b** half of the molecule was severely disordered. Since there are little differences in the structure of these three complexes (Table 7) solely the structure of **33a** will be discussed in details in the following.

Table 7. Selected geometric parameters. The numbering is according to figures 22-24.

	33a	33e	33b
<i>Distances (Å)</i>			
N(1)-Ru(1)	1.985(3)	1.985(4)	1.974(4)
N(2)-Ru(1)	2.081(2)	2.081(4)	2.080(3)
N(4)-Ru(1)	2.093(3)	2.092(4)	2.074(12)-2.100(9)
P(1)-Ru(1)	2.2800(8)	2.2933(13)	2.2883(10)
Cl(1)-Ru(1)	2.4576(8)	2.4706(12)	2.4651(10)
Cl(2)-Ru(1)	2.4664(8)	2.4670(12)	2.4587(11)
<i>Angles (°)</i>			
N(1)-Ru(1)-N(2)	77.35(10)	78.10(16)	77.82(14)
N(1)-Ru(1)-N(4)	78.07(10)	77.67(17)	85.3(3)-71.7(3)
N(2)-Ru(1)-N(4)	154.24(10)	155.16(17)	162.4(4)-149.1(3)
N(1)-Ru(1)-P(1)	94.37(7)	91.42(12)	92.52(10)
N(2)-Ru(1)-P(1)	96.08(7)	91.47(12)	94.59(9)
N(4)-Ru(1)-P(1)	93.34(7)	94.52(12)	91.1(8)-91.7(5)
N(1)-Ru(1)-Cl(1)	90.40(7)	88.21(12)	89.28(10)
N(2)-Ru(1)-Cl(1)	83.59(7)	86.59(12)	87.09(9)
N(4)-Ru(1)-Cl(1)	89.00(7)	87.26(12)	87.7(8)-87.6(5)
P(1)-Ru(1)-Cl(1)	175.03(3)	178.06(5)	177.76(4)
N(1)-Ru(1)-Cl(2)	178.65(7)	177.95(12)	178.34(10)
N(2)-Ru(1)-Cl(2)	103.78(7)	101.52(12)	102.06(8)
N(4)-Ru(1)-Cl(2)	100.71(8)	102.50(12)	94.6(3)-108.2(3)
P(1)-Ru(1)-Cl(2)	86.27(3)	90.61(4)	89.14(4)
Cl(1)-Ru(1)-Cl(2)	88.99(3)	89.75(4)	89.06(4)

Results and Discussion

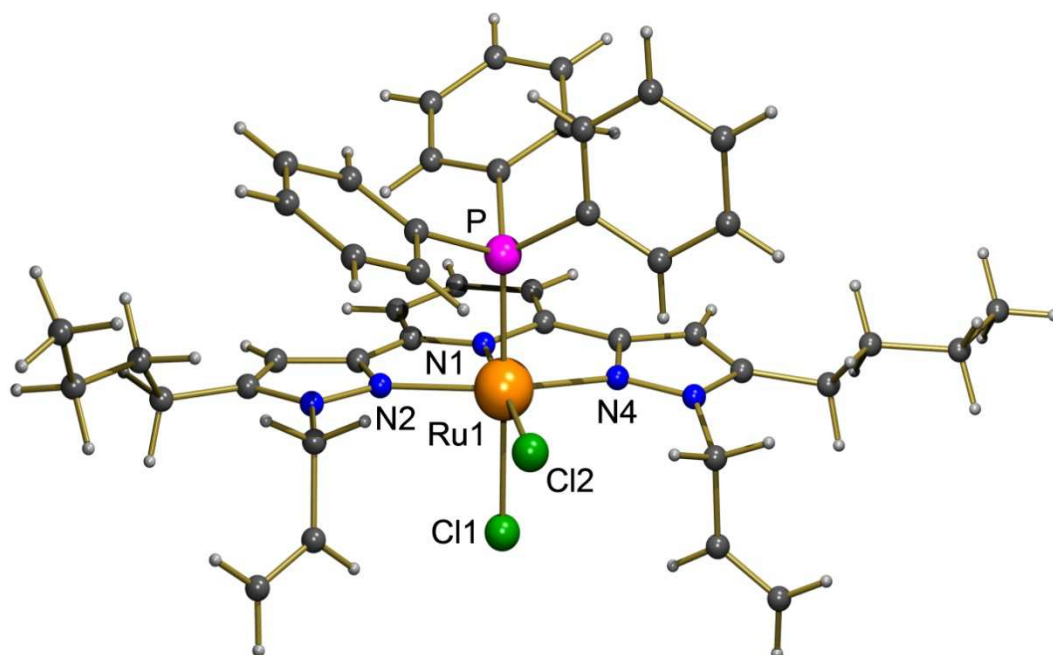


Figure 22. Molecular structure of the ruthenium(II) complex **33b** in the solid state. The disordering of one of the butyl side chains is omitted for clarity.

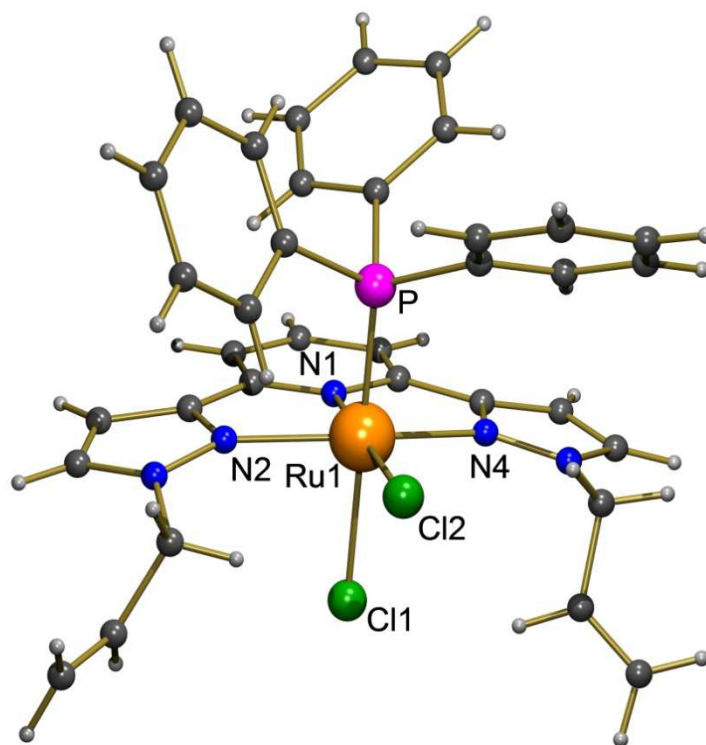


Figure 23. Molecular structure of ruthenium complex **33a** in solid state.

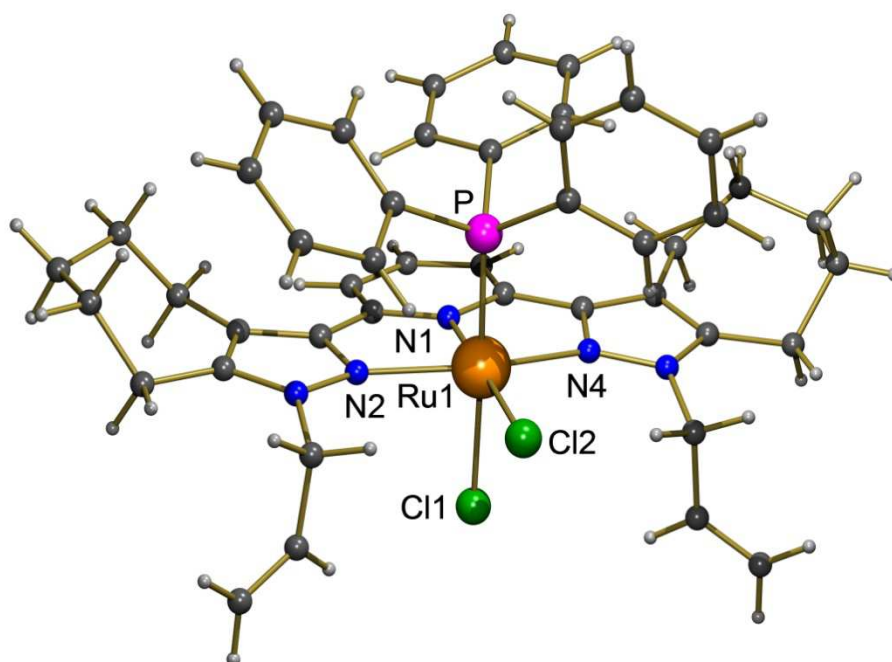
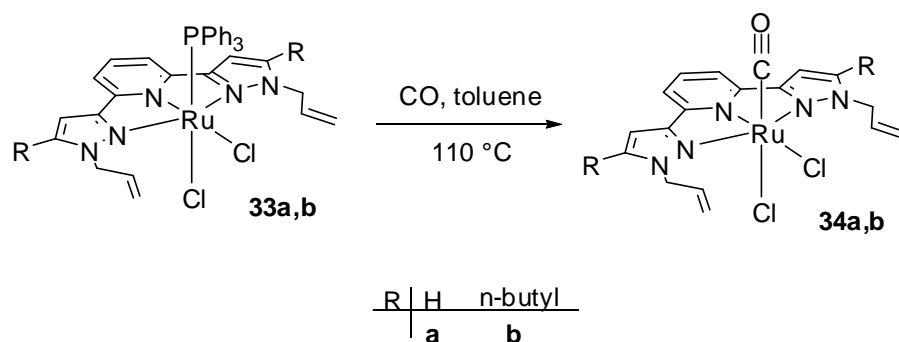


Figure 24. Molecular structure of ruthenium complex **33e** in solid state. The two solvent molecules in the unit cell are omitted for clarity.

Results and Discussion

Since pyridines are generally considered to be better donors than pyrazoles, the large Ru-N bond length difference of about 10 pm can just be explained by the steric requirements of the tridentate ligand.^{127,128} Bidentate pyrazolylpyridine complexes show less pronounced differences in the M-N bond lengths.^{94,127,129} Due to the tridentate coordination of the *N,N,N*-donor, the central nitrogen atom N1 is pushed closer to the ruthenium(II) centre. It therefore applies a *trans*-influence to Cl2 comparable to the *trans*-influence of the phosphine donor to Cl1, which explains the almost identical Ru-Cl bond lengths found in this solid state structure. All P-Ru-N angles are larger than 90° showing the steric influence of the bulky triphenylphosphine onto the chelating ligand.



Scheme 42. Formation of **34a,b** by bubbling CO gas through a solution of **33a** and **33b**.

Bubbling CO into a solution of **33a,b** in refluxing toluene results in the formation of the carbonyl complexes **34a,b** in quantitative yields (Scheme 42), a colour change from red to yellow indicates the end of the reaction. The ³¹P NMR signals of the triphenylphosphine ligands have disappeared proving that the phosphine is substituted by CO which is in contrast to previous findings (Figure 25).¹²⁷ The ¹H NMR spectra of **34a** and **34b** recorded in DMSO-*d*₆ again show two diastereotopic methylene protons (**4a**: 6.12, 5.20; **4b**: 5.55, 5.03 ppm), which means that the chloride ligands are still *cis*-coordinated. In the ¹³C NMR spectrum, the

resonances of the carbonyl ligand are observed at 191.0 ppm for **34a** and at 191.2 ppm for **34b**. Intense CO absorptions in the infrared spectrum at 1936 cm^{-1} for **34a** and at 1948 cm^{-1} for **34b** confirm the attachment of one carbonyl ligand to the ruthenium centre. The slight difference of 12 cm^{-1} can be explained by the steric influence of the bulky butyl chain attached to compound **34b**, which increases the Ru-CO distance, decreases the back donation to the carbonyl ligand and therefore strengthens the C=O bond.

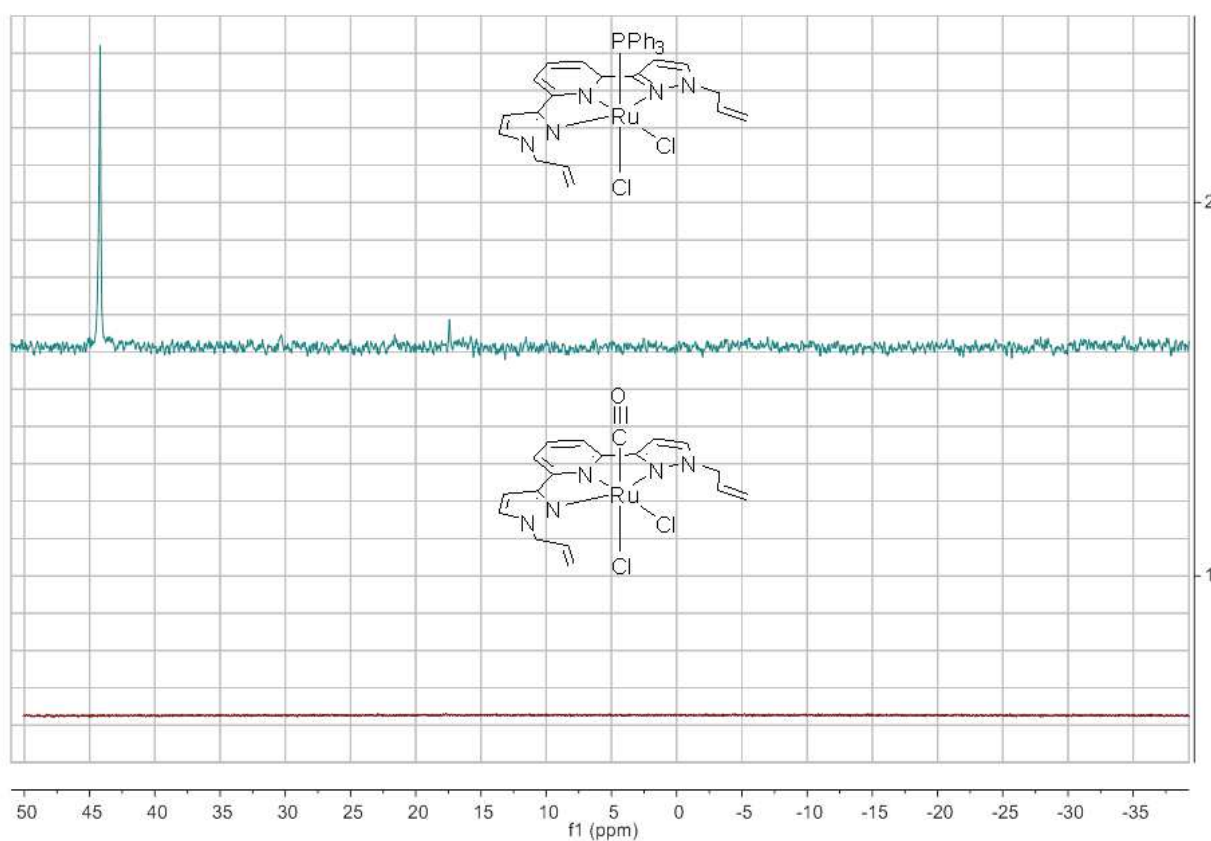


Figure 25. ^{31}P NMR spectrum of **33a** (top) and **34a** (bottom).

Results and Discussion

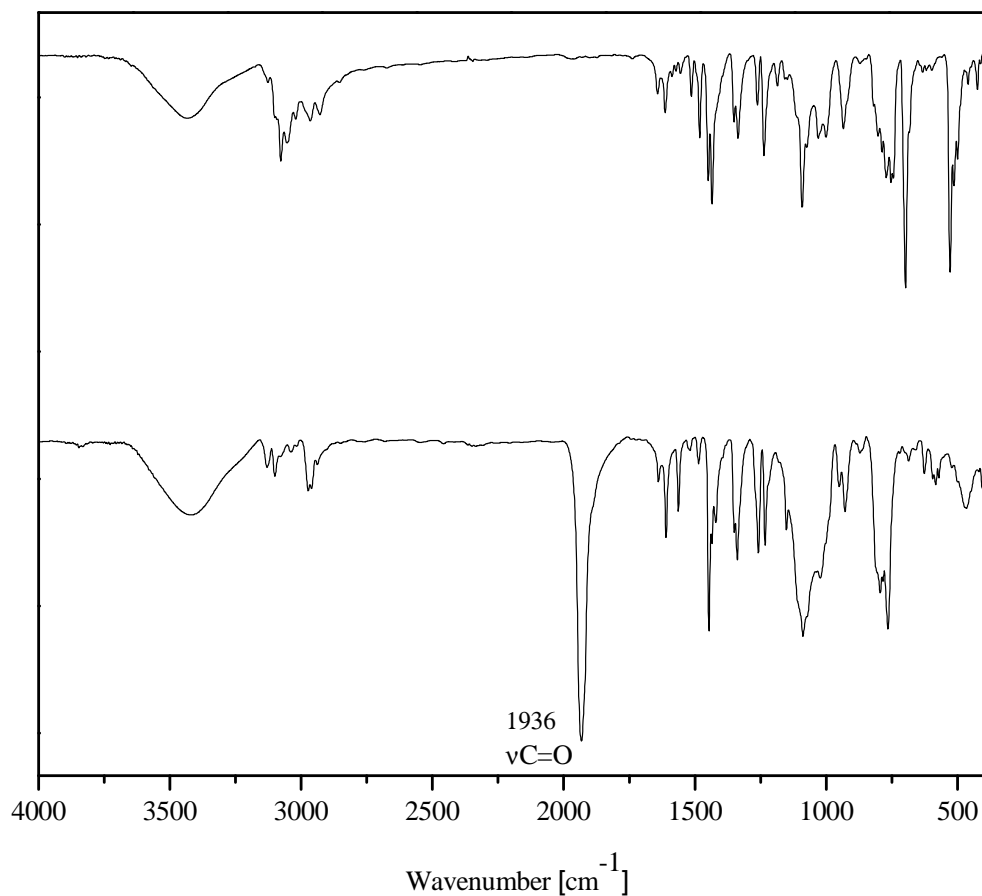
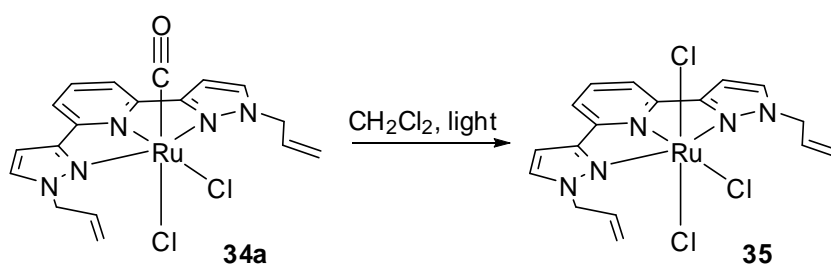


Figure 26. IR spectra of ruthenium complex **33a** (top) and **34a** (bottom)

Attempts to obtain single crystals of **34a** suitable for X-ray structure determination by crystallization from dichloromethane over a long period of time and in the presence of light resulted in oxidation to ruthenium(III) and replacement of the carbonyl against a chloride ligand (Scheme 43, Figure 27).



Scheme 43. Chlorination of the carbonyl complex **34a**.

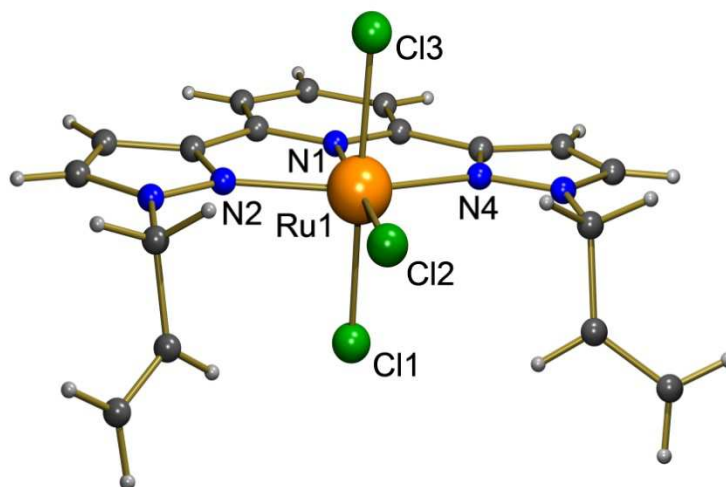


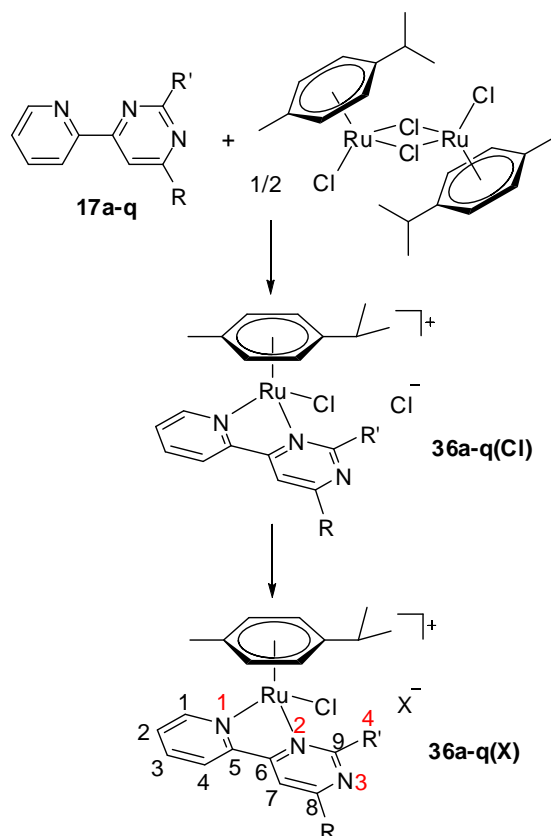
Figure 27. Molecular structure of complex **35** in solid state, characteristic bond lengths [\AA], angles [deg], the co-crystallized dichloromethane molecule is omitted for clarity: Ru1-Cl1 2.4159(18), Ru1-Cl2 2.405(5), Ru1-Cl3 2.358(2), Ru1-N1 2.039(5), Ru1-N2 2.089(5), Ru1-N4 2.043(5), Cl1-Ru1-Cl2 93.88(11), Cl1-Ru1-Cl3 177.59(6), Cl1-Ru1-N1 87.82(15), Cl1-Ru1-N2 89.66(15), Cl1-Ru1-N4 89.56(16), Cl2-Ru1-Cl3 87.79(12), Cl2-Ru1-N1 177.92(18), Cl2-Ru1-N2 101.86(18), Cl2-Ru1-N4 104.24(18), Cl3-Ru1-N1 90.55(16), Cl3-Ru1-N2 91.70(15), Cl3-Ru1-N4 88.34(16), N1-Ru1-N2 76.9(2), N1-Ru1-N4 77.0(2), N2-Ru1-N4 153.9(2).

As in **33a**, the ruthenium centre in **35** is again coordinated in a distorted octahedral geometry with the tridentate *N,N,N*-donor adopting a *mer*-arrangement. The Ru-N on one side and the Ru-Cl distances on the other side are almost identical, slight differences are related to packing effects in the solid state structure. The bond angles Cl3-Ru-N are approaching 90° , corroborating the discussion of the steric influence of the triphenylphosphine ligand on the structure of **33a**.

Results and Discussion

3.2.1.2 Ruthenium Complexes with Bidendate Ligands

Reacting the ligands **17a-q** with the ruthenium(II) precursor $[(\eta^6\text{-cymene})\text{Ru}(\text{Cl})(\mu^2\text{-Cl})_2]$ at room temperature in dichloromethane solution gave red to brown coloured cationic ruthenium(II) complexes of the type $[(\eta^6\text{-cymene})\text{Ru}(\text{Cl})(\text{pdpm})]\text{Cl}$ (**36a-q(Cl)**; pdpm = chelating 2-amino-4-(2-pyridinyl)pyrimidine ligand) in almost quantitative yields (Scheme 44). For catalyst optimization, the chloride anion was exchanged against three larger and thus weaker coordinating anions (BF_4^- , PF_6^- , BPh_4^-) for a part of the ruthenium complexes, which additionally enforced the crystallization of the compounds. Stirring the freshly prepared complexes **36a-q(Cl)** with either NaBPh_4 , NaBF_4 or KPF_6 directly led to the ruthenium(II) complexes **36a-q(X)**.



36	a	b	c	d	e	f
R	H	C ₆ H ₅	1-naphthyl	C ₆ H ₄ OMe	C ₆ H ₄ O ⁿ Bu	^t Bu
R'	NH ₂	NH ₂	NH ₂	NH ₂	NH ₂	NH ₂

36	g	h	i	j	k
R	H	^t Bu	C ₆ H ₄ OMe	H	H
R'	N(CH ₂) ₄	NMe ₂	N(CH ₂) ₄	NMe ₂	N(CH ₂) ₅

X⁻ = BPh₄⁻, BF₄⁻, PF₆⁻

36	l	m	n	o	p	q
R	H	H	H	H	H	H
R'	HN(CH ₂) ₂ CH ₃	HN(CH ₂) ₃ CH ₃	HN(CH ₂) ₇ CH ₃	S-HN(CH)(CH ₃)(C ₆ H ₅)	R-HN(CH)(CH ₃)(C ₆ H ₅)	HN(CH)(CH ₃) ₂

Scheme 44. Synthesis of the ruthenium(II) complexes **36a-q(X)**.

Due to the two different *N*-donor moieties, the metal site becomes a centre of chirality leading to two diastereotopic methyl groups and four magnetically inequivalent aromatic C-H sites at the cymene ligand. This is clearly demonstrated by the ¹H and ¹³C NMR spectra of the ruthenium complexes. The methyl groups of cymene ring appear as two doublets at about 0.8 and 0.9 ppm and four peaks between 82 and 86 ppm can be assigned to the four magnetically

Results and Discussion

inequivalent aromatic carbon atoms of cymene ring. Coordination of the 2-amino-4-(2-pyridinyl)pyrimidines to the Lewis-acidic ruthenium(II) centre causes a shift of the H1 resonance to lower field (for the numbering see Scheme 44): ca. 9.50 ppm for ligands with R = NH₂, ca. 9.48 ppm for ligands with R = NH(alkyl), ca. 9.32 ppm for R = NMe₂ and ca. 9.24 ppm for R = N(CH₂)₄. Obviously, by functionalizing the amino group with more electron donating groups, the resonance of H1 in the complex shifts to higher field. This is a quite pronounced influence of a substituent located far at the other side of the ligand and an indirect hint for the electronic situation at the ruthenium(II) centre, which should become more electron rich in the series R = NH₂ < NHAlkyl < NMe₂ < N(CH₂)₄. The resonances of protons H2 (ca. 7.83 ppm) and H3 (ca. 8.24 ppm) are almost independent from the substituent at the pyrimidine ring, while H4 shows a similar but less pronounced behavior as H1. Protons H7 at the pyrimidine moiety are sensitive to the presence (ca. 8.21-8.39 ppm) or absence (ca. 7.69-7.86 ppm) of aromatic substituents in the 8-position and the shift of protons H8 is almost independent from the amine substituent.

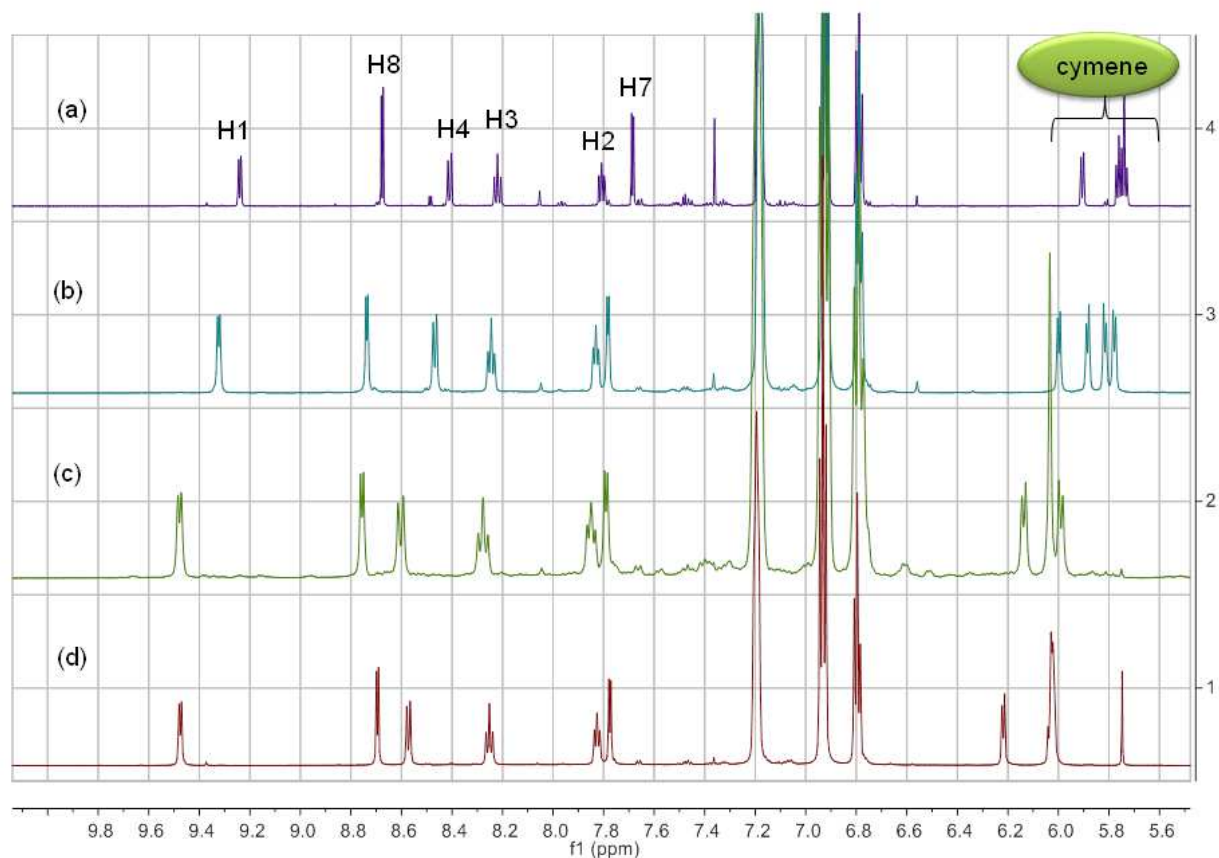


Figure 28. ^1H NMR spectra of (a) **36i**, (b) **36j**, (c) **36n** and (d) **36a**.

In the ^{13}C NMR spectra, nine carbon resonances for the nine carbon atoms of the cymene ligand can be assigned, proving the presence of a centre of chirality in the molecule. Generally the ^{13}C NMR shifts are less sensitive towards the substitution pattern of the 2-amino-4-(2-pyridinyl)pyrimidine system than the ^1H NMR shifts. Solely C7 of complex **36c**(BPh_4) is shifted about 10 ppm towards lower field with respect to the other compounds. This is probably due to a deshielding effect of the naphthyl substituent.

For complexes **36a**(PF_6), **36b**(BPh_4), **36f**(BPh_4), **36h**(BPh_4), **36j**(BPh_4), **36k**(BPh_4) and **36l**(BPh_4) single crystals suitable for X-ray diffraction studies were obtained, and their molecular structures in the solid state are presented in Figures 29-36. All the cationic complexes show a typical piano-stool geometry with Ru(II) centers adopting a distorted

Results and Discussion

octahedral arrangement and being coordinated by a chelating 2-amino-4-(2-pyridinyl)pyrimidine type ligand, an η^6 -cymene ring and a terminal chloride, Table 8. Although the Ru(II) centers are stereogenic, all complexes are obtained as a racemic mixture and crystallized in centrosymmetric space groups (Table 9).

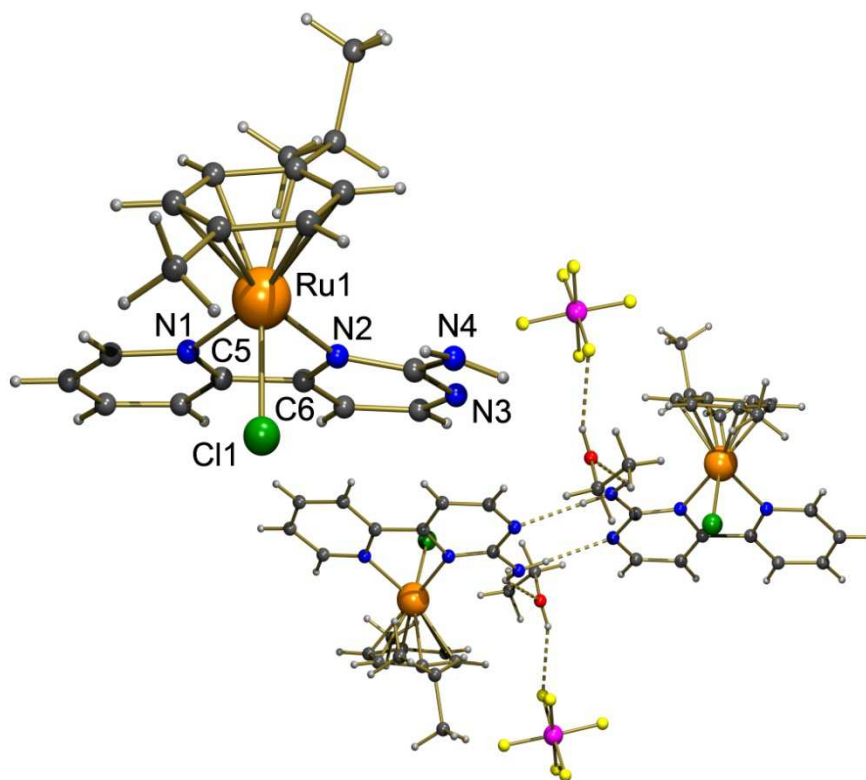


Figure 29. Molecular structure of complex **36a(PF₆)** in solid state at 50 % probability level; top: the cation **36a⁺**, bottom: hydrogen bonds between the NH₂ moiety, the co-crystallized ethanol and the PF₆⁻ anion.

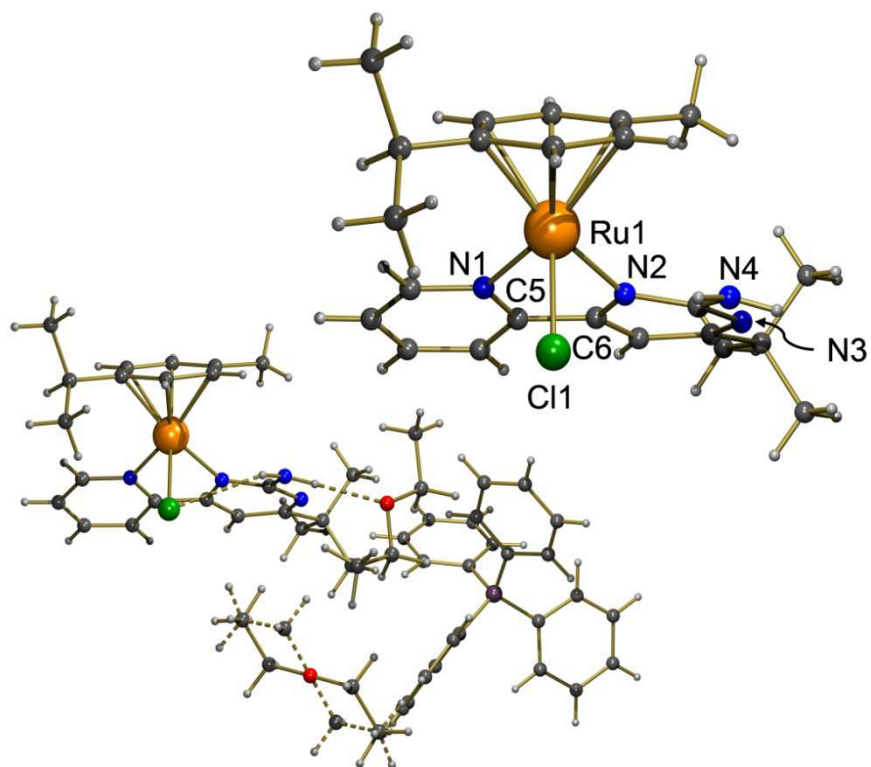


Figure 30. Molecular structure of complex **36f(BPh₄)** in solid state at 50 % probability level; top: the cation **36f⁺**, bottom: hydrogen bonds between the NH₂ moiety, the co-crystallized ethanol.

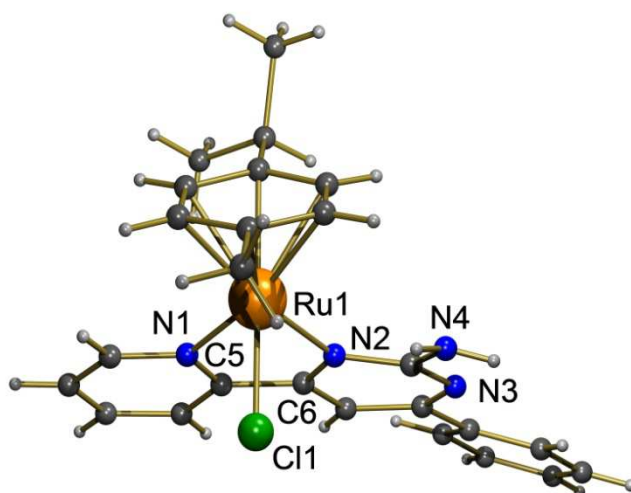


Figure 31. Molecular structure of complex **36b(BPh₄)** in solid state at 50 % probability level with the counter anion and co-crystallized solvents being omitted for clarity.

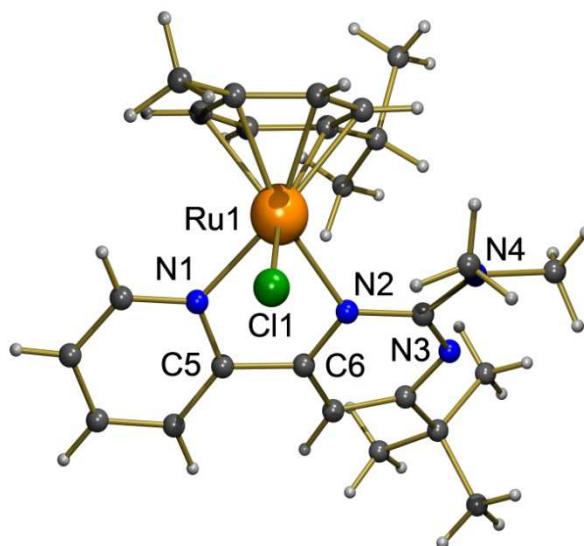


Figure 32. Molecular structure of complex **36h(BPh₄)** in solid state at 50 % probability level with the counter anion and co-crystallized solvents being omitted for clarity.

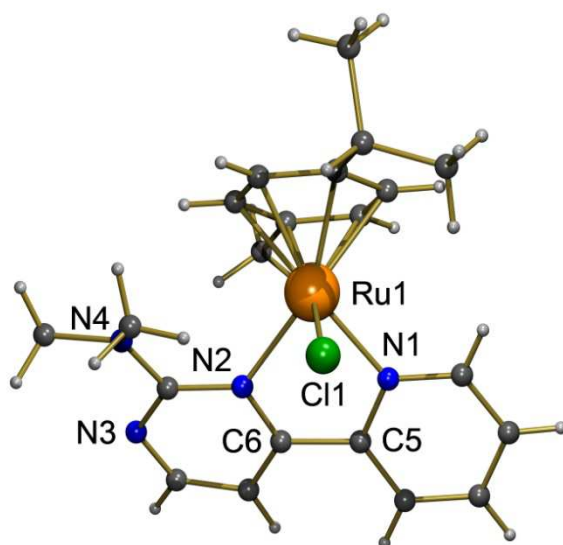


Figure 33. Molecular structure of complex **36j(BPh₄)** in solid state at 50 % probability level with the counter anions and co-crystallized solvents being omitted for clarity.

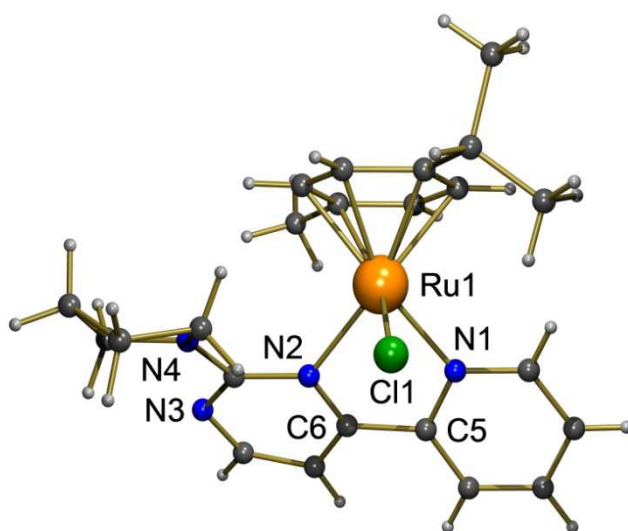


Figure 34. Molecular structure of complex **36g(BPh₄)** in solid state at 50 % probability level with the counter anion and co-crystallized solvents being omitted for clarity.

Results and Discussion

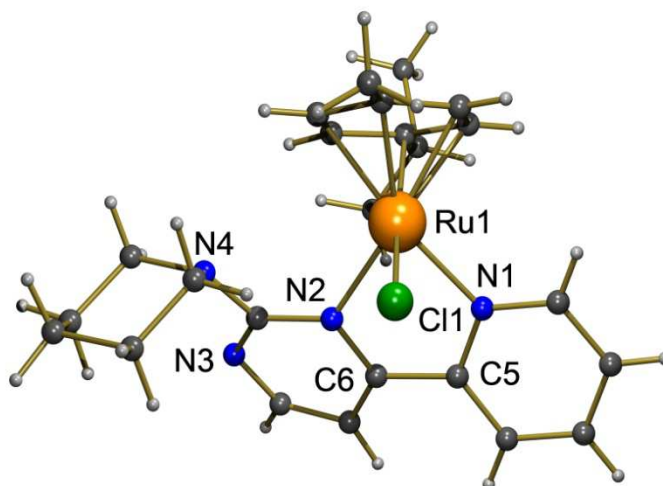


Figure 35. Molecular structure of complex **36k(BPh₄)** in solid state at 50 % probability level with the counter anion and co-crystallized solvents being omitted for clarity.

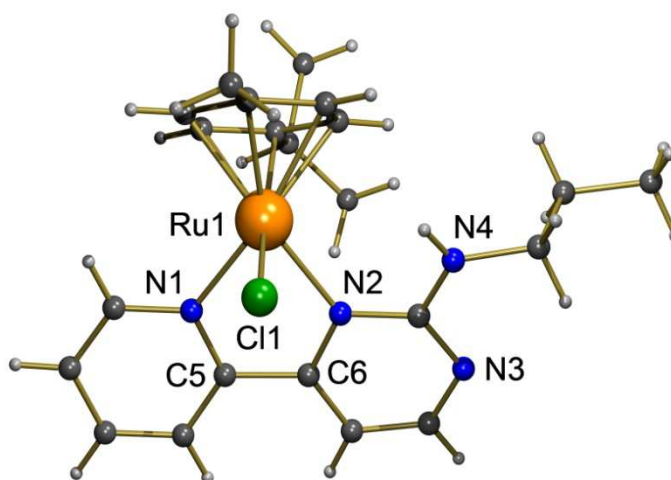


Figure 36. Molecular structure of complex **36l(BPh₄)** in solid state at 50 % probability level with the counter anion and co-crystallized solvents being omitted for clarity.

Table 8. Selected geometric parameters of the cymene ruthenium complexes. The numbering is according to Scheme 44.

	36a(PF₆)	36b(BPh₄)	36f(BPh₄)	36j(BPh₄)	36h(BPh₄)	36k(BPh₄)	36l(BPh₄)
R	H	Ph	<i>t-butyl</i>	H	<i>t-butyl</i>	H	H
R'	NH ₂	NH ₂	NH ₂	NMe ₂	NMe ₂	N(CH ₂) ₄	NH(CH ₂) ₂ CH ₃
<i>distances (Å)</i>							
Ru1-N1	2.0819(19)	2.0845(13)	2.0875(15)	2.0745(15)	2.084(2)	2.0800(17)	2.080(2)
Ru1-N2	2.1200(17)	2.1080(13)	2.0992(15)	2.1446(15)	2.1509(19)	2.1379(16)	2.108(2)
Ru1-cymene ^a	1.6886(9)	-1.6892(7)	-1.6815(7)	1.6747(8)	-1.6913(11)	1.6774(9)	1.6883(11)
Ru1-C11	2.3953(5)	2.3992(4)	2.4028(5)	2.4034(5)	2.4189(7)	2.3891(5)	2.3839(7)
<i>angles (°)</i>							
N1-Ru1-N2	76.55(7)	76.21(5)	76.12(6)	77.84(5)	77.16(8)	77.78(6)	76.57(8)
N1-Ru1-C11	87.61(5)	87.49(4)	89.48(4)	82.56(4)	81.97(6)	81.75(5)	85.88(6)
N2-Ru1-C11	85.49(5)	87.09(4)	84.12(4)	90.30(4)	91.02(5)	87.84(5)	84.50(6)
<i>torsion angle (°)</i>							
N1-C5-C6-N2	0.7(3)	2.72(19)	7.2(2)	-11.0(2)	14.3(3)	14.7(3)	3.4(3)

a. The distance between Ru1 and the mean plane of cymene.

Results and Discussion

Table 9. Summary of the crystallographic data and details of data collection and refinement for compounds **36a**(PF₆), **36b**(BPh₄), **36f**(BPh₄), **36h**(BPh₄), **36j**(BPh₄), **36k**(BPh₄) and **36l**(BPh₄).

	36a (PF ₆)	36b (BPh ₄)	36f (BPh ₄)	36j (BPh ₄)	36h (BPh ₄)	36k (BPh ₄)	36l (BPh ₄)
empirical formula	C ₂₁ H ₂₈ ClF ₆ N ₄ OPRu	C ₄₉ H ₄₆ BClN ₄ Ru	C ₅₃ H ₆₅ BClN ₄ O _{1.5} Ru	C ₄₅ H ₄₆ BClN ₄ Ru	C ₄₉ H ₅₄ BClN ₄ Ru	C ₄₈ H ₅₀ BClN ₄ Ru	C ₄₇ H ₅₀ BCl ₃ N ₄ Ru
formula weight	633.96	838.23	929.42	790.19	846.29	830.25	889.14
crystal size [mm]	0.28x0.21x0.18	0.20x0.13x0.08	0.40x0.17x0.13	0.18x0.12x0.11	0.25x0.09x0.05	0.18 x 0.07 x 0.03	0.16 x 0.08 x 0.06
<i>T</i> [K]	150(2)	150(2)	150(2)	150(2)	150(2)	150(2)	150(2)
λ [Å]	1.54184	1.54184	1.54184	1.54184	1.54184	1.54184	1.54184
crystal system	monoclinic	monoclinic	monoclinic	monoclinic	monoclinic	monoclinic	monoclinic
space group	P2 ₁ /c	P2 ₁ /c	P2 ₁ /c	P2 ₁ /n	P2 ₁ /c	P2 ₁ /c	P2 ₁ /c
<i>a</i> [Å]	10.3751(1)	13.5219(1)	15.2326(1)	13.0910(2)	14.6567(3)	12.2710(1)	12.89110(10)
<i>b</i> [Å]	15.0288(2)	21.5269(2)	13.8012(1)	11.8941(1)	9.6078(2)	14.9669(1)	14.90500(10)
<i>c</i> [Å]	16.0810(2)	14.0468(1)	24.5075(2)	25.6986(3)	33.5405(6)	22.3485(2)	22.7354(2)
α [°]	90	90	90	90	90	90	90
β [°]	102.954(1)	90.424(1)	107.188(1)	95.960(1)	100.226(2)	95.163(1)	98.3670(10)
γ [°]	90	90	90	90	90	90	90
<i>V</i> [Å ³]	2442.77(5)	4088.70(6)	4922.07(6)	3979.79(8)	4648.10(16)	4087.85(6)	4321.93(6)
<i>Z</i>	4	4	4	4	4	4	4
$\rho_{\text{calcd.}}$ [g cm ⁻³]	1.724	1.362	1.254	1.319	1.209	1.349	1.366
μ [mm ⁻¹]	7.452	4.002	3.392	4.076	3.521	3.994	4.925
θ -range [°]	4.08-62.64	3.76-62.64	3.04-62.65	3.46-62.74	3.06-62.63	3.56-62.65	3.47-62.67
refl. coll.	17462	31505	40936	31463	24700	32737	33782
indep. refl.	3903	6538	7866	6363	7402	6515	6916
	[R _{int} = 0.0274]	[R _{int} = 0.0241]	[R _{int} = 0.0225]	[R _{int} = 0.0237]	[R _{int} = 0.0367]	[R _{int} = 0.0336]	[R _{int} = 0.0299]
data/restr./param.	3903/2/327	6538/2/514	7866/40/580	6363/0/474	7402/0/513	6515/0/499	6916/1/512
final <i>R</i> indices [<i>I</i> > 2 σ (<i>I</i>)] ^a	0.0230, 0.0589	0.0200, 0.0529	0.0244, 0.0647	0.0218, 0.0562	0.0310, 0.0771	0.0245, 0.0652	0.0292, 0.0796
<i>R</i> indices (all)	0.0245, 0.0596	0.0225, 0.0535	0.0264, 0.0655	0.0240, 0.0570	0.0390, 0.0797	0.0293, 0.0665	0.0346, 0.0815

data) ^b							
$GooF^c$	1.079	1.034	1.042	1.041	0.946	1.045	1.045
$\Delta\rho_{\max/\min} (e \cdot \text{\AA}^{-3})$	0.319/-0.618	0.227/-0.360	0.414/-0.335	0.292/-0.597	0.402/-0.581	0.536/-0.388	0.679/-0.944
^a $RI = \Sigma F_o - F_c / \Sigma F_o $. ^b $\omega R2 = [\Sigma\omega(F_o^2 - F_c^2)^2 / \Sigma\omega F_o^2]^{1/2}$. ^c $GooF = [\Sigma\omega (F_o^2 - F_c^2)^2 / (n-p)]^{1/2}$							

Results and Discussion

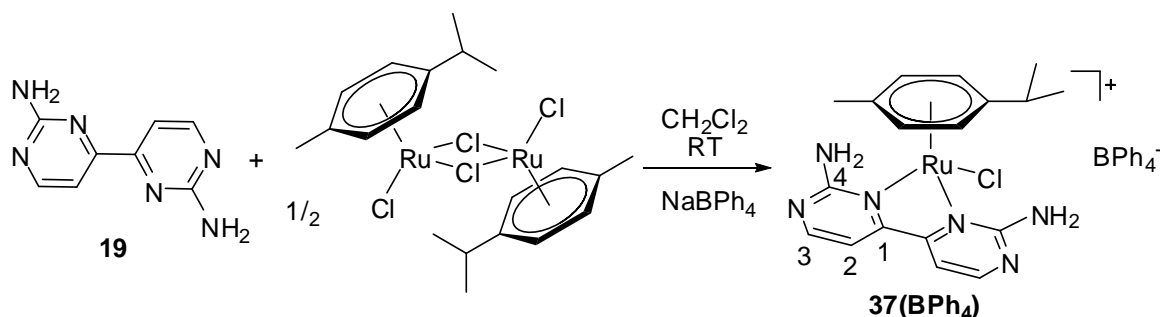
The observed distances of Ru-N1 (2.07-2.09 Å), Ru-cymene (1.67-1.69 Å) and Ru-Cl (2.40-2.42 Å) are comparable to related structures. For published structures of $[(\eta^6\text{-arene})\text{Ru}(N,N')\text{Cl}]^+$ type compounds, wherein N,N' are bidentate N -aromatic heterocycles, the reported Ru-N(pyridine) distances are observed at 2.06-2.12 Å, whereas Ru- $(\eta^6\text{-arene})$ distances and Ru-Cl bonds found at 1.67-1.70 Å and 2.38-2.43 Å, respectively¹³⁰.

Further examination of the metric parameters in Table 8 reveals that in all complexes **36a**(PF₆), **36b**(BPh₄), **36f**(BPh₄), **36h**(BPh₄), **36j**(BPh₄), **36k**(BPh₄) and **36l**(BPh₄) the Ru1-N1 distance is always significantly shorter than the Ru1-N2 distance, proofing a stronger binding of pyridine compared to pyrimidines. The introduction of an electron-donating substituent such as phenyl or ^tbutyl in the pyrimidine ring (**36b**(BPh₄) and **36f**(BPh₄) vs. **36a**(PF₆)) increases the electron density of the coordinating N-atom, which eventually forces the distance of Ru1-N2 shorter (2.1080(13) Å and 2.0992(15) Å vs. 2.1200(17) Å, respectively). At the same time the corresponding Ru1-Cl1 bonds are slightly stretched. The N,N -dimethylation of the NH₂ group is supposed to enhance this trend due to the higher electron-donating ability of the NMe₂ group compared to NH₂. Contrarily a Ru1-N2 bond elongation was observed, 2.1446(15) Å vs. 2.1200(17) Å for complex **36j**(BPh₄) vs. **36a**(PF₆) and 2.1509(19) Å vs. 2.0992 (15) Å for complex **36h**(BPh₄) vs. **36f**(BPh₄). Simultaneously a dramatic increase of the torsion angle of N1-C5-C6-N2 was also observed, -11.0(2) ° vs. 0.7(3) ° for complex **36j**(BPh₄) vs. **36a**(PF₆) and 14.3(3) ° vs. 7.2(2) ° for complex **36h**(BPh₄) vs. **36f**(BPh₄). That suggests that the introduction of the bulkier NMe₂ group in the close proximity to Ru(II) centre distorts the desired co-planarity of the pyridine and pyrimidine rings (last entry in Table 8), which may play an important role in the metal-ligand orbital overlapping. But interestingly, despite the quite large variation in steric and electronic aspects of the applied N,N -chelating ligands, the bite angle at the metal stays almost un-influenced

(N1-Ru1-N2, 76.12-77.84 °) for **36a**(PF₆), **36b**(BPh₄), **36f**(BPh₄), **36h**(BPh₄), **63j**(BPh₄), **36k**(BPh₄) and **36l**(BPh₄).

3.2.1.3 Ruthenium Complex with Symmetrical 4,4'-Bipyrimidine-2,2'-diamine

The ruthenium complex **37**(BPh₄) was synthesized like the others by reacting the ligand **19** with the ruthenium(II) precursor [(η⁶-cymene)Ru(Cl)(μ²-Cl)]₂ at room temperature in dichloromethane solution in almost quantitative yield (Scheme 45). By stirring the freshly prepared complex **37**(Cl) with NaBPh₄, the chloride anion was exchanged against the larger and thus weaker coordinating BPh₄⁻ and directly led to the ruthenium(II) complex **37**(BPh₄).



Scheme 45. Synthesis of the ruthenium(II) complex with the symmetric 4,4'-bipyrimidine-2,2'-diamine.

Due to the two similar *N*-donor moieties, the metal site is no longer a centre of chirality leading to a symmetrical complex therefore the methyl groups as well as the four aromatic C-H sites at the cymene ligand become magnetically equivalent. This is clearly demonstrated by the ¹H and ¹³C NMR spectra of the **37**(BPh₄) (Figures 37 and 38). The methyl groups of the cymene ring appear as one doublet at about 0.87 ppm and two doublets at about 6.15 and 6.02 ppm can be assigned to the aromatic hydrogen atoms of the cymene ring. In the ¹³C NMR spectrum two peaks at 85.9 and 81.9 ppm can be assigned to the four magnetically different aromatic carbon atoms of the cymene ring and the methyl groups at cymene ring appear as one peak at about 21.6 ppm. Coordination of the 4,4'-bipyrimidine-2,2'-diamine to the Lewis-acidic

Results and Discussion

ruthenium(II) centre causes a shift of the H2 and H3 resonances to lower field of about 0.3 ppm.

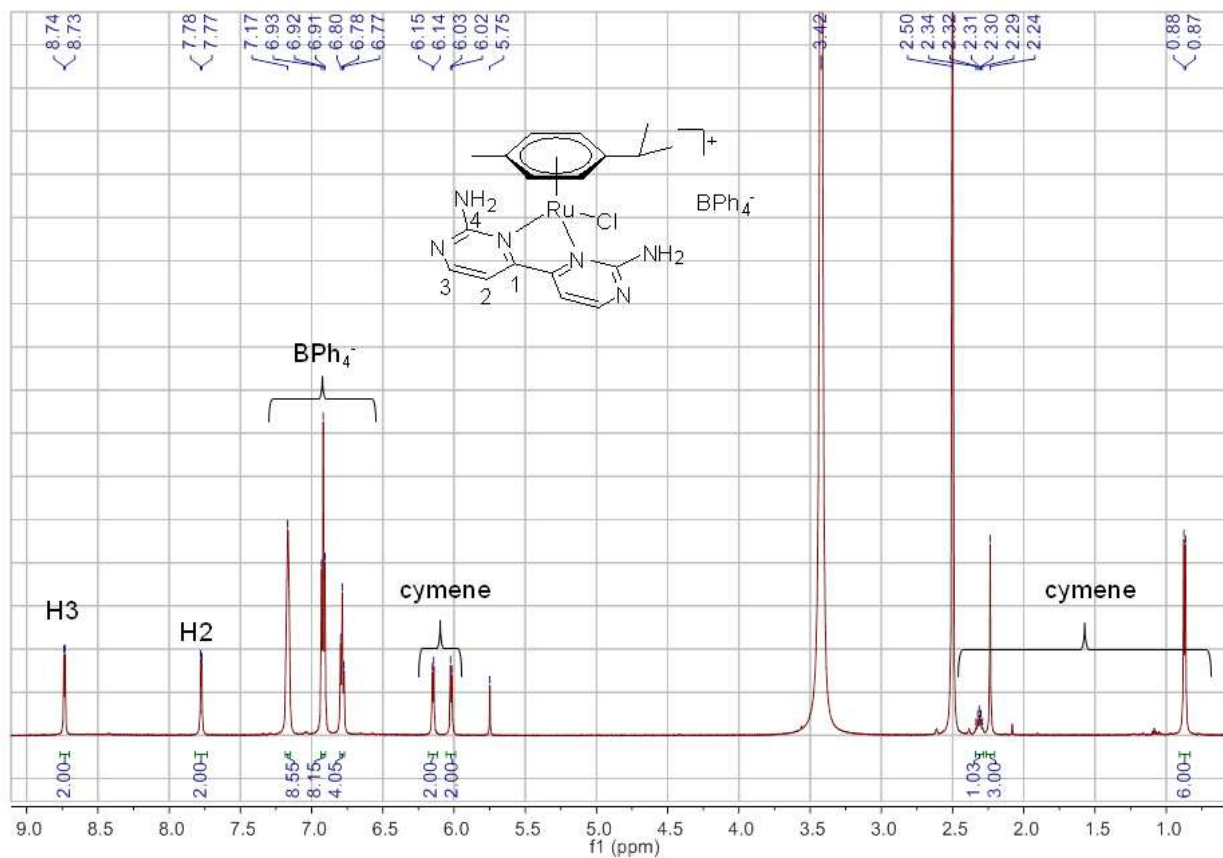


Figure 37. ^1H NMR spectrum of ruthenium complex **37**(BPh_4).

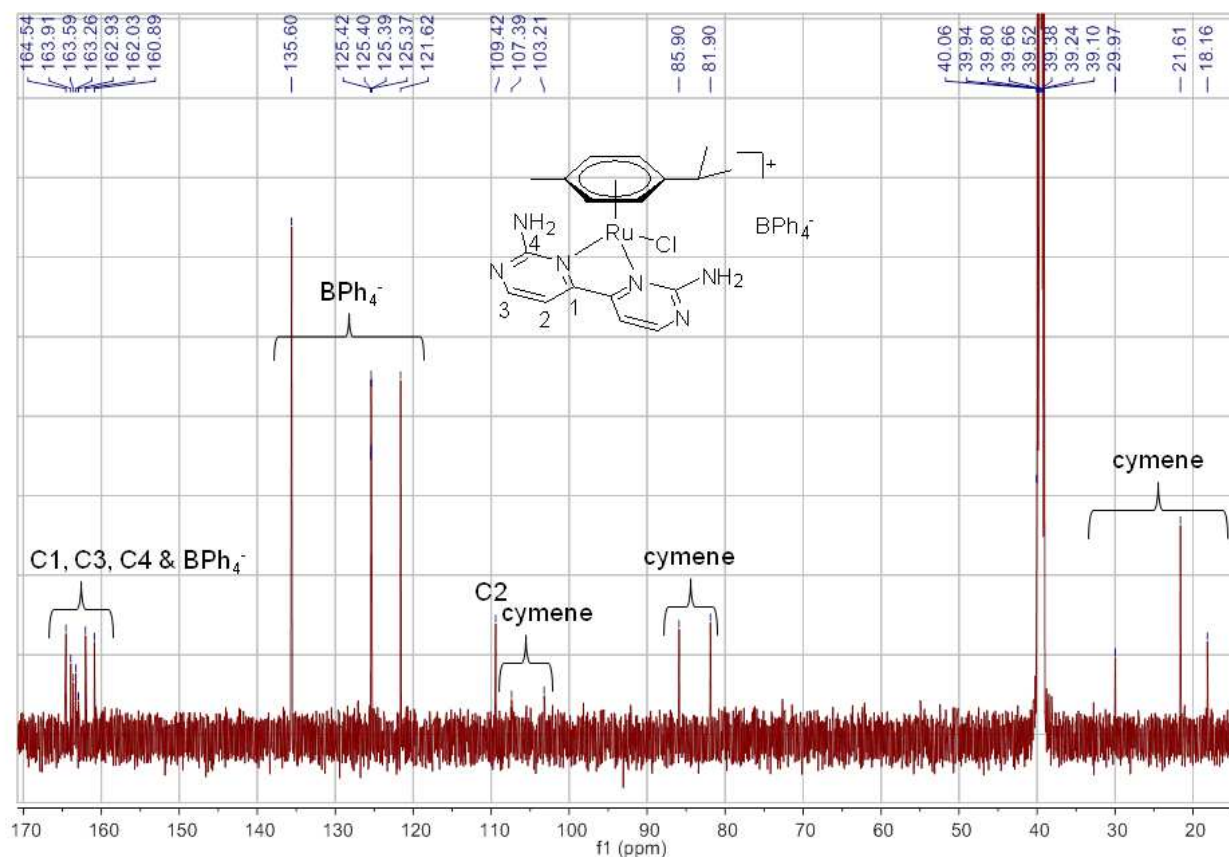
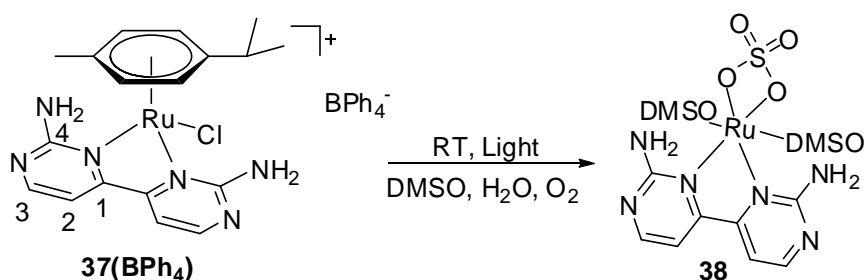


Figure 38. ^{13}C NMR spectrum of ruthenium complex **37**(BPh_4).

Attempts to obtain single crystals of **37**(BPh_4) suitable for X-ray structure determination by crystallization from dimethylsulfoxide over a long period of time and in the presence of oxygen, water and light resulted in ruthenium complex **38**. Replacement of the cymene ligand against two DMSO ligands and the chlorido ligand against one sulfate ligand occurred (Scheme 46, Figure 39). It seems that in the presence of oxygen, water and light DMSO is oxidized to sulfate which coordinates to the ruthenium. In a study on organic pollutants in water and wastewater DMSO was shown to be oxidized leading to sulfate as the thermodynamically most stable product *via* the formation of methanesulfinate and methanesulfonate.¹³¹ Formation of methanesulfonic acid by the reaction of methanesulfinic acid with OH radicals has been reported by Holezman¹³² and Scaduto.¹³³ The oxidation mechanism

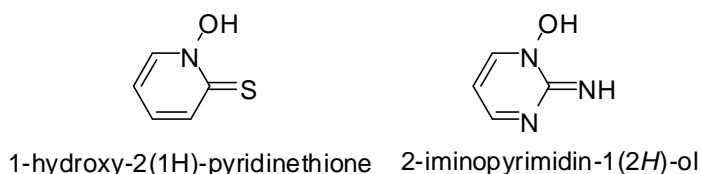
Results and Discussion

of dimethyl sulfoxide (DMSO) by OH radicals in the liquid phase was investigated by Arbilla et. al.¹³⁴



Scheme 46. Formation of complex **38** in DMSO in presence of light and oxygen.

Most notably hydroxyl radicals are produced from the decomposition of hydroperoxides (ROOH) or, in atmospheric chemistry, by the reaction of excited atomic oxygen with water. In organic synthesis hydroxyl radicals are most commonly generated by photolysis of 1-hydroxy-2(1H)-pyridinethione which is structurally similar to 2-iminopyrimidin-1(2H)-ol (Scheme 47).



Scheme 47. Structure of 1-hydroxy-2(1H)-pyridinethione and 2-iminopyrimidin-1(2H)-ol.

Although aerobic oxidation of sulfur atoms in disulfides in the presence of copper(II) is well documented,¹³⁵ according to my knowledge there is no report for ruthenium assisted oxidation of DMSO. There are few ruthenium complexes known with a bidentate coordinating sulfate as ligand.¹³⁶ To synthesize them, silver sulfate salt has been used directly.

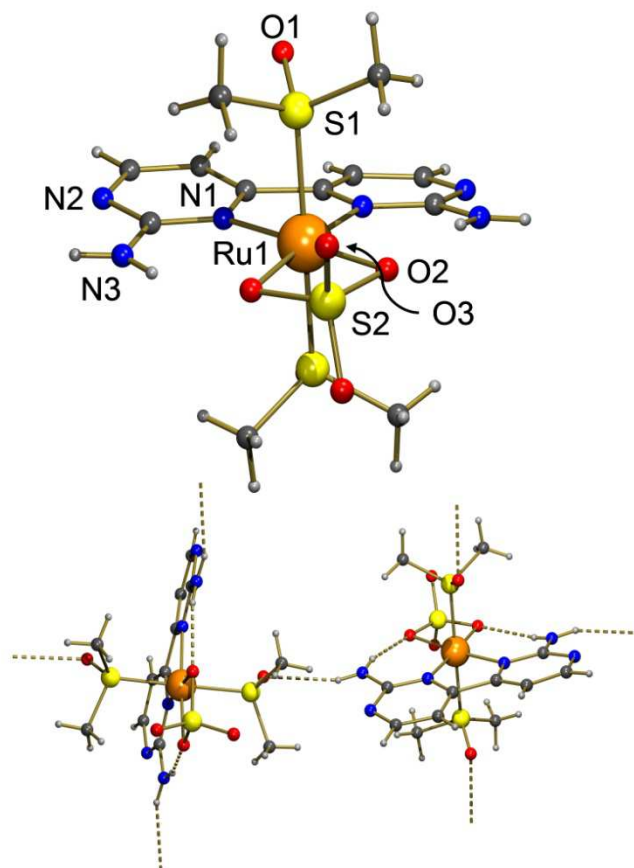


Figure 39. Molecular structure of complex **38** in solid state.

This complex shows a distorted octahedral arrangement with Ru(II) in center being coordinated by the chelating 4,4'-bipyrimidine-2,2'-diamine ligand, two DMSO ligands, coordinating by the sulfur atom which are oriented *trans* to each other and *cis* to the chelating bidentate ligands. The most important aspect of the structure is the bidentate mode of the coordinating sulfate group which is in the *trans* position to the *N,N* ligand. The Ru(1)-O(2) distance is 2.1383(14) Å (even longer than the Ru-O bond in RuCl(SO₄)(NO)(PPh₃)₂, 2.079(7) Å)¹³⁷ and the O(2)#1-Ru(1)-O(2) angle is 67.23(8)°. According to these parameters, and because of the strain involved in the four-membered ring RuOSO ring, the sulfate ligand is not chelated as strong as other bidentate ligands. The O-S-O bond angles are 101.18(11), 109.88(9), 110.69(8) and 113.81(14) which show, that the tetrahedral sulfate is slightly

Results and Discussion

distorted. As expected, the S-O bond lengths of the terminal oxygen atoms are shorter than the corresponding bond lengths of the coordinated oxygen atoms (1.4453(16) vs. 1.5321(15) Å). The angular distortions in the tetrahedron can be explained according to the Gillespie-Nyholm model in which it is assumed that the bonds with greater bond order will achieve a maximum angular separation.

The N(1)-Ru(1) bond length is shorter than the N(2)-Ru(1) length of complex **38** (2.0599(16) vs. 2.1200(17) Å). Ru(1)-S(1) bond length is 2.3076(5) Å which is in the normal range of Ru-S bond lengths of coordinating DMSO.¹³⁸ As the different bond angles in Table 10 shows, DMSO is coordinated as a distorted tetrahedron. S(1)-O(1) bond length is 1.4839(15) Å which is close to the averaged value of 1.475(10) Å for ionic sulfate.¹³⁷

Table 10. Bond angles of coordinated DMSO.

Bond angles (°)	
O(1)-S(1)-C(6)	107.49(10)
O(1)-S(1)-C(5)	107.27(11)
C(6)-S(1)-C(5)	101.13(13)
O(1)-S(1)-Ru(1)	116.19(6)
C(6)-S(1)-Ru(1)	113.00(8)
C(5)-S(1)-Ru(1)	110.55(8)

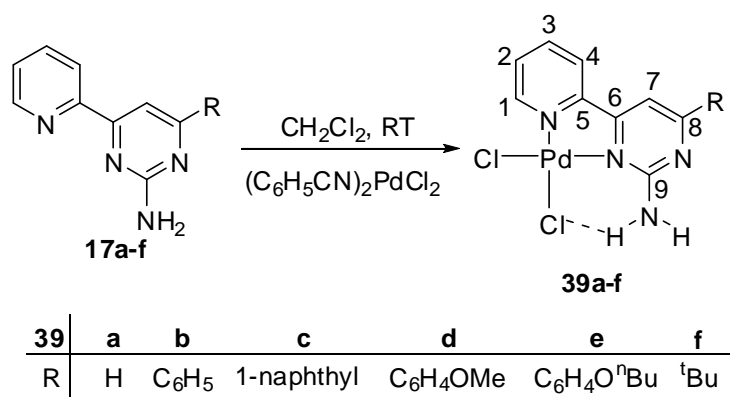
3.2.2 Palladium Complexes

Palladium complexes are widely used as catalysts for carbon-carbon, carbon-nitrogen, carbon-oxygen and even carbon-fluorine bond formations in agrochemicals, pharmaceuticals, and materials.¹³⁹

3.2.2.1 Palladium Complexes with Bidentate Ligands

Di(chloro)(4-(pyridin-2-yl)pyrimidin-2-amine)palladium(II) complexes **39a-f** were obtained by the reaction of the corresponding ligands with PdCl₂(CH₃CN)₂ in dichloromethane at room temperature (Scheme 48). All complexes tended to precipitate from the reaction

solutions, and optimized yields were obtained by adding excessive amounts of ether to the reaction mixtures. The complexes **39a-f** are pale yellow to orange solids.



Scheme 48. Preparation of palladium complexes **39a-f**.

After coordination to palladium, the resonance of all hydrogen atoms in the ¹H NMR spectrum shifted to lower field in comparison to the free ligands (Figure 40). The resonance of the hydrogen atoms of the amino group not only shifted to lower field by about 2 ppm but also show two broad resonances. Therefore, these atoms are no longer magnetically equivalent after coordination to palladium. There may be electronic or steric reasons for this behavior: 1) one of the NH₂ protons is in an ideal position to perform a H···Cl hydrogen bond (Scheme 48) and 2) due to coordination to the Lewis acidic metal site, the π-delocalization from the amino group into the pyrimidine ring will increase. Both effects result in a hindered rotation around the C-NH₂ bond. Generally the ¹³C NMR shifts are less sensitive towards the substitution pattern than the ¹H NMR shifts. C3 is the most influenced carbon atom and is shifted about 4 ppm towards lower field with respect to the free ligands.

Results and Discussion

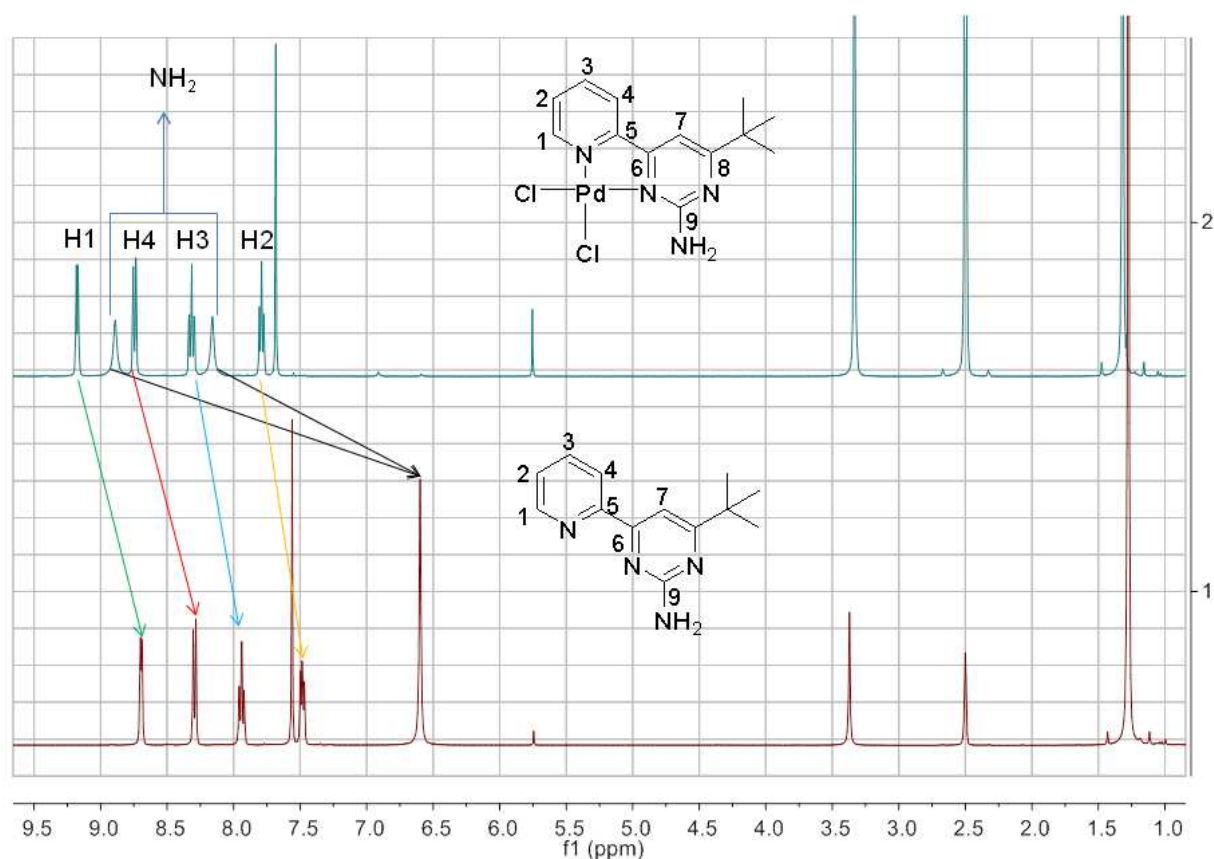
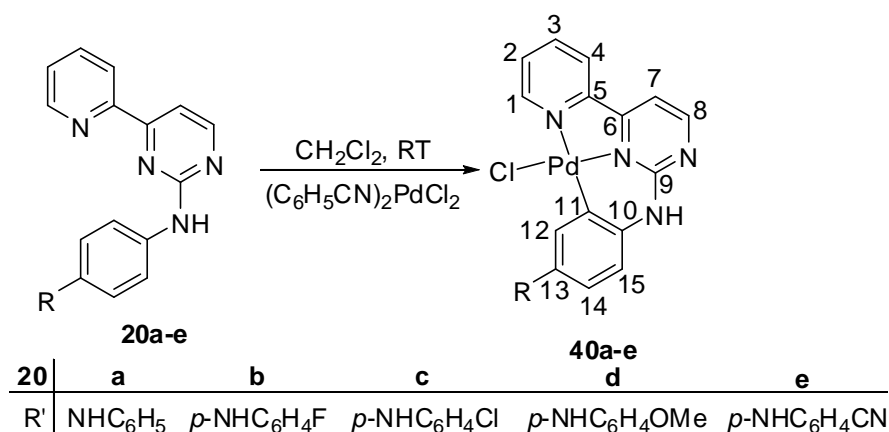


Figure 40. ^1H NMR spectrum of ligand **17f** and complex **39f**.

With ligands **17g-k** no palladium complex was obtained, probably due to steric effects.

3.2.2.2 Palladium Complexes with Tridendate Ligands

$\text{Pd}(N,N,C)\text{Cl}$ type complexes **40a-e** were obtained by the reaction of the corresponding ligands (*N*-(4-aryl)-4-(pyridin-2-yl)pyrimidin-2-amine) with $\text{PdCl}_2(\text{CH}_3\text{CN})_2$ in dichloromethane at room temperature (Scheme 49). All complexes tended to precipitate from the reaction solution and optimized yields were obtained by adding excessive amounts of ether in the reaction mixture. Since the complexes are not very soluble in CH_2Cl_2 they were dissolved in DMSO for further purification, some drops of ethanol were added and then the pure products were precipitated by adding diethylether. The complexes **40a-e** are yellow to deep orange colored solids.



Scheme 49. Synthesis of Pd(*N,N,C*)Cl complexes **40a-e**.

As expected the resonances of the hydrogen atoms in the ^1H NMR spectrum all shifted to lower field after coordination to palladium in comparison to the free ligand. The resonance of the hydrogen atom of the amino group shifted about 1.5 ppm to lower field. In the heterocyclic part of the ligand, H1 was influenced most. Its resonance is shifted by about 0.6 ppm to lower field. Since one of the carbon atoms of the phenyl ring now coordinates to palladium via a CH bond activation, the hydrogen atoms of the phenyl ring become all magnetically inequivalent and the pattern of these resonances in the ^1H NMR spectrum changes dramatically. The resonance of H11 has disappeared completely and a distinguished resonance can be assigned for the other hydrogen atoms (Figure 41). The new substitution pattern has affected the resonances of H12, H13 and H15, so that they appear at higher field for **40d** (8.00, 6.69 and 7.14 ppm, respectively) with the electron donating methoxy group and they shifted to lower field for **40e** (8.71, 7.29 and 7.47 ppm, respectively) with the electron withdrawing cyano group. Generally the ^{13}C NMR shifts are less sensitive towards the substitution pattern than the ^1H NMR shifts belongs to the heterocyclic part of the ligand. The pattern of the ^{13}C NMR spectrum in the phenyl part has become very complex. For each carbon atom of the ring, one signal can be assigned (Figure 42).

Results and Discussion

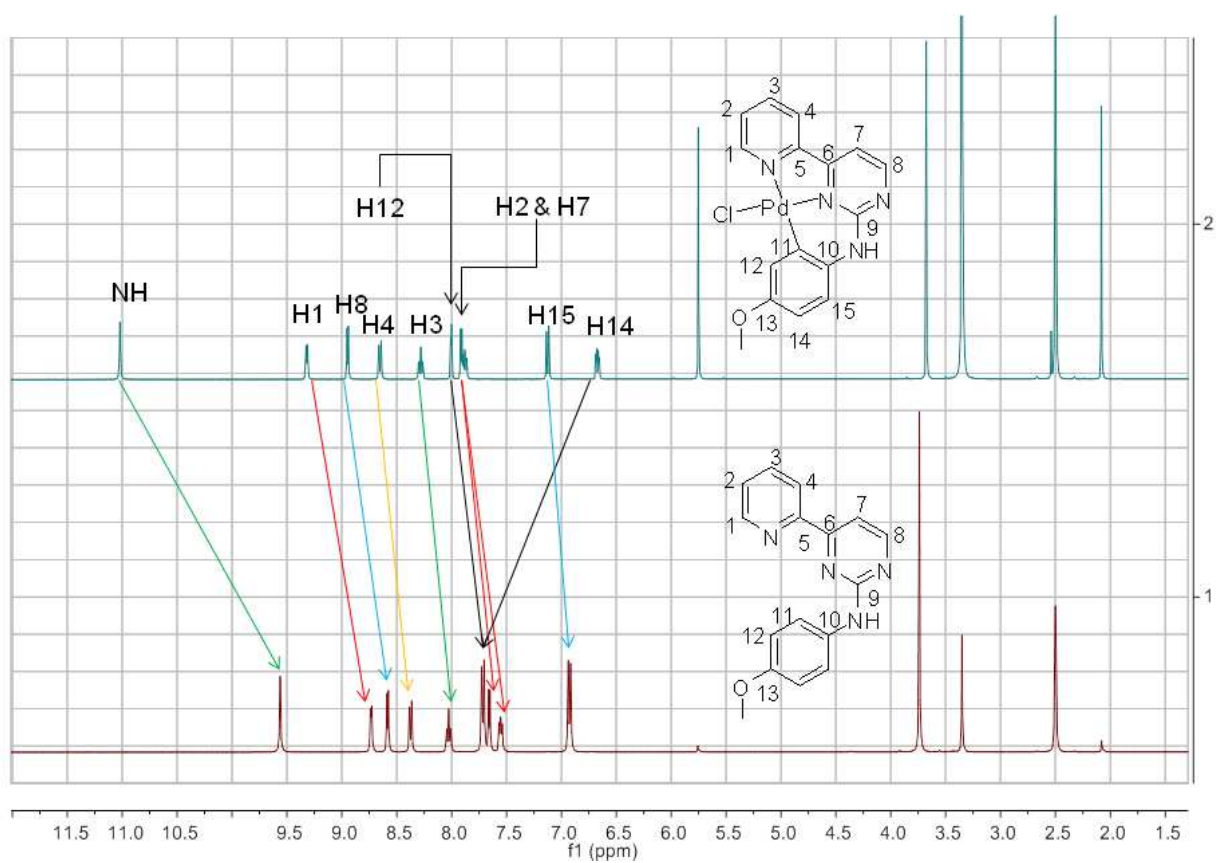


Figure 41. ^1H NMR spectrum of ligand **20d** and complex **40d**.

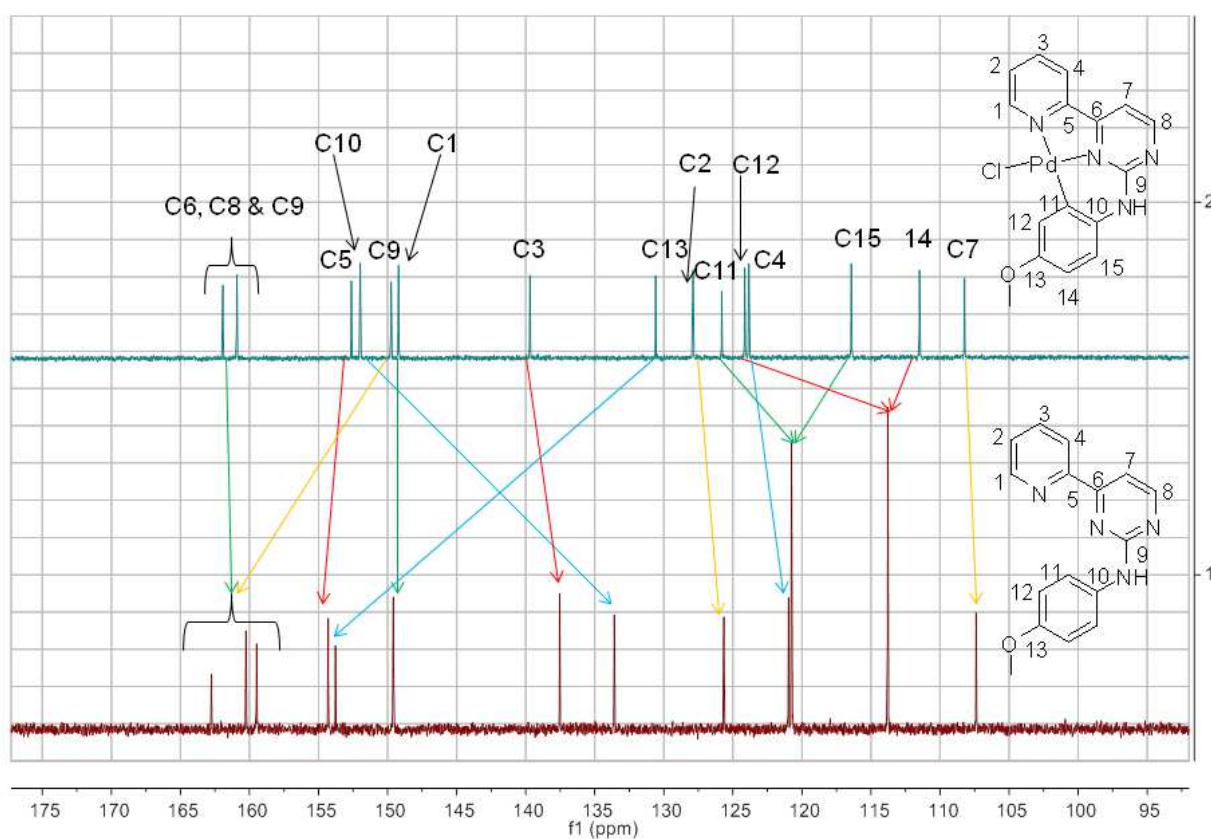


Figure 42. ^{13}C NMR spectrum of ligand **20d** and complex **40d**.

For complexes **40a** and **40d** single crystals suitable for X-ray diffraction studies were obtained from DMSO. Their molecular structures in the solid state are presented in Figures 43 and 44. Both complexes show a typical square-planar geometry with Pd(II) centers adopting a distorted arrangement and being coordinated by a chelating *N,N,C* type and a chloride ligand (Table 11).

Results and Discussion

Table 11 . Selected bond length and angles.

R	40a	40d
<i>Distances (Å)</i>		
C(15)-Pd(1)	1.990(3)	1.993(2)
N(1)-Pd(1)	2.111(2)	2.1161(18)
N(2)-Pd(1)	2.015(2)	2.0068(19)
Cl(1)-Pd(1)	2.3192(7)	2.3226(5)
<i>Angles (°)</i>		
C(15)-Pd(1)-N(2)	93.45(10)	93.20(8)
N(2)-Pd(1)-N(1)	80.27(9)	79.96(7)
C(15)-Pd(1)-Cl(1)	94.76(8)	94.84(7)
N(1)-Pd(1)-Cl(1)	92.04(7)	92.71(5)
C(15)-Pd(1)-N(1)	172.27(10)	171.24(8)
N(2)-Pd(1)-Cl(1)	169.37(7)	168.75(6)

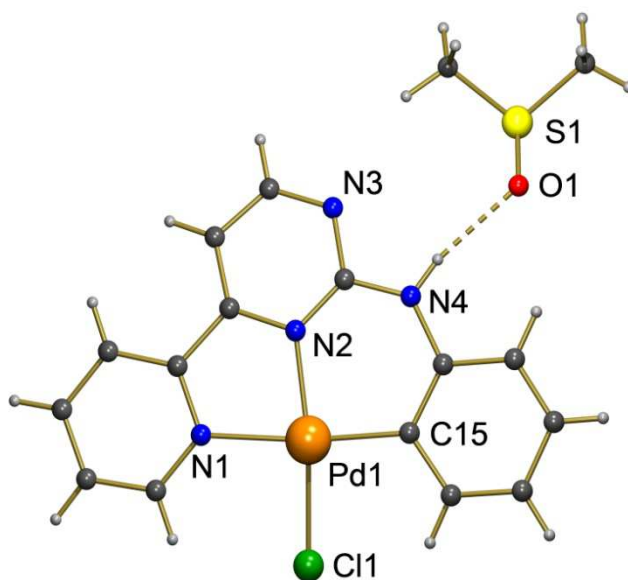


Figure 43. Molecular structure of complex **40a** in solid state.

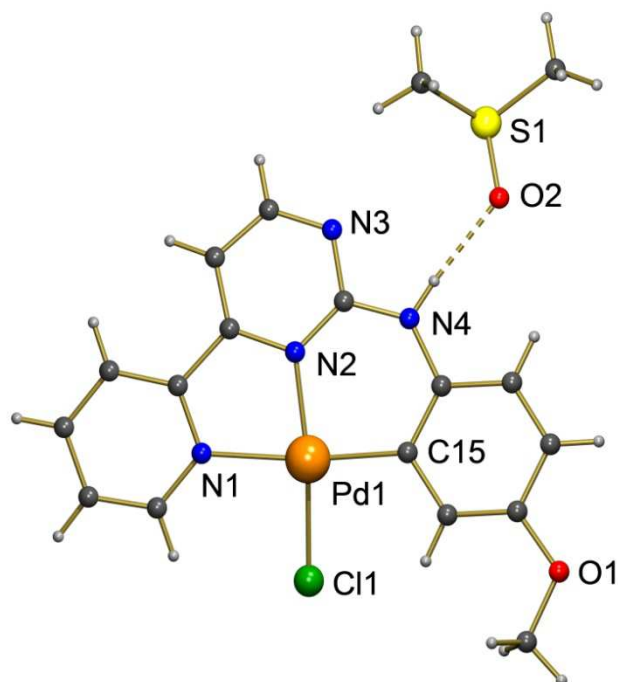


Figure 44. Molecular structure of complex **40d** in solid state.

Both complexes crystallize in the monoclinic space group monoclinic with one additional molecule of DMSO. The aromatic rings are not completely planar, a slight torsion is observed. The distances Pd-N1 (2.111(2) and 2.1161(18) Å for **40a** and **40d**, respectively), Pd-C15 (1.990(3) and 1.993(2) Å for **40a** and **40d**, respectively) and Pd-Cl1 (2.3192(7) and 2.3226(5) Å for **40a** and **40d**, respectively) are similar to related structures. In published molecular structures of Pd(*N,N,C*)Cl type compounds, wherein *N,N,C* are tridentate *N*-aromatic heterocycles, the reported Pd-N(pyridine) bonds lengths fall into the region 1.95-2.15 Å, whereas Pd-C(phenyl) distances and Pd-Cl bonds lie in the region 1.97-1.99 Å and 2.29-2.36 Å, respectively.¹⁴⁰

Further examination of the metric parameters in Table 11 reveals that in both complexes **40a** and **40d** the Pd1-N2 distance is slightly shorter than the corresponding Pd1-N1 distance, which may be due to the steric reasons.

Results and Discussion

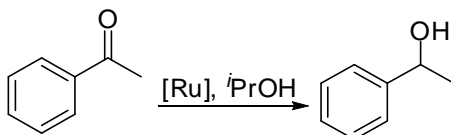
3.3 Catalytic Experiments

The synthesized ruthenium complexes were tested as catalysts for transfer hydrogenation and palladium complexes as catalysts for Suzuki coupling reaction.

3.3.1 Catalytic Activities

3.3.1.1 *Transfer Hydrogenation*

Ruthenium and rhodium complexes are the commonly most efficient catalysts for the transfer hydrogenation of ketones (Scheme 50). It has been shown before in Thiel's group that ruthenium complexes bearing nitrogen containing ligands can catalyze both the direct and the transfer hydrogenation of ketones.^{26h,127}



Scheme 50. Catalytic transfer hydrogenation of acetophenone leading to 1-phenylethanol.

3.3.1.1.1 Catalytic Activities of Ru(NNN)Cl(PPh₃) Complexes

Although more than two complexes of the type Ru(NNN)Cl(PPh₃) were synthesized, just complexes **33a** and **33b** could be obtained in high purity and thus be used as catalyst. Acetophenone has been chosen as a model substrate to explore the catalytic performance of compounds **33a,b** and **34a,b** in transfer hydrogenation. The reaction conditions were optimized by first using **33a** (Table 12). Due to the poor solubility of the catalyst in 2-propanol, dichloromethane was added to obtain a homogeneous solution. All reactions were carried out at room temperature and the catalyst generally showed high activities even under these very mild conditions. It seemed that too much base and a high dilution of the solution reduced the reaction rate (entries 8 and 5, Table 12). As expected, the rate of the reaction increased dramatically by increasing the temperature (entry 7, Table 12). A blank experiment carried out in the absence of the catalyst gave no hydrogenation of acetophenone at all (entry 9, Table 12).

Table 12. Transfer hydrogenation of acetophenone with **33a**^[a].

entry	substrate : catalyst : base ratios			solvent (mL)	yields (%) after		
					0.5 h	1 h	1.5 h
1	200	1	-	25	0	0	0
2	200	1	1	25	92	93	94
3	200	1	2.5	25	88	92	92
4	200	1	5	25	73	87	99 ^[b]
5	200	1	5	50	69	92	92
6	500	1	5	25	48	62	71
7 ^[c]	200	1	5	25	100 ^[d]	0	0
8	200	1	10	25	22	37	49
9	200	-	5	25	0	0	0 ^[e]

[a] Reaction conditions: $2.5 \cdot 10^{-2}$ mmol of **33a**, 20 mL of isopropanol, 5 mL of CH_2Cl_2 , room temperature, N_2 , monitored by GC. [b] Reaction completed after 80 min. [c] Reaction carried out at 82 °C. [d] Reaction completed after 5 min. [e] Even after about 3 h no product was detected without catalyst.

According to these results, the catalyses were carried out using a 0.5 M solution of the substrate, 0.5 mol-% of the catalyst, and 0.025 mol of KOH. For this purpose, a solution of the substrate in 2-propanol was added at room temperature to a 2-propanol/ CH_2Cl_2 solution containing the catalyst and the base. With the addition of the base, the color of the solution turned to a more intense red color, but during the reaction the color of the solution remained unchanged.

Complex **33a** was found to catalyze the reduction of acetophenone to 1-phenylethanol quantitatively in 80 min at room temperature. Substitution of the protons in the 5-position of the pyrazole ring against n-butyl groups dramatically increases the performance: in the presence of catalyst **33b**, the transformation is completed in less than 15 min at room temperature (Table 13), giving a minimum TOF of 800 h^{-1} . We assign this finding to an increase in steric hindrance by the n-butyl groups, which will force the allyl chains to be oriented away from the rear side of the catalyst. This will probably enable the dissociation of the triphenylphosphane ligand and activate the catalyst for the transfer hydrogenation process.

Results and Discussion

This mechanistic idea is corroborated by replacing the triphenylphosphane ligand with a carbon monoxide ligand (compounds **34a,b**), which makes the catalyst almost inactive even at 82 °C.

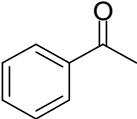
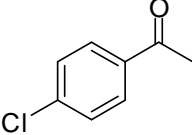
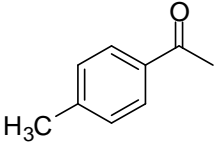
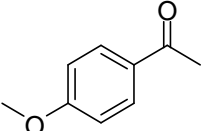
Table 13. Transfer hydrogenation of acetophenone with different ruthenium catalysts^[a].

entry	catalyst	time (min)	yields (%)
1	33a	80	99
2	33b	15	100
3	34a	1080	0
4	34b	1080	traces
5 ^[b]	34a	60	0
		180	traces
6 ^[b]	34b	60	13
		180	16

[a] Reaction conditions: $5 \cdot 10^{-3}$ mmol of catalyst, 1 mmol of substrate, $2.5 \cdot 10^{-2}$ mmol of KOH, 4 mL of isopropanol, 1 mL of CH_2Cl_2 , room temperature, N_2 , monitored by GC. [b] Reaction carried out at 82 °C.

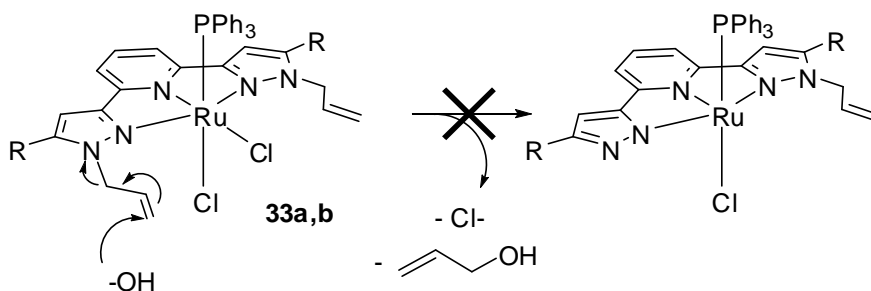
Finally the activity of **33b** was tested with a few different ketones to show its general applicability in transfer hydrogenation (Table 14). The results prove that increasing the electron density at the aromatic ring reduces the reaction rate. Complete conversion for the first two substrates was observed after 10 min at room temperature resulting in a minimum TOF of 1200 h^{-1} .

Table 14. Transfer hydrogenation of different ketones with **33b**^[a].

entry	substrate	yields (%)
1		100
2		100
3		96
4		51

[a] Reaction conditions: 1 mmol of substrate, $5 \cdot 10^{-3}$ mmol of **33b**, $2.5 \cdot 10^{-2}$ mmol of KOH, 4 mL of isopropanol, 1 mL of CH_2Cl_2 , room temperature, N_2 , reactions monitored by GC, samples were taken after 10 min.

Concerning the mechanism of the transfer hydrogenation catalyzed by **33a,b**, a reaction sequence following an inner coordination of the substrate can be suggested. There is no evidence for a ligand-assisted process, which could be initiated by splitting one or both of the allylic chains through an $\text{S}_{\text{N}}2$ or $\text{S}_{\text{N}}2'$ reaction with the base leading to an anionic pyrazolate donor (Scheme 51) and a vacant coordination site at the ruthenium(II) center. This reaction would generate an intermediate suitable for a ligand-assisted, outer-coordination mechanism.



Scheme 51. Cleavage of the allyl–N bond by the base.

Results and Discussion

Treatment of **33a,b** with KOH did not result in cleavage of the N-allyl bond. Cleaving the Ru-P bond, further promoted by the steric demand of the butyl chain in complex **33b**, should therefore be the initial step to generate a reactive 16-VE ruthenium(II) species, which then leads to the formation of the catalytically active ruthenium hydrido species. This is supported by the fact that addition of an excess of PPh₃ to the catalyst strongly decreases the reaction rates of **33a,b**, which is similar to findings reported in the literature.⁴⁶ Comparing the activity of **33b** (TOF $\geq 1200 \text{ h}^{-1}$) at room temperature makes it clear that we have obtained a highly active structural motif. It already had been shown in the literature that ruthenium(II) complexes with *trans*-coordinated chloro ligands are less active in the transfer hydrogenation of ketones than ruthenium(II) complexes with *cis*-coordinated chloro ligands (such as **33a,b**).^{10b}

3.3.1.1.2 Catalytic Activities of Ru(NN)(Cymene)Cl Complexes

Compound **36a(Cl)** was taken to optimize the reaction conditions for the transfer hydrogenation of acetophenone in isopropanol solution. A first series of experiments proved, that the catalyst becomes active at about 82 °C in the presence of KOH as the base. Evaluation of the optimum amount of base showed that with a base to catalyst ratio of 2.5:1 about 64 % of conversion can be observed after 3 h (Table 15, entry 3). However, under these conditions the catalyst becomes inactive and will not reach 100% of conversion, which is possible by increasing the base to catalyst ratio to 10:1 (Table 15, entry 1). The catalyst shows no activity in the absence of the base.

Table 15. Optimization of the base to catalyst ratio.^[a]

entry	base : catalyst	conversion [%] after	
		3h	24h
1	10 : 1	37	100
2	5 : 1	32	94
3	2.5 : 1	64	81
4	0 : 1	0	0

[a] reaction conditions: acetophenone (2.5 mmol), **36a(Cl)** ($1.25 \cdot 10^{-2}$ mmol), isopropanol (25 mL), 82 °C; the reactions were monitored by GC.

After having fixed the reaction conditions, the catalyst structure was optimized by changing A) the counter ion, B) the substitution in the 5-position of the pyrimidine ring (R), and C) the nature of the amine group (R') (see Scheme 44). Table 16 summarizes the influence of the counter ion in the series **36c(X)** (X = Cl⁻, BF₄⁻, PF₆⁻, BPh₄⁻). Although the differences are not pronounced, the weakly coordinating tetraphenylborate anion (Table 16, entry 4) clearly gives the best results at both, short and long reaction times.

Table 16. Effect of the counter ion.^[a]

entry	anion X	conversion [%] after		
		2 h	6 h	24 h
1	Cl ⁻	28	60	100
2	BF ₄ ⁻	26	53	70
3	PF ₆ ⁻	45	69	78
4	BPh ₄ ⁻	49	63	100

[a] reaction conditions: acetophenone (2.5 mmol), **36c(X)** ($1.25 \cdot 10^{-2}$ mmol), KOH ($1.25 \cdot 10^{-1}$ mmol), isopropanol (25 mL), 82 °C; the reactions were monitored by GC.

In the following, the substitution pattern on the pyrimidine ring was changed. As summarized in Table 17, there are pronounced effects of the substituents in the 5-position of the pyrimidine ring, reflecting that increased electron donation of the substituent results in an

Results and Discussion

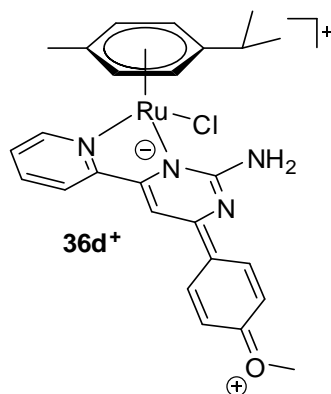
increase of catalytic activity. It is also clear, that substituents with a π -system, which will overlap with the pyrimidine π -system, are beneficial.

Table 17. Influence of the substituent in the 5-position of the pyrimidine ring.^[a]

entry	catalyst	conversion [%] after	
		2h	6h
1	36a(BPh₄)	19	35
2	36b(BPh₄)	69	89
3	36c(BPh₄)	49	63
4	36d(BPh₄)	73	87
5	36f(BPh₄)	79	98

[a] Reaction conditions: acetophenone (2.5 mmol), catalyst ($1.25 \cdot 10^{-2}$ mmol), KOH ($1.25 \cdot 10^{-1}$ mmol), isopropanol (25 mL), 82 °C; the reactions were monitored by GC.

For the 6-*para*-methoxyphenyl functionalized system **36d(BPh₄)**, the delocalization even includes the oxygen atom as outlined in Scheme 52, which will donate additional charge density to the nitrogen donor atom of the pyrimidine ring. This will reduce the strength of the Ru-Cl bond and therefore will allow this ligand easier to be replaced by an isopropanolato ligand and subsequently undergo the transfer of a hydrido ligand to the ruthenium site. Comparing these catalytic data with the structural data of compounds **36a(PF₆)**, **36k(BPh₄)**, and **36p(BPh₄)** (for crystal structures see Figure 29-36) reveals that as the Ru1-N2 distance decreases, the catalytic activity will increase.



Scheme 52. Electron delocalization including the oxygen atom.

It should be mentioned at this point that $[(\eta^6\text{-cymene})\text{Ru}(\text{Cl})(\text{bipy})]^+\text{Cl}^-$ (bipy = 2,2'-bipyridyl) was included into this study. This catalyst shows - with chloride as the counter ion - higher activities than all members of the series **36a-f(BPh₄)** suggesting that the presence of a NH₂ group has a detrimental rather than positive effect on the catalytic performance. Therefore the NH₂ functionalized ligands should not take part in the catalytic process in terms of a bifunctional mechanism. Therefore, it was proposed that like with Baratta's catalysts, this system performs an inner-sphere mechanism in which the alcohol and the ketone coordinate to the metallic center during the catalytic process.^{10,11} Similar results have been reported by Schlaf et al.¹⁴¹ who showed that a NH₂ substituted catalyst failed to show higher activity. They explained their finding with either the low pK_a value of the NH₂ group or with a mismatch of the proton-hydride distance in the active species. The active hydride species could not be trapped but according to the similarity of this catalysts with the Schlaf's system, steric reasons seem to be important.

To overcome the drawbacks of the 2-amino group, a series of catalysts were synthesized, containing either secondary or tertiary amino groups in the 2-position of the pyrimidine ring. The data of these compounds in the catalytic transfer hydrogenation are summarized in Table 18. Generally, the introduction of a tertiary amine improves the

Results and Discussion

conversions dramatically. Contrary to the findings discussed above, electron donating groups in the 4-position of the pyrimidine ring are decreasing the catalytic performance, the best result was found for the pyrrolidinyl functionalized system **36g(BPh₄)** (Table 18, entry 4). Moreover, this compound was also checked for its activity in the absence of the base and it achieved 51% and 85% of conversion after 6h and 24h, respectively, while the NH₂ functionalized catalyst **36a(Cl)** gave no conversion at all under these conditions. Still the reactivity of **36g(BPh₄)** is lower in the absence than in the presence of KOH. However, since the base is required to activate the catalyst by generation of a hydride species, an alternative mechanism has to be found to explain these findings. This will be discussed in the next section.

Table 18. Effects of the amino group.^[a]

entry	catalyst	conversion [%] (time [min])
1	36i(BPh₄)	45 (120)
2	36h(BPh₄)	48 (120)
3	36j(BPh₄)	100 (90)
4	36g(BPh₄)	97 (20)
5	36q(BPh₄)	100 (600)
6	36m(BPh₄)	100 (600)
7	36p(BPh₄)	100 (600)

[a] reaction conditions: acetophenone (2.5 mmol), catalyst ($1.25 \cdot 10^{-2}$ mmol), KOH ($1.25 \cdot 10^{-1}$ mmol), isopropanol (25 mL), 82 °C; the reactions were monitored by GC.

3.3.1.1.3 Investigation of the Mechanism

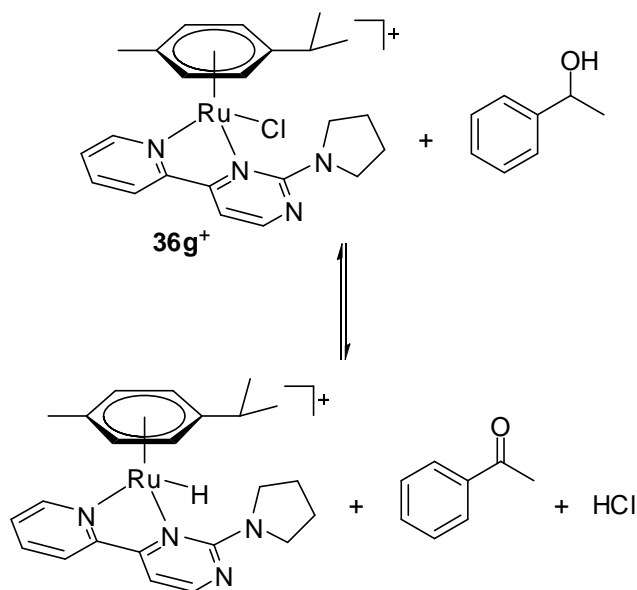
Chanati et al. had reported the activation of sp³ C-H bonds adjacent to the nitrogen atom of an alkylamine group in ruthenium catalyzed coupling reactions¹⁴² and Whittlesey et al. had reported a facile C-H bond activation at room temperature occurring on the *N*-heterocyclic carbene ligand 1,3-bis(2,4,6-trimethylphenyl)imidazol-2-ylidene (IMes) in Ru(IMes)(PPh₃)₂CO(H)₂ in the presence of a sacrificial alkene.¹⁴³ Here the C-H cleavage product readily reforms the starting dihydride upon reaction with H₂.¹⁴³ The same group had

also exploited this ruthenium complex for an indirect Wittig reaction using alcohols as the substrate, in which the catalyst removes hydrogen from the alcohol.¹⁴³ Crucial to the success of this complex for both direct and transfer hydrogenation reactions¹⁴³ is a reversible C-H bond activation process.

These findings led me to the idea, that an intramolecular C-H bond activation occurring in the ligand environment of the catalyst could be the key step in the base-free transfer hydrogenation with catalysts **36g(BPh₄)**, **36j(BPh₄)** and **36k(BPh₄)**. To elucidate the mechanism, the activity of **36g(BPh₄)** was investigated in more details. First its activity was checked for the catalytic dehydrogenation of 1-phenylethanol and it was found that after 48 h at 82 °C in toluene solution just traces of acetophenone could be detected, even in the presence of KOH, which means that there is likely the formation of a rutheniumhydrido species, but this compound cannot lose dihydrogen. So, there is no C-H activation on the ligand, neither by oxidative addition which is discussed in the literature for zero valent ruthenium complexes,^{142,144,145} nor by direct H₂ evolution, otherwise ongoing dehydrogenation of 1-phenylethanol under evolution of dihydrogen would be feasible.¹⁴⁶

Next, it was checked if **36g(BPh₄)** reacted in a 1:2.5 ratio with 1-phenylethanol (approximately quantitative) can dehydrogenize the substrate in the absence of KOH and an hydrogen acceptor (such as acetophenone). After 24 h we found 31% conversion of 1-phenylethanol to acetophenone, which is about 80% corresponding to the amount of **36g(BPh₄)** added in this experiment, which might either be explained by an incomplete conversion or by reaching the equilibrium as shown in Scheme 53. This proves that the formation of a hydridoruthenium species is possible, although this compound could not be isolated up to now. The hydridoruthenium formation can be explained just by a C-H bond activation occurring on the ligand.

Results and Discussion



Scheme 53. Stoichiometric reaction between **36g(BPh₄)** and 1-phenylethanol.

Furthermore, there is no stoichiometric hydrogenation of acetophenone in the absence of isopropanol. To investigate this, a 1.35:1 mixture of acetophenone and **36g(BPh₄)** was stirred for 24 h at 82 °C in toluene solution. No trace of 1-phenylethanol could be detected. This excludes a double C-H activation on the ligand, a pathway that is discussed in the literature, too.¹⁴⁷

To support that there is an intramolecular C-H bond activation occurring in the ligand environment of the catalyst and experimentally elucidate the process of C-H activation, electrospray mass spectrometry investigations were carried out in collaboration with Fabian Menges from the group of Prof. Nieder-Schatteburg, using collision-induced dissociation (CID) mass spectrometry with compounds **36a(BPh₄)**, **36g(BPh₄)**, and **36j(BPh₄)** under variation of the fragmentation amplitude (see below). Under mild conditions (no CID), the corresponding cations **36a⁺**, **36g⁺**, and **36j⁺** were detected without any fragmentation. Inducing fragmentation by increasing the fragmentation amplitude gave directly rise to HCl elimination for all three ruthenium complexes (Figures 45-47). However, the energy required for this process is considerably higher for the cation **36a⁺** than for its *N*-alkylated congeners **36g⁺** and

36j⁺ (Figure 48). Relative abundances of the CID fragments (fragment yield curves) were fitted using a sigmoidal function. The corresponding $E_{50\%}$ values (50% of the fragment ion intensity with respect to the total ion intensity) are thought to represent the relative appearance energies of the related fragmentation processes.

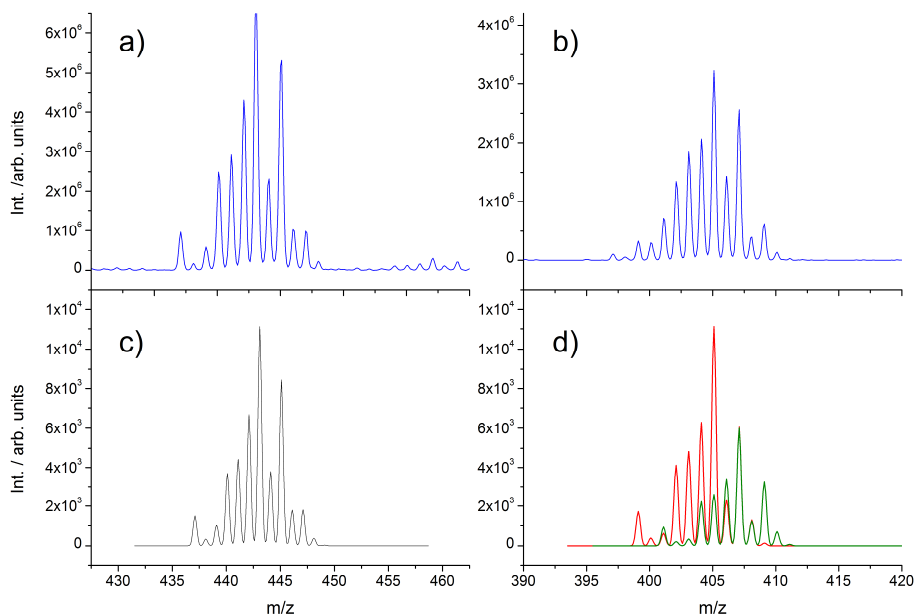


Figure 45. ESI-MS spectra of **36a⁺**. Experimental spectrum of **36a⁺** (a) and of the fragmentation of **36a⁺** (loss of HCl) (b), simulated spectrum of **36a⁺** (c) and of the fragments of **36a⁺** (loss of HCl (green) and HCl and H₂ (red)) (d).

Results and Discussion

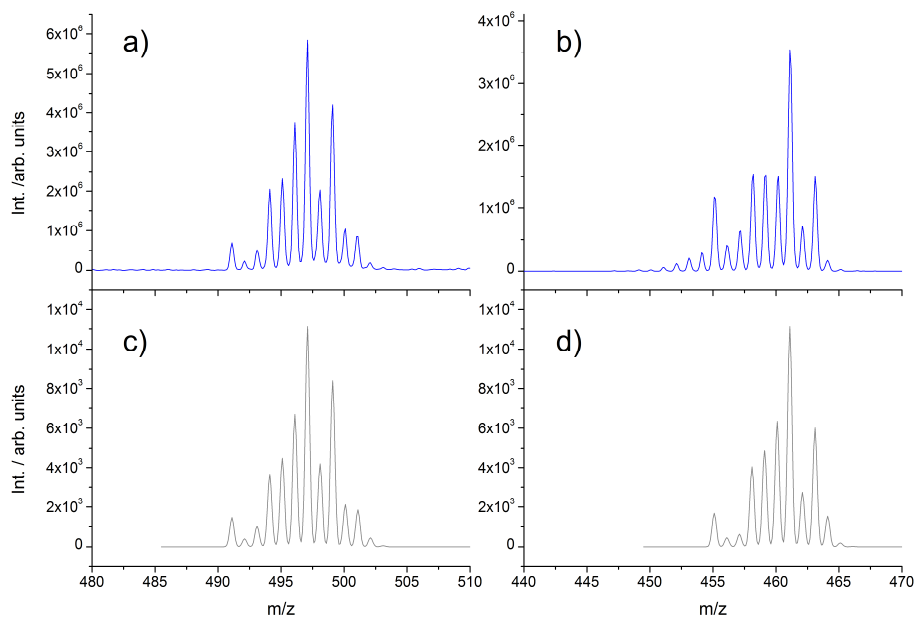


Figure 46. ESI-MS spectra of $36g^+$. Experimental spectrum of $36g^+$ (a) and of the fragmentation of $36g^+$ (loss of HCl) (b), simulated spectrum of $36g^+$ (c) and of the fragment of $36g^+$ (loss of HCl) (d).

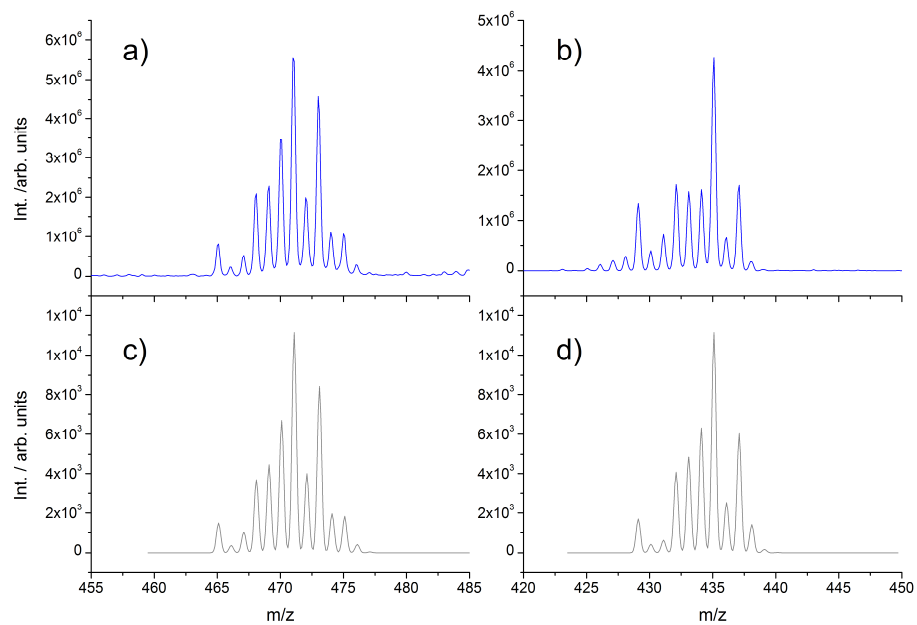


Figure 47. ESI-MS spectra of **36j**⁺. Experimental spectrum of **36j**⁺ (a) and of the fragmentation of **36j**⁺ (loss of HCl) (b), simulated spectrum of **36j**⁺ (c) and of the fragment of **36j**⁺ (loss of HCl) (d).

Results and Discussion

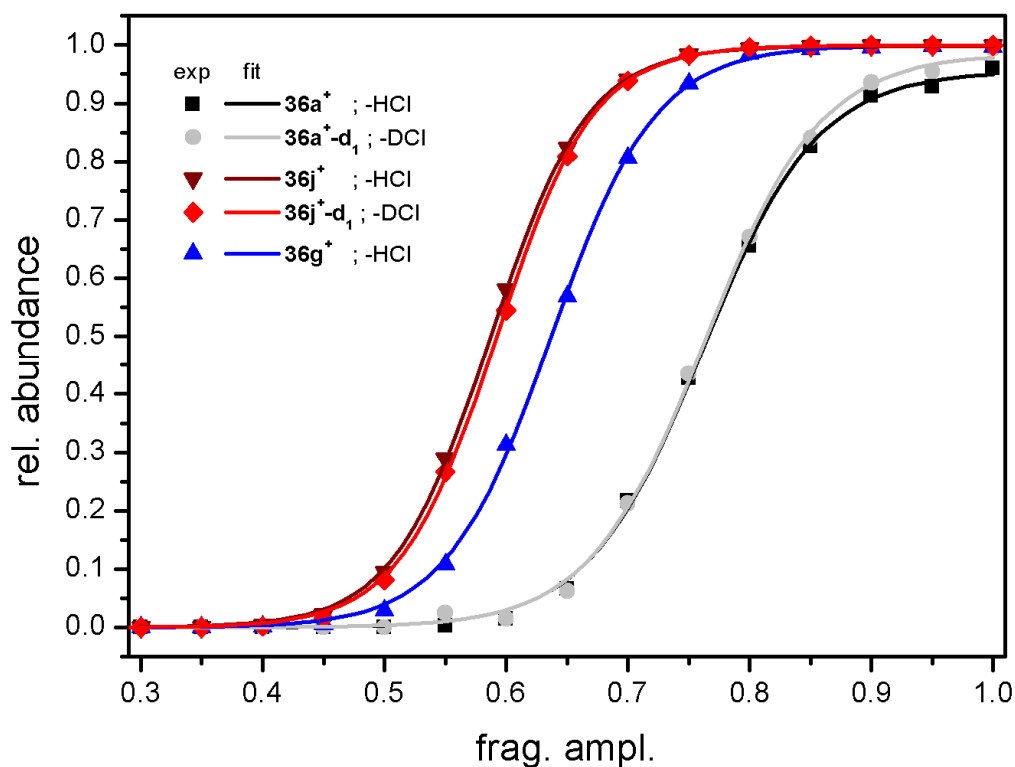
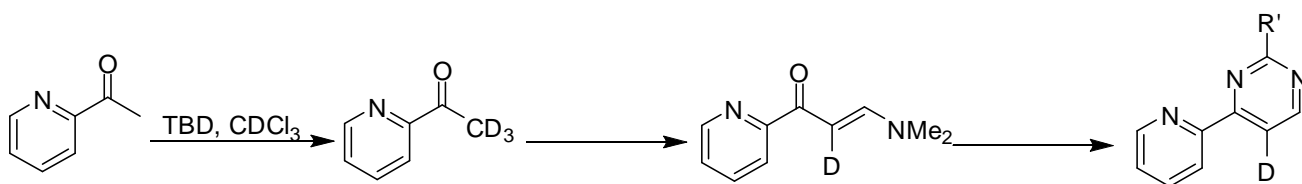


Figure 48. Collision-induced fragmentation of the cations **36a⁺** (■), **36a⁺-d₁** (●), **36j⁺** (▼), **36j⁺-d₁** (◆) and **36g⁺** (▲).

To gain a deeper insight into the transfer hydrogenation mechanism, identification of the location of the C-H activation was started. Since the η^6 -coordinated cymene ligand and the pyridine moiety are common features of **36a(BPh₄)**, **36g(BPh₄)**, and **36j(BPh₄)**, C-H activation at one of these sites should not result in pronounced differences between **36a⁺** on one side and **36g⁺**, **36j⁺** on the other. Therefore the efforts were concentrated on the pyrimidine moiety. The proton H7 was replaced against deuterium using 2,3,4,6,7,8-hexahydro-1*H*-pyrimido[1,2-*a*]pyrimidine (TBD) as an efficient isotope exchanger catalyst in CDCl₃ at room temperature (Scheme 54).¹⁴⁸



Scheme 54. Synthesis of the deuterated ligand **17a⁺-d₁**, **17j⁺-d₁**.

Repeating the ESI-MS experiment with **36a⁺-d₁** and **36j⁺-d₁** revealed exclusively the elimination of DCI (Figure 49), proving that the C-H activation occurs selectively at the 5-position of the pyrimidine ring. Furthermore **36j⁺-d₁** was dissolved in dry isopropanol and the ²H NMR has been measured overnight before and after heating. The deuterium peak vanished after heating which is another evidence for an intramolecular C-H bond activation occurring on the 5-position of the pyrimidine ring (Figure 50).

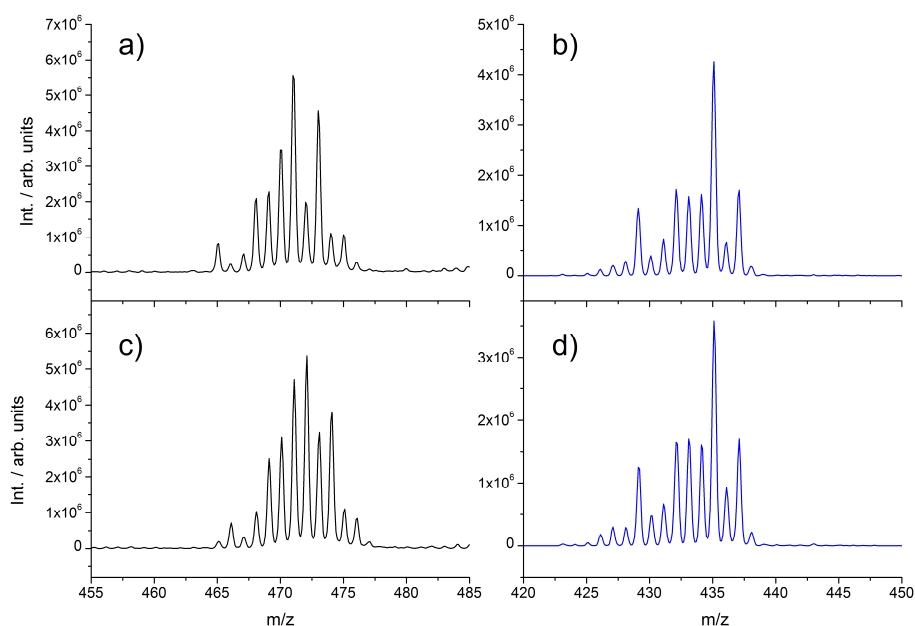


Figure 49. Comparison of the ESI-MS data of **36j⁺** and **36j⁺-d₁**. Experimental spectrum of **36j⁺** (a) and of the fragmentation of **36j⁺** (loss of HCl) (b), experimental spectrum of **36j⁺-d₁** (c) and of the fragment of **36j⁺-d₁** (loss of DCI) (d).

Results and Discussion

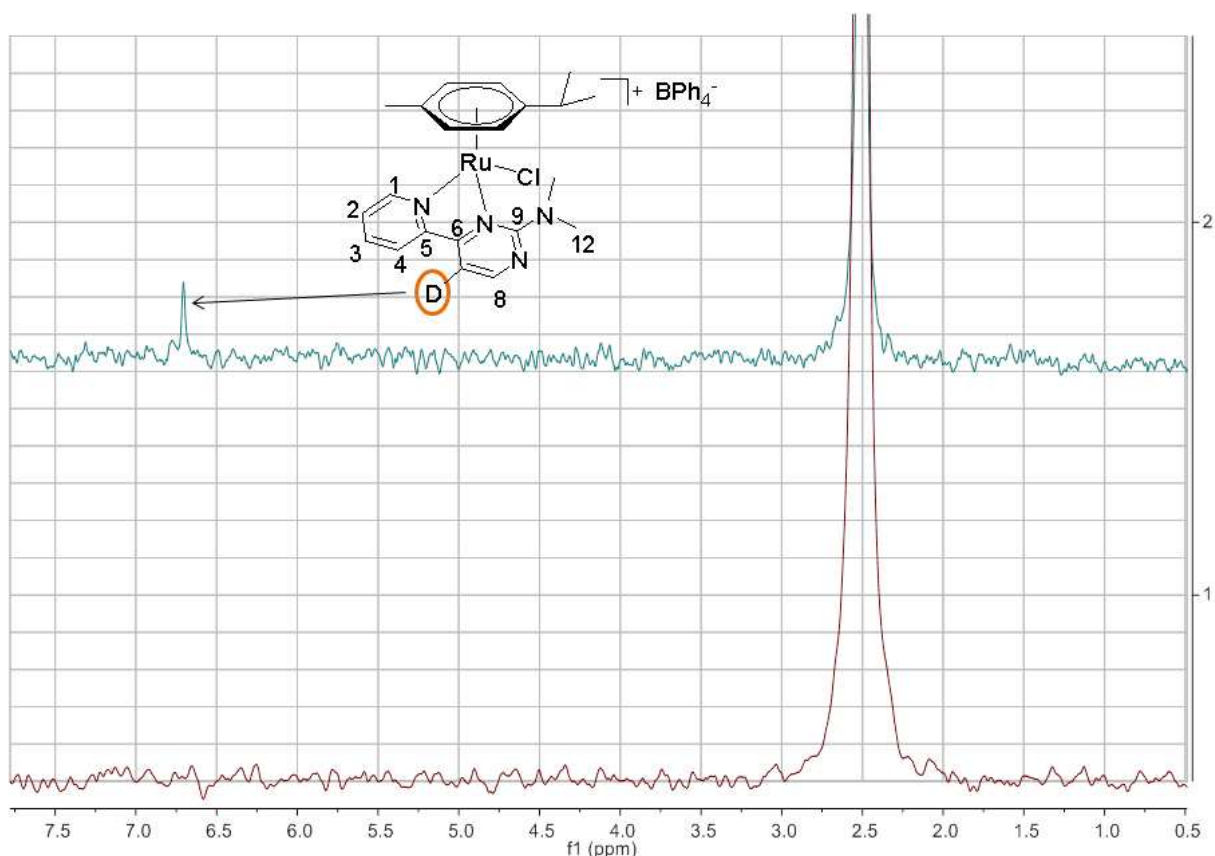


Figure 50. ^2H NMR spectra of $\mathbf{36j}^+-\mathbf{d}_1$ before (top) and after (bottom) heating.

To further evaluate this process, DFT calculations on the cations $\mathbf{36a}^+$, $\mathbf{36g}^+$, and $\mathbf{36j}^{+149}$ were carried out by Prof. Thiel. The elimination of HCl from the 18e systems $\mathbf{36a}^+$, $\mathbf{36g}^+$, and $\mathbf{36j}^+$ is obviously an endothermic, dissociative process in all cases, and is generally induced by breaking the Ru-N(pyrimidine) bond. Subsequently the pyrimidine moiety re-coordinates with C5 and H5 is transferred to the chloride ligand resulting in an HCl-adduct of a C,N-coordinated (η^6 -cymene)Ru complex, which then loses HCl with a very small barrier of activation. Results of the calculations on the C-H activation process are shown in Figure 51. The calculated data (ΔH_f^\ddagger) for the HCl elimination show that all energies are about 10-12 kcal/mol higher for $\mathbf{36a}^+$ than for $\mathbf{36j}^+$ and about 9-11 kcal/mol higher for $\mathbf{36a}^+$ than for $\mathbf{36g}^+$ ($\mathbf{36a}^+ \gg \mathbf{36g}^+ > \mathbf{36j}^+$; Table 19). Since these differences in energy are already found for TS1, the breaking of the Ru-

N(pyrimidine) bond is crucial for the C-H activation. This can be assigned to an increase of steric hindrance with the cymene ligand when the NH₂ group (**36a**⁺) is substituted against a NR₂ group (**36g**⁺ and **36j**⁺). The catalytic activities follow an ordering of **36a**(BPh₄) << **36j**(BPh₄) < **36g**(BPh₄), the inversed ordering of **36j**(BPh₄) and **36g**(BPh₄), with respect to their catalytic activities, may be due to solvent and/or counterion effects.

Table 19. Calculated heats of formation ($\Delta\Delta H_f$), enthalpies ($\Delta\Delta H$, italics) and Gibbs energies ($\Delta\Delta G$, underlined) of the C-H activation steps in kcal/mol.

step	36a ⁺	36j ⁺	36g ⁺
A	0.00 / 0.00 / <u>0.00</u>	0.00 / 0.00 / <u>0.00</u>	0.00 / 0.00 / <u>0.00</u>
TS1	34.81 / 33.66 / <u>32.11</u>	24.64 / 23.60 / <u>20.92</u>	25.29 / 24.28 / <u>22.56</u>
B	24.32 / 23.86 / <u>23.21</u>	12.89 / 12.47 / <u>10.13</u>	12.99 / 12.68 / <u>11.55</u>
TS2	48.11 / 43.56 / <u>42.76</u>	38.20 / 33.93 / <u>31.81</u>	38.52 / 34.35 / <u>32.97</u>
C	45.94 / 43.17 / <u>40.92</u>	36.66 / 34.00 / <u>30.46</u>	37.11 / 34.56 / <u>32.39</u>
TS3	50.03 / 46.54 / <u>40.98</u>	39.43 / 36.09 / <u>31.20</u>	39.81 / 36.53 / <u>32.01</u>
D	49.22 / 45.36 / <u>32.78</u>	38.17 / 34.47 / <u>20.98</u>	38.49 / 34.75 / <u>21.27</u>

Results and Discussion

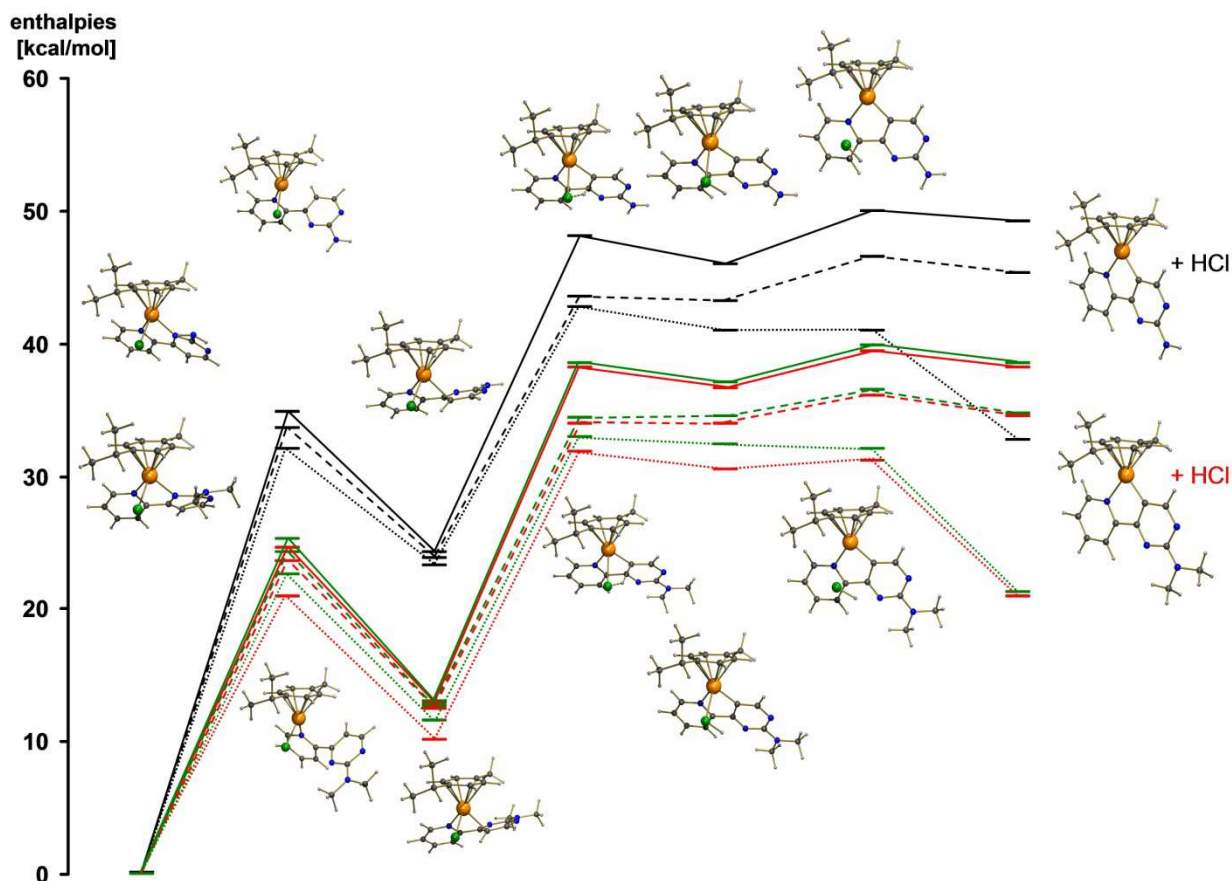


Figure 51. Calculated heats of formation ($\Delta\Delta H_f$, solid lines), enthalpies ($\Delta\Delta H$, dashed lines) and Gibbs energies ($\Delta\Delta G$, dotted lines) leading to the elimination of HCl from the cations $36a^+$ (black curves), $36j^+$ (red curves), and $36g^+$ (green curves). The calculated structures of all intermediates and final products derived from $36a^+$ and $36j^+$ are depicted.

Recently, it was shown that with so-called “thermometer ions” (substituted benzyropyridinium ions), it is possible to calibrate the internal voltage scales of the mass spectrometers fragmentation amplitudes towards appearance energies ($E_{50\%}$) of the fragment ions.¹⁵⁰ The precision of such an approach is compromised if additional fragmentation channels are taken into account. For $36j^+$ and $36g^+$ only one reaction channel, the elimination of HCl (resp. DCl) was found, $36a^+$ showed the additional loss of H_2 . The underlying mechanism of

the C-H activation of **36a**⁺, **36g**⁺ and **36j**⁺ implies a tight transition state (see DFT calculations), which might lead to a kinetic shift in the appearance energies obtained by CID.

Fabian Menges calibrated the CID breakdown curves of **36a**⁺, **36g**⁺ and **36j**⁺ with seven “thermometer ions” (C₅H₅N⁺-CH₂-C₆H₄-R; R=H, o-CH₃, p-CH₃, p-F, p-Cl, p-CN, p-OCH₃) against the calculated enthalpies (ΔH_{calc} ; B3LYP, G6-31*, ZPE-correction, 298.15 K, BSSE corrected) for a bond cleavage regarding the loss of neutral pyridine (with cationic substituted benzylium ions as ionic products (in case of R=H, p-Cl, p-CN, p-OCH₃)). Zins et al. investigated the competing formation of tropylium ions (in case of o-CH₃, p-CH₃, p-F), which also was calculated and used for calibration.^{149c}

Data from CID experiments of benzyropyridinium ions and **36a**⁺, **36g**⁺ and **36j**⁺ were center-of-mass transformed and compared according to their E_{50%} values. A linear fit function (ΔH_{calc} versus CID E_{50%} value of substituted benzyropyridinium ions) was used to estimate the enthalpies of the HCl (DCI) loss for **36a**⁺, **36g**⁺ and **36j**⁺. This analysis results in a qualitative trend of activation energies (loss of HCl or DCI) of the Ru-catalysts **36a**⁺, **36g**⁺ and **36j**⁺ with respect to the “thermometer ions” (Table 20).

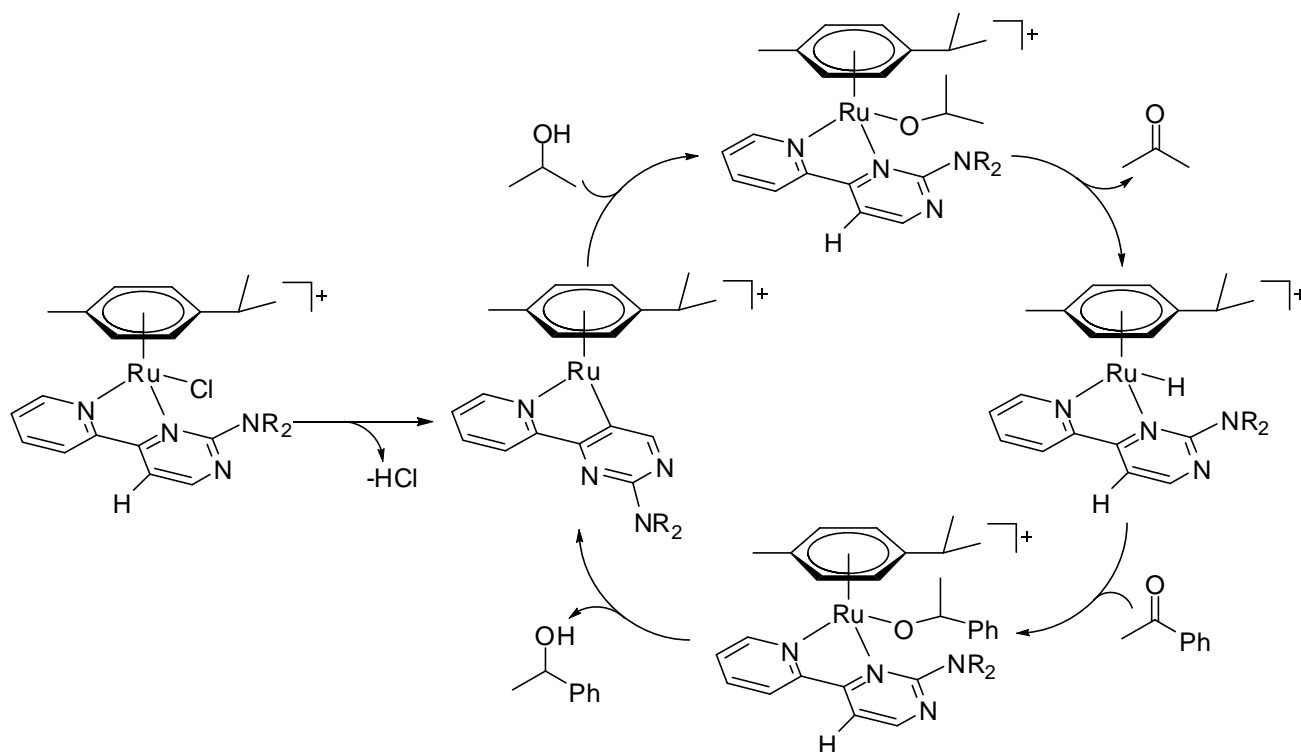
Table 20. Estimated enthalpies of Ru-catalysts **36a**⁺, **36g**⁺ and **36j**⁺ (ΔH_{fit}) from a linear fit function of benzyropyridinium ions (ΔH_{calc} versus CID E_{50%} value) and calculated ZPE corrected enthalpies (ΔH) of the transition state TS3 of the HCl loss.

	ΔH_{fit} (kcal/mol)	ΔH (kcal/mol)
36a ⁺	49	46.5
36a ⁺ -d ₁	49	-
36j ⁺	34	36.1
36j ⁺ -d ₁	35	-
36g ⁺	36	36.5

Since the presence of the base is solely accelerating the reaction but is, as mentioned above, not a condition precedent for the transfer hydrogenation with **36g**(BPh₄), the following

Results and Discussion

mechanism is proposed according to the experiments and calculation which have been done (Scheme 55).



Scheme 55. Reaction mechanism for the transfer hydrogenation in the absence of the base.

Using experimental and theoretical results unusual activities of different catalysts can be explained as follow:

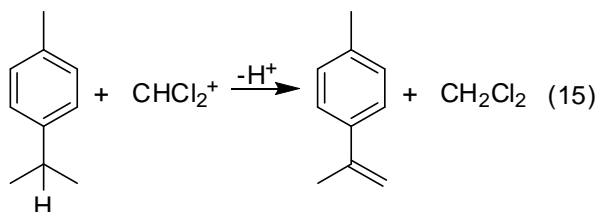
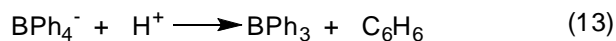
- If there is a substituent at the 5-position of pyrimidine ring, no C-H bond activation will take place because of steric reasons and the mechanism of the reaction is the classical one, meaning that the catalytic cycle requires a base to be completed. Here the catalyst will benefit from electron donating substituent at the 5-position of pyrimidine ring.
- If there is no substituent at the 5-position of the pyrimidine ring so that C-H bond activation can occur the catalyst will benefit from more steric hindrance of alkylated amines which results in a *C,N* coordination mode. This facilitates the elimination of HCl and makes a

coordination site free for coordination of the alcohol. In this case, the carbon atom can perform the role of an internal base so that the catalyst is active also in the absence of external base.

- Since in the first step of catalytic cycle the chloride ligand should leave the coordination sphere and since this can be expedited by the *C,N* coordination mode, the complexes having no substituent at the 5-position of pyrimidine ring seem to be promising catalysts for transfer hydrogenation of ketons in the absence and presence of a base.

In order to trap and characterize the CH activated intermediate some additional experiments were carried out. Heating a NMR probe of **36g(BPh₄)** with CDCl₃ as solvent results in de-coordination of ligands. It is noteworthy that two extra peaks which can be assigned to CH₂Cl₂ ($\delta = 5.30$ ppm) and benzene ($\delta = 7.36$ ppm) are also detectable in the ¹H NMR spectrum. Adding triethylamine as a base to a NMR probe of **36g(BPh₄)** with CDCl₃ as solvent (without heating) results in decomposition of the complex after one day. Parallel to this, the peaks at 5.30 and 7.36 ppm are detected. If again a similar probe is heated for 1h in addition to the peaks at 5.30 and 7.36 ppm a further peak at 11.78 ppm can be detected which can be assigned to the triethylammonium cation. In all cases it seems that the probe's medium is getting acidic and that the counterion has released benzene, a process that can occur in an acidic medium¹⁵¹ (Scheme 56, Equation 13). Also it seems that the formed triphenylborane has reacted with the solvent and produced dichloromethylum (Scheme 56, Equation 14) which may take a hydride from cymene ring and be converted to dichloromethane (Scheme 56, Equation 15). The cymene can release a proton and become stable results in decomposition of the catalyst. This will result in a more acidic medium which autocatalyzes the reaction 13.

Results and Discussion

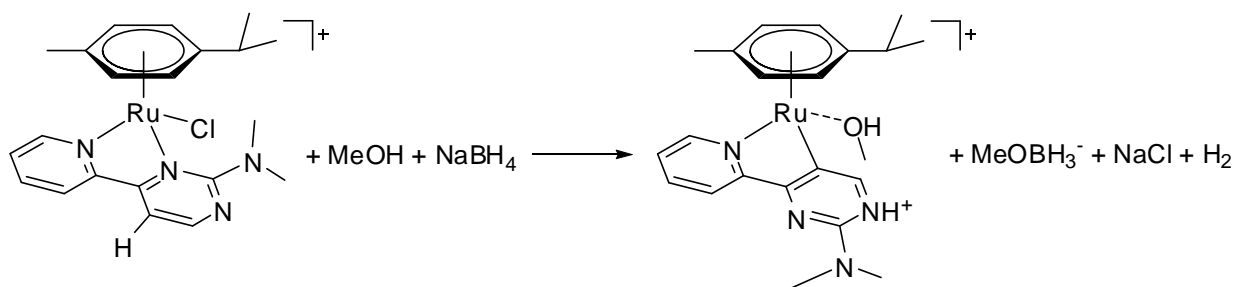


Scheme 56. Benzene formation from tetraphenylborate in an acidic medium (eq. 13), reaction between triphenylborane and solvent (eq. 14), reaction between dichloromethyl cation and cymene ligand (eq. 15).

Obviously these conditions are too harsh and result in complex decomposition. So without adding a base, a NMR probe of **36g(BPh₄)** with CDCl₃ as solvent was heated just to 60 °C for 15 h. In this case no peak at 5.30 ppm is detected but still the complex decomposed and a peak appears at 7.36 ppm which means that the medium gets acidic by heating. This can be a hint for C-H bond activation which results in release of a proton and makes the medium acidic. Using a milder condition AgOAc was added to NMR probe of **36g(BPh₄)** with CDCl₃ as solvent. Here silver can catch the chloride and the acetate, which is a weak base, will capture the proton. But even after 3 days without any heating no changes have been observed in the ¹H NMR spectrum.

It was expected to trap a hydrido ruthenium complex by refluxing **36j(BPh₄)** and NaBH₄ in dry methanol for 15 h. But in the ¹H NMR spectrum no peaks below 0 ppm can be assigned to a hydrido species. However there are some changes in the spectrum. The most important one is that the doublet peak at about 6.70 ppm which was assigned to H7 on the pyrimidine ring vanished and another doublet peak appeared at about 8.7 ppm. Also all the peaks of the *N,N* ligand and counter ion are shifted to lower field. Moreover the peaks of the cymene ring show a more symmetric pattern. This can be explained as follows:

NaBH₄ and methanol form an adduct which will take a proton from the complex and release H₂.¹⁵² This makes the reaction to occur in one direction and will produce BH₃, NaCl and the 16e intermediate simultaneously. Methanol can be activated by liberated BH₃ and donate its proton to the nitrogen atom of the *N,N* ligand (Scheme 57). This proton might appear at low field at about 8.7 ppm in the ¹H NMR spectrum.



Scheme 57. Formation of a 18e intermediate in the presence of NaBH₄ in methanol.

Furthermore no formation of the CH₂Cl₂ and benzene has occurred which is a result of replacing chloroform with methanol. It seems that the formed intermediate is too active and will react with chloroform to produce dichloromethane and this makes the medium acidic which causes the splitting of a benzene ring from counter ion as discussed above. Although the active intermediate in the transfer hydrogenation could not be detected by these experiments, all of them confirm the CH bond activation indirectly.

As it was mentioned in section 1.5.1, there are five classes for CH bond activation according to the Bercaw classification⁶⁵:

- 1) Oxidative addition, which is typical for electron-rich, low-valent complexes of the late transition metals. This will occur for Ru⁰, our complexes cannot undergo this type of reaction.
- 2) Sigma-bond metathesis, which is typical for complexes of the early transition metals in which ruthenium is not included.

Results and Discussion

- 3) Metalloradical activation, which is typical for dimeric complexes.
- 4) 1,2-Addition, which is common for an addition across a metal-nonmetal double bond.
- 5) Electrophilic activation, which occurs in polar or acidic media and is typical for late- or post-transition metal.

In our case the complex should lose HX in the first step. This is not reported for ruthenium complexes until now but all evidences mentioned above confirm that this can be the right class for this type of CH bond activation.

3.3.1.2 Suzuki Coupling

After the first report in 1981, the Suzuki–Miyaura reaction has been used in the construction of varied biaryls,^{74,153} which have many applications in pharmaceutical, material and agricultural chemistry.¹⁵⁴ In the past decades phosphine ligand based palladium catalysts were extensively used due to their extreme donor ability. Despite their toxicity, Pd(II) catalysts with phosphine ligands have shown very high turnover numbers (TONs).¹⁵⁵ Recently, Pd(II) catalysts with different *N*-donor ligands became attractive for catalytic applications as they possess lower toxicity and are easy to handle.^{156,157} As examples, *N*-coordinated palladium-imidazole, imidazoline complexes¹⁵⁸ and palladiumbenzimidazole complexes¹⁵⁹ were found to be catalytically active in the Suzuki–Miyaura reaction. Furthermore, Boykin and co-workers have developed a simple amine–Pd(OAc)₂ catalyst system for the Suzuki–Miyaura reaction.¹⁶⁰ Moreover, bidentate nitrogen donors, which are more air-stable, have also been used as ligands for this reaction.^{157f,161} Here, I focus on the catalytic activity of complexes **39a-f** for the Suzuki–Miyaura reaction.

Complex **39d** was first tested as a catalyst in the model Suzuki–Miyaura reaction of bromobenzene with benzenboronic acid to ascertain the optimum conditions (Table 21). As obvious from the results, this complex is even active at low temperatures near to room temperature and although lowering the loading will decrease the activity but the system is still

active. Since the proper combination of base and solvent was extremely important, several different bases and solvents were examined. Obviously an increase in the polarity of the solvent will increase the activity of the catalyst. Although ethanol is a very good solvent, a mixture of the DMF and water seems to be the best solvent. From the entries 9-13 one can conclude, that the activity benefits from a larger cation in base and carbonate as its counterion which makes Cs₂CO₃ a good base for this system. Furthermore the ratio of DMF and water was tested and therefore the optimized conditions were found using the complex **39d** as follows: the reaction proceeded with 89% in DMF/H₂O with Cs₂CO₃ at 70 °C for 1 h.

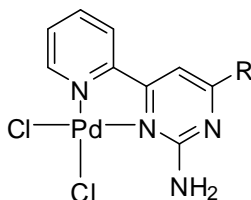
Table 21. Optimization of the reaction conditions using **39d**.^[a]

Entry	Solvent	Solvents ratio	Cat. Loading [mol-%]	base	base [mol-%]	T[°C]	Yield [%]		
							1h	2h	24h
1	1,4-dioxane	-	1	Cs ₂ CO ₃	120	RT	0	0	0
2	1,4-dioxane	-	1	Cs ₂ CO ₃	120	40	trace	trace	Trace
3	1,4-dioxane	-	1	Cs ₂ CO ₃	120	60	24	30	44
4	1,4-dioxane	-	1	Cs ₂ CO ₃	120	75	27	36	71
5	1,4-dioxane	-	1	Cs ₂ CO ₃	120	70	27	-	-
6	DMF	-	1	Cs ₂ CO ₃	120	70	0	-	-
7	Toluene	-	1	Cs ₂ CO ₃	120	70	23	-	-
8	EtOH	-	1	Cs ₂ CO ₃	120	70	81	-	-
9	DMF/H ₂ O	50:50	1	Cs ₂ CO ₃	120	70	89	-	-
10	DMF/H ₂ O	50:50	1	NaOAc	120	70	9	-	-
11	DMF/H ₂ O	50:50	1	Na ₂ CO ₃	120	70	71	-	-
12	DMF/H ₂ O	50:50	1	K ₃ PO ₄	120	70	73	-	-
13	DMF/H ₂ O	50:50	1	K ₂ CO ₃	120	70	81	-	-
14	DMF/H ₂ O	75:25	1	Cs ₂ CO ₃	120	70	46	-	-
15	DMF/H ₂ O	25:75	1	Cs ₂ CO ₃	120	70	65	-	-
16	DMF/H ₂ O	50:50	1	Cs ₂ CO ₃	60	70	60	-	-
17	DMF/H ₂ O	50:50	1	Cs ₂ CO ₃	240	70	92	-	-
18	DMF/H ₂ O	50:50	0.1	Cs ₂ CO ₃	120	70	67	-	-
19	DMF/H ₂ O	50:50	0.01	Cs ₂ CO ₃	120	70	42	-	-

[a] Reaction conditions: phenyl bromide (1 mmol), benzenboronic acid (1.5 mmol), solvent (5 mL,) under N₂. The reactions are monitored by GC.

Results and Discussion

At the end, complexes **39a-f** (Scheme 58) with different substituents on the pyrimidyl ring were tested for this reaction (Table 22). As it is shown, substituents on the pyrimidyl ring decrease the activity of the catalyst.



Scheme 58. (*N,N*)PdCl₂ complexes with different substituents on pyrimidyl ring.

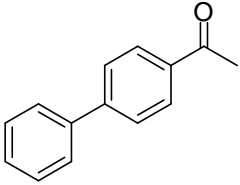
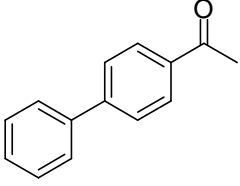
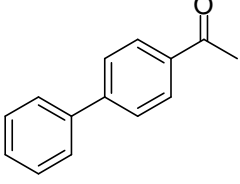
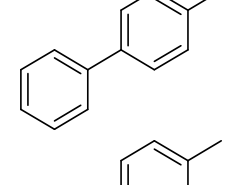
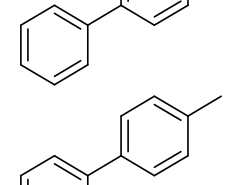
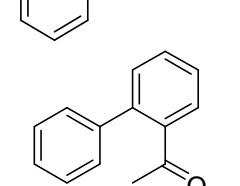
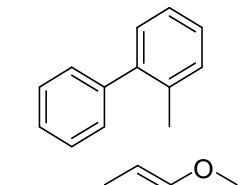
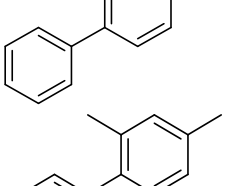
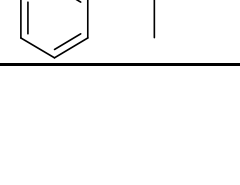

Table 22. Effect of the substituent on the Suzuki-Miyaura reaction of bromobenzene with benzenboronic acid and different palladium catalysts **39a-f**.^[a]

Catalyst	R	Yield
39a	H	100
39b	phenyl	77
39c	naphtyl	96
39d	4-methoxyphenyl	89
39e	4- ⁿ butoxyphenyl	66
39f	^t butyl	85

[a] Reaction conditions: catalyst (0.01 mmol), aryl halide (1 mmol), benzenboronic acid (1.5 mmol), DMF/H₂O (5 ml, 1:1) at 70 °C under N₂. The reactions were monitored by GC.

To elucidate the further potential of complex **39a** in Suzuki–Miyaura transformation, substituted aryl halides were chosen to react with benzenboronic acid, Table 23. Both activated and deactivated aryl bromides and iodides are efficiently converted into biaryls. Aryl chlorides were also examined: unfortunately, the differences in yields determined by GC and ¹H NMR are large for aryl chlorides and the yield could not be determined exactly since different products are formed during the reaction which could not be identified with GC and ¹H NMR.

Table 23. Suzuki-Miyaura reaction of the aryl halides with benzenetricarbonyl acid and **39a**.^[a]

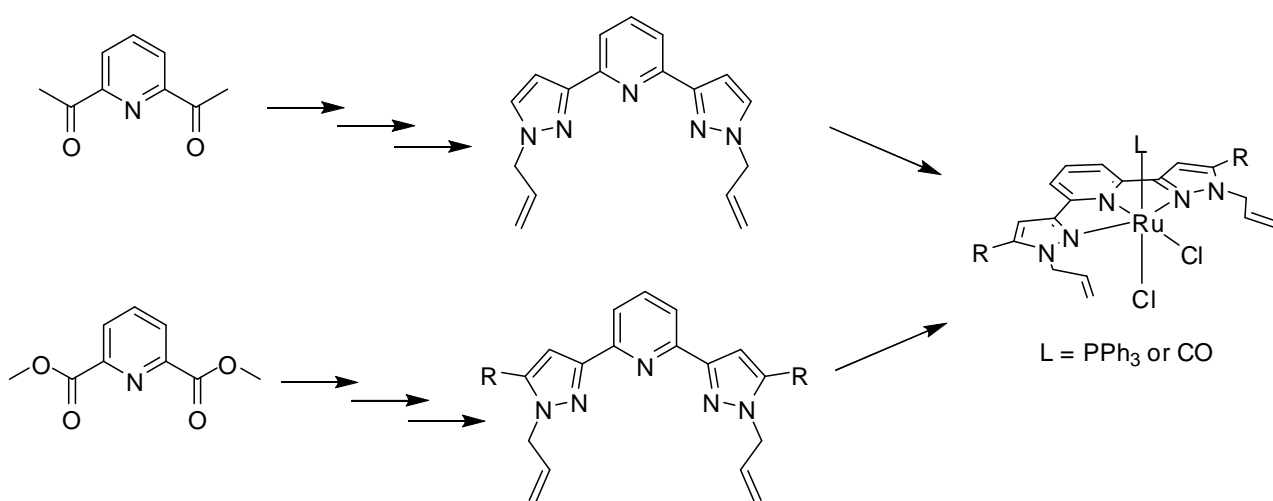
entry	aryl halide	product	yield(%) ^[b]		TOF
			NMR	GC	
1	4-bromoacetophenone		100	100	133
2	4-iodoacetophenone		90	96	120
3	4-chloroacetophenone		22	13	29
4	4-bromotoluene		98	100	131
5	4-iodotoluene		99	100	132
6	4-chlorotoluene		27	4	36
7	2-bromoacetophenone		67	77	89
8	2-bromotoluene		89	90	119
9	1-bromo-4-methoxybenzene		63	74	84
10	4-bromo-xylene		---	2	---

Results and Discussion

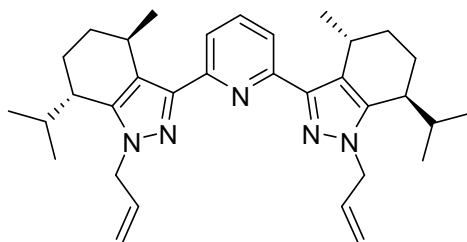
[a] Reaction conditions: **39a** (0.01 mmol), aryl halide (1 mmol), benzenboronic acid (1.5 mmol), DMF/H₂O (5 mL, 1:1) at 70 °C under N₂. [b] after 1h. The reactions are monitored by GC and ¹H NMR.

4 Conclusion and Outlook

The scientific intention of this work was to synthesize and characterize new bidentate, tridentate and multidentate ligands and to apply them in heterogeneous catalysis. For each type of the ligands, new methods of synthesis were developed. Starting from 1,1'-(pyridine-2,6-diyl)diethanone and dimethylpyridine-2,6-dicarboxylate different bispyrazolpyridines were synthesized and novel ruthenium complexes of the type $(L)(NNN)RuCl_2$ could be obtained (Scheme 59). The complexes with $L =$ triphenylphosphine turned out to be highly efficient catalyst precursors for the transfer hydrogenation of aromatic ketones. Introduction of a butyl group in the 5-positions of the pyrazoles leads to a pronounced increase of catalytic activity. Since these catalysts are active at room temperature, the chiral analogues of the dipyrazolpyridine ligands for evaluation of enantioselective transfer hydrogenation shall be synthesized in future (Scheme 60).



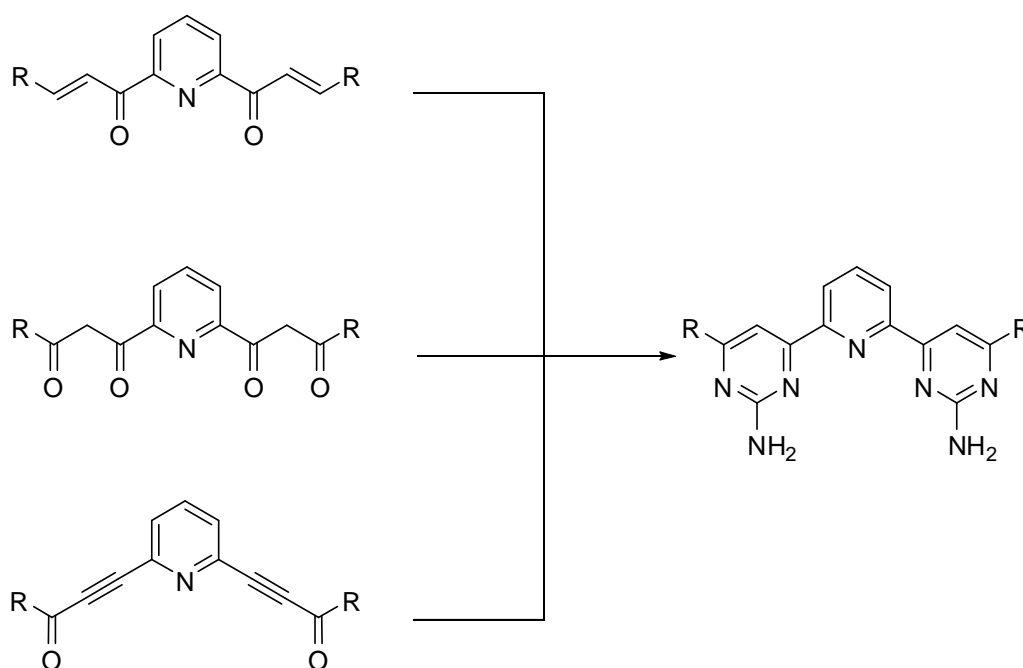
Scheme 59. Synthesis of NNN ligands and their ruthenium complexes.



Scheme 60. An example for a chiral ligand.

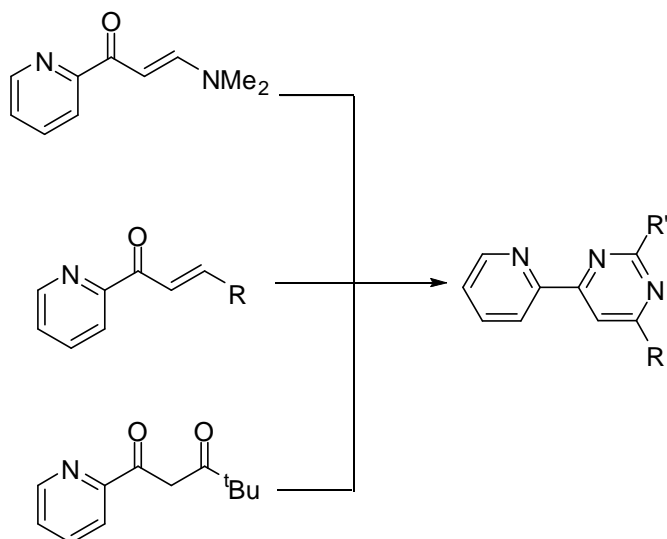
Conclusion and Outlook

To find a method for the synthesis of bispyrimidinepyridines, different reactants (Scheme 61) and condition were applied and it was found that these tridentate ligands can be obtained by mixing and grinding the tetraketone with guanidinium carbonate and silica, which plays the role of a catalyst in this ring closing reaction. In the future, these ligands shall also be investigated for application in catalysis.



Scheme 61. Different reactants examined for synthesizing bispyrimidinepyridines.

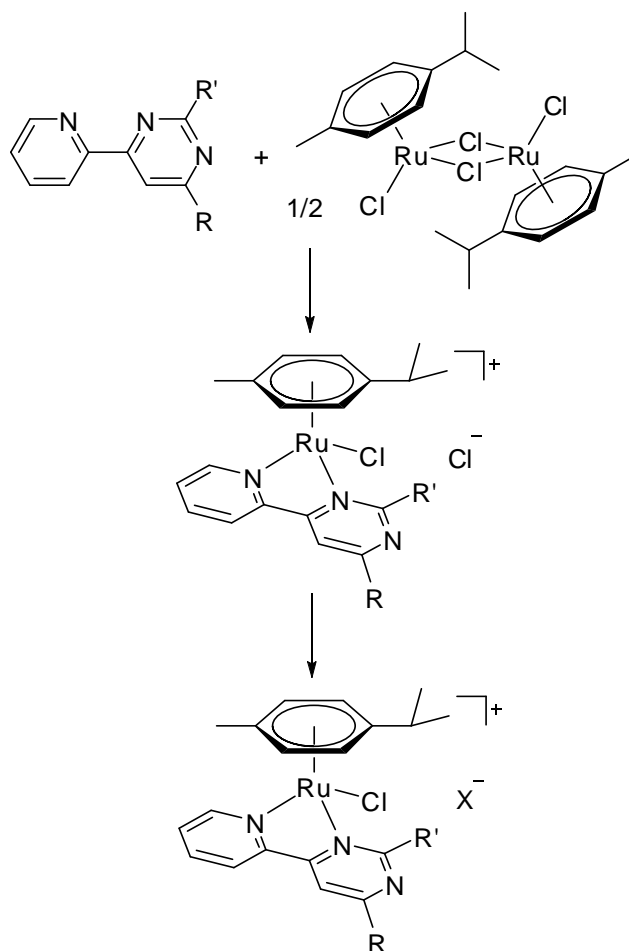
The bidentate 2-amino-4-(2-pyridinyl)pyrimidines were synthesized from different substrates according to the desired substituent on the pyrimidine ring (Scheme 62).



Scheme 62. Different reactants used for synthesizing 2-amino-4-(2-pyridinyl)pyrimidines.

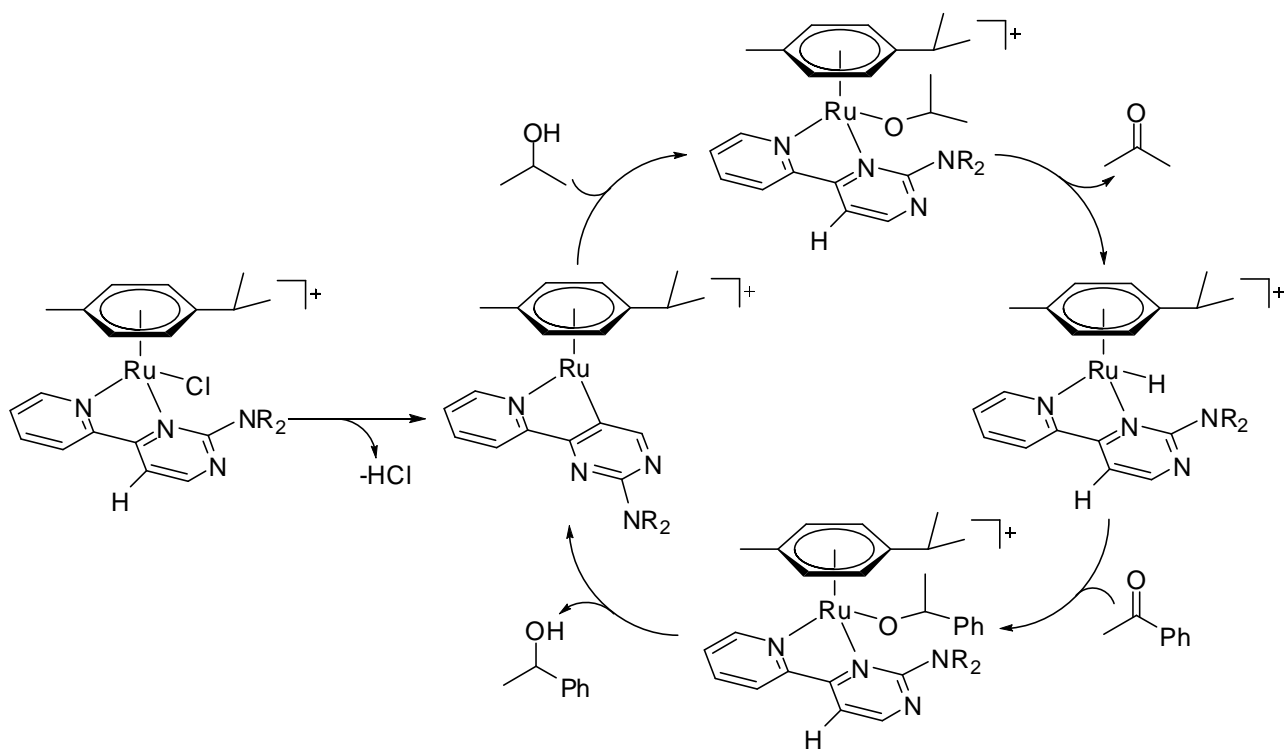
Reacting these bidentate ligands with the ruthenium(II) precursor $[(\eta^6\text{-cymene})\text{Ru}(\text{Cl})(\mu^2\text{-Cl})_2]$ gave cationic ruthenium(II) complexes of the type $[(\eta^6\text{-cymene})\text{Ru}(\text{Cl})(\text{adpm})]\text{Cl}$ (adpm = chelating 2-amino-4-(2-pyridinyl)pyrimidine ligand). Stirring the freshly prepared complexes with either NaBPh_4 , NaBF_4 or KPF_6 , the chloride anion was exchanged against other coordinating anions (BF_4^- , PF_6^- , BPh_4^-) (Scheme 63).

Conclusion and Outlook



Scheme 63. Synthesis of the ruthenium(II) complexes with bidentate ligands.

Some of these ruthenium complexes have shown very special activities in the transfer hydrogenation of ketones by reacting them in the absence of the base. This led to detailed investigations on the mechanism of this reaction. According to the activities and with the help of ESI-MS experiments and DFT calculations, the following mechanism was proposed for the transfer hydrogenation of acetophenone in the absence of the base (Scheme 64). It shows that in the absence of the base, a C-H bond activation at the pyrimidine ring should occur to activate the catalyst. In the future, this concept might be transferred to the other catalytic systems. Additionally, the structure of the ligands can be modified in more details including the synthesis of chiral ligands for enantioselective catalysis.

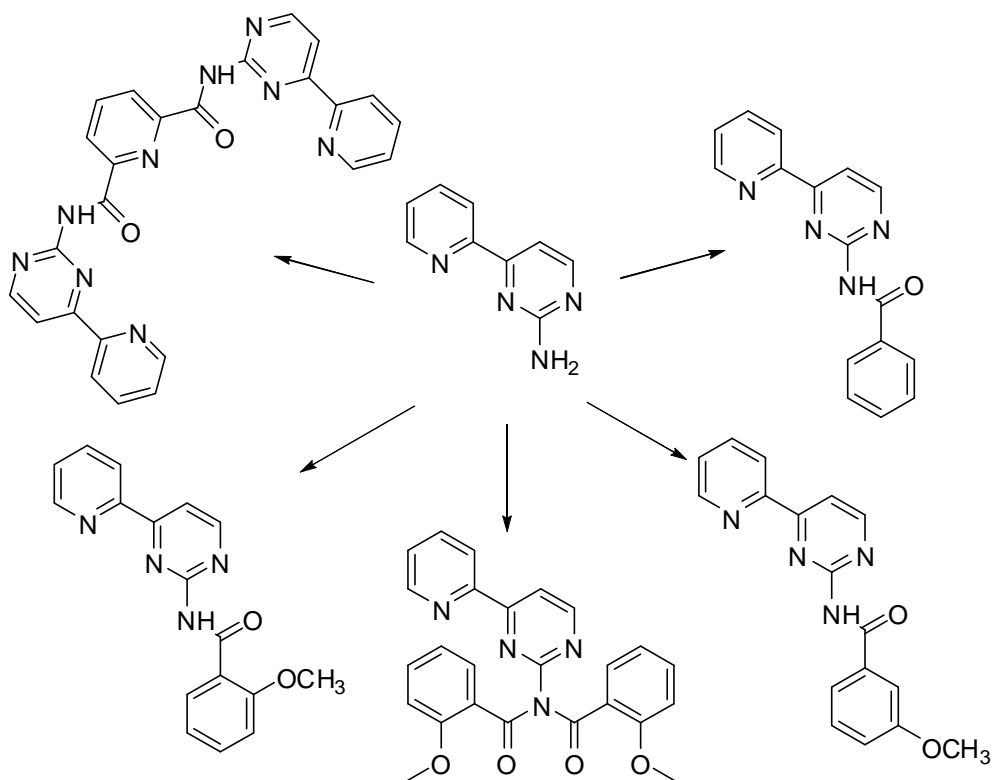


Scheme 64. Reaction mechanism for the transfer hydrogenation in the absence of the base.

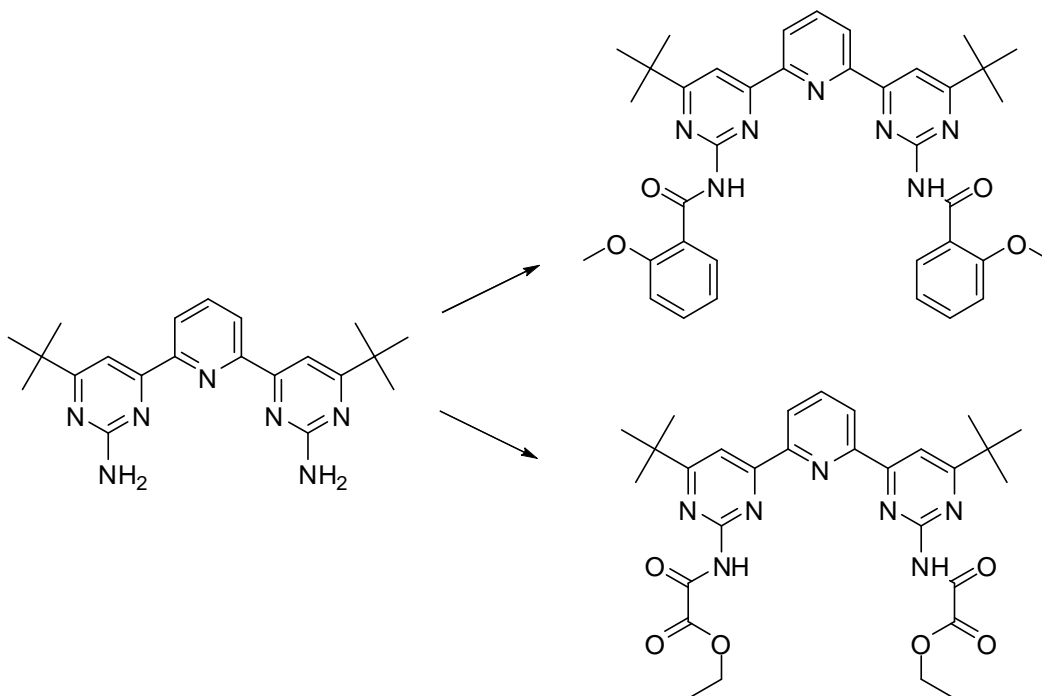
The palladium complexes of bidentate *N,N* ligands were examined in coupling reactions. As expected, they did not show very special activities. However, in future, they should be linked to some phosphine moieties and be investigated for catalytic applications in coupling reactions.

Multidentate ligands, having pyrimidine groups as relatively soft donors for late transition metals and simultaneously possessing a binding position for a hard Lewis-acid, could be obtained using the new synthesized bidentate and tridentate ligands (Scheme 65 and 66). Such systems are matter of interest in the SFB/TRR-88 (3MET) at the TU Kaiserslautern and their complexes should be investigated in future. Hereafter, based on the synthesized bidentate and tridentate ligands more multidentate ligands can be synthesized (Scheme 67).

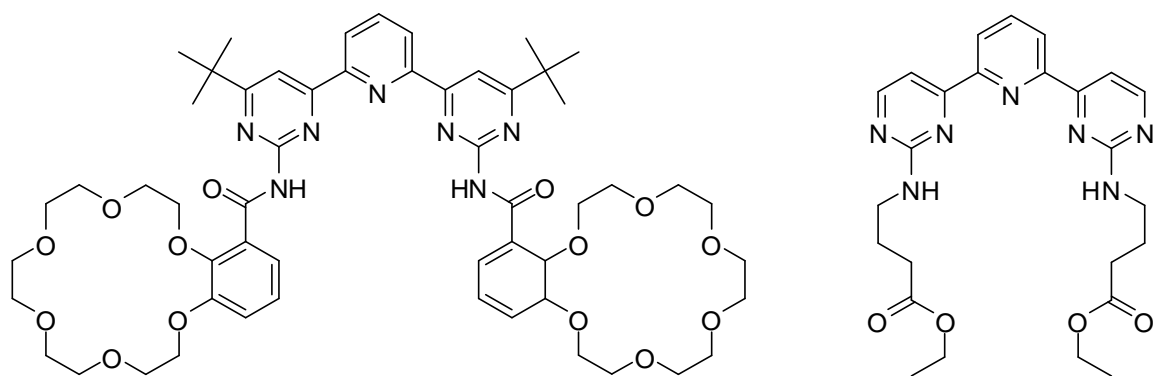
Conclusion and Outlook



Scheme 65. Synthesis of multidentate ligands starting from bidentate ligand.



Scheme 66. Synthesis of multidentate ligands starting from tridentate ligand.



Scheme 67. Two examples of multidentate ligands which might be synthesized in future.

Experimental

5 Experimental

5.1 General Performance

All bought reactants were used without further purification. The silicagel Merck (60, 0.063–0.200 mm) was used for chromatography.

5.2 Used Devices

NMR spectroscopy:

- Bruker DPX 200 (^1H : 200.1 MHz, ^{13}C : 50.3 MHz, ^{31}P : 81.0 MHz)
- Bruker DPX 400 (^1H : 400.1 MHz, ^{13}C : 100.6 MHz, ^{31}P : 162.0 MHz)
- Bruker AVANCE 600 (^1H : 600.1 MHz, ^{13}C : 150.9 MHz)

The chemical shifts are given in δ -values [ppm]. As internal standard for ^1H NMR and ^{13}C NMR spectra the resonance signal of the solvent was concerned according to Gottlieb and Nudelmann; abbreviation: s = singlet, d = doublet, t = triplet, m = multiplet.¹⁶²

Elemental analysis:

The determination of the percentage of carbon, hydrogen, nitrogen and sulfur was done at the analytical laboratory of the TU Kaiserslautern. For this, the following devices were used.

- Perkin Elmer Elemental Analyzer 2400 CHN
- Firma Elementar Analysentechnik: vario Micro cube (CHNS)

Solid state structure analysis:

The measurement of the crystal structures were carried out by Dr. Yu Sun (see index) on a

- Stoe-IPDS X-ray diffractometer and an
- Oxford Diffraction Gemini S Ultra

Gaschromatography/massspectrometry:

GC/MS measurements were done on a Varian 3900 gaschromatograph in combination with a Varian GC/MS Saturn 2100T massspectrometer.

MS spectra were obtained from a

• ESI: Bruker Esquire 3000plus: a 10^{-3} - 10^{-4} molar solution of the sample in acetonitrile was used. The measurements were done by Dipl.-Chem. Fabian Menges from Niedner-Schatteburg's group.

IR-Spectroscopy data were measured as KBr pellets with a

• Jasco FT-IR 6100 spectrometer

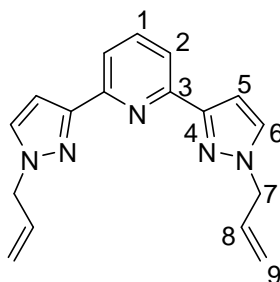
Drying of the solvents:

For THF, toluene, diethylether, pentane and dichloromethane a Mbraun MB-SPS solventdrier was used. All the other solvents were dried according to general methods.¹⁶³

5.3 Ligand Synthesis

5.3.1. Synthesis of the *NNN* Ligands

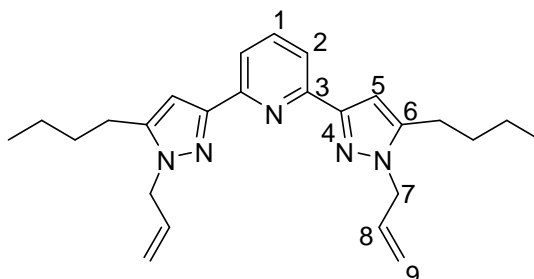
5.3.1.1. *Synthesis of Ligands with a Bispyrazolyipyridine Backbone*



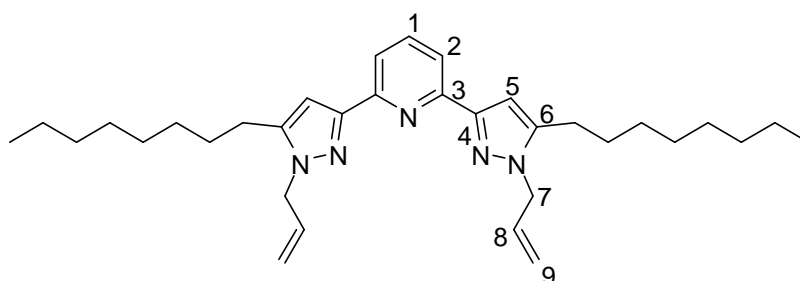
2,6-Di(1-allyl-1H-pyrazol-3-yl)pyridine (5). 0.16 g of LiH (20 mmol) were added to a solution of 2.1 g of 2,6-di(1H-pyrazol-3-yl)pyridine (10 mmol) in 75 mL of dry THF. After the evolution of dihydrogen ceased, 1.2 g of allylicbromide (20 mmol) were added and the reaction mixture and was stirred for 12 h. After evaporating the solvent under vacuum, the product was extracted with chloroform and the organic phase was filtered over sodium sulfate. Removing the solvent under reduced pressure gave the desired product. Yield: 1.9 g (65%, pale yellow solid). Anal. calcd for $C_{17}H_{17}N_5$: C, 70.08; H, 5.88; N, 24.04. Found: C, 70.82; H, 5.74; N, 23.44. 1H NMR (400.1 MHz, $CDCl_3$, 20 °C): δ 8.22 (s, 2H, H2), 7.86 (s br., 1H, H1), 7.75 (d, $J_{HH} = 2.35$ Hz, 2H, H5), 7.55 (d, $J_{HH} = 2.35$ Hz, 2H, H6), 6.08-5.98 (m, 2H, H8), 5.31-5.24 (m,

Experimental

4H, H9), 4.85 (d, $J_{\text{HH}} = 5.87$ Hz, 4H, H7). $^{13}\text{C}\{^1\text{H}\}$ NMR (100.6 MHz, CDCl_3 , 20 °C): δ 147.9 (s, C3), 144.8 (s, C4), 143.3 (s, C1), 132.0 (s, C8), 131.7 (s, C6), 121.4 (s, C2), 119.7 (s, C9), 108.9 (s, C5), 55.4 (s, C7).

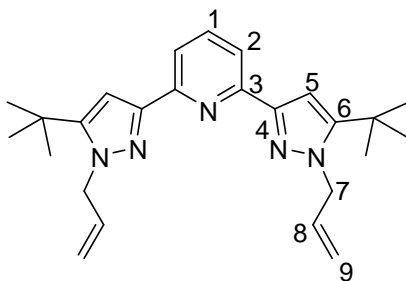


2,6-Di(1-allyl-5-butyl-1H-pyrazol-3-yl)pyridine (6a). The same procedure as for 2,6-di(1-allyl-1H-pyrazol-3-yl)pyridine was applied, just 2,6-bis(5-butyl-1H-pyrazol-3-yl)pyridine was used instead of 2,6-di(1H-pyrazol-3-yl)pyridine. Yield: 2.8 g (70%, pale yellow solid). Anal. calcd for $\text{C}_{25}\text{H}_{33}\text{N}_5$: C, 74.40; H, 8.24; N, 17.35. Found: C, 74.29; H, 8.25; N, 17.40. ^1H NMR (400.1 MHz, CDCl_3 , 20 °C): δ 7.79 (d, $J_{\text{HH}} = 7.83$ Hz, 2H, H2), 7.59 (t, $J_{\text{HH}} = 7.82$ Hz, 1H, H1), 6.76 (s, 2H, H5), 5.95-5.82 (m, 2H, H8), 5.05 (d, $J_{\text{HH}} = 10.17$ Hz, 2H, H9a), 4.88 (d, $J_{\text{HH}} = 17.22$ Hz, 2H, H9b), 4.62 (s br., 4H, H7), 2.46 (t, $J_{\text{HH}} = 7.83$ Hz, 4H, H_{bu}), 1.61-1.54 (m, 4H, H_{bu}), 1.35-1.26 (m, 4H, H_{bu}), 0.84 (t, $J_{\text{HH}} = 7.43$ Hz, 6H, H_{bu}). $^{13}\text{C}\{^1\text{H}\}$ NMR (100.6 MHz, CDCl_3 , 20 °C): δ 151.8 (s, C3), 150.7 (s, C4), 144.4 (s, C1), 136.5 (s, C6), 133.1 (s, C8), 117.9 (s, C2), 116.5 (s, C9), 103.1 (s, C5), 51.6 (s, C7), 30.2 (s, C_{bu}), 24.9 (s, C_{bu}), 22.1 (s, C_{bu}), 13.6 (s, C_{bu}).



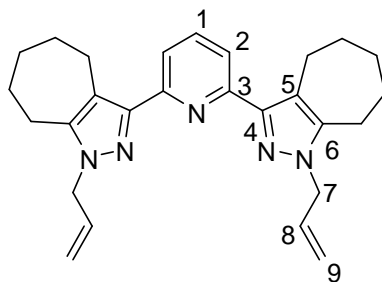
2,6-Di(1-allyl-5-octyl-1H-pyrazol-3-yl)pyridine (6b). The same procedure as for 2,6-di(5-butyl-1H-pyrazol-3-yl)pyridine was applied. Yield: 2.0 g (39%, pale brown solid). Anal. calcd

for $C_{33}H_{49}N_5 + 0.5CH_2Cl_2$: C, 72.08; H, 9.03; N, 12.55. Found: C, 72.11; H, 8.92; N, 11.93. 1H NMR (400.1 MHz, $CDCl_3$, 20 °C): δ 7.83 (d, $J_{HH} = 7.83$ Hz, 2H, H2), 7.65 (t, $J_{HH} = 7.63$ Hz, 1H, H1), 6.81 (s, 2H, H5), 5.99-5.92 (m, 2H, H8), 5.15 (d, $J_{HH} = 10.18$ Hz, 2H, H9a), 4.98 (d, $J_{HH} = 17.16$ Hz, 2H, H9b), 4.72 (d, $J_{HH} = 5.09$, 4H, H7), 2.57 (t, $J_{HH} = 7.63$ Hz, 4H, H_{octyl}), 1.71-1.61 (m, 4H, H_{octyl}), 1.36-1.25 (m, 20H, H_{octyl}), 0.86 (t, $J_{HH} = 6.04$ Hz, 6H, H_{octyl}). $^{13}C\{^1H\}$ NMR (100.6 MHz, $CDCl_3$, 20 °C): δ 152.2 (s, C3), 151.1 (s, C4), 144.6 (s, C1), 136.6 (s, C6), 133.5 (s, C8), 118.2 (s, C2), 116.8 (s, C9), 103.5 (s, C5), 51.9 (s, C7), 31.8 (s, C_{octyl}), 29.3 (s, C_{octyl}), 29.1 (s, C_{octyl}), 28.6 (s, C_{octyl}), 25.6 (s, C_{octyl}), 22.6 (s, C_{octyl}), 14.0 (s, C_{octyl}).

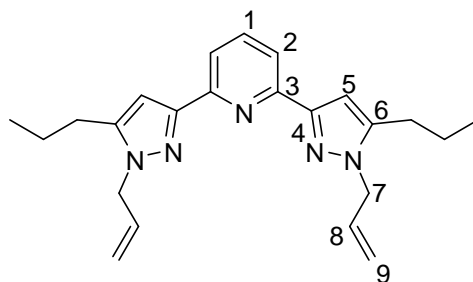


2,6-Di(1-allyl-5-*t*butyl-1*H*-pyrazol-3-yl)pyridine (6c). The same procedure as for 2,6-di(1-allyl-1*H*-pyrazol-3-yl)pyridine was applied, just 2,6-bis(5-*t*butyl-1*H*-pyrazol-3-yl)pyridine was used instead of 2,6-di(1*H*-pyrazol-3-yl)pyridine. Yield: 3.2 g (81%, pale yellow solid). Anal. calcd for $C_{25}H_{33}N_5 + 0.33CH_2Cl_2$: C, 70.45; H, 7.86; N, 16.22. Found: C, 69.36; H, 8.02; N, 16.42. 1H NMR (200.1 MHz, $CDCl_3$, 20 °C): δ 7.85 (d, $J_{HH} = 7.7$ Hz, 2H, H2), 7.71-7.62 (m, 1H, H1), 6.81 (s, 2H, H5), 6.00-5.90 (m, 2H, H8), 5.19 (d, $J_{HH} = 10.8$ Hz, 2H, H9a), 5.01 (d, $J_{HH} = 17.6$ Hz, 2H, H9b), 4.91 (d, $J_{HH} = 4.8$ Hz, 4H, H7), 1.40 (s, 18H, H_{tbu}). $^{13}C\{^1H\}$ NMR (50.3 MHz, $CDCl_3$, 20 °C): δ 152.8 (s, C3), 152.2 (s, C4), 150.5 (s, C1), 136.9 (s, C6), 134.7 (s, C8), 118.5 (s, C2), 116.9 (s, C9), 102.6 (s, C5), 53.7 (s, C7), 31.5 (s, C_{tbu}), 30.3 (s, C_{tbu}).

Experimental



2,6-Bis(1-allyl-5,6,7,8-tetrahydro-4H-cycloheptapyrazol-3-yl)pyridine (6d). The same procedure as for 2,6-di(5-butyl-1*H*-pyrazol-3-yl)pyridine was applied. Yield: 3.7 g (88%, pale brown solid). Anal. calcd for $C_{27}H_{33}N_5 + 0.25CH_2Cl_2$: C, 72.92; H, 7.52; N, 15.60. Found: C, 73.01; H, 7.76; N, 15.14. 1H NMR (400.1 MHz, $CDCl_3$, 20 °C): δ 7.74 (d, $J_{HH} = 7.62$ Hz, 2H, H2), 7.68-7.64 (m, 1H, H1), 5.99-5.90 (m, 2H, H8), 5.15 (d, $J_{HH} = 10.49$ Hz, 2H, H9a), 5.00 (d, $J_{HH} = 17.16$ Hz, 2H, H9b), 4.72 (d, $J_{HH} = 5.09$, 4H, H7), 3.17 (t, $J_{HH} = 5.4$ Hz, 4H, $H_{cycloheptyl}$), 2.68 (t, $J_{HH} = 5.4$ Hz, 4H, $H_{cycloheptyl}$) 1.83-1.80 (m, 4H, $H_{cycloheptyl}$), 1.68-1.67 (m, 8H, $H_{cycloheptyl}$). $^{13}C\{^1H\}$ NMR (100.6MHz, $CDCl_3$, 20 °C): δ 153.5 (s, C3), 147.5 (s, C4), 143.6 (s, C1), 136.4 (s, C6), 133.8 (s, C8), 120.7 (s, C5), 119.8 (s, C2), 116.6 (s, C9), 52.2 (s, C7), 32.0 (s, $C_{cycloheptyl}$), 28.6 (s, $C_{cycloheptyl}$), 26.8 (s, $C_{cycloheptyl}$), 26.4 (s, $C_{cycloheptyl}$), 24.7 (s, $C_{cycloheptyl}$).

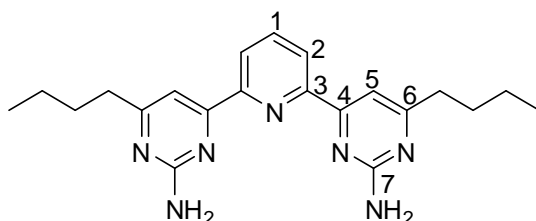


2,6-Di(1-allyl-5-propyl-1*H*-pyrazol-3-yl)pyridine (6e). The same procedure as for 2,6-di(5-butyl-1*H*-pyrazol-3-yl)pyridine was applied. Yield: 3.3 g (89%, pale yellow solid). Anal. calcd for $C_{23}H_{29}N_5$: C, 73.57; H, 7.78; N, 18.65. Found: C, 73.29; H, 8.10; N, 18.40. 1H NMR (400.1 MHz, $CDCl_3$, 20 °C): δ 7.83 (d, $J_{HH} = 7.71$ Hz, 2H, H2), 7.68 (t, $J_{HH} = 7.7$ Hz, 1H, H1), 6.81 (s, 2H, H5), 6.01-5.91 (m, 2H, H8), 5.16 (d, $J_{HH} = 10.27$ Hz, 2H, H9a), 4.98 (d, $J_{HH} = 16.88$

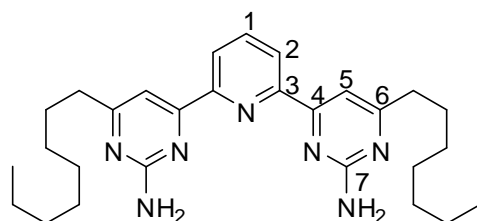
Hz, 2H, H9b), 4.73 (s, 4H, H7), 2.56 (t, $J_{\text{HH}} = 7.33$ Hz, 4H, H_{propyl}), 1.74-1.69 (m, 4H, H_{propyl}), 0.99 (t, $J_{\text{HH}} = 7.34$ Hz, 6H, H_{propyl}). $^{13}\text{C}\{^1\text{H}\}$ NMR (100.6 MHz, CDCl_3 , 20 °C): δ 152.2 (s, C3), 151.2 (s, C4), 143.4 (s, C1), 136.7 (s, C6), 133.5 (s, C8), 118.2 (s, C2), 116.8 (s, C9), 103.6 (s, C5), 52.0 (s, C7), 27.6 (s, C_{propyl}), 21.9 (s, C_{propyl}), 13.9 (s, C_{propyl}).

5.3.1.2 Synthesis of Ligands with a Bispyrimidylpyridine Backbone

General methode for the synthesis of 2,6-bis(2-amino-4-alkyl-6-pyrimidyl)pyridines. 10 mmol of precursor **3**, 10 mmol of guanidinium carbonate and X g of silica (X= [mass of the precursor **3** in grams + mass of the guanidinium carbonate in grams] * 2) were ground together and the mixture was put in an oven at 200° C for 4 h. After cooling to room teperature, the product was washed from the silica with ethanol using a soxhlet extractor.

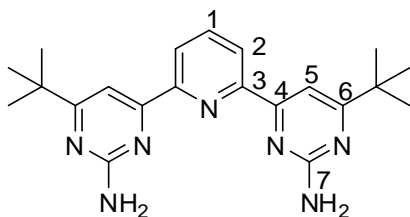


2,6-Bis(2-amino-4-*n*butyl-6-pyrimidyl)pyridine (8a). Since the product was not pure no yield and elemental analysis is reported. ^1H NMR (400.1 MHz, CDCl_3 , 20 °C): δ 8.36 (d, $J_{\text{HH}} = 7.83$ Hz, 2H, H2), 7.92 (t, $J_{\text{HH}} = 7.82$ Hz, 1H, H1), 7.60 (s, 2H, H5), 5.63 (s br., 4H, NH_2), 2.70 (t, $J_{\text{HH}} = 7.82$ Hz, 4H, H_{butyl}), 1.79-1.71 (m, 4H, H_{butyl}), 1.48-1.39 (m, 4H, C_{butyl}), 0.96 (t, $J_{\text{HH}} = 7.44$ Hz, 6H, H_{butyl}). ^{13}C NMR (100.6 MHz, CDCl_3 , 20 °C): δ 173.6 (s, C6), 163.8 (s, C4), 163.4 (s, C7), 154.5 (s, C3), 137.9 (s, C1), 122.8 (s, C2), 107.1 (s, C5), 38.0 (s, C_{butyl}), 31.1 (s, C_{butyl}), 22.7 (s, C_{butyl}), 14.0 (s, C_{butyl}).

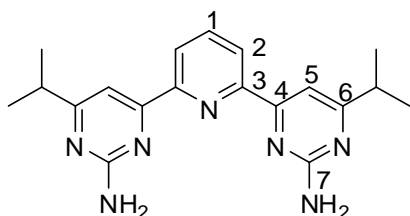


Experimental

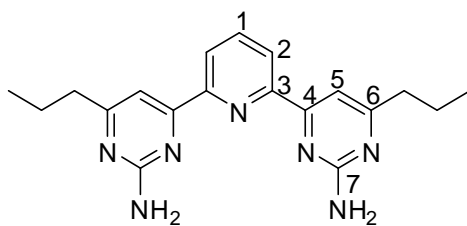
2,6-Bis(2-amino-4-*n*octyl-6-pyrimidyl)pyridine (8b). Since the product was not pure no yield and elemental analysis is reported. ^1H NMR (400.1 MHz, CDCl_3 , 20 °C): δ 8.42 (d, $J_{\text{HH}} = 7.83$ Hz, 2H, H2), 7.94 (t, $J_{\text{HH}} = 7.43$ Hz, 1H, H1), 7.67 (s, 2H, H5), 5.12 (s br, 4H, NH_2), 2.74 (t, $J_{\text{HH}} = 7.83$ Hz, 4H, H_{octyl}), 1.79-1.74 (m, 4H, H_{octyl}), 1.42-1.27 (m, 26H, C_{octyl}). The sample was very impure and ^{13}C NMR could not be interpreted.



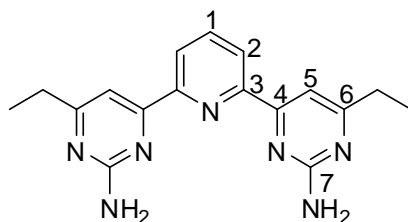
2,6-bis(2-amino-4-*t*butyl-6-pyrimidyl)pyridine (8c). Since the product was not pure no yield and elemental analysis is reported. ^1H NMR (400.1 MHz, CDCl_3 , 20 °C): δ 8.40 (d, $J_{\text{HH}} = 7.83$ Hz, 2H, H2), 7.96-7.91 (m, 3H, H1 & H5), 5.12 (s br., 4H, NH_2), 1.39 (s, 18H, $\text{H}_{t\text{-butyl}}$). ^{13}C NMR (100.6 MHz, CDCl_3 , 20 °C): δ 180.5 (s, C6), 163.9 (s, C4), 163.2 (s, C7), 154.5 (s, C3), 138.0 (s, C1), 122.5 (s, C2), 103.8 (s, C5), 37.6 (s, $\text{C}_{t\text{-butyl}}$), 29.5 (s, $\text{C}_{t\text{-butyl}}$).



2,6-Bis(2-amino-4-isopropyl-6-pyrimidyl)pyridine (8d). Since the product was not pure no yield and elemental analysis is reported. ^1H NMR (400.1 MHz, CDCl_3 , 20 °C): δ 8.41 (d, $J_{\text{HH}} = 7.83$ Hz, 2H, H2), 7.94 (t, $J_{\text{HH}} = 7.82$ Hz, 1H, H1), 7.71 (s br., 2H, H5), 5.15 (s br., 4H, NH_2), 3.00-2.93 (m, 2H, H_{propyl}), 1.36 (d, $J_{\text{HH}} = 7.04$ Hz, 12H, H_{propyl}). ^{13}C NMR (100.6 MHz, CDCl_3 , 20 °C): δ 178.4 (s, C6), 164.0 (s, C4), 163.4 (s, C7), 154.5 (s, C3), 138.0 (s, C1), 122.8 (s, C2), 105.1 (s, C5), 36.3 (s, C_{propyl}), 21.8 (s, C_{propyl}).

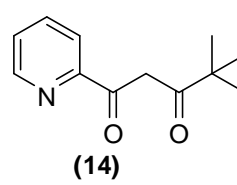
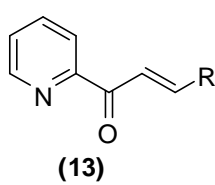
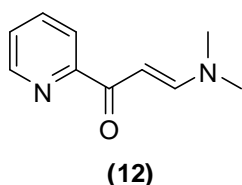


2,6-Bis(2-amino-4-*n*propyl-6-pyrimidyl)pyridine (8e). Since the product was not pure no yield and elemental analysis is reported. ^1H NMR (400.1 MHz, CDCl_3 , 20 °C): δ 8.42 (d, $J_{\text{HH}} = 7.83$ Hz, 2H, H2), 7.94 (t, $J_{\text{HH}} = 7.82$ Hz, 1H, H1), 7.66 (s br., 2H, H5), 5.14 (s br., 4H, NH_2), 2.71 (t, $J_{\text{HH}} = 7.44$ Hz, 4H, H_{propyl}), 1.83-1.79 (m, 4H, H_{propyl}), 1.04 (t, $J_{\text{HH}} = 7.04$ Hz, 6H, H_{propyl}). ^{13}C NMR (100.6 MHz, CDCl_3 , 20 °C): δ 173.4 (s, C6), 163.8 (s, C4), 163.4 (s, C7), 154.5 (s, C3), 138.0 (s, C1), 122.9 (s, C2), 107.3 (s, C5), 40.3 (s, C_{propyl}), 22.3 (s, C_{propyl}), 14.1 (s, C_{propyl}).



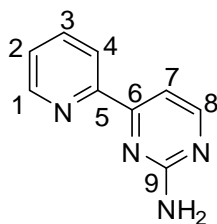
2,6-Bis(2-amino-4-ethyl-6-pyrimidyl)pyridine (8f). Since the product was not pure no yield and elemental analysis is reported. ^1H NMR (400.1 MHz, CDCl_3 , 20 °C): δ 8.43 (d, $J_{\text{HH}} = 7.83$ Hz, 2H, H2), 7.95 (t, $J_{\text{HH}} = 7.83$ Hz, 1H, H1), 7.70 (s br., 2H, H5), 5.12 (s br., 4H, NH_2), 2.79 (q, 4H, H_{ethyl}), 1.36 (t, $J_{\text{HH}} = 7.43$ Hz, 6H, H_{ethyl}). ^{13}C NMR (100.6 MHz, CDCl_3 , 20 °C): δ 174.6 (s, C6), 163.9 (s, C4), 163.3 (s, C7), 154.5 (s, C3), 138.0 (s, C1), 122.9 (s, C2), 106.6 (s, C5), 31.4 (s, C_{ethyl}), 13.1 (s, C_{ethyl}).

5.3.2 Synthesis of NN Ligands

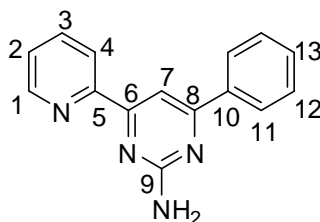


Experimental

Synthesis of precursors 12-14. Precursor **12**,¹⁶⁴ **13**^{102b} and **14**^{91c, 165} were synthesized according to procedures published in the literature.

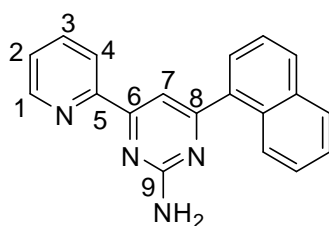


4-(Pyridin-2-yl)pyrimidin-2-amine (17a). Method 1. Under an atmosphere of nitrogen atmosphere 1.0 g of Na (43.5 mmol) was added to a solution of 1.8 g of guanidinium carbonate (18.3 mmol) in dry EtOH (20 ml). When the reaction of Na and EtOH was completed, 3.0 g of precursor **12** (17 mmol) were added and the solution was refluxed for 24 h. After evaporating the solvent, the residue was washed several times with ice-cooled water and the product was recrystallized from CH₂Cl₂/Et₂O. Yield: 2.3 g (80%, pale brown solid). Anal. Calcd for C₉H₈N₄: C, 62.78; H, 4.68; N, 32.54. Found: C, 62.48; H, 4.68; N, 31.87. ¹H NMR (400.1 MHz, DMSO-*d*₆, 20 °C): δ 8.68 (d, *J*_{HH} = 4.3 Hz, 1H, H1), 8.41 (d, *J*_{HH} = 4.7 Hz, 1H, H8), 8.32 (d, *J*_{HH} = 8.22 Hz, 1H, H4), 7.95-7.91 (m, 1H, H3), 7.49-7.45 (m, 2H, H2 & H7), 6.79 (s br., 2H, NH₂). ¹³C NMR (100.6 MHz, DMSO-*d*₆, 20 °C): δ 163.8 (s, C9), 162.9 (s, C6), 159.5 (s, C8), 154.0 (s, C5), 149.4 (s, C1), 137.2 (s, C3), 125.3 (s, C2), 120.7 (s, C4), 106.0 (s, C7).

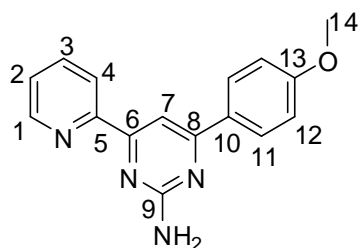


4-Phenyl-6-(pyridin-2-yl)pyrimidin-2-amine (17b). Method 2. 1.67 g of precursor **13b** (8 mmol) were added to a solution of 2.35 g of guanidinium carbonate (24 mmol) in EtOH (25 ml). The solution was refluxed for 24 h. The solvent was evaporated and the residue was dissolved in CH₂Cl₂. The organic phase was washed three times with water and dried over MgSO₄. Yellow crystals were obtained after one day from CH₂Cl₂/Hexane in the refrigerator.

Yield: 1.8 g (92%, pale yellow solid). Anal. calcd for C₁₅H₁₂N₄: C, 72.56; H, 4.87; N, 22.57. Found: C, 71.48; H, 4.91; N, 22.54. ¹H NMR (400.1 MHz, DMSO-*d*₆, 20 °C): δ 8.75 (d, *J*_{HH} = 4.3 Hz, 1H, H1), 8.39 (d, *J*_{HH} = 7.83 Hz, 1H, H4), 8.16-8.13 (m, 2H; H11), 8.06 (s, 1H, H7), 7.98-7.93 (m, 1H, H3), 7.6-7.4 (m, 3H, H2, H12 & H13), 6.92 (s br., 2H, NH₂). ¹³C NMR (100.6 MHz, DMSO-*d*₆, 20 °C): δ 165.2 (s, C6), 164.1 (s, C8), 164.1 (s, C9), 154.2 (s, C5), 149.4 (s, C1), 137.3 (s, C10), 137.2 (s, C3), 130.5 (s, C13), 128.7 (s, C12), 126.8 (s, C11), 125.4 (s, C2), 121.0 (s, C4), 101.8 (s, C7).

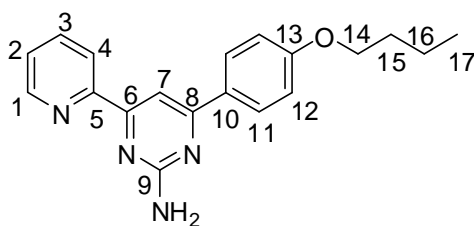


4-(Naphthalen-1-yl)-6-(pyridin-2-yl)pyrimidin-2-amine (17c). The synthesis of **17c** was carried out as described for **17b**, but using 2.07 g of precursor **13c** (8 mmol) and it was crystallized from hexane. Yield: 2.1 g (88%, pale pink solid). Anal. calcd for C₁₉H₁₄N₄ + 0.5 Et₂O: C, 75.15; H, 5.67; N, 16.7. Found: C, 75.65; H, 5.19; N, 17.83. ¹H NMR (400.1 MHz, DMSO-*d*₆, 20 °C): δ 8.70 (d, *J*_{HH} = 3.92 Hz, 1H, H1), 8.42 (d, *J*_{HH} = 7.83 Hz, 1H, H4), 8.26-8.23 (m, 2H, H11), 8.05-7.99 (m, 3H, H3 & H_{naphthyl}), 7.74 (s, 1H, H7), 7.73-7.51 (m, 5H, H2 & H_{naphthyl}), 6.97 (s br., 2H, NH₂). ¹³C NMR (100.6 MHz, DMSO-*d*₆, 20 °C): δ 168.0 (s, C8), 163.9 (s, C6), 163.5 (s, C9), 154.1 (s, C5), 149.5 (s, C1), 137.3 (s, C3), 136.9 (s, C_{naphthyl}), 133.4 (s, C_{naphthyl}), 130.1 (s, C_{naphthyl}), 129.5 (s, C_{naphthyl}), 128.7 (s, C2), 128.4 (s, C_{naphthyl}), 127.0 (s, C_{naphthyl}), 126.6 (s, C_{naphthyl}), 126.1 (s, C4), 125.4 (s, C_{naphthyl}), 125.4 (s, C_{naphthyl}), 125.3 (s, C_{naphthyl}).

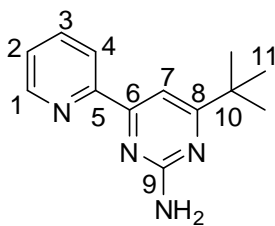


Experimental

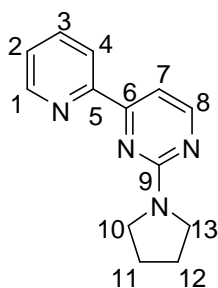
4-(4-Methoxyphenyl)-6-(pyridin-2-yl)pyrimidin-2-amine (17d). The synthesis of **17d** was carried out as described for **17b**, but using 1.91 g of precursor **13d** (8 mmol) and the product was crystallized in EtOH. Yield: 1.5 g (66%, yellow solid). Anal. calcd for C₁₆H₁₄N₄O: C, 69.05; H, 5.07; N, 20.13. Found: C, 68.72; H, 5.18; N, 19.91. ¹H NMR (400.1 MHz, DMSO-*d*₆, 20 °C): δ 8.74 (d, *J*_{HH} = 4.7 Hz, 1H, H1), 8.36 (d, *J*_{HH} = 7.82 Hz, 1H, H4), 8.13 (d, *J*_{HH} = 8.6 Hz, 2H, H11), 8.01-7.95 (m, 2H, H7 & H3), 7.54-7.51 (m, 1H, H2), 7.08 (d, *J*_{HH} = 8.6 Hz, 2H, H12), 6.77 (s br., 2H, NH₂), 3.82 (s, 3H, H14). ¹³C NMR (100.6 MHz, DMSO-*d*₆, 20 °C): δ 165.2 (s, C6), 164.4 (s, C9), 164.2 (s, C8), 161.8 (s, C13), 154.7 (s, C5), 149.8 (s, C1), 137.8 (s, C3), 130.0 (s, C10), 128.8 (s, C12), 125.8 (s, C2), 121.3 (s, C4), 114.6 (s, C11), 101.3 (s, C7), 55.8 (s, C14).



Synthesis of 4-(4-Butoxyphenyl)-6-(pyridin-2-yl)pyrimidin-2-amine (17e). The synthesis of **17e** was carried out as described for **17d**, but 2.25 g of precursor **13e** (8.0 mmol) were applied. Yield: 1.8 g (70%, yellow solid). Anal. calcd for C₁₉H₂₀N₄O: C, 71.23; H, 6.29; N, 17.49. Found: C, 69.69; H, 6.33; N, 17.11. ¹H NMR (400.1 MHz, DMSO-*d*₆, 20 °C): δ 8.74 (d, *J*_{HH} = 4.3 Hz, 1H, H1), 8.36 (d, *J*_{HH} = 7.82 Hz, 1H, H4), 8.10 (d, *J*_{HH} = 8.6 Hz, 2H, H11), 8.01-7.95 (m, 2H, H7 & H3), 7.54-7.51 (m, 1H, H2), 7.05 (d, *J*_{HH} = 9 Hz, 2H, H12), 6.76 (s br., 2H, NH₂), 4.01 (t, *J*_{HH} = 6.65 Hz, 2H, H14), 1.71-1.68 (m, 2H, H15), 1.45-1.40 (m, 2H, H16), 0.91 (t, *J*_{HH} = 7.43, 3H, H17). ¹³C NMR (100.6 MHz, DMSO-*d*₆, 20 °C): δ 164.7 (s, C6), 164.0 (s, C9), 163.7 (s, C8), 160.8 (s, C13), 154.3 (s, C5), 149.4 (s, C1), 137.3 (s, C3), 129.3 (s, C10), 128.3 (s, C12), 125.3 (s, C2), 120.9 (s, C4), 114.5 (s, C11), 100.8 (s, C7), 67.3 (s, C14), 30.7 (s, C15), 18.7 (s, C16), 13.7 (s, C17).



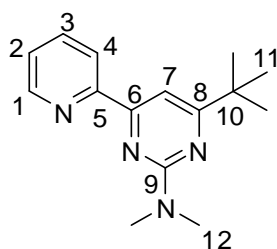
4-tert-Butyl-6-(pyridin-2-yl)pyrimidin-2-amine (17f). Method 3. A solution of 0.8 g of guanidinium carbonate (8.0 mmol) and 0.2 g of Na (8.0 mmol) in dry EtOH (25 ml) was refluxed for 1 h under an atmosphere of nitrogen. 1.64 g of precursor **14** (8 mmol) were added to the solution and it was refluxed for another 24 h. After evaporating the solvent, the residue was washed with cold water and the product was crystallized from EtOH. Yield: 0.5 g (30%, pale yellow crystal). Anal. calcd for C₁₃H₁₆N₄: C, 68.39; H, 7.06; N, 24.54. Found: C, 68.18; H, 6.97; N, 24.13. ¹H NMR (400.1 MHz, DMSO-*d*₆, 20 °C): δ 8.70 (d, *J*_{HH} = 3.92 Hz, 1H, H1), 8.30 (d, *J*_{HH} = 8.22 Hz, 1H, H4), 7.96-7.92 (m, 1H, H3), 7.56 (s, 1H, H7), 7.50-7.47 (m, 1H, H2), 6.60 (s br., 2H, NH₂), 1.27 (s, 9H, H11). ¹³C NMR (100.6 MHz, DMSO-*d*₆, 20 °C): δ 179.2 (s, C8), 163.5 (s, C6), 163.2 (s, C9), 154.4 (s, C5), 149.3 (s, C1), 137.2 (s, C3), 125.1 (s, C2), 120.8 (s, C4), 101.0 (s, C7), 37.1 (s, C10), 29.2 (s, C11).



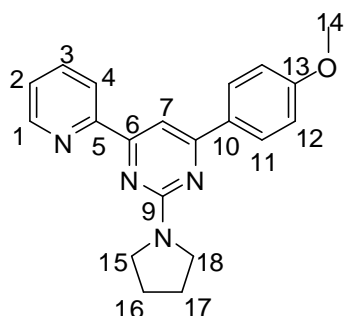
4-(Pyridin-2-yl)-2-(pyrrolidin-1-yl)pyrimidine (17g). Method 1 was applied, using the corresponding guanidinium derivative. Yield: 3.2 g (84%, pale yellow solid). Anal. calcd for C₁₃H₁₄N₄: C, 69.00; H, 6.24; N, 24.76. Found: C, 69.35; H, 6.25; N, 24.30. ¹H NMR (400.1 MHz, DMSO-*d*₆, 20 °C): δ 8.67 (d, *J*_{HH} = 4.31 Hz, 1H, H1), 8.44 (d, *J*_{HH} = 5.09 Hz, 1H, H8), 8.36 (d, *J*_{HH} = 7.83 Hz, 1H, H4), 7.94-7.90 (m, 1H, H3), 7.49-7.45 (m, 2H, H2 & H7), 3.51 (s br., 4H, H10 & H13), 1.91-1.87 (m, 4H, H11 & H12). ¹³C NMR (100.6 MHz, DMSO-*d*₆, 20

Experimental

$^{\circ}\text{C}$): δ 162.3 (s, C6), 160.0 (s, C9), 159.0 (s, C8), 154.2 (s, C5), 149.3 (s, C1), 137.1 (s, C3), 125.3 (s, C2), 120.8 (s, C4), 104.6 (s, C7), 44.2 (s, C10 & C13), 25.0 (s, C11 & C12).

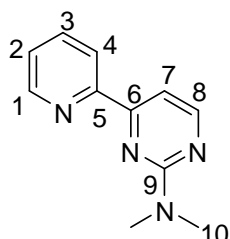


4-*tert*-Butyl-*N,N*-dimethyl-6-(pyridin-2-yl)pyrimidi-2-amine (17h). Method 3 was applied, using the corresponding guanidinium derivative. Yield: 0.7 g (35%, pale yellow solid). Anal. calcd for $\text{C}_{15}\text{H}_{20}\text{N}_4$: C, 70.28; H, 7.86; N, 21.86. Found: C, 69.94; H, 7.69; N, 21.94. ^1H NMR (400.1 MHz, $\text{DMSO-}d_6$, $20\text{ }^{\circ}\text{C}$): δ 8.70 (d, $J_{\text{HH}} = 3.91$ Hz, 1H, H1), 8.40 (d, $J_{\text{HH}} = 7.82$ Hz 1H, H4), 7.97-7.93 (m, 1H, H3), 7.55 (s, 1H, H7), 7.55-7.49 (m, 1H, H2), 3.21 (s, 6H, H12), 1.30 (s, 9H, H11). ^{13}C NMR (100.6 MHz, $\text{DMSO-}d_6$, $20\text{ }^{\circ}\text{C}$): δ 178.7 (s, C8), 162.7 (s, C6), 161.7 (s, C9), 154.5 (s, C1), 149.2 (s, C5), 137.3 (s, C3), 125.2 (s, C2), 121.0 (s, C4), 99.8 (s, C7), 37.4 (s, C10), 36.5 (s, C12), 29.2 (s, C11).

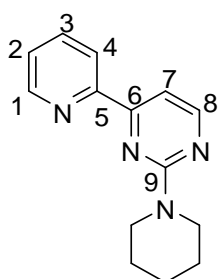


4-(4-Methoxyphenyl)-6-(pyridin-2-yl)-2-(pyrrolidin-1-yl)pyrimidine (17i). Method 2 was applied, using the corresponding guanidinium derivative. Yield: 2.3 g (88%, pale yellow solid). Anal. calcd for $\text{C}_{20}\text{H}_{20}\text{N}_4\text{O}$: C, 72.27; H, 6.06; N, 16.86. Found: C, 71.81; H, 6.03; N, 16.67. ^1H NMR (400.1 MHz, $\text{DMSO-}d_6$, $20\text{ }^{\circ}\text{C}$): δ 8.74 (d, $J_{\text{HH}} = 4.69$ Hz, 1H, H1), 8.45 (d, $J_{\text{HH}} = 7.82$ Hz, 1H, H4), 8.18 (d, $J_{\text{HH}} = 8.61$ Hz, 2H, H11), 8.01-7.97 (m, 1H, H3 & H7), 7.55-7.52 (m, 1H, H2), 7.09 (d, $J_{\text{HH}} = 8.61$ Hz, 2H, H12), 3.84 (s, 3H, H14), 3.67 (s br., 4H, H15 & H18),

1.99 (s br., 4H, H16 & H17). ^{13}C NMR (100.6 MHz, DMSO- d_6 , 20 °C): δ 164.1 (s, C6), 163.2 (s, C8), 161.4 (s, C13), 160.4 (s, C9), 154.4 (s, C5), 149.3 (s, C1), 137.3 (s, C3), 129.7 (s, C10), 128.4 (s, C12), 125.4 (s, C2), 121.0 (s, C4), 114.1 (s, C11), 99.5 (s, C7), 55.3 (s, C14), 46.4 (s, H15 & H18), 25.1 (s, C16 & C17).



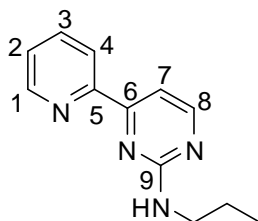
***N,N*-Dimethyl-4-(pyridine-2-yl)pyrimidine (17j)**. Method 1 was applied, using the corresponding guanidinium derivative. Yield: 2.9 g (85%, pale yellow solid). Anal. calcd for $\text{C}_{11}\text{H}_{12}\text{N}_4$: C, 65.98; H, 6.04; N, 27.98. Found: C, 66.19; H, 6.10; N, 26.68. ^1H NMR (400.1 MHz, DMSO- d_6 , 20 °C): δ 8.67 (d, $J_{\text{HH}} = 4.7$ Hz, 1H, H1), 8.47 (d, $J_{\text{HH}} = 5.09$ Hz, 1H, H8), 8.38 (d, $J_{\text{HH}} = 8.22$ Hz, 1H, H4), 7.95-7.92 (m, 1H, H3), 7.5-7.45 (m, 2H, H2 & H7), 3.17 (s br., 6H, H10). ^{13}C NMR (100.6 MHz, DMSO- d_6 , 20 °C): δ 162.3 (s, C6), 161.9 (s, C9), 159.0 (s, C8), 154.1 (s, C5), 149.3 (s, C1), 137.2 (s, C3), 125.4 (s, C2), 120.8 (s, C4), 104.7 (s, C7), 36.5 (s, C10).



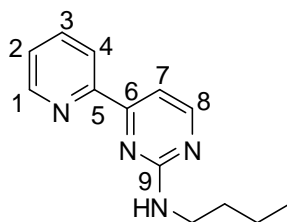
4-(2-Pyridinyl)-2-(1-piperidinyl)-pyrimidin (17k). Method 1 was applied, using the corresponding guanidinium derivative. Yield: 1.3 g (55%, brown oil). Anal. calcd for $\text{C}_{14}\text{H}_{16}\text{N}_4$: C, 69.97; H, 6.71; N, 23.32. Found: C, 69.32; H, 7.18; N, 23.24. ^1H NMR (400.1 MHz, DMSO d_6 , 20 °C): δ 8.65 (d, $J_{\text{HH}} = 3.92$ Hz, 1H, H1), 8.44 (d, $J_{\text{HH}} = 5.08$ Hz, 1H, H8), 8.31 (d, $J_{\text{HH}} = 7.84$ Hz, 1H, H4), 7.87 (t, $J_{\text{HH}} = 7.72$ Hz, 1H, H3), 7.46 (d, $J_{\text{HH}} = 5.08$ Hz, 1H,

Experimental

H7), 7.42 (t, $J_{\text{HH}} = 5.88$ Hz, 1H, H2), 3.37 (t, $J_{\text{HH}} = 5.10$ Hz, 4H, $\text{H}_{\text{piperdinyl}}$), 1.51-1.53 (m, 2H, $\text{H}_{\text{piperdinyl}}$), 1.46-1.47 (m, 4H, $\text{H}_{\text{piperdinyl}}$). ^{13}C NMR (100.6 MHz, $\text{DMSO } d_6$, 20 °C): δ 162.5 (s, C9), 161.2 (s, C8), 158.9 (s, C6), 154.1 (s, C5), 149.2 (s, C1), 136.9 (s, C3), 125.1 (s, C2), 120.7 (s, C4), 104.9 (s, C7), 54.8 (s, $\text{C}_{\text{piperdinyl}}$), 44.1 (s, $\text{C}_{\text{piperdinyl}}$), 25.2 (s, $\text{C}_{\text{piperdinyl}}$).

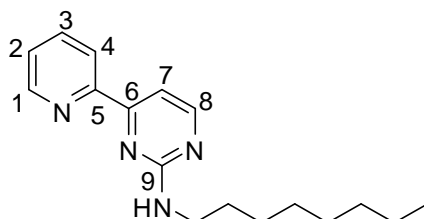


***N*-1-Propyl-4-(2-pyridinyl)pyrimidin-2-amin (17l).** Method 1 was applied, using the corresponding guanidinium derivative. Yield: 1.2 g (58%, light pink solid). Anal. calcd for $\text{C}_{12}\text{H}_{14}\text{N}_4$: C, 67.27; H, 6.59; N, 26.15. Found: C, 67.75; H, 6.83; N, 25.41. ^1H NMR (400.1 MHz, $\text{DMSO } d_6$, 20 °C): δ 8.67 (d, $J_{\text{HH}} = 3.88$ Hz, 1H, H1), 8.40 (d, $J_{\text{HH}} = 3.92$ Hz, 1H, H8), 8.33 (d, $J_{\text{HH}} = 5.88$ Hz, 1H, H4), 7.95 (t, $J_{\text{HH}} = 7.62$ Hz, 1H, H3), 7.49 (t, $J_{\text{HH}} = 6.06$ Hz, 1H, H2), 7.43 (d, $J_{\text{HH}} = 4.68$ Hz, 1H, H7), 7.24 (s, 1H, NH), 3.31 (s, 2H, H_{propyl}), 1.54-1.59 (m, $J_{\text{HH}} = 6.67$ Hz, 2H, H_{propyl}), 0.89 (t, $J_{\text{HH}} = 7.44$ Hz, 3H, H_{propyl}). ^{13}C NMR (100.6 MHz, $\text{DMSO } d_6$, 20 °C): δ 162.6 (s, C9), 159.4 (s, C6, C8), 154.2 (s, C5), 149.5 (s, C1), 137.4 (s, C3), 125.5 (s, C2), 120.9 (s, C4), 105.5 (s, C7), 42.7 (s, C_{Propyl}), 22.3 (s, C_{Propyl}), 11.6 (s, C_{Propyl}).

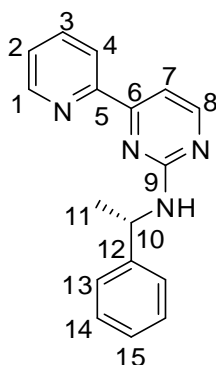


***N*-1-Butyl-4-(2-pyridinyl)pyrimidin-2-amin (17m).** Method 1 was applied, using the corresponding guanidinium derivative. Yield: 1.0 g (45%, light brown solid). Anal. calcd for $\text{C}_{13}\text{H}_{16}\text{N}_4$: C, 68.39; H, 7.06; N, 24.54. Found: C, 68.92; H, 6.53; N, 24.54. ^1H NMR (400.1 MHz, $\text{DMSO } d_6$, 20 °C): δ 8.69 (d, $J_{\text{HH}} = 4.5$ Hz 1H, H1), 8.41 (d, $J_{\text{HH}} = 3.92$ Hz, 1H, H8), 8.34 (s br., 1H, H4), 7.97 (t, $J_{\text{HH}} = 7.82$ Hz, 1H, H3), 7.50 (t, $J_{\text{HH}} = 5.86$ Hz, 1H, H2), 7.44 (d, $J_{\text{HH}} =$

4.88 Hz, 1H, H7), 7.25 (s, 1H, NH), 3.35-3.30 (m, 2H, H_{butyl}), 1.54-1.57 (m, 2H, H_{butyl}), 1.33-1.38 (m, 2H, H_{butyl}), 0.90 (t, $J_{\text{HH}} = 7.24$ Hz, 3H, H_{butyl}). ¹³C NMR (100.6 MHz, DMSO *d*₆, 20 °C): δ 162.5 (s, C9), 159.3 (s, C6, C8), 154.1 (s, C5), 149.4 (s, C1), 137.3 (s, C3), 125.3 (s, C2), 120.7 (s, C4), 105.3 (s, C7), 40.4 (s, C_{butyl}), 31.1 (s, C_{butyl}), 19.7 (s, C_{butyl}), 13.8 (s, C_{butyl}).



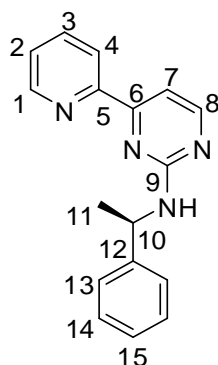
***N*-1-Octyl-4-(2-pyridinyl)pyrimidin-2-amin (17n).** Method 1 was applied, using the corresponding guanidinium derivative. Yield: 1.5 g (54%, light brown solid). Anal. calcd for C₁₇H₂₄N₄: C, 71.79; H, 8.51; N, 19.70. Found: C, 71.14; H, 8.36; N, 19.20. ¹H NMR (400.1 MHz, DMSO *d*₆, 20 °C): δ 8.66 (d, $J_{\text{HH}} = 3.92$ Hz, 1H, H1), 8.40 (d, $J_{\text{HH}} = 4.72$ Hz, 1H, H8), 8.34 (d, $J_{\text{HH}} = 4.00$ Hz, 1H, H4), 7.90 (t, $J_{\text{HH}} = 7.82$ Hz, 1H, H3), 7.46 (t, $J_{\text{HH}} = 4.90$ Hz, 1H, H2), 7.44 (d, $J_{\text{HH}} = 4.68$ Hz, 1H, H7), 7.23 (s, 1H, NH), 1.54 (t, $J_{\text{HH}} = 6.00$ Hz, 2H, H_{octyl}), 1.14-1.27 (m, 12H, H_{octyl}), 0.75 (t, $J_{\text{HH}} = 6.06$ Hz, 3H, H_{octyl}). ¹³C NMR (100.6 MHz, DMSO *d*₆, 20 °C): δ 162.5 (s, C9), 159.1 (s, C6, C8), 154.2 (s, C5), 149.3 (s, C1), 137.0 (s, C3), 125.2 (s, C2), 120.6 (s, C4), 105.3 (s, C7), 40.7 (s, C_{octyl}), 31.3 (s, C_{octyl}), 29.0 (s, C_{octyl}), 28.9 (s, C_{octyl}), 28.8 (s, C_{octyl}), 26.6 (s, C_{octyl}), 22.1 (s, C_{octyl}), 13.8 (s, C_{octyl}).



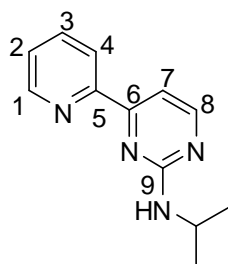
***N*-(*S*)-(+)-1-Phenylethyl-4-(2-pyridinyl)pyrimidin-2-amin (17o).** Method 1 was applied, using the corresponding guanidinium derivative. Yield: 1.3 g (55%, brown oil). Anal. calcd for

Experimental

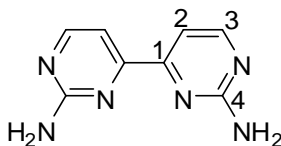
$C_{17}H_{16}N_4 + 0.5 \text{ EtOH}$: C, 72.52; H, 6.58; N, 18.29. Found: C, 73.93; H, 6.52; N, 18.93. ^1H NMR (400.1 MHz, DMSO d_6 , 20 °C): δ 8.66 (d, $J_{\text{HH}} = 3.68$ Hz, 1H, H1), 8.42 (d, $J_{\text{HH}} = 4.92$ Hz, 1H, H8), 8.33 (s, 1H, H4), 7.89-7.92 (m, 2H, H3 & NH), 7.48-7.51 (m, 3H, H7, H13), 7.43 (t, $J_{\text{HH}} = 5.76$ Hz, 1H, H2), 7.28 (t, $J_{\text{HH}} = 7.54$ Hz, 2H, H14), 7.15 (t, $J_{\text{HH}} = 7.34$ Hz, 1H, H15), 5.21-5.27 (m, 1H, H10), 1.51 (d, $J_{\text{HH}} = 7.04$ Hz, 3H, H11). ^{13}C NMR (100.6 MHz, DMSO d_6 , 20 °C): δ 161.7 (s, C9) 159.3 (s, C6 & C8), 154.1 (s, C5), 149.3 (s, C1), 146.0 (s, C12), 137.1 (s, C3), 128.1 (s, C14), 126.1 (s, C13), 126.3 (s, C15), 125.3 (s, C2), 120.8 (s, C4), 105.8 (s, C7), 50.2 (s, C10), 23.0 (s, C11).



***N*-(*R*)-(+)-1-Phenylethyl-4-(2-pyridinyl)pyrimidin-2-amin (17p)**. Method 1 was applied, using the corresponding guanidinium derivative. Yield: 0.6 (45% brown oil). Anal. calcd for $C_{17}H_{16}N_4 + 0.33 \text{ EtOH} + 0.33 \text{ CH}_2\text{Cl}_2$: C, 67.82; H, 6.00; N, 17.26. Found: C, 67.54; H, 5.84; N, 17.11. ^1H NMR (400.1 MHz, DMSO d_6 , 20 °C): δ 8.76 (d, $J_{\text{HH}} = 3.68$ Hz, 1H, H1), 8.48 (d, $J_{\text{HH}} = 4.00$ Hz, 1H, H8), 8.36 (d, $J_{\text{HH}} = 4.00$ Hz, 1H, H4), 7.89-7.87 (m, 2H, H3 & NH), 7.66 (d, $J_{\text{HH}} = 4.00$ Hz, 1H, H7), 7.55 (t, $J_{\text{HH}} = 8.00$ Hz, 2H, H13), 7.43 (t, $J_{\text{HH}} = 6.00$ Hz, 1H, H2), 7.33 (t, $J_{\text{HH}} = 8.00$ Hz, 1H, H15), 7.28 (s br., 2H, H14), 5.37-5.40 (m, 1H, H10), 1.70 (d, $J_{\text{HH}} = 8.00$ Hz, 3H, H11). ^{13}C NMR (100.6 MHz, DMSO d_6 , 20 °C): δ 160.7 (s, C9) 158.1 (s, C6 & C8), 153.7 (s, C5), 148.2 (s, C1), 143.8 (s, C12), 135.8 (s, C3), 127.4 (s, C14), 125.9 (s, C15), 125.0 (s, C13), 123.8 (s, C2), 120.4 (s, C4), 106.0 (s, C7), 49.9 (s, C10), 22.0 (s, C11).



N-Isopropyl-4-(2-pyridinyl)pyrimidin-2-amin (17q). Method 1 was applied, using the corresponding guanidinium derivative. Yield: 1.0 g (48%, colorless crystal). Anal. calcd for $C_{12}H_{14}N_4$: C, 67.27; H, 6.59; N, 26.15. Found: C, 67.30; H, 6.66; N, 25.94. 1H NMR (600.1 MHz, DMSO d_6 , 20 °C): δ 8.68 (d, $J_{HH} = 4.5$ Hz, 1H, H1), 8.41 (d, $J_{HH} = 4.7$ Hz, 1H, H8), 8.34 (d, $J_{HH} = 7.0$ Hz, 1H, H4), 7.95 (td, $J_{HH} = 7.7, 1.5$ Hz, 1H, H3), 7.48 (dd, $J_{HH} = 7.0, 5.0$ Hz, 1H, H2), 7.44 (d, $J_{HH} = 5.0$ Hz, 1H, H7), 7.08 (d, $J_{HH} = 6.8$ Hz 1H, NH), 4.15 (s br., 1H, $H_{isopropyl}$), 1.19 (d, $J_{HH} = 6.65$ Hz, 6H, $H_{isopropyl}$). ^{13}C NMR (151 MHz, DMSO d_6 , 20 °C) δ 162.6 (s, C9), 161.8 (s, C8), 159.3 (s, C6), 154.2 (s, C5), 149.4 (s, C1), 137.2 (s, C3), 125.3 (s, C2), 120.7 (s, C4), 105.3 (s, C7), 42.1 (s, $C_{isoPropyl}$), 22.3 (s, $C_{isoPropyl}$).



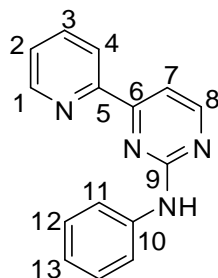
4,4'-Bipyrimidine-2,2'-diamine (19). The synthesis of **19** was carried out as described for **17a**, but using precursor **18** and two equivalents of guanidinium carbonate. Yield: 2.0 g (64%). Anal. calcd for $C_8H_8N_6 + 0.2 CH_2Cl_2$: C, 48.00; H, 4.13; N, 40.96. Found: C, 48.02; H, 4.14; N, 39.53. 1H NMR (400.1 MHz, DMSO- d_6 , 70 °C): δ 8.42 (d, $J_{HH} = 5.0$ Hz, 1H, H3), 7.37 (d, $J_{HH} = 5.0$ Hz, 1H, H2), 6.46 (s, 2H, NH_2). ^{13}C NMR (151 MHz, DMSO- d_6 , 70 °C) δ 163.4 (s, C1), 161.8 (s, C4), 159.1 (s, C3), 106.0 (s, C2).

5.3.3 Synthesis of NNC Ligands

General method for the synthesis of CNN 20a-e. Under an atmosphere of nitrogen 0.5 g of Na (22 mmol) were added to a solution of the proper guanidinium salt (11 mmol) in dry EtOH (50 ml). When the reaction of Na and EtOH was completed, 1.80 g of precursor **12**

Experimental

(10 mmol) were added and the solution was refluxed for 24 h. After cooling the solution to 0 °C the precipitated solid was filtered. The unreacted salt and the excesses of the base were washed out with water. The product was recrystallized from ethanol.



***N*-Phenyl-4-(pyridine-2-yl)pyrimidin-2-amine (20a).** Yield: 1.2 g (50%, pale yellow solid).

Anal. calcd for C₁₅H₁₂N₄: C, 72.56; H, 4.87; N, 22.57. Found: C, 72.35; H, 5.21; N, 22.47. ¹H

NMR (400.1 MHz, DMSO-*d*₆, 20 °C): δ 9.76 (s br., 1H, NH), 8.75 (d, *J*_{HH} = 4.3 Hz, 1H, H1),

8.65 (d, *J*_{HH} = 5.09 Hz, 1H, H8), 8.41 (d, *J*_{HH} = 7.83 Hz, 1H, H4), 8.07-8.02 (m, 1H, H3), 7.85

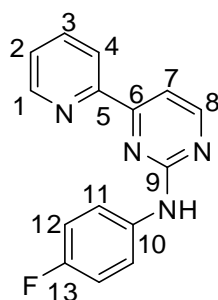
(d, *J*_{HH} = 7.82 Hz, 2H, H11), 7.73 (d, *J*_{HH} = 5.09 Hz, 1H, H7), 7.58-7.55 (m, 1H, H2), 7.33 (t,

*J*_{HH} = 7.82 Hz, 2H, H12), 6.98 (t, *J*_{HH} = 7.04 Hz, 1H, H13). ¹³C NMR (100.6 MHz, DMSO-*d*₆,

20 °C): δ 162.8 (s, C9), 160.1 (s, C6), 159.5 (s, C8), 153.7 (s, C5), 149.6 (s, C1), 140.5 (s,

C10), 137.6 (s, C3), 128.6 (s, C12), 125.7 (s, C2), 121.5 (s, C4), 121.0 (s, C13), 119.0 (s, C11)

108.0 (s, C7).

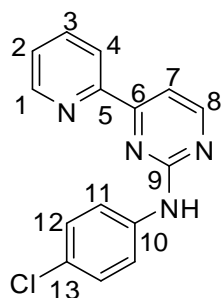


***N*-(4-Fluorophenyl)-4-(pyridine-2-yl)pyrimidin-2-amine (20b).** Yield: 1.4 g (53%, pale

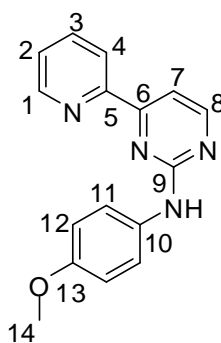
yellow solid). Anal. calcd for C₁₅H₁₁FN₄: C, 67.66; H, 4.16; N, 21.04. Found: C, 67.49; H,

4.28; N, 20.90. ¹H NMR (400.1 MHz, DMSO-*d*₆, 20 °C): δ 9.79 (s br., 1H, NH), 8.74 (d, *J*_{HH} =

4.3 Hz, 1H, H1), 8.63 (d, $J_{\text{HH}} = 4.7$ Hz, 1H, H8), 8.39 (d, $J_{\text{HH}} = 7.83$ Hz, 1H, H4), 8.05-8.00 (m, 1H, H3), 7.85-7.81 (m, 2H, H12), 7.81 (d, $J_{\text{HH}} = 5.08$ Hz, 1H, H7), 7.58-7.55 (m, 1H, H2), 7.17 (t, $J_{\text{HF}} = 9$ Hz, 2H, H11). ^{13}C NMR (100.6 MHz, DMSO- d_6 , 20 °C): δ 162.8 (s, C9), 160.0 (s, C6), 159.5 (s, C8), 158.4 (d, $J_{\text{CF}} = 237.67$ Hz, C13), 153.6 (s, C5), 149.6 (s, C1), 137.6 (s, C3), 136.9 (d, $J_{\text{CF}} = 2.77$ Hz, C10), 125.7 (s, C2), 121.1 (s, C4), 120.7 (d, $J_{\text{CF}} = 7.4$ Hz, C11), 115.2 (d, $J_{\text{CF}} = 22.19$ Hz, C12), 108.0 (s, C7).

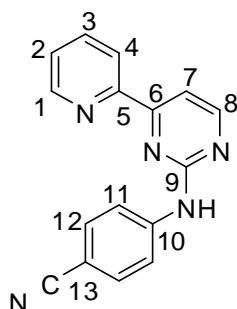


***N*-(4-Chlorophenyl)-4-(pyridine-2-yl)pyrimidin-2-amine (20c)**. Yield: 1.3 g (45%, pale yellow solid). Anal. calcd for $\text{C}_{15}\text{H}_{11}\text{ClN}_4$: C, 63.72; H, 3.92; N, 19.82. Found: C, 63.46; H, 4.10; N, 19.75. ^1H NMR (400.1 MHz, DMSO- d_6 , 20 °C): δ 9.92 (s br., 1H, NH), 8.75 (d, $J_{\text{HH}} = 3.91$ Hz, 1H, H1), 8.66 (d, $J_{\text{HH}} = 4.7$ Hz, 1H, H8), 8.40 (d, $J_{\text{HH}} = 7.83$ Hz, 1H, H4), 8.04 (t, $J_{\text{HH}} = 7.43$ Hz, 1H, H3), 7.89 (d, $J_{\text{HH}} = 9$ Hz, 2H, H12), 7.75 (d, $J_{\text{HH}} = 5.08$ Hz, 1H, H7), 7.58-7.55 (m, 1H, H2), 7.39 (d, $J_{\text{HH}} = 8.61$ Hz, 2H, H11). ^{13}C NMR (100.6 MHz, DMSO- d_6 , 20 °C): δ 162.9 (s, C9), 159.8 (s, C6), 159.6 (s, C8), 153.5 (s, C5), 149.6 (s, C1), 139.5 (s, C10), 137.6 (s, C3), 128.4 (s, C11), 125.8 (s, C2), 124.9 (s, C13), 121.1 (s, C4), 120.3 (s, C12) 108.3 (s, C7).



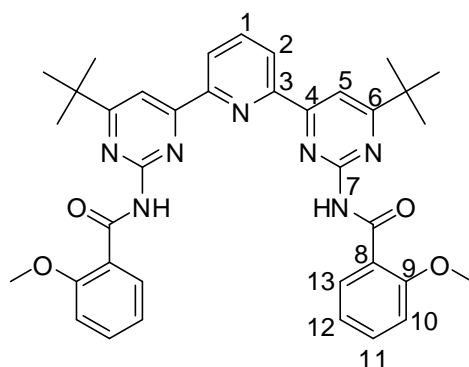
Experimental

***N*-(4-Methoxyphenyl)-4-(pyridine-2-yl)pyrimidin-2-amine (20d)**. Yield: 1.9 g (70%, pale yellow solid). Anal. calcd for C₁₆H₁₄N₄O: C, 69.05; H, 5.07; N, 20.13. Found: C, 66.36; H, 4.81; N, 19.70. ¹H NMR (400.1 MHz, DMSO-*d*₆, 20 °C): δ 9.56 (s br., 1H, NH), 8.74 (d, *J*_{HH} = 4.31 Hz, 1H, H1), 8.59 (d, *J*_{HH} = 4.7 Hz, 1H, H8), 8.38 (d, *J*_{HH} = 7.82 Hz, 1H, H4), 8.02 (t, *J*_{HH} = 7.43 Hz, 1H, H3), 7.73 (d, *J*_{HH} = 9 Hz, 2H, H12), 7.66 (d, *J*_{HH} = 5.09 Hz, 1H, H7), 7.57-7.54 (m, 1H, H2), 6.94 (d, *J*_{HH} = 9 Hz, 2H, H11), 3.74 (s, 3H, H14). ¹³C NMR (100.6 MHz, DMSO-*d*₆, 20 °C): δ 162.7 (s, C9), 160.2 (s, C6), 159.5 (s, C8), 154.3 (s, C5), 153.8 (s, C13), 149.6 (s, C1), 137.5 (s, C3), 133.6 (s, C10), 125.6 (s, C2), 121.0 (s, C4), 120.7 (s, C11), 113.8 (s, C12) 107.4 (s, C7), 55.2 (s, C14).



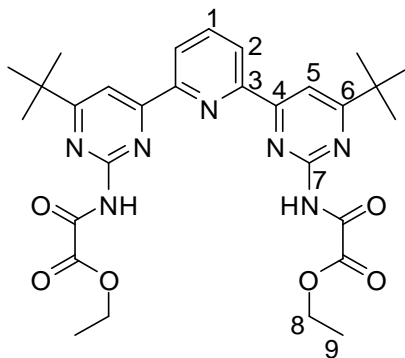
4-(4-(Pyridin-2-yl)pyrimidin-2-ylamino)benzonitrile (20e). Yield: 1.3 g (47%, pale yellow solid). Anal. calcd for C₁₆H₁₁N₅: C, 70.32; H, 4.06; N, 25.63. Found: C, 69.70; H, 4.14; N, 25.01. ¹H NMR (400.1 MHz, DMSO-*d*₆, 20 °C): δ 10.34 (s br., 1H, NH), 8.77 (d, *J*_{HH} = 4.7 Hz, 1H, H1), 8.74 (d, *J*_{HH} = 5.09 Hz, 1H, H8), 8.42 (d, *J*_{HH} = 7.83 Hz, 1H, H4), 8.06-8.04 (m, 3H, H3 & H12), 7.85 (d, *J*_{HH} = 4.7 Hz, 1H, H7), 7.79 (d, *J*_{HH} = 8.6 Hz, 2H, H11), 7.61-7.58 (m, 1H, H2). ¹³C NMR (100.6 MHz, DMSO-*d*₆, 20 °C): δ 163.1 (s, C9), 159.9 (s, C6), 159.5 (s, C8), 153.3 (s, C5), 149.7 (s, C1), 144.9 (s, C10), 137.7 (s, C3), 133.1 (s, C11), 126.0 (s, C2), 121.2 (s, C4), 119.6 (s, C13), 118.4 (s, C12), 109.4 (s, C7), 102.5 (s, CN).

5.3.4 Synthesis of Multidendate Ligands

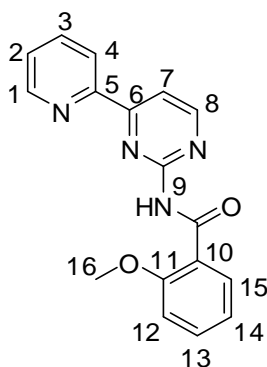


26. Under an atmosphere of nitrogen 331 mg of 2-methoxybenzoic acid (2.18 mmol) were dissolved in 20 ml of thionylchloride. The solution was refluxed for 2.5 h and then the excess of the thionylchloride was distilled off. The residue was dissolved in 20 ml of pyridine and 400 mg of the diamine **7** (1.06 mmol) were added to the solution which was stirred over night. After distillation of the solvent a 10% solution of NaHCO₃ was added to the residue and the product was extracted with dichloromethane. The organic phases were dried over MgSO₄. After evaporation of the solvent, the product was crystallized in ethanol. Yield: 428.0 mg (63%, colorless solid). Anal. calcd for C₃₇H₃₉N₇O₄: C, 68.82; H, 6.09; N, 15.18. Found: C, 68.74; H, 6.05; N, 15.30. ¹H NMR (400.1 MHz, DMSO-*d*₆): δ 10.83 (s, 2H, NH), 8.23-8.20 (m, 4H, H2 & H5), 8.13 (t, *J*_{HH} = 7.6 Hz, 1H, H1), 7.66 (d, *J*_{HH} = 7.4 Hz, 2H, H13), 7.49 (t, *J*_{HH} = 7.8 Hz, 2H, H11), 7.12-7.09 (m, 4H, H10 & H12), 3.71 (s, 6H, H14), 1.28 (s, 18H, H16). ¹³C NMR (100.6 MHz, DMSO-*d*₆): δ 179.9 (s, C6), 165.7 (s, CO), 162.7 (s, C4), 157.6 (s, C7), 156.2 (s, C9), 152.9 (s, C3), 139.0 (s, C1), 132.0 (s, C11), 129.7 (s, C13), 125.2 (s, C8), 123.0 (s, C2), 120.7 (s, C12), 111.9 (s, C10), 107.0 (s, C5), 55.8 (s, C14), 37.4 (s, C15), 28.8 (s, C16). IR (KBr): $\bar{\nu}$ = 3340 cm⁻¹ (s), 3078 (br.), 2959 (s), 2900 (m), 2870 (m), 2838 (br.), 1697 (s), 1600 (s), 1577 (s), 1536 (m), 756 (m).

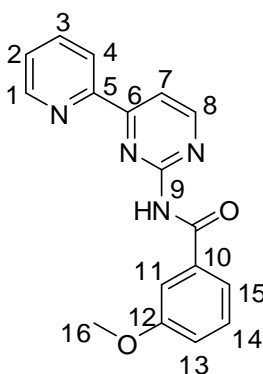
Experimental



27. Under an atmosphere of nitrogen to the solution of 502 mg of the diamine **7** (1.33 mmol) in 20 ml of pyridine 362 mg of ethyl(chlorocarbonyl)formate (2.65 mmol) were added and the solution was stirred over night at room temperature. After distillation of the solvent, a 10% solution of NaHCO_3 was added to the residue and the product was extracted with dichloromethane. The organic phases were washed three times with diluted HCl and then dried over MgSO_4 . Evaporating the solvent resulted in desired product. Yield: 630.0 mg (63%, colorless solid). Anal. calcd for $\text{C}_{29}\text{H}_{35}\text{N}_7\text{O}_6$: C, 60.03; H, 6.11; N, 16.97. Found: C, 60.00; H, 6.04; N, 16.36. ^1H NMR (400.1 MHz, $\text{DMSO}-d_6$): δ 11.70 (s, 2H, NH), 8.42 (d, $J_{\text{HH}} = 7.8$ Hz, 2H, H2), 8.35-8.31 (m, 3H, H1 & H5), 4.31 (q, $J_{\text{HH}} = 7.0$ Hz, 4H, H8), 1.37 (s, 18H, H11), 1.20 (t, $J_{\text{HH}} = 7.0$ Hz, 6H, H9). ^{13}C NMR (100.6 MHz, $\text{DMSO}-d_6$): δ 180.6 (s, C6), 163.0 (s, C4), 160.3 (s, CO), 158.3 (s, CO), 156.3 (s, C7), 152.8 (s, C3), 139.5 (s, C1), 123.3 (s, C2), 108.2 (s, C5), 61.7 (s, C8), 37.7 (s, C10), 28.7 (s, C11), 13.7 (s, C9). IR (KBr): $\bar{\nu} = 3427$ cm^{-1} (w), 3388 (w), 2959 (m), 2926 (m), 2870 (w), 1769 (s), 1744 (s), 1727 (s), 1692 (w), 1604 (s), 1577 (s), 1541 (s), 1523 (s), 1393 (m), 1351 (m), 743 (w).



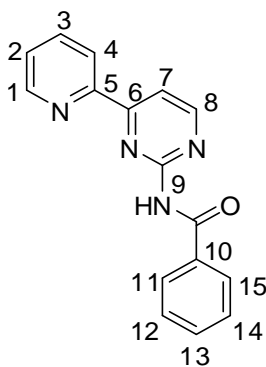
2-Methoxy-*N*-(4-(pyridin-2-yl)pyrimidin-2-yl)benzamide, 28. Under atmosphere of nitrogen 903 mg of 2-methoxybenzoic acid (5.93 mmol) were dissolved in 20 ml of thionylchloride. The solution was refluxed for 2.5 h and then the excess of the thionylchloride was distilled off. The residue was dissolved in 20 ml pyridine and 1.01 g of the monoamine **17a** (5.87 mmol) were added to the solution which was stirred over night. After distillation of the solvent the residue was washed twice with a 10% solution of NaHCO₃, four times with water and then with hot ethanol. Yield: 1.30 g (72%, colorless solid). Anal. calcd for C₁₇H₁₄N₄O₂ · 0.25H₂O: C, 66.13; H, 4.92; N, 17.63; Found: C, 66.04; H, 4.80; N, 17.69. ¹H NMR (400.1 MHz, DMSO-*d*₆): δ 10.85 (s, 1H, NH), 8.81 (d, *J*_{HH} = 5.0 Hz, 1H, H8), 8.73 (d, *J*_{HH} = 3.7 Hz, 1H, H1), 8.02-8.01 (m, 2H, H7 & H15), 7.92 (t, *J*_{HH} = 7.48 Hz, 1H, H3), 7.73 (d, *J*_{HH} = 7.2 Hz, 1H, H4), 7.56-7.51 (m, 2H, H2 & H13), 7.15-7.10 (m, 2H, H12 & H14), 3.80 (s, 3H, H16). ¹³C NMR (100.6 MHz, DMSO-*d*₆): δ 164.8 (s, CO), 162.9 (s, C9), 159.9 (s, C8), 157.7 (s, C6), 156.5 (s, C11), 152.9 (s, C5), 149.7 (s, C1), 137.5 (s, C3), 132.4 (s, C13), 130.0 (s, C15), 126.0 (s, C2), 124.5 (s, C10), 121.4 (s, C4), 120.8 (s, C14), 112.1 (s, C7), 112.0 (s, C12), 56.0 (s, C16), IR (KBr): $\bar{\nu}$ = 3318 cm⁻¹ (br.), 3191 (br.), 3107 (m), 2965 (m), 2906 (m), 1658 (s), 1586 (s), 1556 (s), 815 (m), 756 (s).



3-Methoxy-*N*-(4-(pyridin-2-yl)pyrimidin-2-yl)benzamide, 29. Under an atmosphere of nitrogen 900 mg of 3-methoxybenzoic acid (5.92 mmol) were dissolved in 20 ml of thionylchloride. The solution was refluxed for 1.5 h and then the excess of the thionylchloride was distilled off. The residue was dissolved in 20 ml of pyridine and 1.02 g of the monoamine

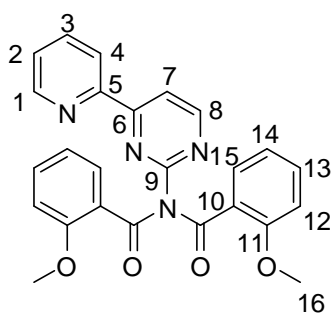
Experimental

17a (5.92 mmol) were added to the solution which was stirred over night. After distillation of the solvent the residue was dissolved in dichloromethane and the organic phase was washed with a saturated solution of NaHCO₃ and dried over MgSO₄. Evaporating the dichloromethane resulted in **29**. Yield: 1.1 g (63%, colorless). Anal. calcd for C₁₇H₁₄N₄O₂: C, 66.66; H, 4.61; N, 18.29; Found: C, 66.18; H, 4.86; N, 18.09. ¹H NMR (400.1 MHz, DMSO-*d*₆): δ 11.12 (s br., 1H, NH), 8.89 (d, *J*_{HH} = 5.1 Hz, 1H, H8), 8.77 (d, *J*_{HH} = 3.9 Hz, 1H, H1), 8.44 (d, *J*_{HH} = 7.8 Hz, 1H, H4), 8.09 (d, *J*_{HH} = 5.1 Hz, 1H, H7), 8.06-8.01 (m, 1H, H3), 7.60-7.57 (m, 3H, H2, H11 & H15), 7.46 (t, *J*_{HH} = 7.8 Hz, 1H, H12), 7.19 (dd, *J* = 2.2, 8.0 Hz, 1H, H13), 3.85 (s, 3H, H16). ¹³C NMR (100.6 MHz, DMSO-*d*₆): δ 165.4 (s, CO), 163.2 (s, C9), 159.8 (s, C8), 159.1 (s, C14), 158.3 (s, C6), 153.1 (s, C5), 149.8 (s, C1), 137.6 (s, C3), 135.7 (s, C10), 129.5 (s, C12), 126.1 (s, C2), 121.5 (s, C4), 120.5 (s, C11), 118.2 (s, C13), 113.0 (s, C15), 112.5 (s, C7), 55.3 (s, C16). IR (KBr): $\bar{\nu}$ = 3244 cm⁻¹ (m), 3208 (m), 3179 (m), 3028 (m), 3005 (m), 2958 (m), 2932 (m), 2834 (m), 1699 (s), 1587 (s), 742 (s).



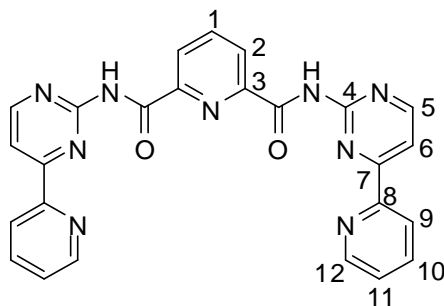
N-(4-(Pyridin-2-yl)pyrimidin-2-yl)benzamide, 30. Under an atmosphere of nitrogen 510 mg of **17a** (2.96 mmol) were dissolved in 15 ml of pyridine and 408 mg of benzoyl chloride (2.96 mmol) were added to the solution which was stirred over night. After distillation of the solvent, the residue was washed with a 10% solution of NaHCO₃ and crystallized from ethanol. Yield: 279.0 mg (34%, colorless solid). Anal. calcd for C₁₆H₁₂N₄O: C, 69.55; H, 4.38; N, 20.28; Found: C, 68.99; H, 4.34; N, 19.88. ¹H NMR (400.1 MHz, DMSO-*d*₆): δ 11.12 (s, NH), 8.89 (d, *J*_{HH} = 5.0 Hz, 1H, H8), 8.77 (d, *J*_{HH} = 3.8 Hz, 1H, H1), 8.41 (d, *J*_{HH} = 7.8 Hz, 1H, H4),

8.15-7.94 (m, 4H, H3, H7, H11 & H15), 7.72-7.45 (m, 4H, H2, H12, H13 & H14). ^{13}C NMR (100.6 MHz, $\text{DMSO-}d_6$): δ 165.9 (s, CO), 163.2 (s, C9), 159.8 (s, C8), 158.4 (s, C6), 153.1 (s, C5), 149.8 (s, C1), 137.6 (s, C3), 134.4 (s, C10), 132.0 (s, C13), 128.4 (s, C12 & C14), 128.2 (s, C11 & C15), 126.1 (s, C2), 121.5 (s, C4), 112.4 (s, C7). IR (KBr): $\bar{\nu}$ = 3218 cm^{-1} (br.), 3170 (m), 3125 (br.), 3082 (br.), 3056 (br.) 2993 (m), 1690 (s), 1601 (s), 1546 (s), 1546 (s), 1516 (s), 803 (s) 731 (s), 701 (s).



31. Under an atmosphere of nitrogen 1.80 g of 2-methoxybenzoic acid (11.8 mmol) were dissolved in 25 ml of thionylchloride. The solution was refluxed for 2 h and then the excess of the thionylchloride was distilled off. The residue was dissolved in 20 ml of pyridine and 1.00 g of the monoamine **17a** (5.81 mmol) were added to the solution which was stirred over night. After distillation of the solvent the residue was washed twice with a 10% solution of NaHCO_3 , four times with water and then with hot ethanol. Yield: 1.0 g (40%, colorless solid), calcd for $\text{C}_{25}\text{H}_{20}\text{N}_4\text{O}_4$: C, 68.17; H, 4.58; N, 12.72; Found: C, 67.87; H, 4.76; N, 12.57. ^1H NMR (400.1 MHz, CDCl_3): δ 8.80 (d, J_{HH} = 5.1 Hz, 1H, H8), 8.65 (d, J_{HH} = 4.4 Hz, 1H, H1), 8.13 (d, J_{HH} = 5.1 Hz, 1H, H7), 8.09 (d, J_{HH} = 8.2 Hz, 1H, H4), 7.75-7.70 (m, 3H, H3 & H15), 7.36-7.29 (m, 3H, H2 & H13), 6.92 (t, J_{HH} = 7.5 Hz, 2H, H14), 6.76 (d, J_{HH} = 8.2 Hz, 2H, H12), 3.72 (s, 6H, H16). ^{13}C NMR (100.6 MHz, CDCl_3): δ 170.0 (s, CO), 164.2 (s, C9), 160.0 (s, C6), 159.5 (s, C8), 157.4 (s, C11), 153.3 (s, C5), 149.5 (s, C1), 137.1 (s, C3), 133.1 (s, C13), 131.2 (s, C15), 125.7 (s, C2), 124.8 (s, C10), 122.1 (s, C4), 120.5 (s, C14), 114.6 (s, C7), 111.1 (s, C12), 55.6 (s, C16). IR (KBr): $\bar{\nu}$ = 3426 cm^{-1} (br.), 3318 (br.), 3088 (br.), 3065 (br.), 3006 (m), 2967 (m), 2942 (m), 2839 (m), 1725 (s), 1668 (s), 1577 (s), 1541 (s), 1489 (s), 815 (s), 757 (s).

Experimental

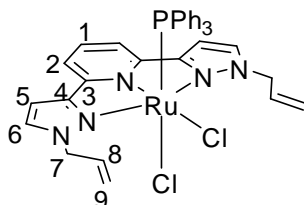


***N*²,*N*⁶-Bis(4-pyridin-2-yl)pyrimidin-2-yl)pyridine-2,6-dicarboxamide 32.** Under an atmosphere of nitrogen 504 mg of pyridine-2,6-dicarboxylic acid (3.02 mmol) were dissolved in 20 ml of thionylchloride. The solution was refluxed for 2 h and then the excess of the thionylchloride was distilled off. The residue was dissolved in 20 ml of pyridine and 1.00 g of the monoamine **17a** (5.81 mmol) were added to the solution which was stirred over night. After distillation of the solvent the residue was washed twice with a 10% solution of NaHCO₃, four times with water and then with hot ethanol. Yield: 892.0 mg (62%, colorless solid). Anal. calcd for C₂₅H₁₇N₉O₂ + 2.5 H₂O: C, 57.69; H, 4.26; N, 24.22; Found: C, 57.54; H, 4.06; N, 23.74. ¹H NMR (400.1 MHz, DMSO-*d*₆): δ 12.06 (s, 2H, NH), 8.99 (d, *J*_{HH} = 5.1 Hz, 2H, H5), 8.79 (d, *J*_{HH} = 4.0 Hz, 2H, H12), 8.57 (d, *J*_{HH} = 7.8 Hz, 2H, H9), 8.48 (d, *J*_{HH} = 7.8 Hz, 2H, H2), 8.38-8.33 (m, 1H, H1), 8.18 (d, *J*_{HH} = 5.1 Hz, 2H, H6), 8.08 (t, *J*_{HH} = 7.8 Hz, 2H, H10), 7.63 (q, *J*_{HH} = 4.0 Hz, 2H, H11). ¹³C NMR (100.6 MHz, DMSO-*d*₆): δ 163.5 (s, CO), 162.1 (s, C4), 160.0 (s, C5), 157.8 (s, C7), 153.0 (s, C8), 149.8 (s, C 12), 148.9 (s, C3), 140.0 (s, C1), 137.7 (s, C10), 126.2 (s, C2), 126.2 (s, C11), 121.7 (s, C9), 113.1 (s, C6). IR (KBr): $\bar{\nu}$ = 3324 cm⁻¹ (m), 3052 (br.), 2922 (br.), 2854 (br.), 1723 (s), 1586 (s), 1541 (s), 782 (s).

5.4 Synthesis of Transitional Metal Complexes

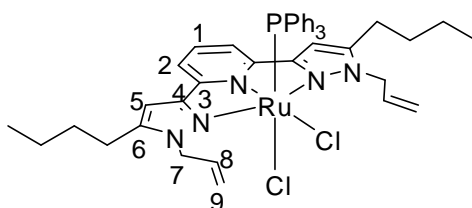
5.4.1 Ruthenium Complexes

5.4.1.1 Ruthenium Complexes with Tridendate Ligands



Dichloro(2,6-di(1-allyl-1H-pyrazol-3-yl)pyridine)triphenylphosphineruthenium(II) (33a).

0.15 g of **5** (0.37 mmol) were added to a solution of 0.355 g of $(PPh_3)_3RuCl_2$ (0.37 mmol) in 10 ml of dry CH_2Cl_2 . The reaction mixture was stirred at room temperature for about 2 h. After concentrating the solution to about 5 mL, 25 mL of dry diethylether were added to precipitate the product, which was filtered off and washed with diethylether to remove liberated triphenylphosphine. Yield: 268.0 mg (100%, red solid). Anal. calcd for $C_{35}H_{32}Cl_2N_5PRu$: C, 57.93; H, 4.45; N, 9.65. Found: C, 57.64; H, 4.45; N, 9.65. 1H NMR (400.1 MHz, $CDCl_3$, 20 °C): δ 7.35 (d, $J_{HH} = 2.72$ Hz, 2H, H6), 7.29 (t, $J_{HH} = 7.49$ Hz, 1H, H1), 7.25-7.18 (m, 5H, H2, H_{Ph}), 7.09-7.06 (m, 12H, H_{Ph}), 6.75 (d, $J_{HH} = 2.72$ Hz, 2H, H5), 6.15-6.04 (m, 2H, H8), 5.80 (dd, 4H, H7), 5.32 (m, 4H, H9), 4.76 (dd, 2H, H7). $^{13}C\{^1H\}$ NMR (100.6 MHz, $CDCl_3$, 20 °C): δ 155.8 (s, C1), 152.6 (s, C4), 134.1 (d, $J_{CP} = 41.62$ Hz, C_{Ph}), 133.4 (d, $J_{CP} = 9.24$ Hz, C_{Ph}), 133.0 (s, C8), 132.5 (s, C6), 132.0 (s, C3), 129.0 (s br., C_{Ph}), 127.8 (d, $J_{CP} = 8.33$ Hz, C_{Ph}), 120.2 (s, C2), 116.9 (s, C9), 105.5 (s, C5), 56.2 (s, C7). $^{31}P\{^1H\}$ NMR (162 MHz, $CDCl_3$, 20 °C): δ 44.2.

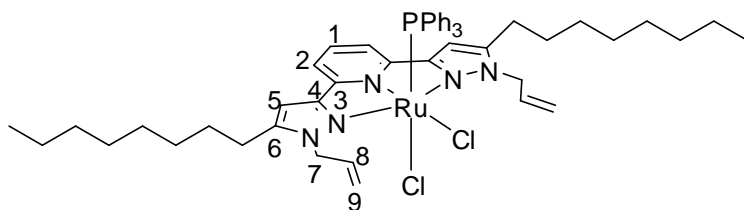


Dichloro(2,6-di(1-allyl-5-butyl-1H-pyrazol-3-yl)pyridine)triphenyl-

phosphineruthenium(II) **33b**. The same procedure as for **33a** was applied. Yield: 310.0 mg

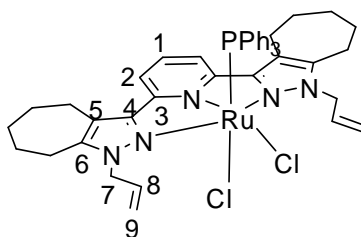
Experimental

(100%, red solid). Anal. calcd for $C_{43}H_{48}Cl_2N_5PRu$: C, 61.67; H, 5.73; N, 8.36. Found: C, 61.95; H, 5.68; N, 7.68. 1H NMR (400.1 MHz, $CDCl_3$, 20 °C): δ 7.34 (t, $J_{HH} = 8.22$ Hz, 1H, H1), 7.21 (m, 3H, H_{Ph}), 7.15 (d, $J_{HH} = 7.44$ Hz, 2H, H2), 7.11-7.07 (m, 12H, H_{Ph}), 6.47 (s, 2H, H5), 6.22-6.19 (m, 4H, H7 & H8), 5.14-5.10 (m, 4H, H9), 4.24-4.18 (m, 2H, H7), 2.59-2.54 (m, 4H, H_{butyl}), 1.60-1.56 (m, 4H, H_{butyl}), 1.39-1.34 (m, 4H, H_{butyl}), 0.94 (t, $J_{HH} = 7.05$ Hz, 6H, H_{butyl}). $^{13}C\{1H\}$ NMR (100.6 MHz, $CDCl_3$, 20 °C): δ 156.2 (s, C1), 151.6 (s, C4), 148.0 (s, C3), 134.5 (d, $J_{CP} = 40.69$ Hz, C_{Ph}), 134.4 (s, C8), 133.4 (d, $J_{CP} = 9.24$ Hz, C_{Ph}), 131.8 (s, C6), 128.8 (s br., C_{Ph}), 127.6 (d, $J_{CP} = 9.25$ Hz, C_{Ph}), 117.6 (s, C2), 116.5 (s, C9), 104.0 (s, C5), 53.8 (s, C7), 30.1 (s, C_{butyl}), 25.8 (s, C_{butyl}), 22.4 (s, C_{butyl}), 14.00 (s, C_{butyl}). $^{31}P\{1H\}$ NMR (162 MHz, $CDCl_3$, 20 °C): δ 42.7.

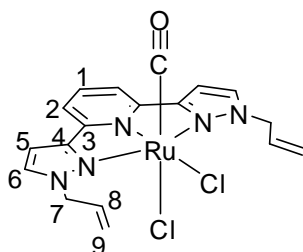


Dichloro(2,6-di(1-allyl-5-octyl-1H-pyrazol-3-yl)pyridine)triphenyl-

phosphineruthenium(II) 33d. The same procedure as for **33a** was applied. Since the product was too much soluble and air sensitive, the high content of free triphenylphosphine oxide and impurities could not be washed out. 1H NMR (400.1 MHz, $CDCl_3$, 20 °C): δ 7.33 (t, $J_{HH} = 7.92$ Hz, 1H, H1), 7.23 (m, 3H, H_{Ph}), 7.15 (d, $J_{HH} = 7.64$ Hz, 2H, H2), 7.10-7.06 (m, 12H, H_{Ph}), 6.47 (s, 2H, H5), 6.22-6.15 (m, 4H, H7 & H8), 5.14-5.10 (m, 4H, H9), 4.24-4.18 (m, 2H, H7), 2.59-2.51 (m, 4H, H_{octyl}), 1.60-1.57 (m, 4H, H_{octyl}), 1.28-1.19 (m, 20H, H_{octyl}), 0.89 (t, $J_{HH} = 6.36$ Hz, 6H, H_{octyl}). $^{31}P\{1H\}$ NMR (162 MHz, $CDCl_3$, 20 °C): δ 44.00.

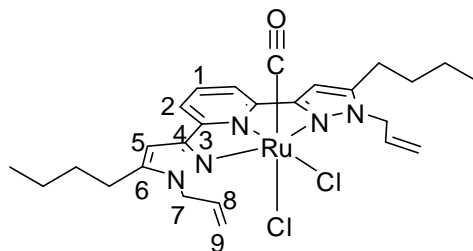


Dichloro(2,6-bis(1-allyl-5,6,7,8-tetrahydro-4H-cycloheptapyrazol-3-yl)pyridine triphenylphosphineruthenium(II) 33e. The same procedure as for **33a** was applied. Because of the high solubility and air sensitivity of the product the high content of free triphenylphosphine oxide and impurities could not be washed out. ^1H NMR (400.1 MHz, CDCl_3 , 20 °C): δ 7.32-7.19 (m, H1, H2 and free OPPh_3), 7.11-7.04 (m, 12H, H_{Ph}), 6.98 (t, $J_{\text{HH}} = 7.5$ Hz, 3H, H_{Ph}), 6.45 (m, 2H, H7), 6.18-6.08 (m, 2H, H8), 5.11-5.06 (m, 4H, H9), 4.31-4.25 (m, 2H, H7), 2.92-2.77 (m, 4H, $\text{H}_{\text{cycloheptyl}}$), 2.65 (t, $J_{\text{HH}} = 5.11$ Hz, 4H, $\text{H}_{\text{cycloheptyl}}$), 1.89-1.80 (m, 4H, $\text{H}_{\text{cycloheptyl}}$), 1.77-1.75 (m, 4H, $\text{H}_{\text{cycloheptyl}}$), 1.70-1.61 (m, 4H, $\text{H}_{\text{cycloheptyl}}$). $^{31}\text{P}\{^1\text{H}\}$ NMR (162 MHz, CDCl_3 , 20 °C): δ 44.67.



Carbonyldichloro(2,6-di(1-allyl-1H-pyrazol-3-yl)pyridine)ruthenium(II), 34a. 0.145 g of **33a** (0.2 mmol) were dissolved in dry toluene/ CH_2Cl_2 (10:1) and CO gas was bubbled into the refluxing solution. The colour of the solution changed from red to yellow. When the reaction mixture cooled down to room temperature, a yellow powder precipitated which was filtered off washed with dry diethylether. Yield: 98.0 mg (100%, yellow solid). Anal. calcd for $\text{C}_{18}\text{H}_{17}\text{Cl}_2\text{N}_5\text{ORu} + \text{CH}_2\text{Cl}_2$: C, 39.60; H, 3.32; N, 12.15. Found: C, 40.05; H, 3.56; N, 12.33. ^1H NMR (400.1 MHz, $\text{DMSO-}d_6$, 20 °C): δ 8.21-8.10 (m, 5H, H1, H2 & H6), 7.36 (d, $J_{\text{HH}} = 2.19$ Hz, 2H, H5), 6.16-6.09 (m, 2H, H8), 5.51-5.47 (dd, 2H, H7), 5.23-5.19 (m, 6H, H7 & H9). $^{13}\text{C}\{^1\text{H}\}$ NMR (100.6 MHz, $\text{DMSO-}d_6$, 20 °C): δ 191.0 (s, CO), 152.8 (s, C3), 152.3 (s, C4), 138.8 (s, C8), 135. (s, C6), 133.7 (s, C1), 119.2 (s, C2), 118.3 (s, C9), 106.7 (s, C5), 53.9 (s, C7). IR (KBr, cm^{-1}): 1936 (C=O).

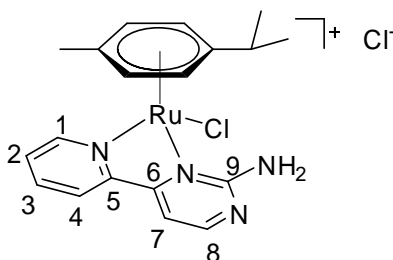
Experimental



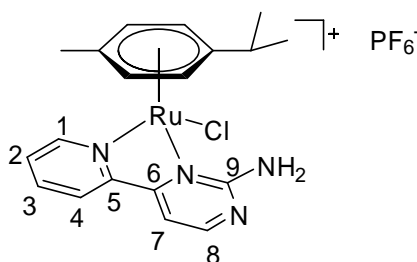
Carbonyldichloro(2,6-di(1-allyl-1H-pyrazol-3-yl)pyridine)ruthenium(II) 34b. The same procedure as for **34a** was applied. Yield: 121.0 mg (100%, yellow solid). Anal. calcd for $C_{26}H_{33}Cl_2N_5ORu$: C, 51.74; H, 5.51; N, 11.60. Found: C, 50.73; H, 5.54; N, 11.60. 1H NMR (400.1 MHz, $DMSO-d_6$, 20 °C): δ 8.15 (t, $J_{HH} = 7.49$ Hz, 1H, H1), 8.05 (d, $J_{HH} = 7.83$ Hz, 2H, H2), 7.21 (s, 2H, H5), 6.05-5.96 (m, 2H, H8), 5.58 (dd, 2H, H7), 5.19 (dd, 4H, H9), 5.07 (d, $J_{HH} = 17.37$ Hz, 2H, H7), 2.76-2.66 (m, 4H, H_{butyl}), 1.70-1.62 (m, 4H, H_{butyl}), 1.43-1.36 (m, 4H, H_{butyl}), 0.96-0.91 (m, 6H, H_{butyl}). $^{13}C\{1H\}$ NMR (100.6 MHz $DMSO-d_6$, 20 °C): δ 191.2 (s, CO), 153.0 (s, C3), 151.4 (s, C4), 148.3 (d, C6), 138.8 (s, C8), 133.3 (s, C1), 119.0 (s, C2), 117.1 (s, C9), 105.0 (s, C5), 51.3 (s, C7), 29.3 (s, C_{butyl}), 24.7 (s, C_{butyl}), 21.8 (s, C_{butyl}), 13.7 (s, C_{butyl}). IR (KBr, cm^{-1}): 1948 (C=O).

5.4.1.2 Ruthenium Complexes with Bidendate Ligands

General synthesis of $[RuCl(p\text{-cymene})L]Cl$. A solution of the ligand (0.32 mmol) in CH_2Cl_2 (5 ml) was added dropwise to a solution of 92.0 mg of $[RuCl_2(p\text{-cymene})]_2$ (0.15 mmol) in CH_2Cl_2 (20 ml). After stirring for 20 h at room temperature the solution was concentrated and the product was precipitated by adding Et_2O (10 ml). The product was filtered, washed twice with Et_2O and dried under vacuum.



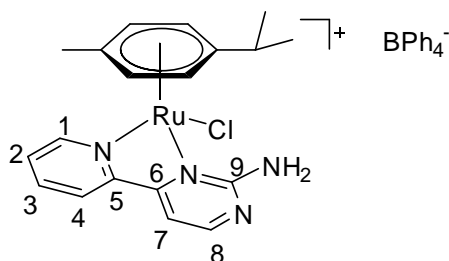
[2-Amino-4-(pyridin-2-yl)pyrimidine(chlorido)(η^6 -*p*-cymene)ruthenium(II)]chloride **36a-Cl. Yield: 122.4 mg (81%, yellow solid). Anal. calcd for C₁₉H₂₂Cl₂N₄Ru: C, 47.70; H, 4.64; N, 11.71. Found: C, 47.54; H, 4.75; N, 11.79. ¹H NMR (600.1 MHz, DMSO-*d*₆, 20 °C): δ 9.50 (d, $J_{\text{HH}} = 4.99$ Hz, 1H, H1), 8.71 (d, $J_{\text{HH}} = 4.7$ Hz, 1H, H8), 8.63 (d, $J_{\text{HH}} = 7.92$ Hz, 1H, H4), 8.30-8.27 (m, 1H, H3), 7.87-7.82 (m, 2H, H2 & H7), 6.23 (d, $J_{\text{HH}} = 6.16$ Hz, 1H, H_{cymene}), 6.07-6.02 (m, 3H, H_{cymene}), 2.50-2.43 (m, 1H, H_{cymene}), 2.22 (s, 3H, H_{cymene}), 0.94 (d, $J_{\text{HH}} = 6.75$ Hz, 3H, H_{cymene}), 0.85 (d, $J_{\text{HH}} = 6.75$ Hz, 3H, H_{cymene}). ¹³C NMR (150.9 MHz, DMSO-*d*₆, 20 °C): δ 164.5 (s, C9), 161.5 (s, C8), 161.2 (s, C6), 156.2 (s, C1), 153.8 (s, C5), 140.1 (s, C3), 129.0 (s, C2), 125.1 (s, C4), 108.2 (s, C7), 105.9 (s, C_{cymene}), 103.6 (s, C_{cymene}), 87.3 (s, C_{cymene}), 86.4 (s, C_{cymene}), 82.8 (s, C_{cymene}), 82.3 (s, C_{cymene}), 30.4 (s, C_{cymene}), 21.6 (s, C_{cymene}), 18.5 (s, C_{cymene}).**



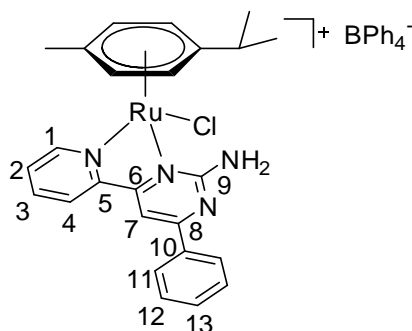
[2-Amino-4-(pyridin-2-yl)pyrimidine(chlorido)(η^6 -*p*-cymene)ruthenium(II)]hexafluorophosphate **36a-PF₆. The synthesis of **36a-PF₆** was carried out as described in general synthesis but 83.0 mg of KPF₆ salt (0.45 mmol) were also added to the solution and before concentrating the excess and formed salts were filtered off. Yield: 164.0 mg (93%, yellow solid). Anal. calcd for C₁₉H₂₂ClF₆N₄PRu: C, 38.82; H, 3.77; N, 9.53. Found: C, 38.60; H, 4.11; N, 9.42. ¹H NMR (600.1 MHz, DMSO-*d*₆, 20 °C): δ 9.48 (d, $J_{\text{HH}} = 4.99$ Hz, 1H, H1), 8.72 (d, $J_{\text{HH}} = 4.69$ Hz, 1H, H8), 8.60 (d, $J_{\text{HH}} = 7.63$ Hz, 1H, H4), 8.29-8.27 (m, 1H, H3), 7.85-7.83 (m, 1H, H2), 7.80 (d, $J_{\text{HH}} = 4.4$ Hz, 1H, H7), 6.23 (d, $J_{\text{HH}} = 5.87$ Hz, 1H, H_{cymene}), 6.05-6.02 (m, 3H, H_{cymene}), 2.47-2.45 (m, 1H, H_{cymene}), 2.22 (s, 3H, H_{cymene}), 0.95 (d, $J_{\text{HH}} = 6.75$ Hz, 3H, H_{cymene}), 0.85 (d, $J_{\text{HH}} = 6.75$ Hz, 3H, H_{cymene}). ¹³C NMR (150.9 MHz, DMSO-*d*₆, 20 °C): δ 164.5 (s, C9), 161.4 (s, C8), 161.1 (s, C6), 156.1 (s, C1), 153.8 (s, C5), 140.1 (s, C3), 128.9 (s,**

Experimental

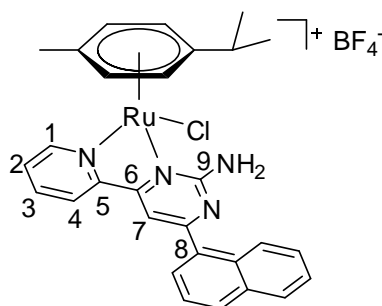
C2), 125.0 (s, C4), 108.1 (s, C7), 105.8 (s, C_{cymene}), 103.6 (s, C_{cymene}), 87.2 (s, C_{cymene}), 86.3 (s, C_{cymene}), 82.8 (s, C_{cymene}), 82.3 (s, C_{cymene}), 30.4 (s, C_{cymene}), 21.6 (s, C_{cymene}), 18.4 (s, C_{cymene}).
³¹P NMR (242.9 MHz, DMSO-*d*₆, 20 °C): δ -144.16 (h; *J*_{PF} = 714.1 Hz, PF₆⁻).



[2-Amino-4-(pyridin-2-yl)pyrimidine(chlorido)(η^6 -*p*-cymene)ruthenium(II)]tetraphenylborate 36a(BPh₄). The synthesis of **36a-BPh₄** was carried out as described in general synthesis but 154.0 mg of NaBPh₄ salt (0.45 mmol) were also added to the solution and before concentrating the excess and formed salts were filtered off. Yield: 217.2 mg (95%, yellow solid). Anal. calcd for C₄₃H₄₂BCIN₄Ru + 1.5CH₂Cl₂: C, 60.02; H, 5.06; N, 6.29. Found: C, 59.00; H, 5.20; N, 6.20. ¹H NMR (600.1 MHz, DMSO-*d*₆, 20 °C): δ 9.48 (d, *J*_{HH} = 5.28 Hz, 1H, H1), 8.70 (d, *J*_{HH} = 4.99 Hz, 1H, H8), 8.58 (d, *J*_{HH} = 7.92 Hz, 1H, H4), 8.27-8.24 (m, 1H, H3), 7.84-7.81 (m, 1H, H2), 7.78 (d, *J*_{HH} = 4.99 Hz, H7), 7.19 (m, 8H, H_{Ph}), 6.92 (m, 8H, H_{Ph}), 6.81-6.78 (m, 4H, H_{Ph}), 6.22 (d, *J*_{HH} = 6.16 Hz, 1H, H_{cymene}), 6.04-6.02 (m, 3H, H_{cymene}), 2.47 (m, 1H, H_{cymene}), 2.22 (s, 3H, H_{cymene}), 0.94 (d, *J*_{HH} = 7.04 Hz, 3H, H_{cymene}), 0.85 (d, *J*_{HH} = 7.05 Hz, 3H, H_{cymene}). ¹³C NMR (150.9 MHz, DMSO-*d*₆, 20 °C): δ 164.5 (s, C9), 163.9-162.9 (q, C_{Ph}), 161.4 (s, C8), 161.1 (s, C6), 156.1 (s, C1), 153.8 (s, C5), 140.0 (s, C3), 135.5 (s, C_{Ph}), 128.9 (s, C2), 125.3 (s, C_{Ph}), 125.0 (s, C4), 121.5 (s, C_{Ph}), 108.1 (s, C7), 105.8 (s, C_{cymene}), 103.5 (s, C_{cymene}), 87.2 (s, C_{cymene}), 86.3 (s, C_{cymene}), 82.8 (s, C_{cymene}), 82.2 (s, C_{cymene}), 30.4 (s, C_{cymene}), 21.6 (s, C_{cymene}), 21.6 (s, C_{cymene}), 18.4 (s, C_{cymene}).

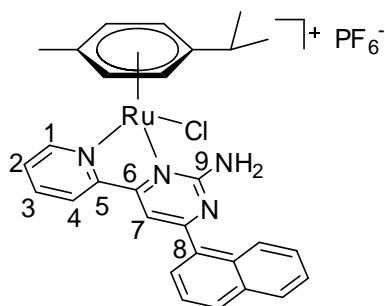


[2-Amino-6-(1-phenyl)-4-(pyridin-2-yl)pyrimidine](chlorido)(η^6 -*p*-cymene)ruthenium(II)] tetraphenylborate **36b-BPh₄. The synthesis of **36b-BPh₄** was carried out as described in general synthesis but 154.0 mg of NaBPh₄ salt (0.45 mmol) were also added to the solution and before concentrating the excess and formed salts were filtered off. Yield: 211.2 mg (84%, fulvous solid). Anal. calcd for C₄₉H₄₆BClN₄Ru: C, 70.21; H, 5.53; N, 6.68. Found: C, 69.48; H, 5.33; N, 6.57. ¹H NMR (600.1 MHz, DMSO-*d*₆, 20 °C): δ 9.50 (d, $J_{\text{HH}} = 4.4$ Hz, 1H, H1), 8.89 (d, $J_{\text{HH}} = 7.93$ Hz, 1H, H4), 8.39 (s, 1H, H7), 8.37 (d, $J_{\text{HH}} = 7.04$ Hz, 2H, H11), 8.34-8.31 (m, 1H, H3), 7.86-7.84 (m, 1H, H2), 7.65-7.63 (m, 3H, H12 & H13), 7.17 (s br., 8H, H_{Ph}), 6.93-6.91 (m, 8H, H_{Ph}), 6.80-6.78 (m, 4H, H_{Ph}), 6.26 (d, $J_{\text{HH}} = 5.28$ Hz, 1H, H_{cymene}), 6.05-6.03 (m, 3H, H_{cymene}), 2.23 (s, 3H, H_{cymene}), 1.08 (d, $J_{\text{HH}} = 6.45$ Hz, 3H, H_{cymene}), 0.85 (d, $J_{\text{HH}} = 6.45$ Hz, 3H, H_{cymene}). ¹³C NMR (150.9 MHz, DMSO-*d*₆, 20 °C): δ 166.5 (s, C9), 164.3 (s, C8), 163.9-162.9 (q, C_{Ph}), 161.9 (s, C6), 156.1 (s, C1), 154.2 (s, C5), 140.0 (s, C3), 135.6 (s, C_{Ph}), 134.6 (s, C10), 132.6 (s, C13), 129.1 (s, C11), 128.8 (s, C2), 127.9 (s, C12), 125.4 (s, C_{Ph}), 125.2 (s, C4), 121.6 (s, C_{Ph}), 105.7 (s, C_{cymene}), 104.6 (s, C7), 103.6 (s, C_{cymene}), 87.2 (s, C_{cymene}), 86.2 (s, C_{cymene}), 83.0 (s, C_{cymene}), 82.4 (s, C_{cymene}), 30.4 (s, C_{cymene}), 21.7 (s, C_{cymene}), 21.6 (s, C_{cymene}), 18.5 (s, C_{cymene}).**



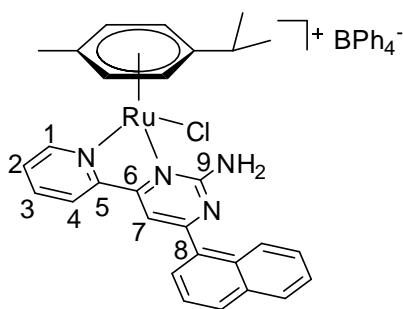
Experimental

[2-Amino-6-(1-naphthyl)-4-(pyridin-2-yl)pyrimidine](chlorido)(η^6 -*p*-cymene)ruthenium(II)] tetrafluoroborate **36c-BF₄. The synthesis of **36c-BF₄** was carried out as described in general synthesis but 49.5 mg of NaBF₄ salt (0.45 mmol) were also added to the solution and before concentrating the excess and formed salts were filtered off. Yield: 186.9 mg (95%, dark tangerine solid). Anal. calcd for C₂₉H₂₈BClF₄N₄Ru: C, 53.11; H, 4.30; N, 8.54. Found: C, 52.23; H, 4.57; N, 8.49. ¹H NMR (600.1 MHz, DMSO-*d*₆, 20 °C): δ 9.53 (d, $J_{\text{HH}} = 4.91$ Hz, 1H, H1), 8.78 (d, $J_{\text{HH}} = 7.92$ Hz, 1H, H8), 8.34-8.28 (m, 2H, H3 & H_{naphthyl}), 8.23 (s, 1H, H7), 8.18 (d, $J_{\text{HH}} = 8.22$ Hz, 1H, H_{naphthyl}), 8.10-8.09 (m, 1H, H_{naphthyl}), 7.92 (d, $J_{\text{HH}} = 7.04$ Hz, 1H, H_{naphthyl}), 7.87 (t, $J_{\text{HH}} = 6.45$ Hz, 1H, H2), 7.71 (t, $J_{\text{HH}} = 7.34$ Hz, 1H, H_{naphthyl}), 7.65-7.62 (m, 2H, H_{naphthyl}), 6.34 (d, $J_{\text{HH}} = 6.16$ Hz, 1H, H_{cymene}), 6.10 (m, 3H, H_{cymene}), 2.58-2.56 (m, 1H, H_{cymene}), 2.28 (s, 3H, H_{cymene}), 1.03 (d, $J_{\text{HH}} = 6.75$ Hz, 3H, H_{cymene}), 0.94 (d, $J_{\text{HH}} = 6.75$ Hz, 3H, H_{cymene}). ¹³C NMR (150.9 MHz, DMSO-*d*₆, 20 °C): δ 169.6 (s, C8), 164.1 (s, C9), 161.5 (s, C6), 156.1 (s, C1), 154.1 (s, C5), 140.0 (s, C3), 134.0 (s, C_{naphthyl}), 133.4 (s, C_{naphthyl}), 131.2 (s, C_{naphthyl}), 129.8 (s, C_{naphthyl}), 128.9 (s, C_{naphthyl}), 128.7 (s, C2), 128.6 (s, C_{naphthyl}), 127.4 (s, C_{naphthyl}), 126.5 (s, C_{naphthyl}), 125.3 (s, C_{naphthyl}), 125.3 (s, C_{naphthyl}), 125.0 (s, C4), 109.3 (s, C7), 105.7 (s, C_{cymene}), 103.7 87.1 (s, C_{cymene}), 86.3 (s, C_{cymene}), 83.0 (s, C_{cymene}), 82.5 (s, C_{cymene}), 30.5 (s, C_{cymene}), 21.8 (s, C_{cymene}), 21.5 (s, C_{cymene}), 18.5 (s, C_{cymene}).**



[2-Amino-6-(1-naphthyl)-4-(pyridin-2-yl)pyrimidine](chlorido)(η^6 -*p*-cymene)ruthenium(II)]hexafluorophosphate **36c-PF₆. The synthesis of **36c-PF₆** was carried out as described in general synthesis but 83.0 mg of KPF₆ salt (0.45 mmol) were also added to the**

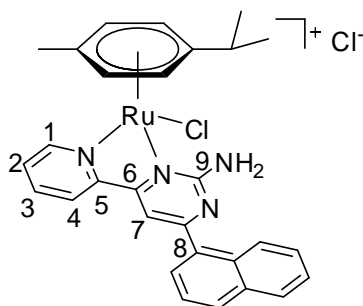
solution and before concentrating the excess and formed salts were filtered off. Yield: 182.1 mg (85%, dark tangerine solid). Anal. calcd for C₂₉H₂₈ClF₆PN₄Ru: C, 48.78; H, 3.95; N, 7.85. Found: C, 48.53; H, 4.08; N, 7.79. ¹H NMR (600.1 MHz, DMSO-*d*₆, 20 °C): δ 9.53 (d, *J*_{HH} = 4.99 Hz, 1H, H1), 8.77 (d, *J*_{HH} = 7.92 Hz, 1H, H4), 8.34-8.27 (m, 2H, H3 & H_{naphthyl}), 8.22 (s, 1H, H7), 8.18 (d, *J*_{HH} = 8.22 Hz, 1H, H_{naphthyl}), 8.10-8.08 (m, 1H, H_{naphthyl}), 7.92 (d, *J*_{HH} = 6.45 Hz, 1H, H_{naphthyl}), 7.87 (t, *J*_{HH} = 7.04 Hz, 1H, H2), 7.71 (t, *J*_{HH} = 7.34 Hz, 1H, H_{naphthyl}), 7.66-7.63 (m, 2H, H_{naphthyl}), 6.34 (d, *J*_{HH} = 6.16 Hz, 1H, H_{cymene}), 6.12-6.09 (m, 3H, H_{cymene}), 2.51-2.50 (m, 1H, H_{cymene}), 2.28 (s, 3H, H_{cymene}), 1.03 (d, *J*_{HH} = 6.75 Hz, 3H, H_{cymene}), 0.94 (d, *J*_{HH} = 6.74 Hz, 3H, H_{cymene}). ¹³C NMR (150.9 MHz, DMSO-*d*₆, 20 °C): δ 169.6 (s, C8), 164.1 (s, C9), 161.5 (s, C6), 156.1 (s, C1), 154.1 (s, C5), 140.0 (s, C3), 134.0 (s, C_{naphthyl}), 133.4 (s, C_{naphthyl}), 131.2 (s, C_{naphthyl}), 129.8 (s, C_{naphthyl}), 128.9 (s, C_{naphthyl}), 128.7 (s, C2), 128.5 (s, C_{naphthyl}), 127.4 (s, C_{naphthyl}), 126.5 (s, C_{naphthyl}), 125.3 (s, C_{naphthyl}), 125.3 (s, C_{naphthyl}), 125.0 (s, C4), 109.3 (s, C7), 105.7 (s, C_{cymene}), 103.7 (s, C_{cymene}), 87.2 (s, C_{cymene}), 86.4 (s, C_{cymene}), 83.0 (s, C_{cymene}), 82.9 (s, C_{cymene}), 30.4 (s, C_{cymene}), 21.8 (s, C_{cymene}), 21.5 (s, C_{cymene}), 18.5 (s, C_{cymene}). ³¹P NMR (242.9 MHz, DMSO-*d*₆, 20 °C): δ -144.18 (h; *J*_{PF} = 711.1 Hz, PF₆).



[2-Amino-6-(1-naphthyl)-4-(pyridin-2-yl)pyrimidine](chlorido)(η⁶-*p*-cymene)ruthenium(II)]tetrafluoroborate **36c-BPh₄. The synthesis of **36c-BPh₄** was carried out as described in general synthesis but 154.0 mg of NaBPh₄ salt (0.45 mmol) were also added to the solution and before concentrating the excess and formed salts were filtered off. Yield: 250.5 mg (94%, dark tangerine solid). Anal. calcd for C₅₃H₄₈BClN₄Ru: C, 71.66; H, 5.45; N, 6.31. Found: C, 71.61; H, 5.8; N, 6.40. ¹H NMR (600.1 MHz, DMSO-*d*₆, 20 °C): δ 9.52 (d, *J*_{HH} =**

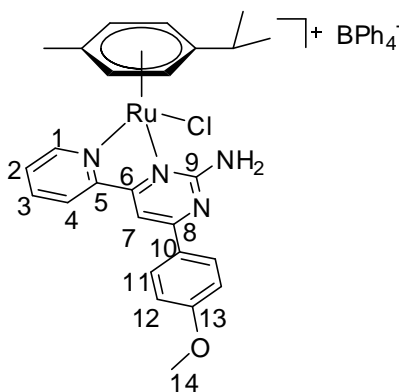
Experimental

5.28 Hz, 1H, H1), 8.74 (d, $J_{\text{HH}} = 7.92$ Hz, 1H, H4), 8.33-8.31 (m, 1H, $\text{H}_{\text{naphthyl}}$), 8.29-8.26 (m, 1H, H3), 8.21 (s, 1H, H7), 8.18 (d, $J_{\text{HH}} = 8.22$ Hz, 1H, $\text{H}_{\text{naphthyl}}$), 8.10-8.08 (m, 1H, $\text{H}_{\text{naphthyl}}$), 7.91 (d, $J_{\text{HH}} = 7.04$ Hz, 1H, $\text{H}_{\text{naphthyl}}$), 7.87-7.85 (m, 1H, H2), 7.71 (t, $J_{\text{HH}} = 7.33$ Hz, 1H, $\text{H}_{\text{naphthyl}}$), 7.65-7.63 (m, 2H, $\text{H}_{\text{naphthyl}}$), 7.20-7.17 (m, 8H, H_{Ph}), 6.94-6.91 (m, 8H, H_{Ph}), 6.80-6.78 (m, 4H, H_{Ph}), 6.32 (d, $J_{\text{HH}} = 6.46$ Hz, 1H, H_{cymene}), 6.09-6.07 (m, 3H, H_{cymene}), 2.59-2.54 (m, 1H, H_{cymene}), 2.28 (s, 3H, H_{cymene}), 1.03 (d, $J_{\text{HH}} = 7.04$ Hz, 3H, H_{cymene}), 0.94 (d, $J_{\text{HH}} = 7.04$ Hz, 3H, H_{cymene}). ^{13}C NMR (150.9 MHz, $\text{DMSO-}d_6$, 20 °C): δ 169.6 (s, C8), 164.1 (s, C9), 163.9-162.9 (q, C_{Ph}), 161.5 (s, C6), 156.1 (s, C1), 154.0 (s, C5), 140.0 (s, C3), 135.5 (s, C_{Ph}), 134.0 (s, $\text{C}_{\text{naphthyl}}$), 133.4 (s, $\text{C}_{\text{naphthyl}}$), 131.2 (s, $\text{C}_{\text{naphthyl}}$), 129.8 (s, $\text{C}_{\text{naphthyl}}$), 128.9 (s, $\text{C}_{\text{naphthyl}}$), 128.8 (s, $\text{C}_{\text{naphthyl}}$), 128.7 (s, C2), 128.5 (s, $\text{C}_{\text{naphthyl}}$), 127.4 (s, $\text{C}_{\text{naphthyl}}$), 126.7 (s, $\text{C}_{\text{naphthyl}}$), 126.5 (s, $\text{C}_{\text{naphthyl}}$), 125.3 (s, C_{Ph}), 125.0 (s, C4), 115.2 (s, C7), 109.3 (s, C_{cymene}), 103.7 (s, C_{cymene}), 87.1 (s, C_{cymene}), 86.3 (s, C_{cymene}), 83.0 (s, C_{cymene}), 82.5 (s, C_{cymene}), 30.4 (s, C_{cymene}), 21.8 (s, C_{cymene}), 21.5 (s, C_{cymene}), 18.5 (s, C_{cymene}).



[2-Amino-6-(1-naphthyl)-4-(pyridin-2-yl)pyrimidine](chlorido)(η^6 -*p*-cymene)ruthenium(II)]chloride **36c-Cl. The synthesis of **36c-Cl** was carried out as described in general synthesis. Yield: 170.5 mg (94%, dark tangerine solid). Anal. calcd for $\text{C}_{29}\text{H}_{28}\text{Cl}_2\text{N}_4\text{Ru} + 0.5 \text{CH}_2\text{Cl}_2$: C, 53.83; H, 4.32; N, 8.65. Found: C, 54.61; H, 5.09; N, 8.97. ^1H NMR (600.1 MHz, $\text{DMSO-}d_6$, 20 °C): δ 9.58 (d, $J_{\text{HH}} = 5.28$ Hz, 1H, H1), 8.81 (d, $J_{\text{HH}} = 7.92$ Hz, 1H, H4), 8.34-8.32 (m, 1H, $\text{H}_{\text{naphthyl}}$), 8.30 (t, $J_{\text{HH}} = 7.63$ Hz, 1H, H3), 8.24 (s, 1H, H7), 8.18 (d, $J_{\text{HH}} = 8.21$ Hz, 1H, $\text{H}_{\text{naphthyl}}$), 8.10-8.08 (m, 1H, $\text{H}_{\text{naphthyl}}$), 7.93 (d, $J_{\text{HH}} = 6.45$ Hz, 1H, $\text{H}_{\text{naphthyl}}$), 7.87 (t, J_{HH}**

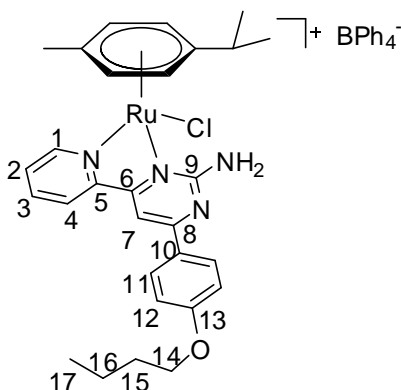
= 6.46 Hz, 1H, H2), 7.71 (t, $J_{\text{HH}} = 7.63$ Hz, 1H, H_{naphthyl}), 7.65-7.63 (m, 2H, H_{naphthyl}), 6.34 (d, $J_{\text{HH}} = 6.17$ Hz, 1H, H_{cymene}), 6.14-6.11 (m, 3H, H_{cymene}), 2.51-2.49 (m, 1H, H_{cymene}), 2.28 (s, 3H, H_{cymene}), 1.02(d, $J_{\text{HH}} = 6.75$ Hz, 3H, H_{cymene}), 0.94 (d, $J_{\text{HH}} = 6.75$ Hz, 3H, H_{cymene}). ¹³C NMR (150.9 MHz, DMSO-*d*₆, 20 °C): δ 169.6 (s, C8), 164.1 (s, C9), 161.5 (s, C6), 156.2 (s, C1), 154.0 (s, C5), 140.0 (s, C3), 134.0 (s, C_{naphthyl}), 133.4 (s, C_{naphthyl}), 131.2 (s, C_{naphthyl}), 129.8 (s, C_{naphthyl}), 128.9 (s, C_{naphthyl}), 128.7 (s, C2), 128.6 (s, C_{naphthyl}), 127.4 (s, C_{naphthyl}), 126.5 (s, C_{naphthyl}), 125.3 (s, C_{naphthyl}), 125.0 (s, C4), 109.2 (s, C7), 105.7 (s, C_{cymene}), 103.6 (s, C_{cymene}), 87.2 (s, C_{cymene}), 86.3 (s, C_{cymene}), 83.0 (s, C_{cymene}), 82.5 (s, C_{cymene}), 30.4 (s, C_{cymene}), 21.8 (s, C_{cymene}), 21.5 (s, C_{cymene}), 18.5 (s, C_{cymene}).



[2-Amino-6-(3-methoxyphenyl)-4-(pyridin-2-yl)pyrimidine](chlorido)(η^6 -*p*-cymene)ruthenium(II)]tetrafluoroborate **36d-BPh₄. The synthesis of **36d-BPh₄** was carried out as described in general synthesis but 154.0 mg of NaBPh₄ salt (0.45 mmol) were also added to the solution and before concentrating the excess and formed salts were filtered off. Yield: 242.3 mg (93%, yellow solid). Anal. calcd for C₅₀H₄₈BClN₄Ru: C, 69.16; H, 5.57; N, 6.45. Found: C, 68.68; H, 6.51; N, 6.58. ¹H NMR (600.1 MHz, DMSO-*d*₆, 20 °C): δ 9.50 (d, $J_{\text{HH}} = 5.29$ Hz, 1H, H1), 8.88 (d, $J_{\text{HH}} = 7.92$ Hz, 1H, H4), 8.39-8.38 (m, 3H, H7 & H11), 8.33-8.30 (m, 1H, H3), 7.85-7.83 (m, 1H, H2), 7.18-7.17 (m, 10H, H_{Ph} & H12), 6.93-6.91 (m, 8H, H_{Ph}), 6.80-6.78 (m, 4H, H_{Ph}), 6.25 (d, $J_{\text{HH}} = 6.17$ Hz, 1H, H_{cymene}), 6.06-6.02 (m, 3H, H_{cymene}), 3.88 (s, 3H, H14), 2.48-2.46 (m, 1H, H_{cymene}), 2.23 (s, 3H, H_{cymene}), 0.96 (d, $J_{\text{HH}} = 6.75$ Hz, 3H, H_{cymene}), 0.86 (d, $J_{\text{HH}} = 7.04$ Hz, 3H, H_{cymene}). ¹³C NMR (150.9 MHz, DMSO-*d*₆, 20 °C): δ 165.8 (s, C9),**

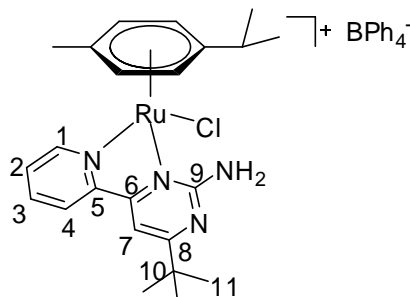
Experimental

164.0 (s, C8), 163.9-162.9 (q, C_{Ph}), 163.0 (s, C6), 161.3 (s, C13), 156.0 (s, C1), 154.3 (s, C5), 139.9 (s, C3), 135.5 (s, C_{Ph}), 129.8 (s, C12), 128.6 (s, C10), 126.8 (s, C2), 125.3 (s, C_{Ph}), 125.0 (s, C4), 114.4 (s, C11), 104.0 (s, C_{cymene} & C7), 103.4 (s, C_{cymene}), 87.1 (s, C_{cymene}), 86.2 (s, C_{cymene}), 82.8 (s, C_{cymene}), 82.2 (s, C_{cymene}), 30.4 (s, C_{cymene}), 21.7 (s, C_{cymene}), 21.5 (s, C_{cymene}), 18.4 (s, C_{cymene}).



[2-Amino-6-(3-butoxyphenyl)-4-(pyridin-2-yl)pyrimidine](chlorido)(η^6 -p-cymene)ruthenium(II)]tetrafluoroborate **36e-BPh₄. The synthesis of **36e-BPh₄** was carried out as described in general synthesis but 154.0 mg of NaBPh₄ salt (0.45 mmol) were also added to the solution and before concentrating the excess and formed salts were filtered off. Yield: 224 mg (82%, fulvous solid). Anal. calcd for C₅₃H₅₄BClN₄Ru: C, 69.93; H, 5.98; N, 6.15. Found: C, 68.33; H, 6.03; N, 6.03. ¹H NMR (600.1 MHz, DMSO-*d*₆, 20 °C): δ 9.48 (d, $J_{\text{HH}} = 4.69$ Hz, 1H, H1), 8.86 (d, $J_{\text{HH}} = 7.63$ Hz, 1H, H4), 8.37-8.36 (m, 3H, H7 & H11), 8.31-8.29 (m, 1H, H3), 7.84-7.82 (m, 1H, H2), 7.18-7.14 (m, 10H, H_{Ph} & H12), 6.93-6.91 (m, 8H, H_{Ph}), 6.80-6.78 (m, 4H, H_{Ph}), 6.24 (d, $J_{\text{HH}} = 5.57$ Hz, 1H, H_{cymene}), 6.02-6.01 (m, 3H, H_{cymene}), 4.10 (t, $J_{\text{HH}} = 5.87$ Hz, 2H, H14), 2.48-2.46 (m, 1H, H_{cymene}), 2.23 (s, 3H, H_{cymene}), 1.75-1.73 (m, 2H, H15), 1.48-1.44 (m, 2H, H16), 0.95-0.94 (m, 6H, H_{cymene} & H17), 0.85 (d, $J_{\text{HH}} = 6.46$ Hz, 3H, H_{cymene}). ¹³C NMR (150.9 MHz, DMSO-*d*₆, 20 °C): δ 165.9 (s, C9), 164.1 (s, C8), 163.9-162.9 (q, C_{Ph}), 162.5 (s, C6), 161.4 (s, C13), 156.0 (s, C1), 154.4 (s, C5), 140.0 (s, C3), 135.6 (s, C_{Ph}), 129.9 (s, C11), 128.7 (s, C2), 126.6 (s, C4), 125.4 (s, C_{Ph}), 125.4 (s, C10), 121.6 (s, C_{Ph}),**

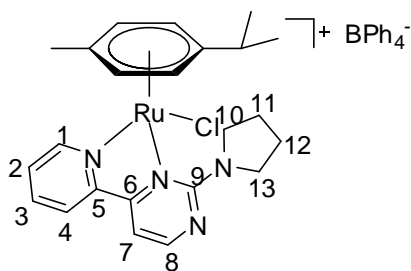
114.9 (s, C12), 105.7 (s, C_{cymene}), 104.0 (s, C7), 103.5 (s, C_{cymene}), 87.1 (s, C_{cymene}), 86.2 (s, C_{cymene}), 82.9 (s, C_{cymene}), 82.3 (s, C_{cymene}), 67.7 (s, C14), 30.7 (s, C15), 30.4 (s, C_{cymene}), 21.7 (s, C_{cymene}), 21.6 (s, C_{cymene}), 18.8 (s, C16), 18.5 (s, C_{cymene}), 13.8 (s, C17).



[2-Amino-6-(tbutyl)-4-(pyridin-2-yl)pyrimidine](chlorido)(η^6 -p-cymene)ruthenium(II)]-

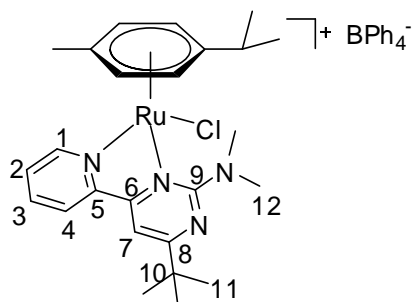
tetrafluoroborate 36f-BPh₄. The synthesis of **36f-BPh₄** was carried out as described in general synthesis but 154.0 mg of NaBPh₄ salt (0.45 mmol) were also added to the solution and before concentrating the excess and formed salts were filtered off. Yield: 220.9 mg (90%, yellow solid). Anal. calcd for C₄₇H₅₀BClN₄Ru: C, 68.99; H, 6.16; N, 6.85. Found: C, 66.58; H, 6.86; N, 6.33. ¹H NMR (600.1 MHz, DMSO-*d*₆, 20 °C): δ 9.45 (d, $J_{\text{HH}} = 5.29$ Hz, 1H, H1), 8.75 (d, $J_{\text{HH}} = 7.92$ Hz, 1H, H4), 8.27-8.25 (m, 1H, H3), 7.86 (s, 1H, H7), 7.83-7.80 (m, 1H, H2), 7.18-7.17 (m, 10H, H_{Ph} & H12), 6.93-6.91 (m, 8H, H_{Ph}), 6.80-6.78 (m, 4H, H_{Ph}), 6.21 (d, $J_{\text{HH}} = 6.46$ Hz, 1H, H_{cymene}), 6.00-5.98 (m, 3H, H_{cymene}), 2.45-2.41 (m, 1H, H_{cymene}), 2.21 (s, 3H, H_{cymene}), 1.36 (s, 9H, H11), 0.92 (d, $J_{\text{HH}} = 6.75$ Hz, 3H, H_{cymene}), 0.85 (d, $J_{\text{HH}} = 7.04$ Hz, 3H, H_{cymene}). ¹³C NMR (150.9 MHz, DMSO-*d*₆, 20 °C): δ 182.0 (s, C8), 163.9 (s, C9), 163.9-162.9 (q, C_{Ph}), 160.9 (s, C6), 156.0 (s, C1), 154.2 (s, C5), 139.9 (s, C3), 135.6 (s, C_{Ph}), 129.0 (s, C2), 125.2 (s, C_{Ph}), 124.9 (s, C4), 121.6 (s, C_{Ph}), 105.5 (s, C_{cymene}), 105.0 (s, C7), 103.4 (s, C_{cymene}), 87.0 (s, C_{cymene}), 86.1 (s, C_{cymene}), 82.9 (s, C_{cymene}), 82.4 (s, C_{cymene}), 38.0 (s, C10), 30.4 (s, C_{cymene}), 28.9 (s, C11), 21.7 (s, C_{cymene}), 21.4 (s, C_{cymene}), 18.4 (s, C_{cymene}).

Experimental



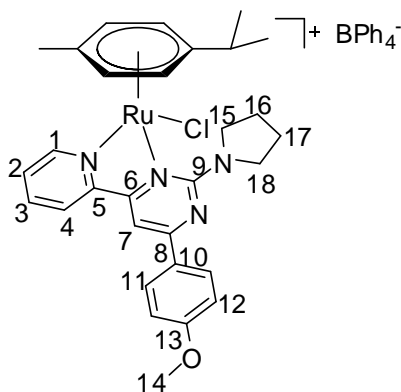
[4-(Pyridin-2-yl)-2-(pyrrolidin-1-yl)pyrimidine(chlorido)(η^6 -*p*-cymene)ruthenium(II)]-tetrafluoroborate **36g-BPh₄.**

The synthesis of **36g-BPh₄** was carried out as described in general synthesis but 154.0 mg of NaBPh₄ salt (0.45 mmol) were also added to the solution and before concentrating the excess and formed salts were filtered off. Yield: 220.4 mg (90%, brown solid). Anal. calcd for C₄₇H₄₈BCIN₄Ru: C, 69.16; H, 5.93; N, 6.86. Found: C, 68.78; H, 5.67; N, 6.74. ¹H NMR (600.1 MHz, DMSO-*d*₆, 20 °C): δ 9.24 (d, $J_{\text{HH}} = 4.99$ Hz, 1H, H1), 8.68 (d, $J_{\text{HH}} = 4.69$ Hz, 1H, H8), 8.41 (d, $J_{\text{HH}} = 7.92$ Hz, 1H, H4), 8.23-8.20 (m, 1H, H3), 7.82-7.79 (m, 1H, H2), 7.69 (d, $J_{\text{HH}} = 4.69$ Hz, 1H, H7), 7.19-7.17 (m, 8H, H_{Ph}), 6.93-6.91 (m, 8H, H_{Ph}), 6.80-6.77 (m, 4H, H_{Ph}), 5.91 (d, $J_{\text{HH}} = 6.16$ Hz, 1H, H_{cymene}), 5.77-5.73 (m, 3H, H_{cymene}), 4.00-3.63 (4s br., 4H, H10 & H13), 2.37-2.33 (m, 1H, H_{cymene}), 2.08-1.95 (m br., 6H, H_{cymene}, H11 & H12), 1.71 (s br., 1H, H12), 1.06 (d, $J_{\text{HH}} = 7.04$ Hz, 3H, H_{cymene}), 0.85 (d, $J_{\text{HH}} = 6.75$ Hz, 3H, H_{cymene}). ¹³C NMR (151 MHz, DMSO *d*₆) δ 165.8 (s, C8), 163.9-162.9 (m, C_{ph}), 163.0 (s, C6), 158.5 (s, C9), 156.0 (s, C1), 153.9 (s, C5), 140.1 (s, C3), 135.6 (s, C_{ph}), 128.3 (s, C2), 125.4 (s, C_{ph}), 124.3 (s, C4), 121.6 (s, C_{ph}), 109.0 (s, C7), 104.5 (s, C_{cymene}), 100.3 (s, C_{cymene}), 85.4 (s, C_{cymene}), 84.5 (s, C_{cymene}), 84.4 (s, C_{cymene}), 83.4 (s, C_{cymene}), 51.5 (s, C10), 49.6 (s, C13), 46.4 (s, C11), 30.4 (s, C_{cymene}), 24.1 (s, C12), 22.0 (s, C_{cymene}), 21.1 (s, C_{cymene}), 17.5 (s, C_{cymene}).

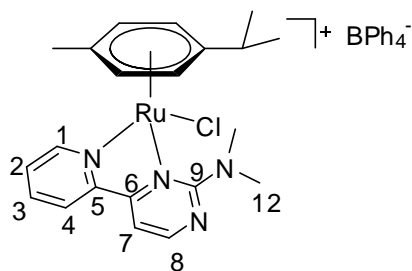


[4-*tert*-Butyl-*N,N*-dimethyl-6-(pyridin-2-yl)pyrimidi-2-amine(chlorido)(η^6 -*p*-cymene)-ruthenium(II)]tetrafluoroborate **36h-BPh₄. The synthesis of **36h-BPh₄** was carried out as described in general synthesis but 154.0 mg of NaBPh₄ salt (0.45 mmol) were also added to the solution and before concentrating the excess and formed salts were filtered off. Yield: 233.6 mg (92%, dark green solid). Anal. calcd for C₄₉H₅₄BClN₄Ru + DMSO(*d*₆): C, 65.77; H, 7.09; N, 6.02. Found: C, 65.42; H, 6.38; N, 6.04. ¹H NMR (600.1 MHz, DMSO-*d*₆, 20 °C): δ 9.29 (d, $J_{\text{HH}} = 5.28$ Hz, 1H, H1), 8.59 (d, $J_{\text{HH}} = 8.22$ Hz, 1H, H4), 8.24-8.21 (m, 1H, H3), 7.83 (s, 1H, H7), 7.83-7.79 (m, 1H, H2), 7.18-7.17 (m, 8H, H_{Ph}), 6.93-6.91 (m, 8H, H_{Ph}), 6.80-6.77 (m, 4H, H_{Ph}), 5.93 (d, $J_{\text{HH}} = 6.16$ Hz, 1H, H_{cymene}), 5.83-5.77 (m, 2H, H_{cymene}), 5.78 (d, $J_{\text{HH}} = 6.16$ Hz, 1H, H_{cymene}), 3.42 (s br., H12 & water), 2.32-2.27 (m, 1H, H_{cymene}), 2.13 (s, 3H, H_{cymene}), 1.37 (s, 9H, H11), 0.96 (d, $J_{\text{HH}} = 7.04$ Hz, 3H, H_{cymene}), 0.79 (d, $J_{\text{HH}} = 6.75$ Hz, 3H, H_{cymene}). ¹³C NMR (150.9 MHz, DMSO-*d*₆, 20 °C): δ 178.9 (s, C8), 167.4 (s, C9), 163.9-162.9 (q, C_{Ph}), 163.6 (s, C6), 155.9 (s, C1), 154.3 (s, C5), 140.0 (s, C3), 135.6 (s, C_{Ph}), 128.2 (s, C2), 125.4 (s, C_{Ph}), 124.5 (s, C4), 121.6 (s, C_{Ph}), 106.8 (s, C7), 103.5 (s, C_{cymene}), 101.5 (s, C_{cymene}), 85.8 (s, C_{cymene}), 85.0 (s, C_{cymene}), 83.6 (s, C_{cymene}), 83.3 (s, C_{cymene}), 38.1 (s, C10), 30.4 (s, C_{cymene}), 28.7 (s, C11), 21.8 (s, C_{cymene}), 21.1 (s, C_{cymene}), 17.8 (s, C_{cymene}).**

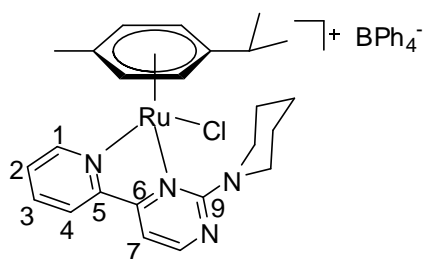
Experimental



[4-(4-Methoxyphenyl)-6-(pyridin-2-yl)-2-(pyrrolidin-1-yl)pyrimidine(chlorido)(η^6 -*p*-cymene)ruthenium(II)]tetrafluoroborate **36i-BPh₄.** The synthesis of **36i-BPh₄** was carried out as described in general synthesis but 154.0 mg of NaBPh₄ salt (0.45 mmol) were also added to the solution and before concentrating the excess and formed salts were filtered off. Yield: 243.5 mg (88%, ginger solid). Anal. calcd for C₅₄H₅₄BClN₄ORu: C, 70.32; H, 5.90; N, 6.07. Found: C, 69.50; H, 5.88; N, 6.02. ¹H NMR (600.1 MHz, DMSO-*d*₆, 20 °C): δ 9.24 (d, $J_{\text{HH}} = 5.29$ Hz, 1H, H1), 8.65 (d, $J_{\text{HH}} = 8.22$ Hz, 1H, H4), 8.40(d, $J_{\text{HH}} = 8.8$ Hz, 1H, H11), 8.31 (s, 1H, H7), 8.27-8.24 (m, 1H, H3), 7.82-7.80 (m, 1H, H2), 7.21-7.18 (m, 8H, H_{Ph}), 7.17 (d, $J_{\text{HH}} = 8.8$ Hz, 1H, H12), 6.94-6.92 (m, 8H, H_{Ph}), 6.81-6.78 (m, 4H, H_{Ph}), 5.89 (d, $J_{\text{HH}} = 6.16$ Hz, 1H, H_{cymene}), 5.78 (d, $J_{\text{HH}} = 5.87$ Hz, 1H, H_{cymene}), 5.75 (d, $J_{\text{HH}} = 6.16$ Hz, 1H, H_{cymene}), 5.72 (d, $J_{\text{HH}} = 6.16$ Hz, 1H, H_{cymene}), 4.04-3.38 (m br., 7H, H14, H15 & H18), 2.44-2.39 (m, 1H, H_{cymene}), 2.24-1.75 (m br., 4H, H16, H17), 2.02 (s, 3H, H_{cymene}), 1.05 (d, $J_{\text{HH}} = 6.74$ Hz, 3H, H_{cymene}), 0.85 (d, $J_{\text{HH}} = 6.75$ Hz, 3H, H_{cymene}). ¹³C NMR (150.9 MHz, DMSO-*d*₆, 20 °C): δ 165.6 (s, C9), 163.9-162.9 (m, C_{Ph}, C6, C8 & C13), 155.9 (s, C1), 154.3 (s, C5), 139.9 (s, C3), 135.6 (s, C_{Ph}), 129.9 (s, C11), 128.0 (s, C10), 126.9 (s, C2), 125.3 (s, C_{Ph}), 121.5 (s, C_{Ph}), 124.3 (s, C4), 114.5 (s, C12), 104.8 (s, C_{cymene}), 104.5 (s, C_{cymene}), 99.9 (s, C7), 85.4 (s, C_{cymene}), 84.7 (s, C_{cymene}), 84.2 (s, C_{cymene}), 83.2 (s, C_{cymene}), 30.4 (s, C_{cymene}), 21.9 (s, C_{cymene}), 21.0 (s, C_{cymene}), 17.4 (s, C_{cymene}).

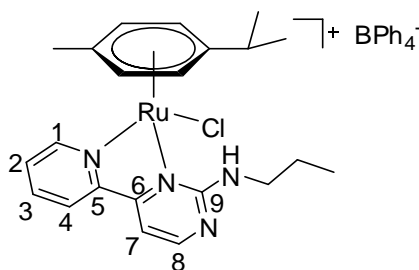


[*N,N*-Dimethyl-4-(pyridine-2-yl)pyrimidine(chlorido)(η^6 -*p*-cymene)ruthenium(II)]tetrafluoroborate **36j-BPh₄.** The synthesis of **36j-BPh₄** was carried out as described in general synthesis but 154.0 mg of NaBPh₄ salt (0.45 mmol) were also added to the solution and before concentrating the excess and formed salts were filtered off. Yield: 222.84 mg (94%, dark green solid). Anal. calcd for C₄₅H₄₆BClN₄Ru: C, 68.40; H, 5.87; N, 7.09. Found: C, 67.30; H, 5.89; N, 7.21. ¹H NMR (600.1 MHz, DMSO-*d*₆, 20 °C): δ 9.33 (d, $J_{\text{HH}} = 5.29$ Hz, 1H, H1), 8.74 (d, $J_{\text{HH}} = 4.69$ Hz, 1H, H8), 8.47 (d, $J_{\text{HH}} = 7.93$ Hz, 1H, H4), 8.26-8.23 (m, 1H, H3), 7.84-7.82 (m, 1H, H2), 7.79 (d, $J_{\text{HH}} = 4.69$ Hz, 1H, H7), 7.19-7.17 (m, 10H, H_{Ph}), 6.93-6.91 (m, 10H, H_{Ph}), 6.80-6.78 (m, 5H, H_{Ph}), 6.00 (d, $J_{\text{HH}} = 5.87$ Hz, 1H, H_{cymene}), 5.89 (d, $J_{\text{HH}} = 5.87$ Hz, 1H, H_{cymene}), 5.82 (d, $J_{\text{HH}} = 5.87$ Hz, 1H, H_{cymene}), 5.78 (d, $J_{\text{HH}} = 5.87$ Hz, 1H, H_{cymene}), 3.52 (s br., 3H, H10), 3.26 (s br., 3H, H11), 2.35-2.33 (m, 1H, H_{cymene}), 2.13 (s, 3H, H_{cymene}), 0.98 (d, $J_{\text{HH}} = 6.75$ Hz, 3H, H_{cymene}), 0.82 (d, $J_{\text{HH}} = 6.75$ Hz, 3H, H_{cymene}). ¹³C NMR (151 MHz, DMSO *d*₆) δ 168.8 (s, C9), 168.0 (s, C8), 163.2 (s, C6), 163.6-162.6 (q, C_{Ph}), 155.5 (s, C1), 153.6 (s, C5), 139.6 (s, C3), 135.2 (s, C_{ph}), 127.8 (s, C2), 124.7 (s; C_{ph}), 124.1 (s, C4), 120.9 (s, C_{ph}), 109.5 (s, C7), 104.5 (s, C_{cymene}), 101.9 (s, C_{cymene}), 84.7 (s, C_{cymene}), 84.5 (s, C_{cymene}), 84.0 (s, C_{cymene}), 82.9 (s, C_{cymene}), 36.2 (s, C10), 29.9 (s, C_{cymene}), 21.2 (s, C_{cymene}), 20.7 (s, C_{cymene}), 17.3 (s, C_{cymene}).



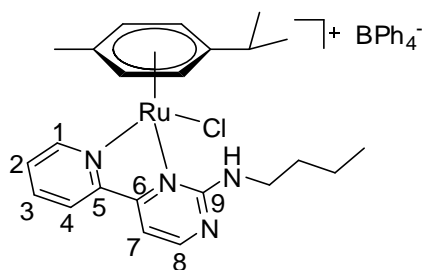
Experimental

[4-(2-Pyridinyl)-2-(1-piperidinyl)-pyrimidin(chlorido)(η^6 -*p*-cymene)ruthenium(II)]tetrafluoroborate **36k-BPh₄. The synthesis of **36k-BPh₄** was carried out as described in general synthesis but 154.0 mg of NaBPh₄ salt (0.45 mmol) were also added to the solution and before concentrating the excess and formed salts were filtered off. Yield: 300.0 mg (72%, green solid). Anal. calcd for C₄₈H₅₀BClN₄Ru: C, 69.44; H, 6.07; N, 6.75. Found: C, 68.83; H, 6.21; N, 6.65. ¹H NMR (400.1 MHz, DMSO *d*₆, 20 °C): δ 9.32 (d, $J_{\text{HH}} = 5.44$ Hz, 1H, H1), 8.75 (d, $J_{\text{HH}} = 4.68$ Hz, 1H, H8), 8.47 (d, $J_{\text{HH}} = 8.20$ Hz, 1H, H4), 8.24 (t, $J_{\text{HH}} = 7.82$ Hz, 1H, H3), 7.82 (t, $J_{\text{HH}} = 6.46$ Hz, 1H, H2), 7.77 (d, $J_{\text{HH}} = 4.72$ Hz, 1H, H7), 7.19 (m, 8H, BPh₄⁻), 6.92 (t, $J_{\text{HH}} = 7.24$ Hz, 8H, BPh₄⁻), 6.79 (t, $J_{\text{HH}} = 7.04$ Hz, 4H, BPh₄⁻), 5.98 (d, $J_{\text{HH}} = 5.88$ Hz, 1H, H_{cymene}), 5.88 (d, $J_{\text{HH}} = 5.92$ Hz, 1H, H_{cymene}), 5.79-5.75 (m, 2H, H_{cymene}), 3.78 (t, $J_{\text{HH}} = 8.22$ Hz, 4H, H_{piperidinyl}), 2.32-2.39 (m, 1H, H_{cymene}), 2.14 (s, 3H, H_{cymene}), 1.66 (m, 6H, H_{piperidinyl}), 0.97 (d, $J_{\text{HH}} = 7.04$ Hz, 3H, H_{cymene}), 0.82 (d, $J_{\text{HH}} = 6.68$ Hz, 3H, H_{cymene}). ¹³C NMR (100.6 MHz, DMSO *d*₆, 20 °C): δ 164.1-162.6 (m, BPh₄⁻), 162.5 (s, C9), 161.3 (s, C8), 159.0 (s, C6), 153.9 (s, C5), 149.4 (s, C1), 140.0 (s, C_{cymene}), 137.4 (s, C3), 135.5 (s, C_{cymene} & BPh₄⁻), 128.4 (s, C_{cymene}), 125.3-125.2 (m, BPh₄⁻), 124.7 (s, C2), 121.5 (s, C_{cymene} & BPh₄⁻), 120.9 (s, C4), 105.0 (s, C7), 64.9 (s, C_{piperidinyl}), 44.2 (s, C_{piperidinyl}), 30.4 (s, C_{cymene}), 25.3 (s, C_{piperidinyl}), 21.8 (s, C_{cymene}), 21.1 (s, C_{cymene}), 17.9 (s, C_{cymene}).**



[N-1-Propyl-4-(2-pyridinyl)pyrimidin-2-amin(chlorido)(η^6 -*p*-cymene)ruthenium(II)]tetrafluoroborate **36l-BPh₄. The synthesis of **36l-BPh₄** was carried out as described in general synthesis but 154.0 mg of NaBPh₄ salt (0.45 mmol) were also added to the solution and before concentrating the excess and formed salts were filtered off. Yield: 380.0 mg (85%, brown**

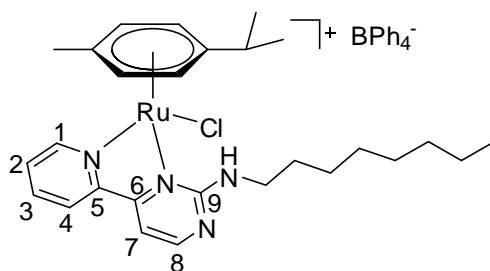
solid). Anal. calcd for C₄₆H₄₈BClN₄Ru: C, 68.70; H, 6.02; N, 6.97. Found: C, 68.17; H, 5.89; N, 7.04. ¹H NMR (400.1 MHz, DMSO *d*₆, 20 °C): δ 9.48 (s br., 1H, H1), 8.77 (s br., 1H, H8), 8.63 (d, *J*_{HH} = 6.8 Hz 1H, H4), 8.29 (s br., 1H, H3), 7.83 (s br., 1H, H2), 7.81 (s br., 1H, H7), 7.18 (s br., 8H, BPh₄⁻), 6.92 (s br., 8H, BPh₄⁻), 6.79 (s br., 5H, BPh₄⁻, NH), 6.15 (s, 1H, H_{cymene}), 6.05-6.01 (m, 3H, H_{cymene}), 3.57 (s br., 2H, H_{propyl}), 2.43 (s br., 1H, H_{cymene}), 2.21 (s, 3H, H_{cymene}), 1.70 (s br., 2H, H_{propyl}), 0.97-0.86 (m, 9H, H_{cymene} & H_{propyl}). ¹³C NMR (100.6 MHz, DMSO *d*₆, 20 °C): δ 164.1-162.6 (m, BPh₄⁻), 162.5 (s, C9), 161.5 (s, C8), 161.0 (s, C6), 156.1 (s, C5), 153.8 (s, C1), 140.1 (s, C_{cymene}), 135.5 (s br., C3, C_{cymene} & BPh₄⁻), 129.0 (s, C_{cymene}), 125.3-125.3 (s br., BPh₄⁻), 125.2 (s, C2), 121.5 (s br., C_{cymene} & BPh₄⁻), 121.2 (s, C4), 105.2 (s, C7), 43.7 (s, C_{propyl}), 30.3 (s, C_{cymene}), 21.9 (s, C_{propyl}), 21.6 (s, C_{cymene}), 21.5 (s, C_{cymene}), 18.3 (s, C_{cymene}), 11.2 (s, C_{propyl}).



[N-1-Butyl-4-(2-pyridinyl)pyrimidin-2-amin(chlorido)(η⁶-*p*-cymene)ruthenium(II)]tetrafluoroborate 36m-BPh₄. The synthesis of **36m-BPh₄** was carried out as described in general synthesis but 154.0 mg of NaBPh₄ salt (0.45 mmol) were also added to the solution and before concentrating the excess and formed salts were filtered off. Yield: 250.0 mg (61%, brown solid). Anal. calcd for C₄₇H₅₀BClN₄Ru: C, 68.99; H, 6.16; N, 6.85. Found: C, 68.92; H, 6.23; N, 6.68. ¹H NMR (400.1 MHz, DMSO *d*₆, 20 °C): δ 9.48 (d, *J*_{HH} = 5.08 Hz, 1H, H1), 8.76 (d, *J*_{HH} = 4.68 Hz, 1H, H8), 8.59 (d, *J*_{HH} = 8.24 Hz, 1H, H4), 8.27 (t, *J*_{HH} = 7.82 Hz, 1H, H3), 7.84 (t, *J*_{HH} = 6.46 Hz, 1H, H2), 7.78 (d, *J*_{HH} = 4.72 Hz, 1H, H7), 7.20 (s br., 8H, BPh₄⁻), 6.93 (t, *J*_{HH} = 7.24 Hz, 8H, BPh₄⁻), 6.78-6.81 (m, 5H, NH & BPh₄⁻), 6.14 (d, *J*_{HH} = 6.24 Hz, 1H, H_{cymene}), 6.03 (s br., 2H, H_{cymene}), 5.99 (d, *J*_{HH} = 6.28 Hz, 1H, H_{cymene}), 3.62 (t, *J*_{HH} = 6.64 Hz, 2H, H_{butyl}),

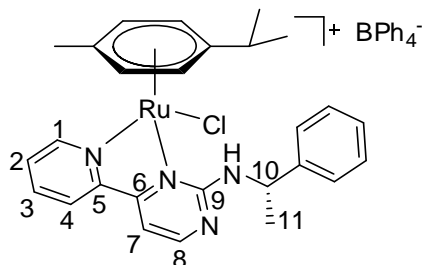
Experimental

2.47-2.40 (m, 1H, H_{cymene}), 2.21 (s, 3H, H_{cymene}), 1.68-1.66 (m, 2H, H_{butyl}), 1.43-1.38 (m, 2H, H_{butyl}), 0.97 (t, $J_{\text{HH}} = 7.42$ Hz, 3H, H_{butyl}), 0.93 (d, $J_{\text{HH}} = 8.04$ Hz, 3H, H_{cymene}), 0.86 (d, $J_{\text{HH}} = 7.04$ Hz, 3H, H_{cymene}). ¹³C NMR (100.6 MHz, DMSO *d*₆, 20 °C): δ 164.1-162.6 (m, BPh₄⁻), 162.5 (s, C9), 161.5 (s, C8), 161.0 (s, C6), 156.1 (s, C5), 153.8 (s, C1), 140.1 (s, C_{cymene}), 135.5 (s, C3, C_{cymene} & BPh₄⁻), 128.9 (s, C_{cymene}), 125.1 (m, C2 & BPh₄⁻), 121.5 (s, C4, C_{cymene} & BPh₄⁻), 105.0 (s, C7), 41.7 (s, C_{butyl}), 30.7 (s, C_{butyl}), 30.3 (s, C_{cymene}), 21.6 (s, C_{cymene}), 21.5 (s, C_{cymene}), 19.6 (s, C_{butyl}), 18.3 (s, C_{cymene}), 13.7 (s, C_{butyl}).



[N-1-Octyl-4-(2-pyridinyl)pyrimidin-2-amin(chlorido)(η^6 -*p*-cymene)ruthenium(II)]tetrafluoroborate **36n-BPh₄. The synthesis of **36n-BPh₄** was carried out as described in general synthesis but 154.0 mg of NaBPh₄ salt (0.45 mmol) were also added to the solution and before concentrating the excess and formed salts were filtered off. Yield: 370.0 mg (85%, brown solid). Anal. calcd for C₅₁H₅₈BClN₄Ru: C, 70.06; H, 6.69; N, 6.41. Found: C, 69.79; H, 6.77; N, 6.42. ¹H NMR (400.1 MHz, DMSO *d*₆, 20 °C): δ 9.48 (d, $J_{\text{HH}} = 5.08$ Hz, 1H, H1), 8.76 (d, $J_{\text{HH}} = 4.68$ Hz, 1H, H8), 8.60 (d, $J_{\text{HH}} = 8.24$ Hz, 1H, H4), 8.28 (t, $J_{\text{HH}} = 7.64$ Hz, 1H, H3), 7.85 (t, $J_{\text{HH}} = 6.44$ Hz, 1H, H2), 7.79 (d, $J_{\text{HH}} = 5.08$ Hz, 1H, H7), 7.19 (d, 8H, BPh₄⁻), 6.93 (t, $J_{\text{HH}} = 7.24$ Hz, 8H, BPh₄⁻), 6.81-6.77 (m, 5H, NH & BPh₄⁻), 6.14 (d, $J_{\text{HH}} = 5.88$ Hz, 1H, H_{cymene}), 6.03 (s br., 2H, H_{cymene}), 5.99 (d, $J_{\text{HH}} = 6.24$ Hz, 1H, H_{cymene}), 2.45-2.41 (m, 1H, H_{cymene}), 2.21 (s, 3H, H_{cymene}), 1.68 (s br., 2H, H_{octyl}), 1.35-1.28 (m, 12H, H_{octyl}), 0.93 (d, $J_{\text{HH}} = 6.68$ Hz, 3H, H_{cymene}), 0.87-0.85 (m, 6H, H_{cymene}, H_{octyl}). ¹³C NMR (100.6 MHz, DMSO *d*₆, 20 °C): δ 164.1-162.6 (m, BPh₄⁻), 162.1 (s, C9), 161.5 (s, C8), 161.0 (s, C6), 156.1 (s, C5), 153.8 (s, C1), 140.1 (s, C_{cymene}), 135.5 (s, C3, C_{cymene} & BPh₄⁻), 128.9 (s, C_{cymene}), 125.3-125.3 (m, BPh₄⁻), 125.2 (s,**

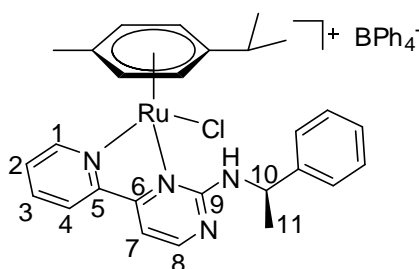
C2), 121.5 (s, C4, C_{cymene} & BPh₄⁻), 105.1 (s, C7), 42.0 (s, C_{octyl}), 31.2 (s, C_{octyl}), 30.3 (s, C_{octyl} & C_{cymene}), 28.7 (s, C_{octyl}), 28.6 (s, C_{octyl}), 26.3 (s, C_{octyl}), 22.1 (s, C_{octyl}), 21.6 (s, C_{cymene}), 21.5 (s, C_{cymene}), 18.3 (s, C_{cymene}), 14.0 (s, C_{octyl}).



[N-(S)-(+)-1-Phenylethyl-4-(2-pyridinyl)pyrimidin-2-amin(chlorido)(η^6 -*p*-cymene)ruthenium(II)]tetrafluoroborate 360-BPh₄. The synthesis of **360-BPh₄** was carried out as described in general synthesis but 154.0 mg of NaBPh₄ salt (0.45 mmol) were also added to the solution and before concentrating the excess and formed salts were filtered off. Yield: 0.34 g (0.39 mmol, 78%, green solid). Anal. calcd for C₅₁H₅₀BClN₄Ru: C, 70.71; H, 5.82; N, 6.47. Found: C, 70.71; H, 5.82; N, 6.53. ¹H NMR (400.1 MHz, DMSO *d*₆, 20 °C): δ 9.54 (d, $J_{\text{HH}} = 5.2$ Hz, 1H, H1), 9.49 (d, $J_{\text{HH}} = 5.2$ Hz, 1H, H1'), 8.83 (d, $J_{\text{HH}} = 4.8$ Hz, 1H, H8), 8.70 (d, $J_{\text{HH}} = 4.8$ Hz, 1H, H8'), 8.65 (t, $J_{\text{HH}} = 7.7$ Hz, 2H, H4 & H4'), 8.32 (t, $J_{\text{HH}} = 7.8$ Hz, 2H, H3 & H3'), 7.90-7.85 (m, 3H, H2 & H_{Ph}), 7.83 (d, $J_{\text{HH}} = 4.9$ Hz, 1H, H2'), 7.67 (d, $J_{\text{HH}} = 7.4$ Hz, 2H, H_{phenyl}), 7.53-7.22 (m, 8H, H7, H7', H_{Ph} & H_{Ph}'), 7.20 (s br., 16H, BPh₄⁻ & BPh₄⁻'), 6.92 (t, $J_{\text{HH}} = 7.3$ Hz, 16H, BPh₄⁻ & BPh₄⁻'), 6.85 (d, $J_{\text{HH}} = 8.7$ Hz, 1H, NH), 6.78 (t, $J_{\text{HH}} = 7.1$ Hz, 8H, BPh₄⁻ & BPh₄⁻'), 6.64 (d, $J_{\text{HH}} = 7.2$ Hz, 1H, NH'), 6.33 (d, $J_{\text{HH}} = 6.0$ Hz, 1H, H_{cymene}), 6.15 (d, $J_{\text{HH}} = 6.0$ Hz, 1H, H_{cymene}'), 6.08 (d, $J_{\text{HH}} = 6.0$ Hz, 1H, H_{cymene}), 5.96 (d, $J_{\text{HH}} = 6.0$ Hz, 1H, H_{cymene}'), 5.86 (t, $J_{\text{HH}} = 6.3$ Hz, 2H, H_{cymene} & H_{cymene}'), 5.79 (d, $J_{\text{HH}} = 6.0$ Hz, 1H, H_{cymene}), 5.53 (d, $J_{\text{HH}} = 6.0$ Hz, 1H, H_{cymene}'), 5.46-5.23 (m, 2H, C10 & C10'), 2.49-2.45 (m, 1H, H_{cymene}), 2.30-2.20 (m, 4H, H_{cymene}' & H_{cymene}), 2.07 (s, 3H, H_{cymene}'), 1.78 (d, $J_{\text{HH}} = 6.9$ Hz, 3H, H11), 1.63 (d, $J_{\text{HH}} = 6.8$ Hz, 3H, H11'), 0.96 (d, $J_{\text{HH}} = 6.8$ Hz, 3H, H_{cymene}), 0.89 (d, $J_{\text{HH}} = 6.9$ Hz, 3H, H_{cymene}'), 0.79 (dd, $J_{\text{HH}} = 6.7, 2.6$ Hz, 6H, H_{cymene} & H_{cymene}'). ¹³C NMR (100.6 MHz, DMSO

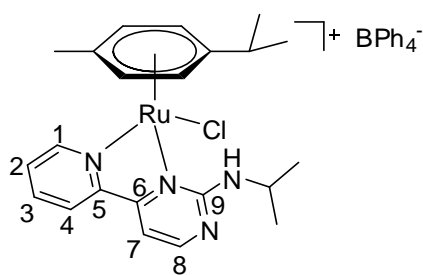
Experimental

d_6 , 20 °C): δ 164.1, 163.6 (s, C9 & C9'), 163.1, 162.6 (s, C8 & C8'), 161.6, 161.4 (s, C6 & C6'), 161.3 (dd, $J_{\text{HH}} = 36.2, 12.6$ Hz, BPh_4^- & BPh_4^-), 156.3 (s, C5 & C5'), 153.7 (s, C1 & C1'), 143.4, 142.3 (s, $\text{C}_{\text{phenylethyl}}$ & $\text{C}_{\text{phenylethyl}}$ '), 140.2 (s br., C_{cymene} & C_{cymene} '), 135.53 (s br., C3, C3', C_{cymene} , C_{cymene} ', BPh_4^- & BPh_4^-), 129.1 (s br., C_{cymene} & C_{cymene} '), 129.0, 128.9 (s, C_{phenyl} & C_{phenyl} '), 128.4, 128.0 (s, C_{phenyl} & C_{phenyl} '), 127.0, 126.6 (s, C_{phenyl} & C_{phenyl} '), 126.6, 125.6 (s, C2 & C2'), 125.3 (dd, $J_{\text{HH}} = 5.3, 2.6$ Hz, BPh_4^- & BPh_4^-), 121.5 (m, C4 & C4'), 108.5, 108.3 (s, C7 & C7'), 104.9-104.1 (m, C_{cymene} , C_{cymene} ', BPh_4^- & BPh_4^-), 87.1, 86.6, 85.6, 84.6, 84.1, 83.7, 83.6 (s, C_{cymene} & C_{cymene} '), 51.8, 51.6 (s, C10 & C10'), 30.4, 30.2 (s, C_{cymene} & C_{cymene} '), 22.9, 21.6 (s, C11 & C11'), 21.6, 21.1 (s, C_{cymene} & C_{cymene} '), 21.4, 20.6 (s, C_{cymene} & C_{cymene} '), 18.3, 18.0 (s, C_{cymene} & C_{cymene} ').



[N-(R)-(+)-1-Phenylethyl-4-(2-pyridinyl)pyrimidin-2-amin(chlorido)(η^6 -*p*-cymene)ruthenium(II)]tetrafluoroborate **36p-BPh₄. The synthesis of **36p-BPh₄** was carried out as described in general synthesis but 154.0 mg of NaBPh₄ salt (0.45 mmol) were also added to the solution and before concentrating the excess and formed salts were filtered off. Yield: 320.0 mg (74%, green solid). Anal. calcd for C₅₁H₅₀BClN₄Ru: C, 70.71; H, 5.82; N, 6.47. Found: C, 68.65; H, 6.01; N, 6.24. ¹H NMR (400.1 MHz, DMSO d_6 , 20 °C): δ 9.53, (d, $J_{\text{HH}} = 5.3$ Hz, 1H, H1), 9.48 (d, $J_{\text{HH}} = 5.3$ Hz, 1H, H1'), 8.81 (d, $J_{\text{HH}} = 4.9$ Hz, 1H, H8), 8.68 (d, $J_{\text{HH}} = 4.8$ Hz, 1H, H8'), 8.62 (t, $J_{\text{HH}} = 7.8$ Hz, 2H, H4 & H4'), 8.29 (t, $J_{\text{HH}} = 7.8$ Hz, 2H, H3 & H3'), 7.91-7.83 (m, 4H, H2 & H_{Ph}), 7.81 (d, $J_{\text{HH}} = 4.9$ Hz, 1H, H2'), 7.67 (d, $J_{\text{HH}} = 7.4$ Hz, 2H, H_{Ph}), 7.53-7.22 (m, 8H, H7, H7', H_{Ph} & H_{Ph}'), 7.18 (s br., 16H, BPh_4^- & BPh_4^-), 6.92 (t, $J_{\text{HH}} = 7.3$ Hz, 16H, BPh_4^- & BPh_4^-), 6.85 (d, $J_{\text{HH}} = 8.7$ Hz, 1H, NH), 6.79 (t, $J_{\text{HH}} = 7.1$ Hz, 8H, BPh_4^- & BPh_4^-), 6.64 (d,**

$J_{\text{HH}} = 7.3 \text{ Hz}$, 1H, NH), 6.31 (d, $J_{\text{HH}} = 6.1 \text{ Hz}$, 1H, H_{Cymene}), 6.13 (d, $J_{\text{HH}} = 6.1 \text{ Hz}$, 1H, H_{Cymene}), 6.06 (d, $J_{\text{HH}} = 6.1 \text{ Hz}$, 1H, H_{Cymene}), 5.94 (d, $J_{\text{HH}} = 6.1 \text{ Hz}$, 1H, H_{Cymene}), 5.84 (t, $J_{\text{HH}} = 7.2 \text{ Hz}$, 2H, H_{Cymene}), 5.77 (d, $J_{\text{HH}} = 6.1 \text{ Hz}$, 1H, H_{Cymene}), 5.51 (d, $J_{\text{HH}} = 6.0 \text{ Hz}$, 1H, H_{Cymene}), 5.45-5.24 (m, 2H, H10 & H10'), 2.45 (m, 1H, H_{Cymene}), 2.27-2.19 (m, 4H, H_{Cymene}), 2.07 (d, $J_{\text{HH}} = 8.7 \text{ Hz}$, 3H, H_{Cymene}), 1.78 (d, $J_{\text{HH}} = 6.9 \text{ Hz}$, 3H, H11), 1.63 (d, $J_{\text{HH}} = 6.8 \text{ Hz}$, 3H, H11'), 0.95 (d, $J_{\text{HH}} = 6.9 \text{ Hz}$, 3H, H_{Cymene}), 0.90 (t, $J_{\text{HH}} = 8.2 \text{ Hz}$, 3H, H_{Cymene}), 0.78 (dd, $J_{\text{HH}} = 6.8, 2.8 \text{ Hz}$, 6H, H_{Cymene}). ^{13}C NMR (100.6 MHz, DMSO d_6 , 20 °C): δ 161.4 (dd, $J_{\text{HH}} = 35.9, 15.8 \text{ Hz}$, BPh_4^- & BPh_4^-), 164.1, 163.6 (s, C9 & C9'), 163.2, 162.7 (s, C8 & C8'), 161.6, 161.5 (s, C6 & C6'), 156.3 (s, C5 & C5'), 153.7 (s, C1 & C1'), 143.5, 142.4 (s, $\text{C}_{\text{phenylethyl}}$ & $\text{C}_{\text{phenylethyl}}$ '), 140.3 (s br., C_{cymene} & C_{cymene} '), 135.57 (s br., C3, C3', C_{cymene} , C_{cymene} '), BPh_4^- & BPh_4^-), 129.1 (s br., C_{cymene} & C_{cymene} '), 129.1, 128.5 (s, C_{phenyl} & C_{phenyl} '), 128.5, 128.0 (s, C_{phenyl} & C_{phenyl} '), 127.0, 126.7 (s, C_{phenyl} & C_{phenyl} '), 126.7, 125.6 (s, C2 & C2'), 125.3 (dd, $J_{\text{HH}} = 5.4, 2.6 \text{ Hz}$, BPh_4^- & BPh_4^-), 121.6 (m, C4, C4', C_{cymene} , C_{cymene} '), BPh_4^- & BPh_4^-), 108.6, 108.4 (s, C7 & C7'), 87.2, 86.7, 85.6, 84.7, 84.1, 83.8, 83.7 (s, C_{cymene} & C_{cymene} '), 51.8, 51.6 (s, C10 & C10'), 30.4, 30.2 (s, C_{cymene} & C_{cymene} '), 22.9, 21.7 (s, C11 & C11'), 21.2 (s, C_{cymene} & C_{cymene} '), 21.5, 20.6 (s, C_{cymene} & C_{cymene} '), 18.3, 18.1 (s, C_{cymene} & C_{cymene} ').

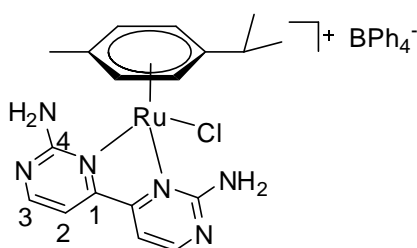


[N-Isopropyl-4-(2-pyridinyl)pyrimidin-2-amin(chlorido)(η^6 -*p*-cymene)ruthenium(II)]-

tetrafluoroborate 36q-BPh₄. The synthesis of **36q-BPh₄** was carried out as described in general synthesis but 154.0 mg of NaBPh₄ salt (0.45 mmol) were also added to the solution and before concentrating the excess and formed salts were filtered off. Yield: 230.0 g (57%, brown solid). Anal. calcd for C₄₆H₄₈BClN₄Ru: C, 68.70; H, 6.02; N, 6.97. Found: C, 68.50; H, 6.21;

Experimental

N, 7.13. ^1H NMR (400.1 MHz, DMSO d_6 , 20 °C): δ 9.49 (d, $J_{\text{HH}} = 5.08$ Hz, 1H, H1). 8.76 (d, $J_{\text{HH}} = 4.68$ Hz, 1H, H8), 8.58 (d, $J_{\text{HH}} = 7.80$ Hz, 1H, H4), 8.25 (t, $J_{\text{HH}} = 7.62$ Hz, 1H, H3), 7.84 (t, $J_{\text{HH}} = 6.26$ Hz, 1H, H2), 7.79 (d, $J_{\text{HH}} = 4.68$ Hz, 1H, H7), 7.23 (d, 8H, BPh_4^-), 6.95 (t, $J_{\text{HH}} = 7.04$ Hz, 8H, BPh_4^-), 6.81 (t, $J_{\text{HH}} = 6.84$ Hz, 4H, BPh_4^-), 6.34 (s, 1H, NH), 6.15 (d, $J_{\text{HH}} = 5.88$ Hz, 1H, H_{cymene}), 6.04-5.99 (m, 2H, H_{cymene}), 5.79 (d, $J_{\text{HH}} = 5.88$ Hz, 1H, H_{cymene}), 4.34-4.29 (m, 1H, $\text{H}_{\text{isopropyl}}$), 2.46-2.39 (m, 1H, H_{cymene}), 2.20 (s, 3H, H_{cymene}), 1.49 (d, $J_{\text{HH}} = 6.24$ Hz, 3H, $\text{H}_{\text{isopropyl}}$), 1.25 (d, $J_{\text{HH}} = 6.64$ Hz, 3H, $\text{H}_{\text{isopropyl}}$), 0.93-0.88 (m, 6H, H_{cymene}). ^{13}C NMR (100.6 MHz, DMSO d_6 , 20 °C): δ 164.1-162.6 (m, BPh_4^-), 161.7 (s, C9), 161.4 (s, C8), 161.1 (s, C6), 156.2 (s, C5), 153.8 (s, C1), 140.1 (s, C_{cymene}), 135.5 (s br., C3, C_{cymene} & BPh_4^-), 129.0 (s, C_{cymene}), 125.3 (s br., BPh_4^-), 125.2 (s, C2), 121.5 (s br., C4, C_{cymene} & BPh_4^-), 108.0 (s, C7), 44.1 (s, $\text{C}_{\text{isopropyl}}$), 30.3 (s, C_{cymene}), 21.7 (s, C_{cymene}), 21.3 (s, C_{cymene}), 21.9 (s, $\text{C}_{\text{isopropyl}}$), 21.8 (s, $\text{C}_{\text{isopropyl}}$), 18.2 (s, C_{cymene}).



[4,4'-Bipyrimidine-2,2'-diamine(chlorido)(η^6 -*p*-cymene)ruthenium(II)]tetrafluoroborate

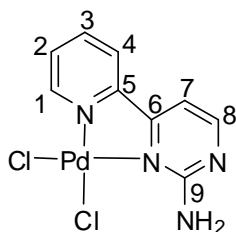
37-BPh₄. The synthesis of **37** was carried out as described in general synthesis but 154.0 mg of NaBPh₄ salt (0.45 mmol) were also added to the solution and before concentrating the excess and formed salts were filtered off. Yield: 224.1 mg (96%, red solid). Anal. calcd for C₄₂H₄₂BClN₆Ru + 0.25 CH₂Cl₂: C, 63.48; H, 5.36; N, 10.51. Found: C, 63.35; H, 5.30; N, 10.38. ^1H NMR (600.1 MHz, DMSO- d_6 , 20 °C): δ 8.74 (d, $J_{\text{HH}} = 4.7$ Hz, 2H, H3), 7.77 (d, $J_{\text{HH}} = 4.7$ Hz, 2H, H2), 7.17 (s br., 8H, H_{Ph}), 6.92 (t, $J_{\text{HH}} = 7.3$ Hz 8H, H_{Ph}), 6.78 (t, $J_{\text{HH}} = 7.1$ Hz, 4H, H_{Ph}), 6.15 (d, $J_{\text{HH}} = 6.1$ Hz, 2H, H_{cymene}), 6.02 (d, $J_{\text{HH}} = 6.1$ Hz 2H, H_{cymene}), 2.31 (m, 1H, H_{cymene}), 2.24 (s, 3H, H_{cymene}), 0.87 (d, $J_{\text{HH}} = 6.8$ Hz, 6H, H_{cymene}). ^{13}C NMR (150.9 MHz,

DMSO-*d*₆, 20 °C): δ 164.5 (s, C4), 163.9-162.9 (q, C_{Ph}), 162.0 (s, C3), 160.9 (s, C1), 135.6 (s, C_{Ph}), 125.4 (s, C_{Ph}), 121.6 (s, C_{Ph}), 109.4 (s, C2), 107.4 (s, C_{cymene}), 103.2 (s, C_{cymene}), 85.9 (s, C_{cymene}), 81.9 (s, C_{cymene}), 30.0 (s, C_{cymene}), 21.6 (s, C_{cymene}), 18.2 (s, C_{cymene}).

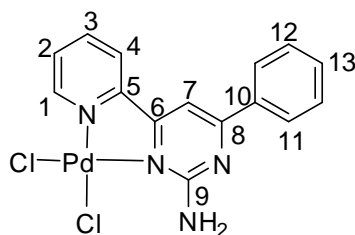
5.4.2 Palladium Complexes

5.4.2.1 Palladium Complexes with Bidentate Ligands

General synthesis of the Pd(NN)Cl₂ type complexes. A solution of the ligand (0.5 mmol) in CH₂Cl₂ (5 ml) was added dropwise to a solution of 191 mg of bis(benzonitrile)palladium(II) chloride (0.5 mmol) in CH₂Cl₂ (20 ml). After stirring for 20 h at room temperature the solution was concentrated and the product was precipitated by adding Et₂O (10 ml). The product was filtered and washed with Et₂O twice and dried under vacuum.

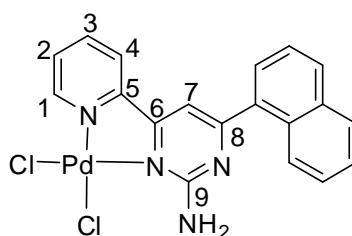


2-Amino-4-(pyridin-2-yl)pyrimidine(dichlorido)palladium(II) 39a. Yield: 78.0 mg (90%, yellow solid). Anal. calcd for C₉H₈Cl₂N₄Pd: C, 30.93; H, 2.31; N, 16.03. Found: C, 30.93; H, 2.54; N, 15.82. ¹H NMR (400.1 MHz, DMSO-*d*₆, 20 °C): δ 9.21 (d, $J_{\text{HH}} = 5.87$ Hz, 1H, H1), 9.00 (s br., 1H, NH₂), 8.70 (d, $J_{\text{HH}} = 4.89$ Hz, 1H, H8), 8.56 (d, $J_{\text{HH}} = 8.32$ Hz, 1H, H4), 8.36-8.8.30 (m, 2H, H3 & NH₂), 7.83 (t, $J_{\text{HH}} = 6.85$ Hz, 1H, H2), 7.65 (d, $J_{\text{HH}} = 4.89$ Hz, 1H, H7). ¹³C NMR (100.6 MHz, DMSO-*d*₆, 20 °C): δ 163.9 (s, C9), 162.5 (s, C6), 161.8 (s, C8), 152.3 (s, C5), 150.0 (s, C1), 141.2 (s, C3), 127.9 (s, C4), 124.9 (s, C2), 107.2 (s, C7).

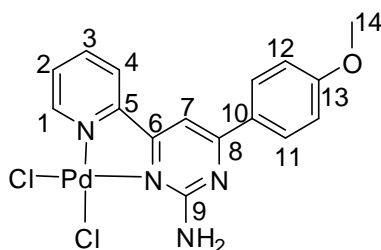


Experimental

2-Amino-6-(1-phenyl)-4-(pyridin-2-yl)pyrimidine(dichlorido)palladium(II) 39b. Yield: 211.0 mg (99%, yellow solid). Anal. calcd for C₁₅H₁₂Cl₂N₄Pd: C, 42.33; H, 2.84; N, 13.16. Found: C, 42.93; H, 2.68; N, 12.72. ¹H NMR (400.1 MHz, DMSO-*d*₆, 20 °C): δ 9.22 (d, *J*_{HH} = 4.89 Hz, 1H, H1), 9.01 (s br., 1H, NH₂), 8.88 (d, *J*_{HH} = 8.32 Hz, 1H, H4), 8.40-8.32 (m, 4H, H3, NH₂ & H11), 8.22 (s, 1H, H7), 7.84 (t, *J*_{HH} = 6.36 Hz, 1H, H2), 7.66-7.58 (m, 3H, H12 & H13). ¹³C NMR (100.6 MHz, DMSO-*d*₆, 20 °C): δ 166.8 (s, C8), 163.7 (s, C6), 163.4 (s, C9), 157.0 (s, C5), 150.0 (s, C1), 141.1 (s, C3), 134.6 (s, C10), 132.6 (s, C13), 129.0 (s, C12), 127.9 (s, C4 & C11), 125.2 (s, C2), 103.8 (s, C7).

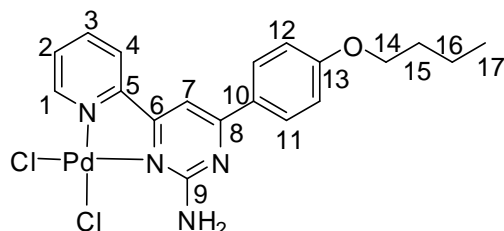


2-Amino-6-(1-naphthyl)-4-(pyridin-2-yl)pyrimidine(dichlorido)palladium(II) 39c. Yield: 226.0 mg (95%, yellow solid). Anal. calcd for C₁₉H₁₄Cl₂N₄Pd: C, 47.98; H, 2.97; N, 11.78. Found: C, 44.96; H, 3.24; N, 11.35. ¹H NMR (400.1 MHz, DMSO-*d*₆, 20 °C): δ 9.25 (d, *J*_{HH} = 5.87 Hz, 1H, H1), 9.09 (s br., 1H, NH₂), 8.73 (d, *J*_{HH} = 7.82 Hz, 1H, H4), 8.47 (s br., 1H, NH₂), 8.36-8.28 (m, 2H, H3 & H_{naphthyl}), 8.17 (d, *J*_{HH} = 8.32 Hz, 1H, H_{naphthyl}), 8.07-8.05 (m, 1H, H_{naphthyl}), 8.01 (s, 1H, H7), 7.88 (d, *J*_{HH} = 6.35 Hz, 1H, H_{naphthyl}), 7.81 (t, *J*_{HH} = 5.87 Hz, 1H, H2), 7.7-7.5 (m, 3H, H_{naphthyl}). ¹³C NMR (100.6 MHz, DMSO-*d*₆, 20 °C): δ 170.3 (s, C8), 163.6 (s, C6), 162.9 (s, C9), 156.9 (s, C5), 150.0 (s, C1), 141.1 (s, C3), 134.2-125.2 (12s, C2, C4 & C_{naphthyl}), 108.5 (s, C7).



2-Amino-6-(3-methoxyphenyl)-4-(pyridin-2-yl)pyrimidine(dichlorido)palladium(II) 39d.

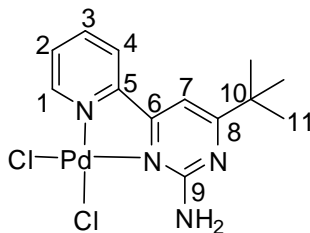
Yield: 191.0 mg (84%, yellow solid). Anal. calcd for C₁₆H₁₄Cl₂N₄OPd: C, 42.18; H, 3.10; N, 12.30. Found: C, 42.10; H, 3.54; N, 12.55. ¹H NMR (400.1 MHz, DMSO-*d*₆, 20 °C): δ 9.22 (d, *J*_{HH} = 4.89 Hz, 1H, H1), 8.94 (s br., 1H, NH₂), 8.87 (d, *J*_{HH} = 7.82 Hz, 1H, H4), 8.39-8.32 (m, 3H, H3 & H11), 8.22 (s br., 1H, NH₂), 8.17 (s, 1H, H7), 7.82 (t, *J*_{HH} = 6.36 Hz, 1H, H2), 7.16 (d, *J*_{HH} = 8.81 Hz, 2H, H12), 3.88 (s, 1H, H14). ¹³C NMR (100.6 MHz, DMSO-*d*₆, 20 °C): δ 166.0 (s, C13), 163.6, 163.0, 162.9 (3s, C9, C6 & C8), 157.1 (s, C5), 149.9 (s, C1), 141.0 (s, C3), 129.8 (s, C11), 127.7 (s, C4), 126.8 (s, C10), 124.9 (s, C2), 114.4 (s, C12), 103.1 (s, C7), 55.6 (s, C14).



2-Amino-6-(3-butoxyphenyl)-4-(pyridin-2-yl)pyrimidine(dichlorido)palladium(II) 39e.

Yield: 202.0 mg (81%, yellow solid). Anal. calcd for C₁₉H₂₀Cl₂N₄OPd: C, 45.85; H, 4.05; N, 11.26. Found: C, 45.52; H, 4.27; N, 11.07. ¹H NMR (400.1 MHz, DMSO-*d*₆, 20 °C): δ 9.20 (d, *J*_{HH} = 5.38 Hz, 1H, H1), 8.92 (s br., 1H, NH₂), 8.85 (d, *J*_{HH} = 7.82 Hz, 1H, H4), 8.35 (t, *J*_{HH} = 7.34 Hz, 1H, H3), 8.30 (d, *J*_{HH} = 8.8 Hz, 1H, H11), 8.17 (s br., 1H, NH₂), 8.12 (s, 1H, H7), 7.80 (t, *J*_{HH} = 6.36 Hz, 1H, H2), 7.11 (d, *J*_{HH} = 8.8 Hz, 2H, H12), 4.09 (t, *J*_{HH} = 6.36 Hz, 2H, H14), 1.77-1.72 (m, 2H, H15), 1.49-1.40 (m, 2H, H16), 0.95 (t, *J*_{HH} = 7.34 Hz, 3H, H17). ¹³C NMR (100.6 MHz, DMSO-*d*₆, 20 °C): δ 166.0 (s, C13), 163.6, 162.8, 162.5 (3s, C9, C6 & C8), 157.1 (s, C5), 149.6 (s, C1), 141.0 (s, C3), 129.8 (s, C11), 127.6 (s, C4), 126.6 (s, C10), 124.9 (s, C2), 114.8 (s, C12), 103.1 (s, C7), 67.6 (s, C14), 30.7 (s, C15), 18.7 (s, C16), 13.7 (s, C17).

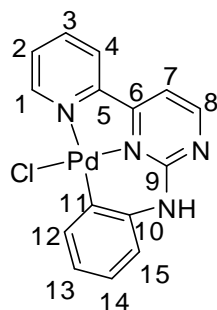
Experimental



2-Amino-6-(*t*butyl)-4-(pyridin-2-yl)pyrimidine(dichlorido)palladium(II) 39f. Yield: 170.0 mg (84%, orange solid). Anal. calcd for $C_{13}H_{16}Cl_2N_4OPd$: C, 38.49; H, 3.98; N, 13.81. Found: C, 38.48; H, 4.09; N, 13.75. 1H NMR (400.1 MHz, $DMSO-d_6$, 20 °C): δ 9.18 (d, $J_{HH} = 5.38$ Hz, 1H, H1), 8.89 (s br., 1H, NH_2), 8.75 (d, $J_{HH} = 7.82$ Hz, 1H, H4), 8.31 (t, $J_{HH} = 7.83$ Hz, 1H, H3), 8.16 (s br., 1H, NH_2), 7.79 (t, $J_{HH} = 6.36$ Hz, 1H, H2), 7.68 (s, 1H, H7), 1.32 (s, 9H, H11). ^{13}C NMR (100.6 MHz, $DMSO-d_6$, 20 °C): δ 182.3 (s, C8), 163.3 (s, C6), 162.3 (s, C9), 156.9 (s, C5), 149.9 (s, C1), 141.0 (s, C3), 127.6 (s, C4), 124.9 (s, C2), 104.1 (s, C7), 38.1 (s, C10), 28.5 (s, C11).

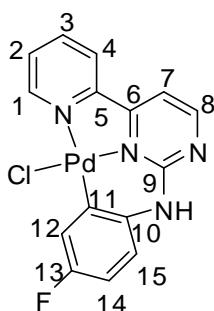
5.4.2.2 Palladium Complexes with Tridentate Ligands

General method of synthesis of the $Pd(NNC)Cl$ type complexes. To a solution of 0.5 mmol bis(benzonitrile)palladium(II)chloride in 10 ml of dichloromethane a solution of 0.5 mmol of the ligand in 10 ml dichloromethane was added dropwise. The reaction mixture was stirred at room temperature over night. The precipitated product was filtered and washed with dichloromethane. The product can be crystallized from DMSO.



***N*-Phenyl- κC^2 -4-(pyridine-2-yl- κN^1)pyrimidin- κN^3 -2-amine(chlorido)palladium(II) 40a.** Yield: 360.0 mg (93%, orange solid). Anal. calcd for $C_{15}H_{11}ClN_4Pd + 0.33CH_2Cl_2$: C, 44.14; H, 2.80; N, 13.43. Found: C, 44.58; H, 2.90; N, 13.73. 1H NMR (400.1 MHz, $DMSO-d_6$, 20

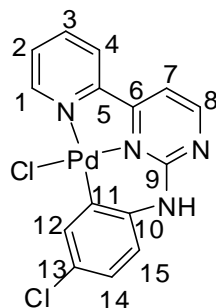
°C): δ 11.10 (s br., 1H, NH), 9.33 (d, $J_{\text{HH}} = 4.69$ Hz, 1H, H1), 9.00 (d, $J_{\text{HH}} = 4.69$ Hz, 1H, H8), 8.67 (d, $J_{\text{HH}} = 7.82$ Hz, 1H, H4), 8.37 (d, $J_{\text{HH}} = 8.19$ Hz, 1H, H12), 8.28 (t, $J_{\text{HH}} = 7.04$ Hz, 1H, H3), 7.99 (d, $J_{\text{HH}} = 5.08$ Hz, 1H, H7), 7.88 (t, $J_{\text{HH}} = 6.26$ Hz, 1H, H2), 7.19 (d, $J_{\text{HH}} = 7.43$ Hz, 1H, H13), 7.04 (t, $J_{\text{HH}} = 7.04$ Hz, 1H, H15), 6.71 (t, $J_{\text{HH}} = 7.04$ Hz, 1H, H14). ^{13}C NMR (100.6 MHz, DMSO- d_6 , 20 °C): δ 162.1 (s, C6), 161.1 (s, C8), 152.5 (s, C5), 150.0 (s, C9), 149.2 (s, C1), 140.3 (s, C10), 139.8 (s, C3), 136.6 (s, C14), 128.0 (s, C2), 125.0 (s, C11), 124.5 (s, C12), 123.9 (s, C4), 120.6 (s, C13), 116.2 (s, C15), 108.8 (s, C7).



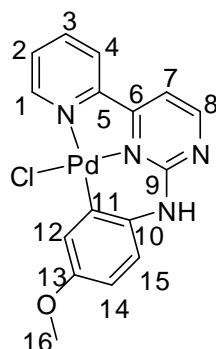
***N*-(4-Fluorophenyl- κC^2)-4-(pyridine-2-yl- κN^1)pyrimidin- κN^3 -2-amine(chlorido)palla-**

dium(II) 40b. Yield: 380.0 mg (94%, orange solid). Anal. calcd for $\text{C}_{15}\text{H}_{10}\text{ClFN}_4\text{Pd}$ + DMSO: C, 42.08; H, 3.32; N, 11.55. Found: C, 41.80; H, 3.42; N, 11.46. ^1H NMR (400.1 MHz, DMSO- d_6 , 20 °C): δ 11.03 (s br., 1H, NH), 9.18 (d, $J_{\text{HH}} = 5.04$ Hz, 1H, H1), 8.90 (d, $J_{\text{HH}} = 4.70$ Hz, 1H, H8), 8.56 (d, $J_{\text{HH}} = 8.21$ Hz, 1H, H4), 8.21-8.17 (m, 1H, H3), 8.04 (dd, $J_{\text{HH}} = 11.4, 2.9$ Hz, 1H, H12), 7.87 (d, $J_{\text{HH}} = 4.69$ Hz, 1H, H7), 7.79-7.77 (m, 1H, H2), 7.13 (dd, $J_{\text{HH}} = 3.13, 5.48$ Hz, 1H, H15), 6.84-6.79 (m, 1H, H14). ^{13}C NMR (100.6 MHz, DMSO- d_6 , 20 °C): δ 162.0 (s, C6), 161.2 (s, C8), 156.2 (d, $J_{\text{CF}} = 240$ Hz, C13), 152.6 (s, C5), 150.0 (s, C9), 149.2 (s, C1), 139.8 (s, C3), 133.5 (s, C10), 128.0 (s, C2), 126.5 (d, $J_{\text{CF}} = 5.0$ Hz, C11), 124.9 (d, $J_{\text{CF}} = 20.6$ Hz, C12), 123.9 (s, C4), 116.8 (d, $J_{\text{CF}} = 7.7$ Hz, C15), 112.0 (d, $J_{\text{CF}} = 23.4$ Hz, C14), 108.7 (s, C7).

Experimental

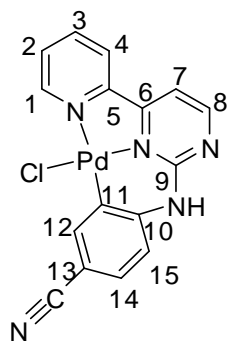


***N*-(4-Chlorophenyl- κ C²)-4-(pyridine-2-yl- κ N¹)pyrimidin- κ N³-2-amine(chlorido)palladium(II) 40c.** Yield: 370.0 mg (88%, orange solid). Anal. calcd for C₁₅H₁₀Cl₂N₄Pd + 0.33 CH₂Cl₂: C, 40.71; H, 2.36; N, 12.39. Found: C, 40.95; H, 2.41; N, 12.70. ¹H NMR (400.1 MHz, DMSO-*d*₆, 20 °C): δ 11.19 (s br., 1H, NH), 9.27 (d, $J_{\text{HH}} = 5.08$ Hz, 1H, H1), 9.00 (d, $J_{\text{HH}} = 5.08$ Hz, 1H, H8), 8.66 (d, $J_{\text{HH}} = 8.22$ Hz, 1H, H4), 8.32-8.26 (m, 2H, H3 & H12), 7.99 (d, $J_{\text{HH}} = 4.70$ Hz, 1H, H7), 7.88 (t, $J_{\text{HH}} = 6.26$ Hz, 1H, H2), 7.17-7.15 (m, 1H, H15), 7.09-7.06 (m, 1H, H14). ¹³C NMR (100.6 MHz, DMSO-*d*₆, 20 °C): δ 162.1 (s, C6), 161.3 (s, C8), 152.6 (s, C5), 150.1 (s, C9), 149.3 (s, C1), 139.9 (s, C3), 138.6 (s, C13), 135.9 (s, C10), 128.0 (s, C2), 126.4 (s, C11), 124.7 (s, C12), 124.0 (s, C4), 123.9 (s, C14), 117.3 (s, C15), 109.1 (s, C7).



***N*-(4-Methoxyphenyl- κ C²)-4-(pyridine-2-yl- κ N¹)pyrimidin- κ N³-2-amine(chlorido)palladium(II) 40d.** Yield: 400 mg (95%, red solid). Anal. calcd for C₁₆H₁₃ClN₄OPd: C, 45.85; H, 3.13; N, 13.37. Found: C, 45.30; H, 3.30; N, 13.15. ¹H NMR (400.1 MHz, DMSO-*d*₆, 20 °C): δ 11.02 (s br., 1H, NH), 9.33 (d, $J_{\text{HH}} = 4.7$ Hz, 1H, H1), 8.95 (d, $J_{\text{HH}} = 4.69$ Hz, 1H, H8), 8.66 (d, $J_{\text{HH}} = 8.22$ Hz, 1H, H4), 8.28 (t, $J_{\text{HH}} = 8.33$ Hz, 1H, H3), 8.00 (d, $J_{\text{HH}} = 2.74$ Hz, 1H, H12), 7.91-7.86 (m, 2H, H7 & H2), 7.14 (d, $J_{\text{HH}} = 9$ Hz, 1H, H15), 6.69 (dd, $J_{\text{HH}} = 2.74, 5.87$ Hz, 1H,

H14), 3.68 (s, 3H, H16). ^{13}C NMR (100.6 MHz, $\text{DMSO-}d_6$, 20 °C): δ 161.9 (s, C6), 160.9 (s, C8), 152.6 (s, C5), 152.0 (s, C10), 149.7 (s, C9), 149.2 (s, C1), 139.7 (s, C3), 130.6 (s, C13), 127.9 (s, C2), 125.8 (s, C11), 124.1 (s, C12), 123.8 (s, C4), 116.4 (s, C15), 111.5 (s, C14), 108.2 (s, C7), 54.9 (s, C16).



4-(4-(Pyridin-2-yl- κN^1)pyrimidin- κN^3 -2-ylamino)benzonitrile- κC^2 (chlorido)palladium(II)

40e. Yield: 370.0 mg (90%, yellow solid). Anal. calcd for $\text{C}_{16}\text{H}_{10}\text{ClN}_5\text{Pd}$ + DMSO: C, 43.92; H, 3.28; N, 14.23. Found: C, 44.04; H, 3.33; N, 14.47. ^1H NMR (400.1 MHz, $\text{DMSO-}d_6$, 20 °C): δ 11.51 (s br., 1H, NH), 9.29 (d, $J_{\text{HH}} = 4.7$ Hz, 1H, H1), 9.08 (d, $J_{\text{HH}} = 4.69$ Hz, 1H, H8), 8.71-8.69 (m, 2H, H4 & H12), 8.31-8.29 (m, 1H, H3), 8.10 (d, $J_{\text{HH}} = 4.7$ Hz, 1H, H7), 7.90-7.88 (m, 1H, H2), 7.47 (d, $J_{\text{HH}} = 8.22$ Hz, 1H, H15), 7.29 (d, $J_{\text{HH}} = 8.22$ Hz, 1H, H14). ^{13}C NMR (100.6 MHz, $\text{DMSO-}d_6$, 20 °C): The complex was not soluble enough, so the ^{13}C NMR spectrum could not be measured.

References

6 References

- (1) <http://www.catalysis.de/Research.6.0.html?&L=1>, Catalysis—a Key to Sustainability, Beller, M.
- (2) (a) Shang, G.; Li, W.; Zhang, X. In *Catalytic Asymmetric Synthesis*, 3rd ed.; Ojima, I., Ed.; John Wiley & Sons: Hoboken, **2010**; Chapter 7. (b) *The Handbook of Homogeneous Hydrogenation*, Vols. 1-3; de Vries, J. G., Elsevier, C. J., Eds.; Wiley-VCH: Weinheim, **2007**. (c) *Transition Metals for Organic Synthesis*, 2nd ed.; Beller, M., Bolm, C., Eds.; Wiley-VCH: Weinheim, **2004**; p 29. (d) *Asymmetric Catalysis on Industrial Scale*; Blaser, H.-U., Schmidt, E., Eds.; Wiley-VCH: Weinheim, **2004**.
- (3) (a) Morris, R. H. *Chem. Soc. Rev.* **2009**, *38*, 2282. (b) Baratta, W.; Rigo, P. *Eur. J. Inorg. Chem.* **2008**, 4041. (c) Wang, C.; Wu, X.; Xiao, J. *Chem. Asian J.* **2008**, *3*, 1750. (d) Morris, D. J.; Wills, M. *Chim. Oggi- Chem. Today* **2007**, *25*, 11. (e) Ikariya, T.; Blacker, A. *J. Acc. Chem. Res.* **2007**, *40*, 1300. (f) Samec, J. S. M.; Bäckvall, J. E.; Andersson, P. G.; Brandt, P. *Chem. Soc. Rev.* **2006**, *35*, 237. (g) Gladiali, S.; Alberico, E. *Chem. Soc. Rev.* **2006**, *35*, 226. (h) Ikariya, T.; Murata, K.; Noyori, R. *Org. Biomol. Chem.* **2006**, *4*, 393.
- (4) (a) Doucet, H.; Ohkuma, T.; Murata, K.; Yokozawa, T.; Kozawa, M.; Katayama, E.; England, A. F.; Ikariya, T.; Noyori, R. *Angew. Chem., Int. Ed.* **1998**, *37*, 1703. (b) Haack, K. J.; Hashiguchi, S.; Fujii, A.; Ikariya, T.; Noyori, R. *Angew. Chem., Int. Ed. Engl.* **1997**, *36*, 285.
- (5) (a) Ohkuma, T.; Ooka, H.; Yamakawa, M.; Ikariya, T.; Noyori, R. *J. Org. Chem.* **1996**, *61*, 4872. (b) Ohkuma, T.; Koizumi, M.; Doucet, H.; Pham, T.; Kozawa, M.; Murata, K.; Katayama, E.; Yokozawa, T.; Ikariya, T.; Noyori, R. *J. Am. Chem. Soc.* **1998**, *120*, 13529. (c) Ohkuma, T.; Doucet, H.; Pham, T.; Mikami, K.; Korenaga, T.; Terada, M.; Noyori, R. *J. Am. Chem. Soc.* **1998**, *120*, 1086.

- (6) (a) Nordin, S. J. M.; Roth, P.; Tarnai, T.; Alonso, D. A.; Brandt, P.; Andersson, P. G. *Chem. Eur. J.* **2001**, *7*, 1431. (b) Faller, J. W.; Lavoie, A. R. *Organometallics* **2002**, *21*, 3493. (c) Pasto', M.; Riera, A.; Perica's, M. A. *Eur. J. Org. Chem.* **2002**, 2337. (d) Everaere, K.; Mortreux, A.; Carpentier, J. F. *Adv. Synth. Catal.* **2003**, *345*, 67. (e) Petra, D. G. I.; Kamer, P. C. J.; Van Leeuwen, P. W. N. M.; Goubitz, K.; Van Loon, A. M.; De Vries, J. G.; Schoemaker, H. E. *Eur. J. Inorg. Chem.* **1999**, 2335. (f) Brandt, P.; Roth, P.; Andersson, P. G. *J. Org. Chem.* **2004**, *69*, 4885.
- (7) Pelagatti, P.; Carcelli, M.; Calbiani, F.; Cassi, C.; Elviri, L.; Pelizzi, C.; Rizzotti, U.; Rogolino, D. *Organometallics* **2005**, *24*, 5836.
- (8) (a) Carmona, D.; Lamata, M. P.; Oro, L. A. *Eur. J. Inorg. Chem.* **2002**, 2239. (b) Carmona, D.; Lamata, M. P.; Viguri, F.; Dobrinovich, I.; Lahoz, F. J.; Oro, L. A. *Adv. Synth. Catal.* **2002**, *344*, 499. (c) Boegevig, A.; Pastor, I. M.; Adolfsson, H. *Chem. Eur. J.* **2004**, *10*, 294.
- (9) (a) Abdur-Rashid, K.; Lough, A. J.; Morris, R. H. *Organometallics* **2000**, *19*, 2655. (b) Abdur-Rashid, K.; Lough, A. J.; Morris, R. H. *Organometallics* **2001**, *20*, 1047. (c) Leyssens, T.; Peeters, D.; Harvey, J. N. *Organometallics* **2008**, *27*, 1514. (d) Doherty, S.; Knight, J. G.; Bell, A. L.; Harrington, R. W.; Clegg, W. *Organometallics* **2007**, *26*, 2465. (e) Clapham, S. E.; Hadzovic, A.; Morris, R. H. *Coord. Chem. Rev.* **2004**, *248*, 2201.
- (10) (a) Baratta, W.; Schütz, J.; Herdtweck, E.; Herrmann, W. A.; Rigo, P. *J. Organomet. Chem.* **2005**, *690*, 5570. (b) Baratta, W.; Herdtweck, E.; Siega, K.; Toniutti, M.; Rigo, P. *Organometallics* **2005**, *24*, 1660. (c) Baratta, W.; Chelucci, G.; Gladiali, S.; Siega, K.; Toniutti, M.; Zanette, M.; Zangrando, E.; Rigo, P. *Angew. Chem., Int. Ed.* **2005**, *44*, 6214. (d) Baratta, W.; Ballico, M.; Esposito, G.; Rigo, P. *Chem. Eur. J.* **2008**, *14*, 5588. (e) Baratta, W.; Chelucci, G.; Herdtweck, E.; Magnolia, S.; Siega, K.; Rigo, P. *Angew. Chem., Int. Ed.* **2007**, *46*, 7651. (f) Baratta, W.; Siega, K.; Rigo, P. *Chem. Eur. J.* **2007**, *13*, 7479. (g) Baratta, W.; Siega, K.; Rigo, P. *Adv. Synth. Catal.* **2007**, *349*, 1633. (h) Baratta, W.; Bosco, M.; Chelucci,

References

- G.; Del Zotto, A.; Siega, K.; Toniutti, M.; Zangrando, E.; Rigo, P. *Organometallics* **2006**, *25*, 4611.
- (11) Carmen Carrión, M.; Sepúlveda, F.; Jalón, F. A.; Manzano, B. R.; Rodríguez, A. M. *Organometallics* **2009**, *28*, 3822.
- (12) (a) Bäckvall, J. E. *J. Organomet. Chem.* **2002**, *652*, 105. (f) Pàmies, O.; Bäckvall, J. E. *Chem. Eur. J.* **2001**, *7*, 5052. (b) Noyori, R.; Yamakawa, M.; Hashiguchi, S. *J. Org. Chem.* **2001**, *66*, 7931.
- (13) (a) de Araujo, M. P.; de Figueiredo, A. T.; Bogado, A. L.; von Poelhsitz, G.; Ellena, J.; Castellano, E. E.; Donnici, C. L.; Comasseto, J. V.; Batista, A. A. *Organometallics* **2005**, *24*, 6159. (b) V. Rautenstrauch, X. Hoang-Cong, R. Churlaud, K. Abdur-Rashid, R. H. Morris, *Chem. Eur. J.* **2003**, *9*, 4954. (c) Z. L. Lu, K. Eichele, I. Warad, H. A. Mayer, E. Lindner, Z. J. Jiang, V. Z. Schurig, *Anorg. Allg. Chem.* **2003**, *629*, 1308.
- (14) (a) Crochet, P.; Gimeno, J.; Borge, J.; García-Granda, S. *New J. Chem.* **2003**, *27*, 414. (b) Crochet, P.; Gimeno, J.; García-Granda, S.; Borge, J. *Organometallics* **2001**, *20*, 4369. (c) Sammakia, T.; Stangeland, E. L. *J. Org. Chem.* **1997**, *62*, 6104. (d) Nishibayashi, Y.; Takei, I.; Uemura, S.; Hidai, M. *Organometallics* **1999**, *18*, 2291. (e) Arikawa, Y.; Ueoka, M.; Matoba, K.; Nishibayashi, Y.; Hidai, M.; Uemura, S. *J. Organomet. Chem.* **1999**, *572*, 163.
- (15) Dahlenburg, L.; Kühnlein, C. *J. Organomet. Chem.* **2005**, *690*, 1.
- (16) Thoumazet, C.; Melaimi, M.; Ricard, L.; Mathey, F.; Le Floch, P. *Organometallics* **2003**, *22*, 1580.
- (17) (a) Canivet, J.; Süß-Fink, G. *Green Chem.* **2007**, *9*, 391. (b) Canivet, J.; Karmazin-Brelot, L.; Süß-Fink, G.; *J. Organomet. Chem.* **2005**, *690*, 3202. (c) Canivet, J.; Labat, G.; Stoeckli-Evans, H.; Süß-Fink, G. *Eur. J. Inorg. Chem.* **2005**, 4493.
- (18) Braunstein, P.; Fryzuk, M. D.; Naud, F.; Rettig, S. J. *J. Chem. Soc., Dalton Trans.* **1999**, 589.

- (19) Braunstein, P.; Naud, F.; Pfaltz, A.; Rettig, S. *J. Organometallics* **2000**, *19*, 2676.
- (20) Cuervo, D.; Gamasa, M. P.; Gimeno, J. *Chem. Eur. J.* **2004**, *10*, 425.
- (21) Baratta, W.; Benedetti, F.; Del Zotto, A.; Fanfoni, L.; Felluga, F.; Magnolia, S.; Putignano, E.; Rigo, P. *Organometallics*, **2010**, *29*, 3563.
- (22) (a) Gao, J. X.; Zhang, H.; Yi, X. D.; Xu, P. P.; Tang, C. L.; Wan, H. L.; Tsai, K. R.; Ikariya, T. *Chirality* **2000**, *12*, 383. (b) Gao, J. X.; Xu, P. P.; Yi, X. D.; Yang, C. B.; Zhang, H.; Cheng, S. H.; Wan, H. L.; Tsai, K. R.; Ikariya, T. *J. Mol. Catal. A: Chem.* **1999**, *147*, 105. (c) Gao, J. X.; Ikariya, T.; Noyori, R. *Organometallics* **1996**, *15*, 1087.
- (23) (a) Togni, A.; Venanzi, L. M. *Angew. Chem.* **1994**, *106*, 517; *Angew. Chem. Int. Ed. Engl.* **1994**, *33*, 497. (b) Fache, F.; Schulz, E.; Tommasino, M. L.; Lemaire, M. *Chem. Rev.* **2000**, *100*, 2159.
- (24) For recent reviews on the chemistry of complexes containing phosphorus & nitrogen ligands, see: (a) Helmchen, G.; Pfaltz, A. *Acc. Chem. Res.* **2000**, *33*, 336. (b) Gómez, M.; Muller, G.; Rocamora, M. *Coord. Chem. Rev.* **1999**, *193*, 769. (c) Espinet, P.; Soulantica, K. *Coord. Chem. Rev.* **1999**, *193*, 499. (d) Braunstein, P.; Naud, F. *Angew. Chem.* **2001**, *113*, 702; *Angew. Chem. Int. Ed.* **2001**, *40*, 680.
- (25) (a) Son, S.; Fu, G. C. *J. Am. Chem. Soc.* **2008**, *130*, 2756. (b) Sean, W.; Fu, G. C. *J. Am. Chem. Soc.* **2008**, *130*, 12645.
- (26) (a) Small, B. L.; Brookhart, M.; Bennet, A. M. A. *J. Am. Chem. Soc.* **1998**, *120*, 4049. (b) Small, B. L.; Brookhart, M. *J. Am. Chem. Soc.* **1998**, *120*, 7143. (c) Small, B. L.; Brookhart, M. *Macromolecules* **1999**, *32*, 2120. (d) Dias, E. L.; Brookhart, M.; White, P. S. *Organometallics* **2000**, *19*, 4995. (e) Britovsek, G. J. P.; Gibson, V. C.; Kimberley, B. S.; Maddox, P. J.; McTavish S. J.; Solan, G. A.; White, A. J. P.; Williams, D. J. *Chem. Commun.* **1998**, 849. (f) Glentsmith, G. K. B.; Gibson, V. C.; Hitcock, P. B.; Kimberley, B. S.; Rees, C. W. *Chem. Commun.* **2002**, 1498. (g) Gibson, V. C.; Tellmann, K. P.; Humphries, M. J.; Wass,

References

- D. F. *Chem. Commun.* **2002**, 2316. (h) Zabel, D.; Schubert, A.; Wolmershäuser, G.; Jones Jr, R. L.; Thiel, W. R. *Eur. J. Inorg. Chem.* **2008**, 3648.
- (27) (a) Zassinovich, G.; Mestroni, G.; Gladiali, S. *Chem. Rev.* **1992**, *92*, 1051; (b) Gladiali, S.; Mestroni, G. in *Transition Metal for Organic Synthesis*, Vol. 2 (Eds.: M. Beller, C. Bolm), Wiley-VCH, Weinheim, **1998**, p. 97.
- (28) (a) Evans, D.; Osborn, J.A.; Jardine, F.H.; Wilkinson, G. *Nature*, **1965**, *208*, 1203. (b) Halpern, J.; Harrod, J.F.; James, B.R. *J. Am. Chem. Soc.*, **1966**, *88*, 5150.
- (29) (a) Noyori, R.; Takaya, H. *Acc. Chem. Res.*, **1990**, *23*, 345. (b) James, B.R. *Catal. Today*, **1997**, *37*, 209. (c) Fache, F.; Schulz, E.; Tommasino, M.L.; Lemaire, M. *Chem. Rev.*, **2000**, *100*, 2159. (d) Noyori, R. *Angew. Chem. Int. Ed. Engl.*, **2002**, *41*, 2008. (e) Blaser, H.-U.; Malan, C.; Pugin, B.; Spindler, F.; Steiner, H.; Studer, M. *Adv. Synth. Catal.*, **2003**, *345*, 103.
- (30) (a) Noyori, R.; Ohkuma, T. *Angew. Chem. Int. Ed. Engl.*, **2001**, *40*, 40. (b) James, B.R.; *Homogeneous Hydrogenation*, Wiley, New York, 1973. (c) James, B.R. *Adv. Organomet. Chem.*, **1979**, *17*, 319. (d) Noyori, R.; Hashiguchi, S. *Acc. Chem. Res.*, **1997**, *30*, 97. (e) Naota, T.; Takaya, H.; Murahashi, S.-I. *Chem. Rev.*, **1998**, *98*, 2599. (f) Sanchez-Delgado, R.A.; Rosales, M. *Coord. Chem. Rev.*, **2000**, *196*, 249. (g) Bäckvall, J.-E. *J. Organomet. Chem.*, **2002**, *652*, 105. (h) Joó, F. *Acc. Chem. Res.*, **2002**, *35*, 738.
- (31) (a) Kubas, G.J. *Metal Dihydrogen and Sigma-Bond Complexes*, Kluwer Academic Publishers/Plenum Press, New York, 2001. (b) Esteruelas, M.A.; Oro, L.A. *Chem. Rev.*, **1998**, *98*, 577. (c) Sabo-Etienne, S.; Chaudret, B. *Coord. Chem. Rev.*, **1998**, *180*, 381. (d) Jessop, P.G.; Morris, R.H. *Coord. Chem. Rev.*, **1992**, *121*, 155.
- (32) (a) Salvini, A.; Frediani, P.; Gallerini, S. *Appl. Organomet. Chem.*, **2000**, *14*, 570. (b) Joó, F.; Kovacs, J.; Benyei, A.C.; Katho, A. *Catal. Today*, **1998**, *42*, 441.
- (33) Crabtree, R.H. *Organometallic Chemistry of the Transition Metals*, Wiley, New York, 1994.

- (34) Yamagishi, T.; Mizushima, E.; Sato, H.; Yamachi, M. *Chem. Lett.*, **1998**, 1255.
- (35) (a) Ohkuma, T.; Kitamura, M.; Noyori, R.; Ojima, I. (Ed.), *Catalytic Asymmetric Synthesis, second ed.*, Wiley VCH, New York, **2000**. (b) Gladiali, S.; Mestroni, G.; *Transit. Met. Org. Synth.*, **1998**, 2, 97. (c) Fehring, V.; Selke, R. *Angew. Chem. Int. Ed. Engl.*, **1998**, 37, 1827.
- (36) Chaloner, P.A.; Esteruelas, M.A.; Joó, F.; Oro, L.A. *Homogeneous Hydrogenation*, Kluwer Academic Publishers, Dordrecht, The Netherlands, **1994** (Chapter 3).
- (37) (a) Lin, Y.; Zhou, Y.; *J. Organomet. Chem.*, **1990**, 381, 135. (b) Imai, H.; Nishiguchi, T.; Fukuzumi, K. *J. Org. Chem.*, **1976**, 41, 665. (c) Chowdhury, R.L.; Bäckvall, J.-E. *J. Chem. Soc. Chem. Commun.*, **1991**, 1063. (d) Watanabe, Y.; Ohta, T.; Tsuji, Y. *Bull. Chem. Soc. Jpn.*, **1982**, 55, 2441. (e) Bianchini, C.; Farnetti, E.; Graziani, M.; Peruzzini, M.; Polo, A. *Organometallics*, **1993**, 12, 3753. (f) Gordon, E.M.; Gaba, D.C.; Jebber, K.A.; Zacharias, D.M.; *Organometallics*, **1993**, 12(12), 5020. (g) Bianchi, M.; Matteoli, U.; Menchi, G.; Frediani, P.; Pratesi, S.; Piacenti, F.; Botteghi, C. *J. Organomet. Chem.*, **1980**, 198, 73. (h) Dani, P.; Karlen, T.; Gossage, R.A.; Gladiali, S.; van Koten, G. *Angew. Chem. Int. Ed. Engl.*, **2000**, 39, 743. (i) Benyei, A.C.; Joó, F.; *J. Mol. Catal.*, **1990**, 58, 151. (j) Everaere, K.; Mortreux, A.; Bulliard, M.; Brussee, J.; van der Gen, A.; Nowogrocki, G.; Carpentier, J.-F. *Eur. J. Org. Chem.*, **2001**, 275. (k) Wills, M.; Gamble, M.; Palmer, M.; Smith, A.; Studley, J.; Kenny, J.; *J. Mol. Catal. A: Chem.*, **1999**, 146, 139. (m) Gao, J.-X.; Zhang, H.; Yi, X.-D.; Xu, P.-P.; Tang, C.-L.; Wan, H.-L.; Tsai, K.-R.; Ikariya, T. *Chirality*, **2000**, 12, 383. (n) Mizushima, E.; Ohi, H.; Yamaguchi, M.; Yamagishi, T. *J. Mol. Catal. A: Chem.*, **1999**, 149, 43.
- (38) Yamakawa, M.; Ito, H.; Noyori, R. *J. Am. Chem. Soc.*, **2000**, 122, 1466.

References

- (39) (a) Cole-Hamilton, D.J.; Wilkinson, G. *New J. Chem.*, **1977**, *1*, 141. (b) Mizushima, E.; Yamaguchi, M.; Yamagishi, T. *J. Mol. Catal. A: Chem.*, **1999**, *148*, 69. (c) Mizushima, E.; Yamaguchi, M.; Yamagishi, T. *Chem. Lett.*, **1997**, 237.
- (40) Standfest-Hauser, C.; Slugovc, C.; Mereiter, K.; Schmid, R.; Kirchner, K.; Xiao, L.; Weissensteiner, W. *J. Chem. Soc. Dalton Trans.*, **2001**, 2989.
- (41) Jalon, F.A.; Otero, A.; Rodriguez, A.; Perez-Manrique, M.; *J. Organomet. Chem.*, **1996**, *508*, 69.
- (42) Vicente, C.; Shulpin, G.B.; Moreno, B.; Sabo-Etienne, S.; Chaudret, B. *J. Mol. Catal. A: Chem.*, **1995**, *98*, L5.
- (43) Yang, H.; Alvarez, M.; Lugan, N.; Mathieu, R. *J. Chem. Soc. Chem. Commun.*, **1995**, 1721.
- (44) Rahman, M.S.; Prince, P.D.; Steed, J.W.; Hii, K.K. *Organometallics*, **2002**, *21*, 4927.
- (45) Bhaduri, S.; Sharma, K.; Mukesh, D. *J. Chem. Soc. Dalton Trans.*, **1993**, 1191.
- (46) Yi, C.S.; He, Z.; Guzei, I.A. *Organometallics*, **2001**, *20*, 3641.
- (47) Ogo, S.; Abura, T.; Watanabe, Y. *Organometallics*, **2002**, *21*, 2964.
- (48) (a) Yamakawa, M.; Yamada, I.; Noyori, R. *Angew. Chem. Int. Ed. Engl.*, **2001**, *40*, 2818. (b) Fujii, A.; Hashiguchi, S.; Uematsu, N.; Ikariya, T.; Noyori, R. *J. Am. Chem. Soc.*, **1996**, *118*, 2521. (c) Hashiguchi, S.; Fujii, A.; Haack, K.J.; Matsumura, K.; Ikariya, T.; Noyori, R. *Angew. Chem. Int. Ed. Engl.*, **1997**, *36*, 288.
- (49) Menashe, N.; Salant, E.; Shvo, Y. *J. Organomet. Chem.*, **1996**, *514*, 97.
- (50) Labinger, J. A.; Bercaw J. E. *Nature*, **2002**, *417*, 507.
- (51) Collman, J. P.; Hegedus, L. S.; Norton, J. R.; Finke, R. G. *Principles and Applications of Organotransition Metal Chemistry* Ch. 7, 2nd edn (Univ. Science, Mill Valley, **1987**).
- (52) Sheldon, R. A.; Kochi, J. K. *Metal-Catalyzed Oxidations of Organic Compounds* Ch. 4 (Academic, New York, **1981**).

- (53) Fryzuk, M. D.; Johnson, S. A. *Coord. Chem. Rev.* **2000**, *202*, 379.
- (54) Green, M. L. H.; Knowles, P. J. *J. Chem. Soc. Chem. Commun.* **1970**, 1677.
- (55) Foley, P.; Whitesides, G. M. *J. Am. Chem. Soc.* **1979**, *101*, 2732.
- (56) Bennett, M. A.; Milner, D. L. *Chem. Commun.* **1967**, 581.
- (57) Janowicz, A. H.; Bergman, R. G. *J. Am. Chem. Soc.*, **1982**, *104*, 352.
- (58) Rothwell, I. P. *Acc. Chem. Res.*, **1988**, *21*, 153.
- (59) (a) Watson, P. L. *J. Am. Chem. Soc.*, **1983**, *105*, 6491. (b) Thompson, M. E. *J. Am. Chem. Soc.*, **1987**, *109*, 203.
- (60) (a) Vidal, V.; Theolier, A.; Thivolle-Cazat, J.; Basset, J. M.; Corker, J. *J. Am. Chem. Soc.*, **1996**, *118*, 4595. (b) Niccolai, G. P.; Basset, J. M. *Appl. Catal. A*, **1996**, *146*, 145.
- (61) (a) Sherry, A. E.; Wayland, B. B. *J. Am. Chem. Soc.*, **1990**, *112*, 1259. (b) Wayland, B. B.; Ba, S.; Sherry, A. E. *J. Am. Chem. Soc.*, **1991**, *113*, 5305.
- (62) Cummins, C. C.; Baxter, S. M.; Wolczanski, P. T. *J. Am. Chem. Soc.*, **1988**, *110*, 8731.
- (63) Walsh, P. J.; Hollander, F. J.; Bergman, R. G. *Generation J. Am. Chem. Soc.*, **1988**, *110*, 8729.
- (64) (a) Bennett, J. L.; Wolczanski, P. T. *J. Am. Chem. Soc.*, **1997**, *119*, 10696. (b) Schafer, D. F.; Wolczanski, P. T. *J. Am. Chem. Soc.*, **1998**, *120*, 4881. (c) Tran, E.; Legzdins, P. *J. Am. Chem. Soc.*, **1997**, *119*, 5071.
- (65) Stahl, S. S.; Labinger, J. A.; Bercaw, J. E. *Angew. Chem. Int. Edn Engl.*, **1998**, *37*, 2180.
- (66) Wu, X. F.; Anbarasan, P.; Neumann, H.; Beller, M. *Angew. Chem. Int. Ed.* **2010**, *49*, 9047.
- (67) Jira, R. *Angew. Chem.* **2009**, *121*, 9196; *Angew. Chem. Int. Ed.* **2009**, *48*, 9034.
- (68) (a) Heck, R. F. *J. Am. Chem. Soc.* **1968**, *90*, 5518; (b) Heck, R. F. *J. Am. Chem. Soc.* **1968**, *90*, 5526; (c) Heck, R. F. *J. Am. Chem. Soc.* **1968**, *90*, 5531; (d) Heck, R. F. *J. Am. Chem. Soc.*

References

- 1968**, 90, 5535; e) Heck, R. F. *J. Am. Chem. Soc.* **1968**, 90, 5538; (f) Heck, R. F. *J. Am. Chem. Soc.* **1968**, 90, 5542; g) Heck, R. F. *J. Am. Chem. Soc.* **1968**, 90, 5546.
- (69) Heck, R. F. Nolley, J. P. *J. Org. Chem.* **1972**, 37, 2320.
- (70) a) Mizoroki, T.; Mori, K.; Ozaki, A. *Bull. Chem. Soc. Jpn.* **1971**, 44, 581; b) Mizoroki, T.; Mori, K.; Ozaki, A. *Bull. Chem. Soc. Jpn.* **1973**, 46, 1505.
- (71) Sonogashira, K.; Tohda, Y.; Hagihara, N. *Tetrahedron Lett.* **1975**, 16, 4467.
- (72) Negishi, E.; King, A. O.; Okukado, N. *J. Org. Chem.* **1977**, 42, 1821.
- (73) Yamamura, M.; Moritani, I.; Murahashi, S.-I. *J. Organomet. Chem.* **1975**, 91, C39.
- (74) Miyaura, N.; Yanaga, T.; Suzuki, A. *Synth. Commun.* **1981**, 11, 513.
- (75) Stille, J. K. *Angew. Chem.* **1986**, 98, 504; *Angew. Chem. Int. Ed. Engl.* **1986**, 25, 508.
- (76) (a) Hatanaka, Y.; Hiyama, T.; *J. Org. Chem.* **1988**, 53, 918; (b) Hatanaka, Y.; Hiyama, T.; *J. Org. Chem.* **1989**, 54, 268.
- (77) (a) Surry, D. S.; Buchwald, S. L. *Angew. Chem. Int. Ed.* **2008**, 47, 6338; (b) Hartwig, J. F. *Acc. Chem. Res.* **1998**, 31, 852.
- (78) (a) Nicolaou, K. C.; Bulger, P. G.; Sarlah, D. *Angew. Chem.* **2005**, 117, 4516; *Angew. Chem. Int. Ed.* **2005**, 44, 4442; b) Torborg, C.; Beller, M. *Adv. Synth. Catal.* **2009**, 351, 3027.
- (79) (a) Jozak, T. *Diplomarbeit*, Kaiserslautern, **2007**. (b) Jozak, T. *Dissertation*, Kaiserslautern, **2011**.
- (80) Zabel, D. *Dissertation*, Kaiserslautern, **2007**.
- (81) Selected recent reviews and papers: (a) Bianchini, C.; Meli, A. *Coord. Chem. Rev.* **2002**, 225, 35. (b) Braunstein, P.; Naud, F. *Angew. Chem., Int. Ed.* **2001**, 40, 680. (c) Nakao, Y.; Imanaka, H.; Sahoo, A. K.; Yada, A.; Hiyama, T. *J. Am. Chem. Soc.* **2005**, 127, 6952. (d) Trost, B. M.; Fandrick, D. R.; Dinh, D. C. *J. Am. Chem. Soc.* **2005**, 127, 14186.
- (82) Hofmeier, H.; Schubert, U. S. *Chem. Soc. Rev.* **2004**, 33, 373.

- (83) Tellmann, K. P.; Gibson, V. C.; White, A. J. P.; Williams, D. J. *Organometallics* **2005**, *24*, 280 and references therein.
- (84) For selected recent reviews and papers on pybox-based transitionmetal catalysts, see: (a) Desimoni, G.; Faita, G.; Quadrelli, P. *Chem. Rev.* **2003**, *103*, 3119. (b) Lu, J.; Ji, S.-J.; Teo, Y.-C.; Loh, T.-P. *Org. Lett.* **2005**, *7*, 159.
- (85) Fusco, R. In *The Chemistry of Heterocyclic Compounds: Pyrazoles, Pyrazolines, Pyrazolidines, Indazoles and Condensed Rings*, Wiley, R. H., Ed.; Wiley: New York, **1967**; Vol. 22, pp 1-174.
- (86) (a) De, D.; Mague, J. T.; Byers, L. D.; Krogstad, D. J. *Tetrahedron Lett.* **1995**, *36*(2), 205. (b) Kusumoto, T.; Ogino, K.; Sato, K.; Hiyama, T.; Takehara, S.; Nakamura, K. *Chem. Lett.* **1993**, *7*, 1243.
- (87) (a) Papet, A. L.; Marsura, A.; Ghermani, N.; Lecomte, C.; Friant, P.; Rivail, J. L. *New J. Chem.* **1993**, *17*(3), 181. (b) Regnouf de Vains, J.-B.; Lehn, J.-M.; Ghermani, N. E.; Dusausoy, O.; Dusausoy, Y.; Papet, A.-L.; Marsura, A.; Friant, P.; Rivail, J. L. *New J. Chem.* **1994**, *18*(6), 701.
- (88) (a) Case, F. H.; Koft, E. *J. Am. Chem. Soc.* **1959**, *81*, 905. (b) Lafferty, J. J.; Case, F. H. *J. Org. Chem.* **1967**, *32*(5), 1591. (c) Kawanishi, Y.; Kitamura, N.; Tazuke, S. *Inorg. Chem.* **1989**, *28*(15), 2968.
- (89) Bejan, E.; Ait Haddou, H.; Daran, J. C.; Balavoine, G. G. A. *Synthesis*, **1996**, *8*, 1012.
- (90) Zabel, D.; *Dissertation*, Technische Universität Kaiserslautern, **2007**.
- (91) (a) Pleier, A. K.; Glas, H.; Grosche, M.; Sirsch, P.; Thiel, W. R. *Synthesis* **2001**, 55. (b) Foxa, M. A.; Harrisa, J. E.; Heidera, S.; Pérez-Gregoria, V.; Zakrzewskaa, M. E.; Farmer, J. D.; Yufita, D. S.; Howarda, J. A. K.; Low, P. J. *J. Organomet. Chem.*, **2009**, *694*, 2350. (c) Thiel, W. R.; Eppinger, J. *Chem. Eur. J.* **1997**, *3*, 696.

References

- (92) (a) Schubert, A.; *Diplomarbeit*, Technische Universität Chemnitz, **2003**. (b) Saalfrank, R. W.; Löw, N.; Trummer, S.; Sheldrick, G. M.; Teichert, M.; Stalke, D. *Eur. J. Inorg. Chem.*, **1998**, 559.
- (93) van der Valk, P.; Potwin, P. G. *J. Org. Chem.*, **1994**, 59, 1766.
- (94) Thiel, W. R.; Angstl, M.; Priermeier, T. *Chem. Ber.* **1994**, 127, 2373.
- (95) Thiel, W. R.; Priermeier, T. *Angew. Chem., Int. Ed. Engl.* **1995**, 34, 1737.
- (96) Thiel, W. R. *Chem. Ber.* **1996**, 129, 575.
- (97) Glas, H.; Spiegler, M.; Thiel, W. R. *Eur. J. Inorg. Chem.* **1998**, 1, 275.
- (98) Glas, H.; Herdtweck, E.; Artus, G. R. J.; Thiel, W. R. *Inorg. Chem.* **1998**, 37, 3644.
- (99) Hroch, A.; Gemmecker, G.; Thiel, W. R. *Eur. J. Inorg. Chem.* **2000**, 3, 1107.
- (100) Pleier, A.; Glas, H.; Grosche, M.; Sirsch, P.; Thiel, W. R. *Synthesis* **2001**, 1, 55.
- (101) He, W.; Yang, D.; Cui, Y.; Xu, Y.; Guo, C. *Acta Crystallogr. E.*, **2008**, E64, o1126.
- (102) (a) Constable, E. C.; Daniels, M. A. M.; Drew, M. G. B.; Tocher, D. A.; Walker, J. V.; Wood, P. D. *J. Chem. Soc. Dalton. Trans.*, **1993**, 13, 1947. (b) Cordaro, J. G.; McCusker, J. K.; Bergman, R. G. *Chem. Commun.*, **2002**, 1496.
- (103) Marshall, J. A.; Adams, N. D. *J. Org. Chem.*, **1998**, 63, 3812.
- (104) Holmes, B. T.; Padgett, C. W.; Krawiec, M.; Pennington, W. T. *Crystal Growth & Design*, **2002**, 2, 619.
- (105) Wendelin, W.; Harler, A. *Monatshefte für Chemie*, **1975**, 106, 1479.
- (106) Mariella, R.; Zelko, J. *J. Org. Chem.*, **1960**, 25 (4), 647.
- (107) (a) Carver, C. T.; Williams, B. N.; Ogilby, K. R.; Diaconescu, P. L. *Organometallics* **2010**, 29, 835. (b) Concepcion, J. J.; Tsai, M.; Muckerman, J. M.; Meyer, T. J. *J. Am. Chem. Soc.*, **2010**, 132, 1545. (c) Sakamoto, M.; Ohki, Y.; Tatsumi, K. *Organometallics*, **2010**, 29, 1761. (d) Iron, M. A.; Sundermann, A.; Martin, J. M. L. *J. Am. Chem. Soc.*, **2003**, 125, 11430.

- (108) (a) Steffen, A.; Sladek, M. I.; Braun, T.; Neumann, B.; Stammeler, H. *Organometallics* **2005**, *24*, 4057. (b) Dufresne, S.; Hanan, G. S.; Skene, W. G. *J. Phys. Chem. B* **2007**, *111*, 11407. (c) LaChance-Galang, K. J.; Maldonado, I.; Gallagher, M. L.; Jian, W.; Prock, A.; Chacklos, J.; Galang, R. D.; Clarke, M. J. *Inorg. Chem.* **2001**, *40*, 485. (d) Demeter, A.; Weber, C.; Brlik, J. *J. Am. Chem. Soc.*, **2003**, *125*, 2535. (e) Field, L. M.; Morón, C.; Lahti, P. M.; Palacio, F.; Paduan-Filho, A.; Oliveira Jr, N. F. *Inorg. Chem.* **2006**, *45*, 2562. (f) Hutchinson, D. J.; Hanton, L. R.; Moratti, S. C. *Inorg. Chem.* **2010**, *49*, 5923. (g) Meyer, D.; Taige, M. A.; Zeller, A.; Hohlfeld, K.; Ahrens, S.; Strassner, T. *Organometallics* **2009**, *28*, 2142. (h) Braga, D.; D'Addario, D.; Polito, M.; Grepioni, F. *Organometallics* **2004**, *23*, 2810. (i) Fischer, G.; Cai, Z.; Reimers, J. R.; Wormell, P. *J. Phys. Chem. A* **2003**, *107*, 3093. (j) Jagtap, S. V.; Deshpande, R. M. *Catalysis Today* **2008**, *131* 353.
- (109) Yamada, S.; Tokugawa, Y. *J. Am. Chem. Soc.*, **2009**, *131*, 2098.
- (110) Fishbien, L.; Gallaghan, J. A. *J. Am. Chem. Soc.*, **1954**, *76*, 3217.
- (111) Balbo, P. B.; Patel, C. N.; Sell, K. G.; Adcock, R. S.; Neelakantan, S.; Crooks, P. A.; Oliveira, M. A. *Biochemistry*, **2003**, *42*, 15189.
- (112) Tavares, F. X.; Boucheron, J. A.; Dickerson, S. H.; Griffin, R. J.; Preugschat, F.; Thomson, S. A.; Wang, T. Y.; Zhou, H. *J. Med. Chem.*, **2004**, *47*, 4716.
- (113) (a) Marvel, C. S.; Coleman, L.; Scott, G. P. *J. Org. Chem.*, **1955**, *20*, 1785. (b) Mubofu, E. B.; Engberts, J. B.F.N. *J. Phys. Org. Chem.* **2007**; *20*, 764.
- (114) Allen, F. H.; Kennard, O.; Watson, D. G.; Brammer, L.; Orpen, A. G. *J. Chem. Soc. Perkin Trans. II* **1987**, S1.
- (115) Effenberger, F. *Chemische Berichte*, **1965**, *98*, 2260.
- (116) (a) Ohkita, M.; Lehn, J.-M.; Baum, G.; Fenske D. *Heterocycles* **2000**, *52*, 103. (b) Ohkita, M.; Lehn, J.-M.; Baum, G.; Fenske, D. *Chem. Eur. J.* **1999**, *5*, 3471. (c) Bassani, D. M.; Lehn, J.-M. *Bull Soc. Chim. Fr.* **1997**, *134*, 897.

References

- (117) (a) Wright, A. T.; Anslyn, E. V.; *Org. Lett.* **2004**, *6*, 1341. (b) Ziener, U.; Breuning, E.; Lehn, J.-M.; Wegelius, E.; Rissanen, K.; Baum, G.; Fenske, D.; Vaughan, G. *Chem. Eur. J.* **2000**, *6*, 4132.
- (118) (a) Aït-Haddou, H.; Sumaoka, J.; Wiskur, S.L.; Folmer-Andersen, J.F.; Anslyn, E.V. *Angew. Chem. Int. Ed.* **2002**, *41*, 4013. (b) Aït-Haddou, H.; Wiskur, S.L.; Lynch, V.M.; Anslyn, E.V. *J. Am. Chem. Soc.* **2001**, *123*, 11296.
- (119) Liu, S.; Luo, Z.; Hamilton, A.D. *Angew. Chem.* **1997**, *109*, 2794.
- (120) Fritsky, I. O.; Ott, R.; Krämer, R. *Angew. Chem.* **2000**, *112*, 3403.
- (121) Hanan, G.S.; Arana, C.R.; Lehn, J. M.; Fenske, D. *Angew. Chem.* **1995**, *107*, 1191.
- (122) (a) Castro-Juiz, S.; Fernández, A.; López-Torres, M.; Vázquez-García, D.; Suárez, A.J.; Vila, J.M.; Fernández, J.J. *Organometallics* **2009**, *28*, 6657. (b) Fernández, A.; López-Torres, M.; Castro-Juiz, S.; Merino, M.; Vázquez-García, D.; Vila, J.M.; Fernández, J.J. *Organometallics* **2011**, *30*, 386. (c) Vázquez-García, D.; Fernández, A.; López-Torres, M.; Rodríguez, A.; Varela, A.; Pereira, M.T.; Vila, J.M.; Fernández, J.J. *Organometallics* **2011**, *30*, 396.
- (123) Kamala, K.; Rao, P.J.; Reddy, K.K. *Bull. Chem. Soc. Jpn.* **1988**, *61*, 3791.
- (124) (a) Ohkuma, T.; Ooka, H.; Ikariya, T.; Noyori, R. *J. Am. Chem. Soc.* **1995**, *117*, 10417. (b) Mikami, K.; Korenaga, T.; Terada, M.; Ohkuma, T.; Pham, T.; Noyori, R. *Angew. Chem., Int. Ed.* **1999**, *38*, 495. (c) Wu, X.; Xiao, J. *Chem. Commun.* **2007**, 2449.
- (125) (a) Ghebreyessus, K. Y.; Nelson, J. H. *J. Organomet. Chem.* **2003**, *669*, 48. (b) Rath, R. K.; Nethaji, M.; Chakravarty, A. R. *Polyhedron* **2001**, *20*, 2735. (c) Braunstein, P.; Naud, F.; Rettig, S. J. *New J. Chem.* **2001**, *25*, 32. (d) Reetz, M. T.; Li, X. *J. Am. Chem. Soc.* **2006**, *128*, 1044.
- (126) (a) Zeng, F.; Yu, Z. *Organometallics* **2008**, *27*, 2898. (b) Zeng, F.; Yu, Z. *Organometallics* **2009**, *28*, 1855.

- (127) Jozak, T.; Zabel, D.; Schubert, A.; Sun, Y.; Thiel, W. R. *Eur. J. Inorg. Chem.* **2010**, *32*, 5135.
- (128) Glas, H.; Köhler, K.; Herdtweck, E.; Maas, P.; Spiegler, M.; Thiel, W. R. *Eur. J. Inorg. Chem.* **2001**, 2075.
- (129) (a) Thiel, W. R.; Priermeier, T.; Fiedler, D.; Bond, A. M.; Mattner, M. R. *J. Organomet. Chem.* **1996**, *514*, 137. (b) Rößler, K.; Kluge, T.; Schubert, A.; Sun, Y.; Herdtweck, E.; Thiel, W. R. *Z. Naturforsch.* **2004**, *59b*, 1253.
- (130) (a) Mishra, H.; Mukherjee, R. *J. Organomet. Chem.* **2006**, *691*, 3545. (b) Gupta, G.; Yap, G. P. A.; Therrien, B.; Rao, K. M. *Polyhedron* **2009**, *28*, 844. (c) Tocher, D. A.; Drew, M. G. B.; Nag, S.; Pal, P. K.; Datta, D. *Chem. Eur. J.* **2007**, *13*, 2230. (d) Therrien, B.; Saïd-Mohamed, C.; Süß-Fink, G. *Inorg. Chim. Acta* **2008**, *361*, 2601.
- (131) Lee, C.; Lee, Y. *Chemospher*, **2006**, *65*, 1163.
- (132) Sehested, K.; Holcman, J. *Radiat. Phys. Chem.*, **1996**, *47*, 357.
- (133) Russell C.; Scaduto Jr. *Free Radical Biol. Med.*, **1995**, *18*, 271.
- (134) Baptista, L.; Clemente Da Silva, E.; Arbilla, G. *Phys. Chem. Chem. Phys.* **2008**, *10*, 6867.
- (135) (a) Kimura, K.; Kimura, T.; Kinoshita, I.; Nakashima, N.; Kitano, K.; Nishioka, T.; Isobe, K. *Chem. Commun.*, **1999**, 497. (b) Lobana, T. S.; Sultana, R.; Hundal, G.; Butcher, R. *J. Dalton Trans.*, **2010**, *39*, 7870.
- (136) (a) Zhang, N.; Shapley, P. A. *Inorg. Chem.*, **1988**, *27*, 976. (b) Volland, M. A. O.; Hansen, S. M.; Rominger, F.; Hofmann, P. *Organometallics*, **2004**, *23*, 800. (c) Gruber, S.; Zaitsev, A. B.; Wörle, M.; Pregosin, P. S. *Organometallics*, **2009**, *28*, 3437. (d) Zheng, C.; Inoki, D.; Matsumoto, T.; Ogo, S. *Chemistry Letters*, **2010**, *39*, 130. (e) Balakrishna, M. S.; Panda, R.; Mague, J. *Polyhedron*, **2003**, *22*, 587.
- (137) Reed, J.; Soled, S. L.; Eisenberg, R. *Inorg. Chem.*, **1974**, *13*, 3001.

References

- (138) Leung, W.; Zheng, H.; Chim, J. L. C.; Chan, J.; Wong, W.; Williams, I. D. *J. Chem. Soc., Dalton Trans.*, **2000**, 423.
- (139) Drahl, C. *Science & Technology*, **2008**, 86, 53.
- (140) (a) Bianchini, C.; Lenoble, G.; Oberhauser, W.; Parisel, S.; Zanobini, F. *Eur. J. Inorg. Chem.* **2005**, 4794. (b) Dietrich, B. L.; Egbert, J.; Morris, A. M.; Wicholas, M. *Inorg. Chem.*, **2005**, 44, 6476.
- (141) Dykeman, R. R.; Luska, K. L.; Thibault, M. E.; Jones, M. D.; Schlaf, M.; Khanfar, M.; Taylor, N. J.; Britten, J. F.; Harrington, L. *J. Mol. Catal. A-Chem.*, **2007**, 277, 233.
- (142) (a) Tobisu, M.; Chanati, N. *Angew. Chem. Int. Ed. Engl.* **2006**, 45, 1683. (b) Sezen, B.; Sames, D. *J. Am. Chem. Soc.* **2005**, 127, 5284. (c) Pastin, S. J.; Sames, D. *Org. Lett.* **2005**, 7, 5429. (d) Pastin, S. J.; McQuaid, K. M.; Sames, D. *J. Am. Chem. Soc.* **2005**, 127, 12180. (e) Burling, S.; Mahon, M. F.; Paine, B. M.; Whittlesey, M. K.; Williams, J. M. J. *Organometallics* **2004**, 23, 4537. (f) Murahashi, S.; Komiya, N.; Terai, H.; Nakae, T. *J. Am. Chem. Soc.* **2003**, 125, 15312. (g) Chatani, N.; Yorimitsu, S.; Asaumi, T.; Kakiuchi, F.; Murai, S. *J. Org. Chem.* **2002**, 67, 7557. (h) Dangel, B. D.; Johnson, J. A.; Sames, D. *J. Am. Chem. Soc.* **2001**, 123, 8149. (i) Chatani, N.; Asaumi, T.; Yorimitsu, S.; Ikeda, T.; Kakiuchi, F.; Murai, S. *J. Am. Chem. Soc.* **2001**, 123, 10935.
- (143) (a) Jazzar, R. F. R.; Macgregor, S. A.; Mahon, M. F.; Richards, S. P.; Whittlesey, M. K. *J. Am. Chem. Soc.* **2002**, 124, 4944. (b) Edwards, M. G.; Jazzar, R. F. R.; Paine, B. M.; Shermer, D. J.; Whittlesey, M. K.; Williams, J. M. J.; Edney, D. D. *Chem. Commun.* **2004**, 90. (c) Burling, S.; Whittlesey, M. K.; Williams, J. M. J. *Adv. Synth. Catal.* **2005**, 347, 591.
- (144) Chen, H.; Schlecht, S.; Semple, T. C.; Hartwig, J. F. *Science* **2000**, 287, 1995.
- (145) Jun, C.; Hwang, D.; Na, S. *Chem. Commun.* **1998**, 13, 1405.
- (146) (a) Zhang, J.; Gandelman, M.; Shimon, L. J. W.; Milstein, D. *Dalton Trans.* **2007**, 107. (b) Buijtenen, J.; Meuldijk, J.; Vekeman, A. J. M.; Hulshof, L. A.; Kooijman, H.; Spek, A. L.

Organometallics, **2006**, *25*, 873. (c) Zhang, J.; Gandelman, M.; Shimon, L.J. W.; Rozenberg, H.; Milstein, D. *Organometallics* **2004**, *23*, 4026. (d) Lin, Y.; Ma, D.; Lu, X. *Tetrahedron Lett.* **1987**, *28*, 3115.

(147) (a) Lee, D.; Chen, J.; Faller, J. W.; Crabtree, R. H. *Chem. Commun.* **2001**, *2*, 213. (b) Nugent, W. A.; Ovenall, D. W.; Holmes, S. J. *Organometallics* **1983**, *2*, 161.

(148) Sabot, C.; Kumar, K. A.; Antheaume, C.; Mioskowski, C. *J. Org. Chem.*, **2007**, *72*, 5001.

(149) (a) Gaussian 03, Revision E.01, Gaussian, Inc., Wallingford CT, 2004. Calculations with B3LYP and 6-31G* for C,H,N,Cl and the Stuttgart/Dresden-ECP for Ru (see refs. (54-58)). (b) Lee, C.; Yang, W.; Parr, R. G.; *Phys. Rev. B*, **1988**, *37*, 785. (c) Becke, A. D. *Phys. Rev.*, **1988**, *A38*, 3098. (d) Miehlich, B.; Savin, A.; Stoll, H.; Preuss, H. *Chem. Phys. Lett.*, **1989**, *157*, 200. (e) Hariharan, P. C.; Pople, J. A. *Theoret. Chim. Acta*, **1973**, *28*, 213. (f) Andrae, D.; Haeussermann, U.; Dolg, M.; Stoll, H.; Preuss, H. *Theor. Chem. Acc.*, **1990**, *77*, 123.

(150) (a) Gabelica, V.; De Pauw, E., *Mass Spectrom. Rev.* **2005**, *24*, 566. (b) Zins, E.-L.; Pepe, C.; Rondeau, D.; Rochut, S.; Galland, N.; Tabet, J.-C., *J. Mass. Spectrom.* **2009**, *44(1)*, 12. (c) Zins, E.-L.; Rondeau, D.; Karoyan, P.; Fosse, C. Rochut, S.; Pepe, C., *J. Mass. Spectrom.* **2009**, *44*, 1668. (d) Zins, E.-L.; Pepe, C.; Schröder, D., *J. Mass Spectrom.* **2010**, *45*, 1253. (e) Barylyuk, K.V.; Chingin, K.; Balabin, R.M.; Zenobi, R., *J. Am. Soc. Mass Spectrom.* **2010**, *21*, 172.

(151) Li, T.; Lough, A. J.; Zuccaccia, C.; Macchioni, A.; Morris, R. H. *Can. J. Chem.* **2006**, *84*, 164.

(152) da Costa, J. C. S.; Pais, K. C.; Fernandes, E. L.; de Oliveira, P. S. M.; Mendonça, J. S.; de Souza, M. V. N.; Peralta, M. A.; Vasconcelos, T. R. A. *Arkivoc*, **2006**, *i*, 128.

(153) (a) Miyaura, N.; Yamada, K.; Suzuki, A. *Tetrahedron Lett.* **1979**, *20*, 3437. (b) Miyaura, N.; Suzuki, A. *Chem. Rev.* **1995**, *95*, 2457. (c) Suzuki, A. *J. Organomet. Chem.* **1999**, *576*, 147.

References

- (154) (a) Siddiqui, M. A.; Snieckus, V. *Tetrahedron Lett.* **1990**, *31*, 1523. (b) Kim, Y. H.; Webster, O. W. *J. Am. Chem. Soc.* **1990**, *112*, 4592. (c) Wang, X.; Snieckus, V. *Tetrahedron Lett.* **1991**, *32*, 4883. (d) Lamba, J. J. S.; Tour, J. M. *J. Am. Chem. Soc.* **1994**, *116*, 11723. (e) Nicolaou, K. C.; Boddy, C. N. C.; Braese, S.; Winssinger, N. *Angew. Chem., Int. Ed.* **1999**, *38*, 2097. (f) Miura, M. *Angew. Chem. Int. Ed.* **2004**, *43*, 2201.
- (155) (a) Anderson, J. C.; Namli, H.; Roberts, C. A. *Tetrahedron* **1997**, *53*, 15123. (b) Littke, A. F.; Fu, G. C. *Angew. Chem. Int. Ed.* **1998**, *37*, 3387. (c) Old, D. W.; Wolfe, J. P.; Buchwald, S. L. *J. Am. Chem. Soc.* **1998**, *120*, 9722. (d) Wolfe, J. P.; Buchwald, S. L. *Angew. Chem., Int. Ed.* **1999**, *38*, 2413. (e) Liu, S. Y.; Choi, M. J.; Fu, G. C. *Chem. Commun.* **2001**, 2408. (f) Colacot, T. J.; Gore, E. S.; Kuber, A. *Organometallics* **2002**, *21*, 3301. (g) Kataoka, N.; Shelby, Q.; Stambuli, J. P.; Hartwig, J. F. *J. Org. Chem.* **2002**, *67*, 5553. (h) Bedford, R. B. *Chem. Commun.* **2003**, 1787. (i) Nguyen, H. N.; Huang, X.; Buchwald, S. L. *J. Am. Chem. Soc.* **2003**, *125*, 11818. (j) Walker, S. D.; Barder, T. E.; Martinelli, J. R.; Buchwald, S. L. *Angew. Chem. Int. Ed.* **2004**, *43*, 1871.
- (156) (a) Cabri, W.; Candiani, I.; Bedeschi, A.; Santi, R. *J. Org. Chem.* **1993**, *58*, 7421. (b) Buchmeiser, M. R.; Wurst, K. *J. Am. Chem. Soc.* **1999**, *121*, 11101. (c) Kawano, T.; Shinomaru, T.; Ueda, I. *Org. Lett.* **2002**, *4*, 2545. (d) Grasa, G. A.; Singh, R.; Stevens, E. D.; Nolan, S. P. *J. Organomet. Chem.* **2003**, *687*, 269. (e) Mino, T.; Shirae, Y.; Sasai, Y.; Sakamoto, M.; Fujita, T. *J. Org. Chem.* **2006**, *71*, 6834. (f) Zhang, W.; Sun, W.-H.; Wu, B.; Zhang, S.; Ma, H.; Li, Y.; Chen, J.; Hao, P. *J. Organomet. Chem.* **2006**, *691*, 4759.
- (157) (a) Mathews, C. J.; Smith, P. J.; Welton, T. *J. Mol. Catal. A: Chem.* **2003**, *206*, 77. (b) Najera, C.; Gil-Molto, J.; Karlstroem, S. *Adv. Synth. Catal.* **2004**, *346*, 1798. (c) Weng, Z.; Teo, S.; Koh, L. L.; Hor, T. S. A. *Organometallics* **2004**, *23*, 3603. (d) Mukherjee, A.; Sarkar, A. *Tetrahedron Lett.* **2004**, *46*, 15. (e) Gil-Molto, J.; Karlstroem, S.; Najera, C. *Tetrahedron* **2005**, *61*, 12168. (f) Mino, T.; Shirae, Y.; Sakamoto, M.; Fujita, T. *J. Org. Chem.* **2005**, *70*,

2191. (g) Haneda, S.; Ueba, C.; Eda, K.; Hayashi, M. *Adv. Synth. Catal.* **2007**, *349*, 833. (h) Liu, Y.; Wu, Y.; Xi, C. *Appl. Organomet. Chem.* **2009**, *23*, 329.
- (158) (a) Özdemir, I.; Cetinkaya, B. C.; Demir, S. *J. Mol. Catal. A: Chem.* **2004**, *208*, 109. (b) Mathews, C. J.; Smith, P. J.; Welton, T. *J. Mol. Catal. A: Chem.* **2004**, *214*, 27. (c) Done, M. C.; Ruther, T.; Cavell, K. J.; Kilner, M.; Peacock, E. J.; Braussaud, N.; Skelton, B. W.; White, A. *J. Organomet. Chem.* **2000**, *607*, 78.
- (159) (a) Özdemir, I.; Şahin, N.; Gök, Y.; Demir, S.; Cetinkaya, B. *J. Mol. Catal. A: Chem.* **2005**, *234*, 181. (b) Xi, C.; Wu, Y.; Yan, X. *J. Organomet. Chem.* **2008**, *693*, 3842.
- (160) (a) Tao, B.; Boykin, D. W. *Tetrahedron Lett.* **2003**, *44*, 7993. (b) Tao, B.; Boykin, D. W. *J. Org. Chem.* **2004**, *69*, 4330.
- (161) Takashi, M.; Yoshiaki, S.; Yousuke, S.; Masami, S.; Tsutomu, F. *J. Org. Chem.* **2006**, *71*, 6834.
- (162) Gottlieb, H. E.; Kotlyar, V.; Nudelman, A. *J. Org. Chem.* **1997**, *62*, 7512.
- (163) *Arbeitsmethoden in der Organischen Chemie*; Hünig, S.; Kreitmeier, P.; Märkl, G.; Sauer, J. LOB-Lehmanns, Berlin, **2008**.
- (164) Pleier, A. K.; Glas, H.; Grosche, M.; Sirsch, P.; Thiel, W. R. *Synthesis*, **2001**, *1*, 55.
- (165) Foxa, M. A.; Harrisa, J. E.; Heidera, S.; Pérez-Gregorioa, V.; Zakrzewskaa, M. E.; Farmera, J. D.; Yufita, D. S.; Howarda, J. A. K.; Low, P. J. *J. Organomet. Chem.*, **2009**, *694*, 2350.

Index

7 Index

7.1 Crystal Structure Data

7.1.1 Crystal Data and Structure Refinement for 9

Empirical formula	$C_{27}H_{27}N_3O_2$	
Formula weight	425.52	
Crystal colour and habit	yellow needle	
Crystal size (mm)	0.28 x 0.11 x 0.07	
Temperature (K)	150(2)	
Wavelength (Å)	1.54184	
Crystal system	Monoclinic	
Space group	$P2_1/c$	
Unit cell dimensions	$a = 9.1667(2)$ Å	$\alpha = 90^\circ$
	$b = 15.0261(3)$ Å	$\beta = 99.078(2)^\circ$
	$c = 16.8345(4)$ Å	$\gamma = 90^\circ$
Volume (Å ³)	2289.74(9)	
Z	4	
Calculated density (Mg/m ³)	1.234	
Absorption coefficient (mm ⁻¹)	0.624	
F(000)	904	
Theta-range for data collection (°)	3.97/62.62	
Index ranges	$-10 \leq h \leq 10, -17 \leq k \leq 17, -18 \leq l \leq 19$	
Reflections collected	16200	
Independent reflections	3656 ($R_{int} = 0.0269$)	
Completeness to theta = 62.62°	99.6 %	
Absorption correction	Semi-empirical from equivalents (Multiscan)	

Max. and min. transmission	1.00000 and 0.54119
Refinement method	Full-matrix least-squares on F^2
Data/restraints/parameters	3656/0/294
Goodness-of-fit on F^2	1.024
Final R indices [$I > 2\sigma(I)$]	$R_1 = 0.0325$, $wR_2 = 0.0874$
R indices (all data)	$R_1 = 0.0413$, $wR_2 = 0.0909$
Extinction coefficient	0.00165(19)
Largest diff. peak and hole ($e \cdot \text{\AA}^{-3}$)	0.140/-0.186

Definitions:

$$R_1 = \frac{\sum \|F_o\| - \|F_c\|}{\sum \|F_o\|} \qquad wR_2 = \sqrt{\frac{\sum [w(F_o^2 - F_c^2)^2]}{\sum [w(F_o^2)^2]}}$$

$$Goof = \sqrt{\frac{\sum [w(F_o^2 - F_c^2)]}{(n - p)}} \quad n = \text{number of reflections; } p = \text{number of parameters}$$

Notes on the refinement of 9.

All the hydrogen atoms were placed in calculated positions and refined by using a riding model.

7.1.2 Crystal Data and Structure Refinement for 16

Empirical formula	$C_{36}H_{26}N_2O_2$
Formula weight	518.59
Crystal colour and habit	colorless prism
Crystal size (mm)	0.14 x 0.09 x 0.08

Index

Temperature (K)	150(2)	
Wavelength (Å)	1.54184	
Crystal system	Monoclinic	
Space group	P2 ₁ /n	
Unit cell dimensions	$a = 8.2096(2) \text{ \AA}$	$\alpha = 90^\circ$
	$b = 11.6997(2) \text{ \AA}$	$\beta = 91.195(2)^\circ$
	$c = 27.2887(4) \text{ \AA}$	$\gamma = 90^\circ$
Volume (Å ³)	2620.51(9)	
Z	4	
Calculated density (Mg/m ³)	1.314	
Absorption coefficient (mm ⁻¹)	0.642	
F(000)	1088	
Theta-range for data collection (°)	4.11/62.69	
Index ranges	$-9 \leq h \leq 7, -13 \leq k \leq 13, -31 \leq l \leq 31$	
Reflections collected	22940	
Independent reflections	4188 ($R_{int} = 0.0373$)	
Completeness to theta = 62.69°	99.1 %	
Absorption correction	Semi-empirical from equivalents (Multiscan)	
Max. and min. transmission	1.00000 and 0.67762	
Refinement method	Full-matrix least-squares on F ²	
Data/restraints/parameters	4188/0/361	
Goodness-of-fit on F ²	0.854	
Final R indices [$I > 2\sigma(I)$]	$R_1 = 0.0335, wR_2 = 0.0719$	
R indices (all data)	$R_1 = 0.0500, wR_2 = 0.0755$	
Largest diff. Peak and hole (e·Å ⁻³)	0.119/-0.203	

Definitions:

$$R_1 = \frac{\sum \|F_o\| - \|F_c\|}{\sum \|F_o\|}$$

$$wR_2 = \sqrt{\frac{\sum [w(F_o^2 - F_c^2)^2]}{\sum [w(F_o^2)^2]}}$$

$$GooF = \sqrt{\frac{\sum [w(F_o^2 - F_c^2)]}{(n - p)}} \quad n = \text{number of reflections; } p = \text{number of parameters}$$

Notes on the refinement of 16.

All the hydrogen atoms were placed in calculated positions and refined by using a riding model.

7.1.3 Crystal Data and Structure Refinement for Guanidinium Salt

Empirical formula	C ₁₈ H ₄₄ N ₆ O ₄ S	
Formula weight	440.65	
Temperature	150(2) K	
Wavelength	1.54184 Å	
Crystal system	Monoclinic	
Space group	C2/c	
Unit cell dimensions	a = 11.5847(6) Å	α = 90°.
	b = 7.6008(4) Å	β = 98.688(5)°.
	c = 28.0681(15) Å	γ = 90°.
Volume	2443.1(2) Å ³	
Z	4	
Density (calculated)	1.198 Mg/m ³	

Index

Absorption coefficient	1.452 mm ⁻¹
F(000)	968
Crystal colour and habit	Colorless prism
Crystal size	0.14 x 0.06 x 0.04 mm ³
Theta range for data collection	3.19 to 62.64°.
Index ranges	-13<=h<=13, -8<=k<=7, -32<=l<=20
Reflections collected	7080
Independent reflections	1945 [R(int) = 0.0279]
Completeness to theta = 62.64°	99.7 %
Absorption correction	Semi-empirical from equivalents (Multiscan)
Max. and min. transmission	1.00000 and 0.49315
Refinement method	Full-matrix least-squares on F ²
Data / restraints / parameters	1945 / 49 / 153
Goodness-of-fit on F ²	1.104
Final R indices [I>2σ(I)]	R1 = 0.0330, wR2 = 0.0967
R indices (all data)	R1 = 0.0371, wR2 = 0.0984
Extinction coefficient	0.00041(9)
Largest diff. peak and hole	0.269 and -0.305 e.Å ⁻³

Definitions:

$$R_1 = \frac{\sum \|F_o\| - \|F_c\|}{\sum \|F_o\|}$$

$$wR_2 = \sqrt{\frac{\sum [w(F_o^2 - F_c^2)]^2}{\sum [w(F_o^2)]^2}}$$

$$GooF = \sqrt{\frac{\sum [w(F_o^2 - F_c^2)]}{(n - p)}}$$

n = number of reflections; p = number of parameters

Notes on the refinement of guanidinium salt.

All hydrogen atoms were placed in calculated positions and refined by using a riding model.

7.1.4 Crystal Data and Structure Refinement for 17d

Empirical formula	C ₁₆ H ₁₄ N ₄ O	
Formula weight	278.31	
Crystal colour and habit	yellow needle	
Crystal size (mm)	0.41 x 0.15 x 0.11	
Temperature (K)	150(2)	
Wavelength (Å)	1.54184	
Crystal system	Monoclinic	
Space group	P2 ₁ /c	
Unit cell dimensions	$a = 12.3576(2) \text{ \AA}$	$\alpha = 90^\circ$
	$b = 6.9698(1) \text{ \AA}$	$\beta = 96.270(1)^\circ$
	$c = 15.8623(2) \text{ \AA}$	$\gamma = 90^\circ$
Volume (Å ³)	1358.05(3)	
Z	4	
Calculated density (Mg/m ³)	1.361	
Absorption coefficient (mm ⁻¹)	0.720	
F(000)	584	
Theta-range for data collection (°)	5.61/62.68	
Index ranges	$-14 \leq h \leq 14, -7 \leq k \leq 7, -18 \leq l \leq 17$	
Reflections collected	11721	

Index

Independent reflections	2150 ($R_{int} = 0.0295$)
Completeness to $\theta = 62.68^\circ$	99.0 %
Absorption correction	Semi-empirical from equivalents (Multiscan)
Max. and min. transmission	1.00000 and 0.69702
Refinement method	Full-matrix least-squares on F^2
Data/restraints/parameters	2150/0/192
Goodness-of-fit on F^2	0.954
Final R indices [$I > 2\sigma(I)$]	$R_1 = 0.0331$, $wR_2 = 0.0865$
R indices (all data)	$R_1 = 0.0411$, $wR_2 = 0.0893$
Extinction coefficient	0.0029(4)
Largest diff. Peak and hole ($e \cdot \text{\AA}^{-3}$)	0.168/-0.159

Definitions:

$$R_1 = \frac{\sum \|F_o\| - \|F_c\|}{\sum \|F_o\|} \qquad wR_2 = \sqrt{\frac{\sum [w(F_o^2 - F_c^2)^2]}{\sum [w(F_o^2)^2]}}$$

$$Goof = \sqrt{\frac{\sum [w(F_o^2 - F_c^2)]}{(n - p)}} \qquad n = \text{number of reflections; } p = \text{number of parameters}$$

Notes on the refinement of 17d.

All the hydrogen atoms were placed in calculated positions and refined by using a riding model.

7.1.5 Crystal Data and Structure Refinement for 17f

Empirical formula $C_{13}H_{16}N_4$

Formula weight	228.30	
Crystal colour and habit	colorless needle	
Crystal size (mm)	0.19 x 0.18 x 0.14	
Temperature (K)	150(2)	
Wavelength (Å)	1.54184	
Crystal system	Monoclinic	
Space group	P2 ₁ /c	
Unit cell dimensions	$a = 16.5007(2)$ Å	$\alpha = 90^\circ$
	$b = 9.0395(1)$ Å	$\beta = 98.147(1)^\circ$
	$c = 16.9197(2)$ Å	$\gamma = 90^\circ$
Volume (Å ³)	2498.24(5)	
Z	8	
Calculated density (Mg/m ³)	1.214	
Absorption coefficient (mm ⁻¹)	0.599	
F(000)	976	
Theta-range for data collection (°)	5.28/62.70	
Index ranges	$-13 \leq h \leq 18, -10 \leq k \leq 10, -19 \leq l \leq 19$	
Reflections collected	18102	
Independent reflections	4003 ($R_{int} = 0.0222$)	
Completeness to theta = 62.70°	99.7 %	
Absorption correction	Semi-empirical from equivalents (Multiscan)	
Max. and min. transmission	1.00000 and 0.78505	
Refinement method	Full-matrix least-squares on F ²	
Data/restraints/parameters	4003/4/325	
Goodness-of-fit on F ²	1.071	

Index

Final R indices [$I > 2\sigma(I)$]	$R_1 = 0.0410$, $wR_2 = 0.1185$
R indices (all data)	$R_1 = 0.0461$, $wR_2 = 0.1214$
Largest diff. peak and hole ($e \cdot \text{\AA}^{-3}$)	0.553/-0.276

Definitions:

$$R_1 = \frac{\sum \|F_o\| - \|F_c\|}{\sum \|F_o\|} \qquad wR_2 = \sqrt{\frac{\sum [w(F_o^2 - F_c^2)^2]}{\sum [w(F_o^2)^2]}}$$

$$Goof = \sqrt{\frac{\sum [w(F_o^2 - F_c^2)]}{(n - p)}} \quad n = \text{number of reflections; } p = \text{number of parameters}$$

Notes on the refinement of 17f.

The hydrogen atoms H4A and H4B, H8A and H8B, which are bound to the nitrogen atoms N4 and N8, respectively, were located in the difference Fourier synthesis, and were refined semi-freely with the help of a distance restraint, while constraining their U -values to 1.2 times the $U(eq)$ values of N4 and N8, respectively. All the other hydrogen atoms were placed in calculated positions and refined by using a riding model.

7.1.6 Crystal Data and Structure Refinement for 17h

Empirical formula	$C_{15}H_{20}N_4$
Formula weight	256.35
Crystal colour and habit	colorless prism
Crystal size (mm)	0.18 x 0.11 x 0.09
Temperature (K)	150(2)
Wavelength (\AA)	1.54184

Crystal system	Orthorhombic	
Space group	Pnma	
Unit cell dimensions	$a = 12.0897(3) \text{ \AA}$	$\alpha = 90^\circ$
	$b = 6.9231(2) \text{ \AA}$	$\beta = 90^\circ$
	$c = 16.5369(5) \text{ \AA}$	$\gamma = 90^\circ$
Volume (\AA^3)	1384.11(7)	
Z	4	
Calculated density (Mg/m^3)	1.230	
Absorption coefficient (mm^{-1})	0.593	
F(000)	552	
Theta -range for data collection ($^\circ$)	4.53/62.64	
Index ranges	$-13 \leq h \leq 13, -7 \leq k \leq 7, -18 \leq l \leq 18$	
Reflections collected	7939	
Independent reflections	1206 ($R_{int} = 0.0552$)	
Completeness to theta = 62.64°	99.8 %	
Absorption correction	Semi-empirical from equivalents (Multiscan)	
Max. and min. transmission	1.00000 and 0.87531	
Refinement method	Full-matrix least-squares on F^2	
Data/restraints/parameters	1206/4/125	
Goodness-of-fit on F^2	1.090	
Final R indices [$I > 2\sigma(I)$]	$R_1 = 0.0347, wR_2 = 0.1024$	
R indices (all data)	$R_1 = 0.0443, wR_2 = 0.1065$	
Extinction coefficient	0.0019(6)	
Largest diff. peak and hole ($\text{e} \cdot \text{\AA}^{-3}$)	0.185/-0.252	

Index

Definitions:

$$R_1 = \frac{\sum \|F_o\| - \|F_c\|}{\sum \|F_o\|} \qquad wR_2 = \sqrt{\frac{\sum [w(F_o^2 - F_c^2)^2]}{\sum [w(F_o^2)^2]}}$$

$$Goof = \sqrt{\frac{\sum [w(F_o^2 - F_c^2)]}{(n - p)}} \quad n = \text{number of reflections; } p = \text{number of parameters}$$

Notes on the refinement of 17h.

The hydrogen atoms which are bound to C11 and C14, were located in the difference Fourier synthesis, and were refined semi-freely with the help of a distance restraint, while constraining their U -values to 1.5 times the $U(eq)$ value of bonding C-atom. All the other hydrogen atoms were placed in calculated positions and refined by using a riding model. The methyl group C(15)H₃- was treated as disorder on special position.

7.1.7 Crystal Data and Structure Refinement for 33b

Empirical formula	C ₄₃ H ₄₈ Cl ₂ N ₅ PRu	
Formula weight	837.80	
Crystal colour and habit	red prism	
Crystal size (mm)	0.19 x 0.14 x 0.06	
Temperature (K)	150(2)	
Wavelength (Å)	1.54184	
Crystal system	Monoclinic	
Space group	I2/a	
Unit cell dimensions	$a = 22.9187(2) \text{ \AA}$	$\alpha = 90^\circ$
	$b = 12.84570(10) \text{ \AA}$	$\beta = 101.6280(10)^\circ$

	$c = 27.3925(2) \text{ \AA}$	$\gamma = 90^\circ$
Volume (\AA^3)	7899.03(11)	
Z	8	
Calculated density (Mg/m^3)	1.409	
Absorption coefficient (mm^{-1})	5.127	
F(000)	3472	
Theta-range for data collection ($^\circ$)	3.82/62.65	
Index ranges	$-26 \leq h \leq 26, -13 \leq k \leq 14, -25 \leq l \leq 30$	
Reflections collected	19278	
Independent reflections	6216 ($R_{int} = 0.0244$)	
Completeness to theta = 62.65°	98.2 %	
Absorption correction	Semi-empirical from equivalents (Multiscan)	
Max. and min. transmission	1.00000 and 0.49019	
Refinement method	Full-matrix least-squares on F^2	
Data/restraints/parameters	6216/387/581	
Goodness-of-fit on F^2	1.008	
Final R indices [$I > 2\sigma(I)$]	$R_1 = 0.0405, wR_2 = 0.1182$	
R indices (all data)	$R_1 = 0.0499, wR_2 = 0.1232$	
Largest diff. Peak and hole ($\text{e} \cdot \text{\AA}^{-3}$)	1.239/-0.720	

Definitions:

$$R_1 = \frac{\sum \|F_o\| - |F_c|}{\sum |F_o|}$$

$$wR_2 = \sqrt{\frac{\sum [w(F_o^2 - F_c^2)^2]}{\sum [w(F_o^2)^2]}}$$

Index

$$GooF = \sqrt{\frac{\sum [w(F_o^2 - F_c^2)]}{(n - p)}} \quad n = \text{number of reflections}; p = \text{number of parameters}$$

Notes on the refinement of 33b.

All hydrogen atom positions were calculated in ideal positions (riding model). And half of the molecule was severely disordered.

7.1.8 Crystal Data and Structure Refinement for 33a

Empirical formula	C ₃₅ H ₃₂ Cl ₂ N ₅ PRu	
Formula weight	725.60	
Crystal colour and habit	red prism	
Crystal size (mm)	0.19 x 0.17 x 0.06	
Temperature (K)	150(2)	
Wavelength (Å)	1.54184	
Crystal system	Triclinic	
Space group	P-1	
Unit cell dimensions	$a = 13.0148(9) \text{ \AA}$	$\alpha = 102.805(6)^\circ$
	$b = 14.8928(10) \text{ \AA}$	$\beta = 92.194(5)^\circ$
	$c = 16.8628(10) \text{ \AA}$	$\gamma = 93.225(5)^\circ$
Volume (Å ³)	3177.8(4)	
Z	4	
Calculated density (Mg/m ³)	1.517	
Absorption coefficient (mm ⁻¹)	6.280	
F(000)	1480	
Theta-range for data collection (°)	3.41/62.92	
Index ranges	$-14 \leq h \leq 14, -16 \leq k \leq 16, -18 \leq l \leq 19$	

Reflections collected	27114
Independent reflections	9952 ($R_{int} = 0.0352$)
Completeness to $\theta = 62.92^\circ$	97.0 %
Absorption correction	Semi-empirical from equivalents (Multiscan)
Max. and min. transmission	1.00000 and 0.41078
Refinement method	Full-matrix least-squares on F^2
Data/restraints/parameters	9952/0/793
Goodness-of-fit on F^2	0.985
Final R indices [$I > 2\sigma(I)$]	$R_1 = 0.0299$, $wR_2 = 0.0787$
R indices (all data)	$R_1 = 0.0362$, $wR_2 = 0.0823$
Largest diff. Peak and hole ($e \cdot \text{\AA}^{-3}$)	0.880/-0.749

Definitions:

$$R_1 = \frac{\sum \|F_o\| - \|F_c\|}{\sum \|F_o\|}$$

$$wR_2 = \sqrt{\frac{\sum [w(F_o^2 - F_c^2)^2]}{\sum [w(F_o^2)^2]}}$$

$$Goof = \sqrt{\frac{\sum [w(F_o^2 - F_c^2)]}{(n - p)}} \quad n = \text{number of reflections; } p = \text{number of parameters}$$

Notes on the refinement of 33a.

All hydrogen atom positions were calculated in ideal positions (riding model).

7.1.9 Crystal Data and Structure Refinement for 33e

Empirical formula	$C_{47}H_{52}Cl_6N_5PRu$
Formula weight	1031.68

Index

Crystal colour and habit	red plate
Crystal size (mm)	0.42 x 0.10 x 0.04
Temperature (K)	150(2)
Wavelength (Å)	1.54184
Crystal system	Monoclinic
Space group	P2 ₁ /c
Unit cell dimensions	$a = 14.9916(3)$ Å $\alpha = 90^\circ$ $b = 18.2917(3)$ Å $\beta = 110.460(2)^\circ$ $c = 18.7007(4)$ Å $\gamma = 90^\circ$
Volume (Å ³)	4804.64(16)
Z	4
Calculated density (Mg/m ³)	1.426
Absorption coefficient (mm ⁻¹)	6.323
F(000)	2120
Theta-range for data collection (°)	4.93/62.65
Index ranges	$-15 \leq h \leq 17$, $-20 \leq k \leq 20$, $-21 \leq l \leq 21$
Reflections collected	20732
Independent reflections	7571 ($R_{int} = 0.0450$)
Completeness to theta = 62.65°	98.4 %
Absorption correction	Analytical
Max. and min. transmission	0.801 and 0.323
Refinement method	Full-matrix least-squares on F ²
Data/restraints/parameters	7571/0/541
Goodness-of-fit on F ²	1.027
Final R indices [$I > 2\sigma(I)$]	$R_1 = 0.0535$, $wR_2 = 0.1535$

R indices (all data) $R_1 = 0.0694, wR_2 = 0.1595$

Largest diff. Peak and hole ($e \cdot \text{\AA}^{-3}$) 2.900/-1.517

Definitions:

$$R_1 = \frac{\sum \|F_o\| - \|F_c\|}{\sum \|F_o\|} \quad wR_2 = \sqrt{\frac{\sum [w(F_o^2 - F_c^2)^2]}{\sum [w(F_o^2)^2]}}$$

$$Goof = \sqrt{\frac{\sum [w(F_o^2 - F_c^2)]}{(n - p)}} \quad n = \text{number of reflections; } p = \text{number of parameters}$$

Notes on the refinement of 33e.

All the hydrogen atoms were placed in calculated positions and refined by using a riding model.

7.1.10 Crystal Data and Structure Refinement for 35

Empirical formula	$C_{18}H_{19}Cl_5N_5Ru$	
Formula weight	583.70	
Crystal colour and habit	brown plate	
Crystal size (mm)	0.20 x 0.13 x 0.03	
Temperature (K)	150(2)	
Wavelength (\AA)	1.54184	
Crystal system	Triclinic	
Space group	P-1	
Unit cell dimensions	$a = 8.0575(4) \text{\AA}$	$\alpha = 71.813(4)^\circ$
	$b = 10.4714(4) \text{\AA}$	$\beta = 81.249(4)^\circ$

Index

	$c = 14.3250(7) \text{ \AA}$	$\gamma = 76.049(4)^\circ$
Volume (\AA^3)	1110.51(9)	
Z	2	
Calculated density (Mg/m^3)	1.746	
Absorption coefficient (mm^{-1})	11.381	
F(000)	582	
Tetha-range for data collection ($^\circ$)	3.26/62.60	
Index ranges	$-9 \leq h \leq 9, -11 \leq k \leq 12, -16 \leq l \leq 16$	
Reflections collected	8213	
Independent reflections	3539 ($R_{int} = 0.0252$)	
Completeness to tetha = 62.60°	99.5 %	
Absorption correction	Semi-empirical from equivalents (Multiscan)	
Max. and min. transmission	1.00000 and 0.37481	
Refinement method	Full-matrix least-squares on F^2	
Data/restraints/parameters	3539/0/262	
Goodness-of-fit on F^2	1.096	
Final R indices [$I > 2 \sigma(I)$]	$R_1 = 0.0556, wR_2 = 0.1596$	
R indices (all data)	$R_1 = 0.0595, wR_2 = 0.1626$	
Largest diff. peak and hole ($\text{e} \cdot \text{\AA}^{-3}$)	1.573/-1.549	

Definitions:

$$R_1 = \frac{\sum \|F_o\| - \|F_c\|}{\sum \|F_o\|}$$
$$wR_2 = \sqrt{\frac{\sum [w(F_o^2 - F_c^2)^2]}{\sum [w(F_o^2)^2]}}$$

$$GooF = \sqrt{\frac{\sum [w(F_o^2 - F_c^2)]}{(n - p)}} \quad n = \text{number of reflections; } p = \text{number of parameters}$$

Notes on the refinement of 35.

All the hydrogen atoms were placed in calculated positions and refined by using a riding model.

7.1.11 Crystal Data and Structure Refinement for 36a

Empirical formula	C ₂₁ H ₂₈ ClF ₆ N ₄ OPRu	
Formula weight	633.96	
Crystal colour and habit	red prism	
Crystal size (mm)	0.28 x 0.21 x 0.18	
Temperature (K)	150(2)	
Wavelength (Å)	1.54184	
Crystal system	Monoclinic	
Space group	P2 ₁ /c	
Unit cell dimensions	$a = 10.3715(1) \text{ \AA}$	$\alpha = 90^\circ$
	$b = 15.0288(2) \text{ \AA}$	$\beta = 102.954(1)^\circ$
	$c = 16.0810(2) \text{ \AA}$	$\gamma = 90^\circ$
Volume (Å ³)	2442.77(5)	
Z	4	
Calculated density (Mg/m ³)	1.724	
Absorption coefficient (mm ⁻¹)	7.452	
F(000)	1280	
Tetha-range for data collection (°)	4.08/62.64	
Index ranges	$-11 \leq h \leq 11, -17 \leq k \leq 16, -18 \leq l \leq 18$	

Index

Reflections collected	17462
Independent reflections	3903 ($R_{int} = 0.0274$)
Completeness to tetha = 62.64°	99.9 %
Absorption correction	Semi-empirical from equivalents (Multiscan)
Max. and min. transmission	1.00000 and 0.59416
Refinement method	Full-matrix least-squares on F^2
Data/restraints/parameters	3903/2/327
Goodness-of-fit on F^2	1.079
Final R indices [$I > 2 \sigma(I)$]	$R_1 = 0.0230$, $wR_2 = 0.0589$
R indices (all data)	$R_1 = 0.0245$, $wR_2 = 0.0596$
Largest diff. peak and hole ($e \cdot \text{\AA}^{-3}$)	0.319/-0.618

Definitions:

$$R_1 = \frac{\sum \|F_o\| - \|F_c\|}{\sum \|F_o\|} \qquad wR_2 = \sqrt{\frac{\sum [w(F_o^2 - F_c^2)^2]}{\sum [w(F_o^2)^2]}}$$

$$Goof = \sqrt{\frac{\sum [w(F_o^2 - F_c^2)]}{(n - p)}} \quad n = \text{number of reflections}; p = \text{number of parameters}$$

Notes on the refinement of 36a.

The hydrogen atoms H4A and H4B, which are bound to the nitrogen atom N4, were located in the difference Fourier synthesis, and were refined semi-freely with the help of a distance restraint, while constraining their U -values to 1.2 times the $U(eq)$ value of N4. All the other hydrogen atoms were placed in calculated positions and refined by using a riding model.

One EtOH molecule was co-crystallized with the target complex.

7.1.12 Crystal Data and Structure Refinement for 36b

Empirical formula	C ₄₉ H ₄₆ BClN ₄ Ru	
Formula weight	838.23	
Crystal colour and habit	yellow prism	
Crystal size (mm)	0.20 x 0.13 x 0.08	
Temperature (K)	150(2)	
Wavelength (Å)	1.54184	
Crystal system	Monoclinic	
Space group	P2 ₁ /n	
Unit cell dimensions	$a = 13.5219(1) \text{ \AA}$	$\alpha = 90^\circ$
	$b = 21.5269(2) \text{ \AA}$	$\beta = 90.424(1)^\circ$
	$c = 14.0468(1) \text{ \AA}$	$\gamma = 90^\circ$
Volume (Å ³)	4088.70(6)	
Z	4	
Calculated density (Mg/m ³)	1.362	
Absorption coefficient (mm ⁻¹)	4.002	
F(000)	1736	
Tetha-range for data collection (°)	3.76/62.64	
Index ranges	$-15 \leq h \leq 15, -22 \leq k \leq 24, -16 \leq l \leq 14$	
Reflections collected	31505	
Independent reflections	6538 ($R_{int} = 0.0241$)	
Completeness to tetha = 62.64°	99.8 %	
Absorption correction	Semi-empirical from equivalents (Multiscan)	
Max. and min. transmission	1.00000 and 0.66444	

Index

Refinement method	Full-matrix least-squares on F^2
Data/restraints/parameters	6538/2/514
Goodness-of-fit on F^2	1.034
Final R indices [$I > 2 \sigma(I)$]	$R_1 = 0.0200$, $wR_2 = 0.0529$
R indices (all data)	$R_1 = 0.0225$, $wR_2 = 0.0535$
Largest diff. peak and hole ($e \cdot \text{\AA}^{-3}$)	0.227/-0.360

Definitions:

$$R_1 = \frac{\sum \|F_o\| - \|F_c\|}{\sum \|F_o\|} \qquad wR_2 = \sqrt{\frac{\sum [w(F_o^2 - F_c^2)^2]}{\sum [w(F_o^2)^2]}}$$

$$Goof = \sqrt{\frac{\sum [w(F_o^2 - F_c^2)]}{(n - p)}} \quad n = \text{number of reflections; } p = \text{number of parameters}$$

Notes on the refinement of 36b.

The hydrogen atoms H4A and H4B, which are bound to the nitrogen atom N4, were located in the difference Fourier synthesis, and were refined semi-freely with the help of a distance restraint, while constraining their U -values to 1.2 times the $U(eq)$ value of N4. All the other hydrogen atoms were placed in calculated positions and refined by using a riding model.

7.1.13 Crystal Data and Structure Refinement for 36f

Empirical formula	$C_{53}H_{65}BClN_4O_{1.5}Ru$
Formula weight	929.42
Crystal colour and habit	yellow prism

Crystal size (mm)	0.40 x 0.17 x 0.13	
Temperature (K)	150(2)	
Wavelength (Å)	1.54184	
Crystal system	Monoclinic	
Space group	P2 ₁ /c	
Unit cell dimensions	$a = 15.2326(1) \text{ \AA}$	$\alpha = 90^\circ$
	$b = 13.8012(1) \text{ \AA}$	$\beta = 107.188(1)^\circ$
	$c = 24.5075(2) \text{ \AA}$	$\sigma = 90^\circ$
Volume (Å ³)	4922.07(6)	
Z	4	
Calculated density (Mg/m ³)	1.254	
Absorption coefficient (mm ⁻¹)	3.392	
F(000)	1956	
Tetha-range for data collection (°)	3.04/62.65	
Index ranges	$-14 \leq h \leq 17, -15 \leq k \leq 15, -27 \leq l \leq 17$	
Reflections collected	40936	
Independent reflections	7866 ($R_{int} = 0.0225$)	
Completeness to tetha= 62.65°	99.7 %	
Absorption correction	Semi-empirical from equivalents (Multiscan)	
Max. and min. transmission	1.00000 and 0.68249	
Refinement method	Full-matrix least-squares on F ²	
Data/restraints/parameters	7866/40/580	
Goodness-of-fit on F ²	1.042	
Final R indices [$I > 2 \sigma(I)$]	$R_1 = 0.0244, wR_2 = 0.0647$	
R indices (all data)	$R_1 = 0.0264, wR_2 = 0.0655$	

Index

Largest diff. peak and hole ($e \cdot \text{\AA}^{-3}$) 0.414/-0.335

Definitions:

$$R_1 = \frac{\sum \|F_o\| - \|F_c\|}{\sum \|F_o\|} \qquad wR_2 = \sqrt{\frac{\sum [w(F_o^2 - F_c^2)^2]}{\sum [w(F_o^2)^2]}}$$

$$GoodF = \sqrt{\frac{\sum [w(F_o^2 - F_c^2)]}{(n - p)}} \quad n = \text{number of reflections}; p = \text{number of parameters}$$

Notes on the refinement of 36f.

The hydrogen atoms H4A and H4B, which are bound to the nitrogen atom N4, were located in the difference Fourier synthesis, and were refined semi-freely with the help of a distance restraint, while constraining their U -values to 1.2 times the $U(eq)$ value of N4. All the other hydrogen atoms were placed in calculated positions and refined by using a riding model. One target molecule was co-crystallized with 1.5 Et₂O, one of which was disordered.

7.1.14 Crystal Data and Structure Refinement for 36g

Empirical formula	C ₄₈ H ₄₉ BCl ₄ N ₄ Ru	
Formula weight	935.59	
Temperature	150(2) K	
Wavelength	1.54184 Å	
Crystal system	Monoclinic	
Space group	P2 ₁ /c	
Unit cell dimensions	a = 9.3478(2) Å	α = 90°.
	b = 24.5559(5) Å	β = 90.376(2)°.

$$c = 19.0534(5) \text{ \AA} \quad \gamma = 90^\circ.$$

Volume	4373.49(17) \AA^3
Z	4
Density (calculated)	1.421 Mg/m^3
Absorption coefficient	5.446 mm^{-1}
F(000)	1928
Crystal colour and habit	orange prism
Crystal size	0.11 x 0.09 x 0.05 mm^3
Theta range for data collection	2.94 to 62.72°
Index ranges	-10<=h<=9, -28<=k<=28, -21<=l<=21
Reflections collected	47086
Independent reflections	7017 [R(int) = 0.0534]
Completeness to theta = 62.72°	99.9 %
Absorption correction	Multiscan
Max. and min. transmission	1.00000 and 0.47266
Refinement method	Full-matrix least-squares on F ²
Data / restraints / parameters	7017 / 0 / 526
Goodness-of-fit on F ²	0.955
Final R indices [I>2sigma(I)]	R1 = 0.0253, wR2 = 0.0583
R indices (all data)	R1 = 0.0373, wR2 = 0.0697
Largest diff. peak and hole	0.420 and -0.456 e.\AA^{-3}

Definitions:

Index

$$R_1 = \frac{\sum \|F_o\| - \|F_c\|}{\sum \|F_o\|} \quad wR_2 = \sqrt{\frac{\sum [w(F_o^2 - F_c^2)^2]}{\sum [w(F_o^2)^2]}}$$

$$GoodF = \sqrt{\frac{\sum [w(F_o^2 - F_c^2)]}{(n - p)}} \quad n = \text{number of reflections}; p = \text{number of parameters}$$

Notes on the refinement of 36g.

All hydrogen atoms were placed in calculated positions and refined by using a riding model.

7.1.15 Crystal Data and Structure Refinement for 36h

Empirical formula	C ₄₉ H ₅₄ BClN ₄ Ru	
Formula weight	846.29	
Crystal colour and habit	yellow prism	
Crystal size (mm)	0.25 x 0.09 x 0.05	
Temperature (K)	150(2)	
Wavelength (Å)	1.54184	
Crystal system	Monoclinic	
Space group	P2 ₁ /c	
Unit cell dimensions	$a = 14.6567(3) \text{ \AA}$	$\alpha = 90^\circ$
	$b = 9.6078(2) \text{ \AA}$	$\beta = 100.226(2)^\circ$
	$c = 33.5405(6) \text{ \AA}$	$\gamma = 90^\circ$
Volume (Å ³)	4648.10(16)	
Z	4	
Calculated density (Mg/m ³)	1.209	
Absorption coefficient (mm ⁻¹)	3.521	
F(000)	1768	
Tetha-range for data collection (°)	3.06/62.63	

Index ranges	$-16 \leq h \leq 15, -9 \leq k \leq 11, -38 \leq l \leq 38$
Reflections collected	24700
Independent reflections	7402 ($R_{int} = 0.0367$)
Completeness to $\theta = 62.63^\circ$	99.7 %
Absorption correction	Semi-empirical from equivalents (Multiscan)
Max. and min. transmission	1.00000 and 0.40065
Refinement method	Full-matrix least-squares on F^2
Data/restraints/parameters	7402/0/513
Goodness-of-fit on F^2	0.946
Final R indices [$I > 2\sigma(I)$]	$R_1 = 0.0310, wR_2 = 0.0771$
R indices (all data)	$R_1 = 0.0390, wR_2 = 0.0797$
Largest diff. peak and hole ($e \cdot \text{\AA}^{-3}$)	0.402/-0.581

Definitions:

$$R_1 = \frac{\sum ||F_o| - |F_c||}{\sum |F_o|}$$

$$wR_2 = \sqrt{\frac{\sum [w(F_o^2 - F_c^2)^2]}{\sum [w(F_o^2)^2]}}$$

$$Goof = \sqrt{\frac{\sum [w(F_o^2 - F_c^2)]}{(n - p)}} \quad n = \text{number of reflections; } p = \text{number of parameters}$$

Notes on the refinement of 36h.

All the hydrogen atoms were placed in calculated positions and refined by using a riding model. Because of the existence of severely disordered solvents, most possibly Et₂O,

Index

SQUEEZE process integrated in PLATON has been used. And the detailed information has also been posted in the final CIF file.

7.1.16 Crystal Data and Structure Refinement for 36j

Empirical formula	C ₄₅ H ₄₆ BClN ₄ Ru	
Formula weight	790.19	
Crystal colour and habit	orange needle	
Crystal size (mm)	0.18 x 0.12 x 0.11	
Temperature (K)	150(2)	
Wavelength (Å)	1.54184	
Crystal system	Monoclinic	
Space group	P2 ₁ /n	
Unit cell dimensions	$a = 13.0910(2) \text{ \AA}$	$\alpha = 90^\circ$
	$b = 11.8941(1) \text{ \AA}$	$\beta = 95.960(1)^\circ$
	$c = 25.6986(3) \text{ \AA}$	$\gamma = 90^\circ$
Volume (Å ³)	3979.79(8)	
Z	4	
Calculated density (Mg/m ³)	1.319	
Absorption coefficient (mm ⁻¹)	4.076	
F(000)	1640	
Tetha-range for data collection (°)	3.46/62.74	
Index ranges	$-15 \leq h \leq 14, -13 \leq k \leq 13, -29 \leq l \leq 22$	
Reflections collected	31463	
Independent reflections	6363 ($R_{int} = 0.0237$)	
Completeness to tetha = 62.74°	99.5 %	
Absorption correction	Semi-empirical from equivalents (Multiscan)	

Max. and min. transmission	1.00000 and 0.77087
Refinement method	Full-matrix least-squares on F^2
Data/restraints/parameters	6363/0/474
Goodness-of-fit on F^2	1.041
Final R indices [$I > 2 \sigma(I)$]	$R_1 = 0.0218$, $wR_2 = 0.0562$
R indices (all data)	$R_1 = 0.0240$, $wR_2 = 0.0570$
Largest diff. peak and hole ($e \cdot \text{\AA}^{-3}$)	0.292/-0.597

Definitions:

$$R_1 = \frac{\sum \|F_o\| - \|F_c\|}{\sum \|F_o\|} \qquad wR_2 = \sqrt{\frac{\sum [w(F_o^2 - F_c^2)^2]}{\sum [w(F_o^2)^2]}}$$

$$GoodF = \sqrt{\frac{\sum [w(F_o^2 - F_c^2)]}{(n - p)}} \quad n = \text{number of reflections; } p = \text{number of parameters}$$

Notes on the refinement of 36j.

All hydrogen atoms were placed in calculated positions and refined by using a riding model.

7.1.17 Crystal Data and Structure Refinement for 36k

Empirical formula	$C_{48}H_{50}BClN_4Ru$
Formula weight	830.25
Temperature	150(2) K
Wavelength	1.54184 \AA
Crystal system	Monoclinic
Space group	$P2_1/c$

Index

Unit cell dimensions	$a = 12.2710(1) \text{ \AA}$	$\alpha = 90^\circ$.
	$b = 14.9669(1) \text{ \AA}$	$\beta = 95.163(1)^\circ$.
	$c = 22.3485(2) \text{ \AA}$	$\gamma = 90^\circ$.
Volume	$4087.85(6) \text{ \AA}^3$	
Z	4	
Density (calculated)	1.349 Mg/m^3	
Absorption coefficient	3.994 mm^{-1}	
F(000)	1728	
Crystal colour and habit	Brown plate	
Crystal size	$0.18 \times 0.07 \times 0.03 \text{ mm}^3$	
Theta range for data collection	3.56 to 62.65° .	
Index ranges	$-13 \leq h \leq 14$, $-17 \leq k \leq 16$, $-25 \leq l \leq 22$	
Reflections collected	32737	
Independent reflections	6515 [R(int) = 0.0336]	
Completeness to theta = 62.65°	99.6 %	
Absorption correction	Semi-empirical from equivalents (Multiscan)	
Max. and min. transmission	1.00000 and 0.58561	
Refinement method	Full-matrix least-squares on F^2	
Data / restraints / parameters	6515 / 0 / 499	
Goodness-of-fit on F^2	1.045	
Final R indices [$I > 2\sigma(I)$]	R1 = 0.0245, wR2 = 0.0652	
R indices (all data)	R1 = 0.0293, wR2 = 0.0665	
Largest diff. peak and hole	0.536 and $-0.388 \text{ e.\AA}^{-3}$	

Definitions:

$$R_1 = \frac{\sum \|F_o\| - \|F_c\|}{\sum \|F_o\|}$$

$$wR_2 = \sqrt{\frac{\sum [w(F_o^2 - F_c^2)^2]}{\sum [w(F_o^2)^2]}}$$

$$GooF = \sqrt{\frac{\sum [w(F_o^2 - F_c^2)]}{(n - p)}}$$

n = number of reflections; p = number of parameters

Notes on the refinement of 36k.

All hydrogen atoms were placed in calculated positions and refined by using a riding model.

7.1.18 Crystal Data and Structure Refinement for 36l

Empirical formula	C ₄₇ H ₅₀ BCl ₃ N ₄ Ru	
Formula weight	889.14	
Temperature	150(2) K	
Wavelength	1.54184 Å	
Crystal system	Monoclinic	
Space group	P2 ₁ /c	
Unit cell dimensions	a = 12.89110(10) Å	α = 90°.
	b = 14.90500(10) Å	β = 98.3670(10)°.
	c = 22.7354(2) Å	γ = 90°.
Volume	4321.93(6) Å ³	
Z	4	
Density (calculated)	1.366 Mg/m ³	
Absorption coefficient	4.925 mm ⁻¹	
F(000)	1840	

Index

Crystal size	0.16 x 0.08 x 0.06 mm ³
Crystal colour and habit	Red prism
Theta range for data collection	3.47 to 62.67°.
Index ranges	-14<=h<=12, -17<=k<=16, -26<=l<=25
Reflections collected	33782
Independent reflections	6916 [R(int) = 0.0299]
Completeness to theta = 62.67°	99.8 %
Absorption correction	Semi-empirical from equivalents (Multiscan)
Max. and min. transmission	1.00000 and 0.36187
Refinement method	Full-matrix least-squares on F ²
Data / restraints / parameters	6916 / 1 / 512
Goodness-of-fit on F ²	1.045
Final R indices [I>2sigma(I)]	R1 = 0.0292, wR2 = 0.0796
R indices (all data)	R1 = 0.0346, wR2 = 0.0815
Largest diff. peak and hole	0.679 and -0.944 e.Å ⁻³

Definitions:

$$R_1 = \frac{\sum ||F_o| - |F_c||}{\sum |F_o|}$$

$$wR_2 = \sqrt{\frac{\sum [w(F_o^2 - F_c^2)^2]}{\sum [w(F_o^2)^2]}}$$

$$Goof = \sqrt{\frac{\sum [w(F_o^2 - F_c^2)]}{(n - p)}}$$

n = number of reflections; p = number of parameters

Notes on the refinement of 36l.

The hydrogen atom H4N, which is bound to the nitrogen atom N4, was located in the difference Fourier synthesis, and was refined semi-freely with the help of a distance restraint, while constraining its U -value to 1.2 times the $U(eq)$ values of the corresponding nitrogen atom. All the other hydrogen atoms were placed in calculated positions and refined by using a riding model.

7.1.19 Crystal Data and Structure Refinement for 38

Empirical formula	$C_{12}H_{20}N_6O_6RuS_3$	
Formula weight	541.59	
Crystal colour and habit	red prism	
Crystal size (mm)	0.14 x 0.11 x 0.09	
Temperature (K)	150(2)	
Wavelength (\AA)	1.54184	
Crystal system	Orthorhombic	
Space group	Pbcn	
Unit cell dimensions	$a = 13.1591(2) \text{\AA}$	$\alpha = 90^\circ$
	$b = 10.5891(1) \text{\AA}$	$\beta = 90^\circ$
	$c = 13.5448(2) \text{\AA}$	$\gamma = 90^\circ$
Volume (\AA^3)	1887.37(4)	
Z	4	
Calculated density (Mg/m^3)	1.906	
Absorption coefficient (mm^{-1})	10.250	
F(000)	1096	
Tetha-range for data collection ($^\circ$)	5.36/62.66	
Index ranges	$-15 \leq h \leq 15, -9 \leq k \leq 12, -15 \leq l \leq 15$	

Index

Reflections collected	11302
Independent reflections	1513 ($R_{int} = 0.0253$)
Completeness to tetha = 62.66°	99.9 %
Absorption correction	Semi-empirical from equivalents (Multiscan)
Max. and min. transmission	1.00000 and 0.01465
Refinement method	Full-matrix least-squares on F^2
Data/restraints/parameters	1513/0/168
Goodness-of-fit on F^2	1.129
Final R indices [$I > 2 \text{ sigma } (I)$]	$R_1 = 0.0189$, $wR_2 = 0.0502$
R indices (all data)	$R_1 = 0.0201$, $wR_2 = 0.0507$
Largest diff. peak and hole ($e \cdot \text{\AA}^{-3}$)	0.232/-0.533

Definitions:

$$R_1 = \frac{\sum \|F_o\| - \|F_c\|}{\sum \|F_o\|} \qquad wR_2 = \sqrt{\frac{\sum [w(F_o^2 - F_c^2)^2]}{\sum [w(F_o^2)^2]}}$$

$$GooF = \sqrt{\frac{\sum [w(F_o^2 - F_c^2)]}{(n - p)}} \qquad n = \text{number of reflections}; p = \text{number of parameters}$$

Notes on the refinement of 38.

All hydrogen atoms were located in the difference Fourier synthesis, and then were refined with individual isotopic displacement parameters.

7.1.20 Crystal Data and Structure Refinement for 40a

Empirical formula $C_{17}H_{17}ClN_4OPdS$

Formula weight	467.26	
Temperature	150(2) K	
Wavelength	1.54184 Å	
Crystal system	Monoclinic	
Space group	P2 ₁ /c	
Unit cell dimensions	a = 11.3161(2) Å	α = 90°
	b = 20.3112(4) Å	β = 97.815(2)°
	c = 7.6539(1) Å	γ = 90°
Volume	1742.86(5) Å ³	
Z	4	
Density (calculated)	1.781 Mg/m ³	
Absorption coefficient	11.233 mm ⁻¹	
F(000)	936	
Crystal colour and habit	red needle	
Crystal size	0.32 x 0.15 x 0.14 mm ³	
Theta range for data collection	3.94 to 62.62°.	
Index ranges	-13<=h<=13, -21<=k<=23, -8<=l<=5	
Reflections collected	10892	
Independent reflections	2777 [R(int) = 0.0293]	
Completeness to theta = 62.62°	99.8 %	
Absorption correction	Multiscan	
Max. and min. transmission	1.00000 and 0.61247	
Refinement method	Full-matrix least-squares on F ²	
Data / restraints / parameters	2777 / 1 / 232	
Goodness-of-fit on F ²	1.189	

Index

Final R indices [$I > 2\sigma(I)$]	R1 = 0.0229, wR2 = 0.0636
R indices (all data)	R1 = 0.0258, wR2 = 0.0745
Extinction coefficient	0.00230(13)
Largest diff. peak and hole	0.509 and -0.854 e.Å ⁻³

Definitions:

$$R_1 = \frac{\sum \|F_o\| - |F_c|}{\sum |F_o|} \quad wR_2 = \sqrt{\frac{\sum [w(F_o^2 - F_c^2)^2]}{\sum [w(F_o^2)^2]}}$$

$$GoodF = \sqrt{\frac{\sum [w(F_o^2 - F_c^2)]}{(n - p)}} \quad n = \text{number of reflections}; p = \text{number of parameters}$$

Notes on the refinement of 40a.

The hydrogen atom H4N, which is bound to the nitrogen atom N4, was located in the difference Fourier synthesis, and was refined semi-freely with the help of a distance restraint, while constraining its U -value to 1.2 times the $U(eq)$ value of N4. All the hydrogen atoms were placed in calculated positions and refined by using a riding model.

7.1.21 Crystal Data and Structure Refinement for 40b

Empirical formula	C ₁₈ H ₁₉ ClN ₄ O ₂ PdS	
Formula weight	497.28	
Temperature	150(2) K	
Wavelength	1.54184 Å	
Crystal system	Monoclinic	
Space group	P2 ₁ /n	
Unit cell dimensions	a = 9.0633(2) Å	α = 90°.
	b = 16.6341(3) Å	β = 109.739(2)°.

$$c = 13.2038(3) \text{ \AA} \quad \gamma = 90^\circ.$$

Volume	1873.64(7) \AA^3
Z	4
Density (calculated)	1.763 Mg/m^3
Absorption coefficient	10.534 mm^{-1}
F(000)	1000
Crystal colour and habit	red prism
Crystal size	0.26 x 0.07 x 0.06 mm^3
Theta range for data collection	4.44 to 62.62°.
Index ranges	-10<=h<=9, -19<=k<=18, -14<=l<=15
Reflections collected	13076
Independent reflections	3004 [R(int) = 0.0304]
Completeness to theta = 62.62°	99.8 %
Absorption correction	Semi-empirical from equivalents (Multiscan)
Max. and min. transmission	1.00000 and 0.39813
Refinement method	Full-matrix least-squares on F ²
Data / restraints / parameters	3004 / 1 / 250
Goodness-of-fit on F ²	1.069
Final R indices [I>2sigma(I)]	R1 = 0.0211, wR2 = 0.0521
R indices (all data)	R1 = 0.0230, wR2 = 0.0527
Largest diff. peak and hole	0.316 and -0.677 e.\AA^{-3}

Definitions:

| Index

$$R_1 = \frac{\sum ||F_o| - |F_c||}{\sum |F_o|}$$

$$wR_2 = \sqrt{\frac{\sum [w(F_o^2 - F_c^2)^2]}{\sum [w(F_o^2)^2]}}$$

$$GooF = \sqrt{\frac{\sum [w(F_o^2 - F_c^2)]}{(n - p)}}$$

n = number of reflections; p = number of parameters

Notes on the refinement of 40d.

The hydrogen atom H4N, which is bound to the nitrogen atom N4, was located in the difference Fourier synthesis, and was refined semi-freely with the help of a distance restraint, while constraining its *U*-value to 1.2 times the *U*(*eq*) value of N4. All the other hydrogen atoms were placed in calculated positions and refined by using a riding model.

7.2 DFT calculations

Quantum chemical calculations on the cations **36a**⁺, **36j**⁺ and **36g**⁺ and of HCl were performed with the program Gaussian03^[1] using the B3LYP gradient corrected exchange-correlation functional in combination with the 6-31G* basis set for C, H, N, Cl and the Stuttgart/Dresden ECP basis set for Ru (see ref.^[2] in the manuscript). Full geometry optimizations were carried out in *C*₁ symmetry using analytical gradient techniques and the resulting structures were confirmed to be true minima by diagonalization of the analytical Hessian Matrix. The starting geometries for the calculations of the cations **A**⁺, **B**⁺, and **C**⁺ were taken from solid state structures of appropriate compounds. Different orientations of the cymene ligand were not evaluated. This may lead to small variations of the calculated energies.

7.2.1 Calculation of HCl

SCF Done: E(RB+HF-LYP) = -460.795694055 A.U. after 1 cycles

Low frequencies --- -0.0047 -0.0047 -0.0047 78.8246 78.8246 2930.0342

Zero-point correction= 0.006675 (Hartree/Particle)

Thermal correction to Energy= 0.009036

Thermal correction to Enthalpy= 0.009980

Thermal correction to Gibbs Free Energy= -0.011218

Sum of electronic and zero-point Energies= -460.789019

Sum of electronic and thermal Energies= -460.786658

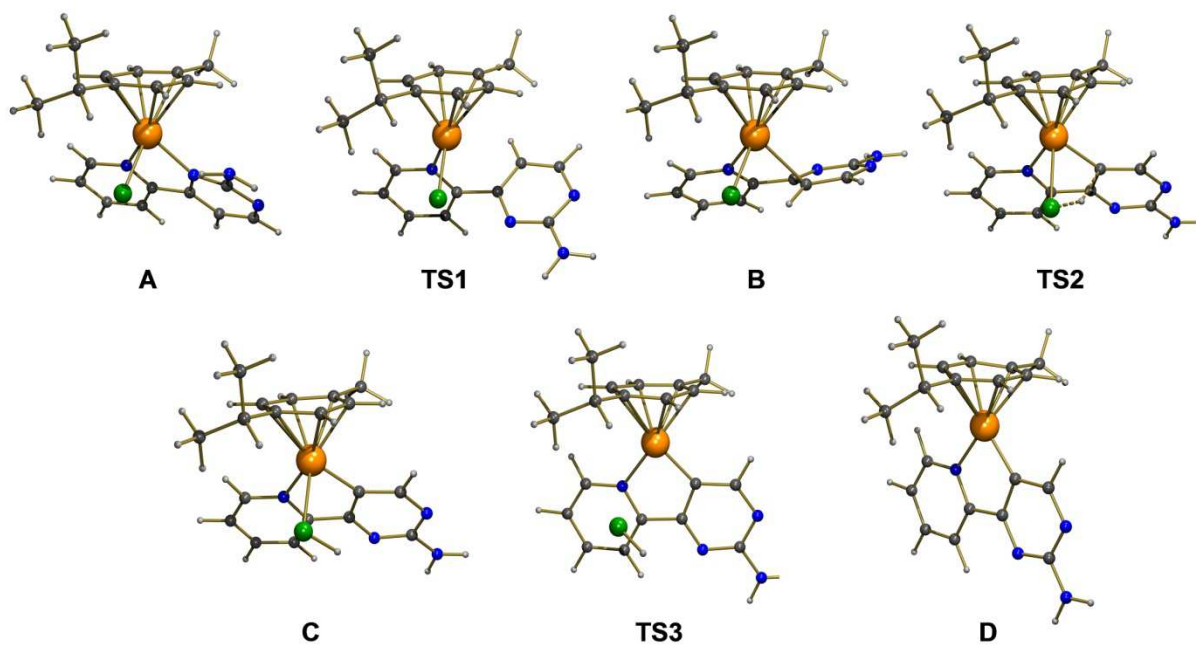
[1] Gaussian 03, Revision E.01, M. J. Frisch, G. W. Trucks, H. B. Schlegel, G. E. Scuseria, M. A. Robb, J. R. Cheeseman, J. A. Montgomery, Jr., T. Vreven, K. N. Kudin, J. C. Burant, J. M. Millam, S. S. Iyengar, J. Tomasi, V. Barone, B. Mennucci, M. Cossi, G. Scalmani, N. Rega, G. A. Petersson, H. Nakatsuji, M. Hada, M. Ehara, K. Toyota, R. Fukuda, J. Hasegawa, M. Ishida, T. Nakajima, Y. Honda, O. Kitao, H. Nakai, M. Klene, X. Li, J. E. Knox, H. P. Hratchian, J. B. Cross, V. Bakken, C. Adamo, J. Jaramillo, R. Gomperts, R. E. Stratmann, O. Yazyev, A. J. Austin, R. Cammi, C. Pomelli, J. W. Ochterski, P. Y. Ayala, K. Morokuma, G. A. Voth, P. Salvador, J. J. Dannenberg, V. G. Zakrzewski, S. Dapprich, A. D. Daniels, M. C. Strain, O. Farkas, D. K. Malick, A. D. Rabuck, K. Raghavachari, J. B. Foresman, J. V. Ortiz, Q. Cui, A. G. Baboul, S. Clifford, J. Cioslowski, B. B. Stefanov, G. Liu, A. Liashenko, P. Piskorz, I. Komaromi, R. L. Martin, D. J. Fox, T. Keith, M. A. Al-Laham, C. Y. Peng, A. Nanayakkara, M. Challacombe, P. M. W. Gill, B. Johnson, W. Chen, M. W. Wong, C. Gonzalez, and J. A. Pople, Gaussian, Inc., Wallingford CT (2004).

[2] a) C. Lee, W. Yang, R. G. Parr, *Phys. Rev. B* **1988**, 37, 785-789; b) A. D. Becke, *Phys. Rev.* **1988**, A38, 3098-3100; c) B. Miehlich, A. Savin, H. Stoll, H. Preuss, *Chem. Phys. Lett.* **1989**, 157, 200-206; d) P. C. Hariharan, J. A. Pople, *Theoret. Chim. Acta* **1973**, 28, 213-222; e) D. Andrae, U. Haeussermann, M. Dolg, H. Stoll, H. Preuss, *Theor. Chem. Acc.* **1990**, 77, 123-141.

Index

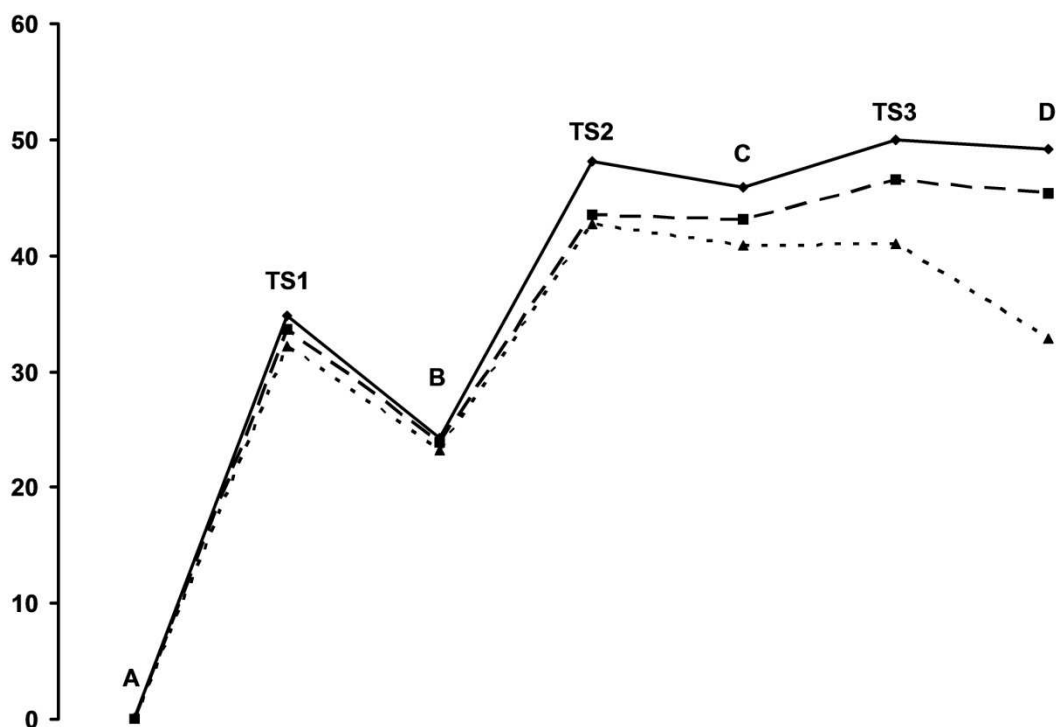
Sum of electronic and thermal Enthalpies= -460.785714
Sum of electronic and thermal Free Energies= -460.806912

7.2.2 Calculations of cation $36a^+$



Calculated geometries of $36a^+$ leading to C-H activation. The calculation results are given below.

Index



Calculated heats of formation ($\square\square H_f$, solid lines), enthalpies ($\square\square H$, dashed lines) and Gibbs energies ($\square\square G$, dotted lines) leading to the elimination of HCl from **36a⁺**.

Geometry A

SCF Done: E(RB+HF-LYP) = -1511.31596928 A.U. after 11 cycles

Low frequencies --- -0.0019 -0.0014 0.0009 5.5565 7.0455

Zero-point correction= 0.384382 (Hartree/Particle)

Thermal correction to Energy= 0.408229

Thermal correction to Enthalpy= 0.409174

Thermal correction to Gibbs Free Energy= 0.331402

Sum of electronic and zero-point Energies= -1510.931587

Sum of electronic and thermal Energies= -1510.907740

Sum of electronic and thermal Enthalpies= -1510.906796

Sum of electronic and thermal Free Energies= -1510.984568

Geometry TS1

SCF Done: E(RB+HF-LYP) = -1511.26049449 A.U. after 11 cycles

Low frequencies --- -46.0545 -7.0925 0.0010 0.0018 0.0022

***** 1 imaginary frequencies (negative Signs) *****

Zero-point correction= 0.382193 (Hartree/Particle)

Thermal correction to Energy= 0.406403

Thermal correction to Enthalpy= 0.407347

Thermal correction to Gibbs Free Energy= 0.327102

Sum of electronic and zero-point Energies= -1510.878302

Sum of electronic and thermal Energies= -1510.854092

Sum of electronic and thermal Enthalpies= -1510.853148

Sum of electronic and thermal Free Energies= -1510.933392

Geometry B

SCF Done: E(RB+HF-LYP) = -1511.27720975 A.U. after 1 cycles

Low frequencies --- -8.5946 0.0011 0.0012 0.0019 5.8451

Zero-point correction= 0.383121 (Hartree/Particle)

Thermal correction to Energy= 0.407499

Thermal correction to Enthalpy= 0.408443

Thermal correction to Gibbs Free Energy= 0.329634

Sum of electronic and zero-point Energies= -1510.894089

Sum of electronic and thermal Energies= -1510.869711

Sum of electronic and thermal Enthalpies= -1510.868766

Sum of electronic and thermal Free Energies= -1510.947576

Geometry TS2

SCF Done: E(RB+HF-LYP) = -1511.23929634 A.U. after 1 cycles

Low frequencies --- -396.9974 -4.9530 -0.0004 0.0013 0.0013

***** 1 imaginary frequencies (negative Signs) *****

Index

Zero-point correction= 0.376562 (Hartree/Particle)
Thermal correction to Energy= 0.400973
Thermal correction to Enthalpy= 0.401917
Thermal correction to Gibbs Free Energy= 0.322867
Sum of electronic and zero-point Energies= -1510.862734
Sum of electronic and thermal Energies= -1510.838323
Sum of electronic and thermal Enthalpies= -1510.837379
Sum of electronic and thermal Free Energies= -1510.916429

Geometry C

SCF Done: E(RB+HF-LYP) = -1511.24275769 A.U. after 3 cycles

Low frequencies --- 0.0001 0.0012 0.0015 5.2357 6.6925

Zero-point correction= 0.378403 (Hartree/Particle)
Thermal correction to Energy= 0.403811
Thermal correction to Enthalpy= 0.404756
Thermal correction to Gibbs Free Energy= 0.323397
Sum of electronic and zero-point Energies= -1510.864355
Sum of electronic and thermal Energies= -1510.838946
Sum of electronic and thermal Enthalpies= -1510.838002
Sum of electronic and thermal Free Energies= -1510.919360

Geometry TS3

SCF Done: E(RB+HF-LYP) = -1511.23624180 A.U. after 19 cycles

Low frequencies --- -25.1010 -9.9084 -5.9022 -0.0018 -0.0018

***** 1 imaginary frequencies (negative Signs) *****

Zero-point correction= 0.376878 (Hartree/Particle)
Thermal correction to Energy= 0.402673
Thermal correction to Enthalpy= 0.403617
Thermal correction to Gibbs Free Energy= 0.316982
Sum of electronic and zero-point Energies= -1510.859364

Sum of electronic and thermal Energies= -1510.833569
Sum of electronic and thermal Enthalpies= -1510.832624
Sum of electronic and thermal Free Energies= -1510.919260

Geometry D

SCF Done: E(RB+HF-LYP) = -1050.44183852 A.U. after 1 cycles

Low frequencies --- -3.3682 0.0005 0.0005 0.0006 4.0179

Zero-point correction= 0.369493 (Hartree/Particle)

Thermal correction to Energy= 0.392095

Thermal correction to Enthalpy= 0.393039

Thermal correction to Gibbs Free Energy= 0.316423

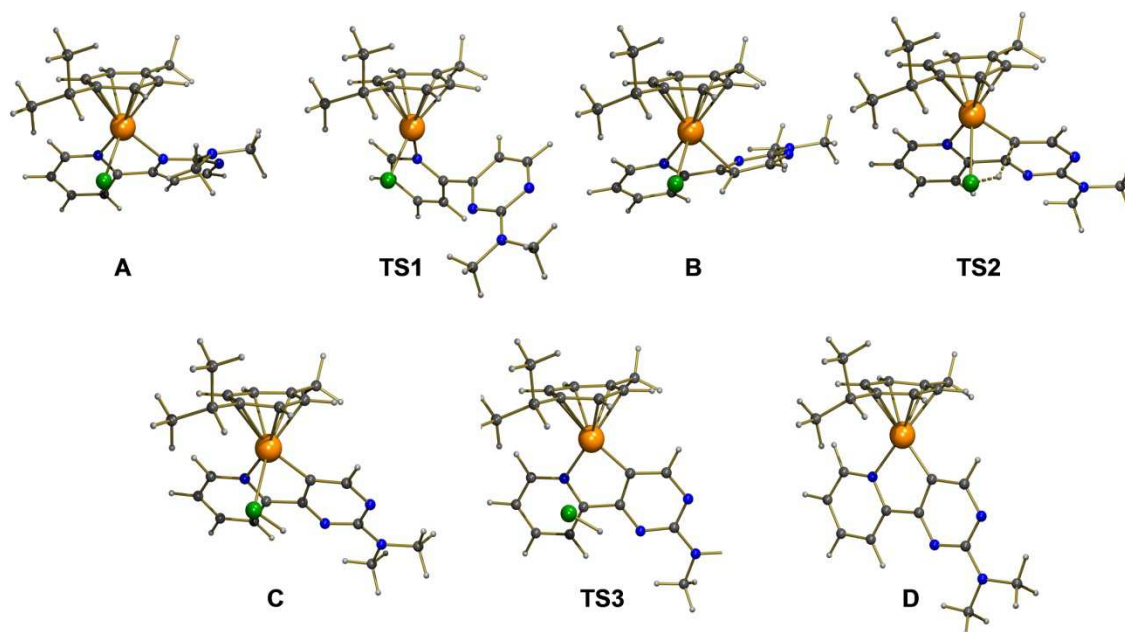
Sum of electronic and zero-point Energies= -1050.072345

Sum of electronic and thermal Energies= -1050.049743

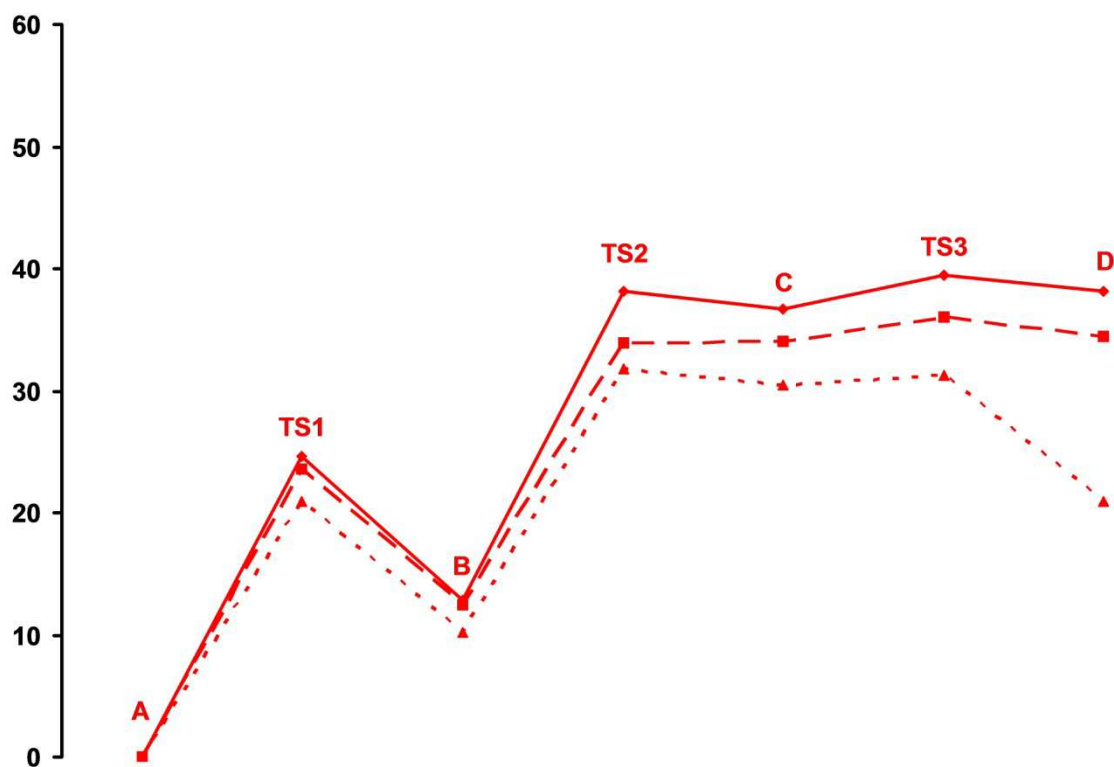
Sum of electronic and thermal Enthalpies= -1050.048799

Sum of electronic and thermal Free Energies= -1050.125415

7.2.3 Calculations of cation $36j^+$



Calculated geometries of $36j^+$ leading to C-H activation. The calculation results are given below.



Calculated heats of formation (□□H_f, solid lines), enthalpies (□□H, dashed lines) and Gibbs energies (□□G, dotted lines) leading to the elimination of HCl from **36j**⁺

Geometry A

SCF Done: E(RB+HF-LYP) = -1589.91791235 A.U. after 1 cycles

Low frequencies --- -0.0009 0.0011 0.0022 3.3602 5.5602

Zero-point correction= 0.440704 (Hartree/Particle)

Thermal correction to Energy= 0.467647

Thermal correction to Enthalpy= 0.468591

Thermal correction to Gibbs Free Energy= 0.384637

Sum of electronic and zero-point Energies= -1589.477208

Sum of electronic and thermal Energies= -1589.450265

Sum of electronic and thermal Enthalpies= -1589.449321

Sum of electronic and thermal Free Energies= -1589.533275

Index

Geometry TS1

SCF Done: E(RB+HF-LYP) = -1589.87864391 A.U. after 1 cycles

Low frequencies --- -42.1364 -2.7747 -0.0015 -0.0010 0.0013

***** 1 imaginary frequencies (negative Signs) *****

Zero-point correction= 0.438572 (Hartree/Particle)

Thermal correction to Energy= 0.465988

Thermal correction to Enthalpy= 0.466932

Thermal correction to Gibbs Free Energy= 0.378714

Sum of electronic and zero-point Energies= -1589.440072

Sum of electronic and thermal Energies= -1589.412656

Sum of electronic and thermal Enthalpies= -1589.411711

Sum of electronic and thermal Free Energies= -1589.499929

Geometry B

SCF Done: E(RB+HF-LYP) = -1589.89737080 A.U. after 1 cycles

Low frequencies --- -13.2204 -9.4610 -5.0836 -0.0015 -0.0005 -

Zero-point correction= 0.439247 (Hartree/Particle)

Thermal correction to Energy= 0.466971

Thermal correction to Enthalpy= 0.467916

Thermal correction to Gibbs Free Energy= 0.380245

Sum of electronic and zero-point Energies= -1589.458124

Sum of electronic and thermal Energies= -1589.430399

Sum of electronic and thermal Enthalpies= -1589.429455

Sum of electronic and thermal Free Energies= -1589.517126

Geometry TS2

SCF Done: E(RB+HF-LYP) = -1589.85703645 A.U. after 1 cycles

Low frequencies --- -356.8770 -8.3221 -5.1598 -0.0023 -0.0020 -

***** 1 imaginary frequencies (negative Signs) *****

Zero-point correction= 0.433202 (Hartree/Particle)
Thermal correction to Energy= 0.460846
Thermal correction to Enthalpy= 0.461790
Thermal correction to Gibbs Free Energy= 0.374448
Sum of electronic and zero-point Energies= -1589.423834
Sum of electronic and thermal Energies= -1589.396190
Sum of electronic and thermal Enthalpies= -1589.395246
Sum of electronic and thermal Free Energies= -1589.482588

Geometry C

SCF Done: E(RB+HF-LYP) = -1589.85949379 A.U. after 1 cycles

Low frequencies --- -8.5904 -5.0578 -0.0013 -0.0005 0.0006

Zero-point correction= 0.434920 (Hartree/Particle)
Thermal correction to Energy= 0.463413
Thermal correction to Enthalpy= 0.464357
Thermal correction to Gibbs Free Energy= 0.374765
Sum of electronic and zero-point Energies= -1589.424573
Sum of electronic and thermal Energies= -1589.396081
Sum of electronic and thermal Enthalpies= -1589.395137
Sum of electronic and thermal Free Energies= -1589.484729

Geometry TS3

SCF Done: E(RB+HF-LYP) = -1589.85508271 A.U. after 1 cycles

Low frequencies --- -27.2579 -7.9043 -4.6512 -0.0010 0.0008

***** 1 imaginary frequencies (negative Signs) *****

Zero-point correction= 0.433662 (Hartree/Particle)
Thermal correction to Energy= 0.462329
Thermal correction to Enthalpy= 0.463273

Index

Thermal correction to Gibbs Free Energy=	0.371535
Sum of electronic and zero-point Energies=	-1589.421421
Sum of electronic and thermal Energies=	-1589.392754
Sum of electronic and thermal Enthalpies=	-1589.391810
Sum of electronic and thermal Free Energies=	-1589.483548

Geometry D

SCF Done: E(RB+HF-LYP) = -1129.06138969 A.U. after 1 cycles

Low frequencies --- -0.0004 -0.0002 0.0005 3.3181 7.6402

Zero-point correction= 0.425996 (Hartree/Particle)

Thermal correction to Energy= 0.451775

Thermal correction to Enthalpy= 0.452720

Thermal correction to Gibbs Free Energy= 0.368457

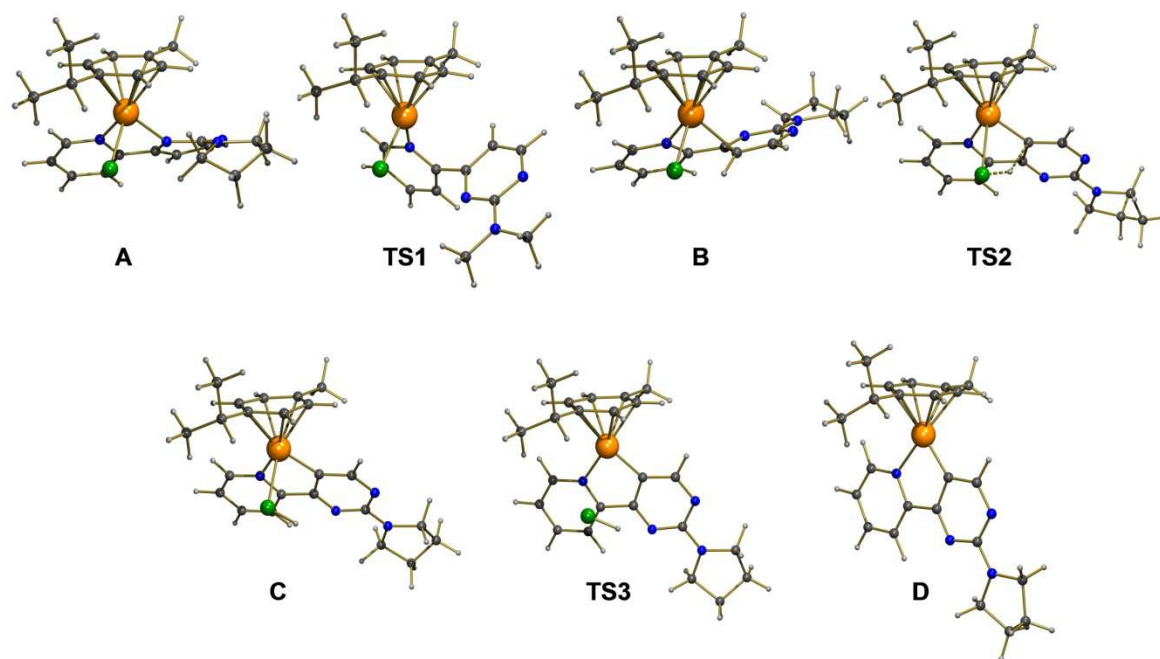
Sum of electronic and zero-point Energies= -1128.635393

Sum of electronic and thermal Energies= -1128.609614

Sum of electronic and thermal Enthalpies= -1128.608670

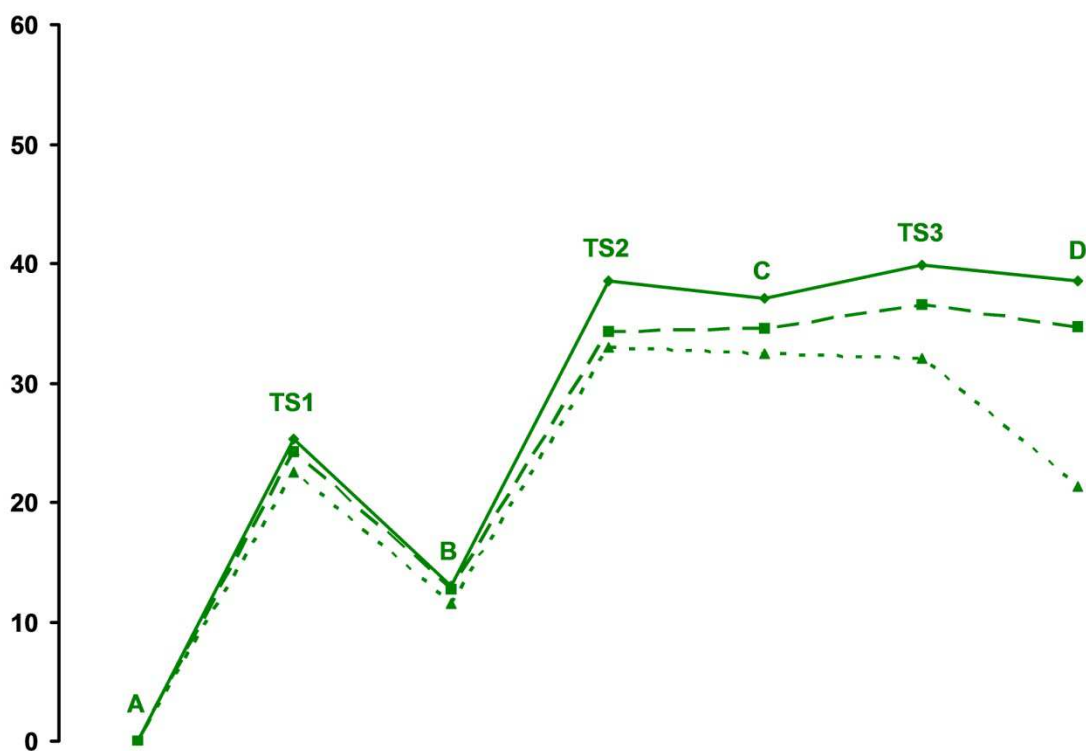
Sum of electronic and thermal Free Energies= -1128.692933

7.2.4 Calculations of cation $36g^+$



Calculated geometries of $36g^+$ leading to C-H activation. The calculation results are given below.

Index



Calculated heats of formation ($\square\square H_f$, solid lines), enthalpies ($\square\square H$, dashed lines) and Gibbs energies ($\square\square G$, dotted lines) leading to the elimination of HCl from $36g^+$.

Geometry A

SCF Done: E(RB+HF-LYP) = -1667.34386736 A.U. after 10 cycles

Low frequencies --- -12.2086 -0.0022 -0.0013 -0.0003 5.6055

Zero-point correction= 0.477635 (Hartree/Particle)

Thermal correction to Energy= 0.505326

Thermal correction to Enthalpy= 0.506270

Thermal correction to Gibbs Free Energy= 0.420205

Sum of electronic and zero-point Energies= -1666.866232

Sum of electronic and thermal Energies= -1666.838541

Sum of electronic and thermal Enthalpies= -1666.837597

Sum of electronic and thermal Free Energies= -1666.923662

Geometry TS1

SCF Done: E(RB+HF-LYP) = -1667.30356205 A.U. after 1 cycles

Low frequencies --- -40.9446 -1.3930 0.0015 0.0022 0.0024

***** 1 imaginary frequencies (negative Signs) *****

Zero-point correction= 0.475965 (Hartree/Particle)

Thermal correction to Energy= 0.503717

Thermal correction to Enthalpy= 0.504661

Thermal correction to Gibbs Free Energy= 0.415856

Sum of electronic and zero-point Energies= -1666.827597

Sum of electronic and thermal Energies= -1666.799845

Sum of electronic and thermal Enthalpies= -1666.798901

Sum of electronic and thermal Free Energies= -1666.887706

Geometry B

SCF Done: E(RB+HF-LYP) = -1667.32317386 A.U. after 1 cycles

Low frequencies --- -7.2257 -0.0004 0.0004 0.0016 0.4847 Zero-point correction=

0.476861 (Hartree/Particle)

Thermal correction to Energy= 0.504837

Thermal correction to Enthalpy= 0.505781

Thermal correction to Gibbs Free Energy= 0.417916

Sum of electronic and zero-point Energies= -1666.846313

Sum of electronic and thermal Energies= -1666.818337

Sum of electronic and thermal Enthalpies= -1666.817393

Sum of electronic and thermal Free Energies= -1666.905258

Geometry TS2

SCF Done: E(RB+HF-LYP) = -1667.28247706 A.U. after 1 cycles

Low frequencies --- -350.4000 -6.0964 -4.1291 -0.0020 -0.0014 -

Index

***** 1 imaginary frequencies (negative Signs) *****

Zero-point correction= 0.470632 (Hartree/Particle)
Thermal correction to Energy= 0.498678
Thermal correction to Enthalpy= 0.499622
Thermal correction to Gibbs Free Energy= 0.411361
Sum of electronic and zero-point Energies= -1666.811845
Sum of electronic and thermal Energies= -1666.783799
Sum of electronic and thermal Enthalpies= -1666.782855
Sum of electronic and thermal Free Energies= -1666.871116

Geometry C

SCF Done: E(RB+HF-LYP) = -1667.28473447 A.U. after 1 cycles

Low frequencies --- -5.8963 -0.0026 -0.0012 -0.0011 4.8874

Zero-point correction= 0.472488 (Hartree/Particle)
Thermal correction to Energy= 0.501262
Thermal correction to Enthalpy= 0.502207
Thermal correction to Gibbs Free Energy= 0.412697
Sum of electronic and zero-point Energies= -1666.812246
Sum of electronic and thermal Energies= -1666.783472
Sum of electronic and thermal Enthalpies= -1666.782528
Sum of electronic and thermal Free Energies= -1666.872038

Geometry TS3

SCF Done: E(RB+HF-LYP) = -1667.28042733 A.U. after 12 cycles

Low frequencies --- -25.0881 -5.3180 -0.0021 -0.0020 0.0010

***** 1 imaginary frequencies (negative Signs) *****

Zero-point correction= 0.471042 (Hartree/Particle)
Thermal correction to Energy= 0.500104
Thermal correction to Enthalpy= 0.501048

Thermal correction to Gibbs Free Energy= 0.407772
Sum of electronic and zero-point Energies= -1666.809385
Sum of electronic and thermal Energies= -1666.780323
Sum of electronic and thermal Enthalpies= -1666.779379
Sum of electronic and thermal Free Energies= -1666.872655

Geometry D

SCF Done: E(RB+HF-LYP) = -1206.48684254 A.U. after 1 cycles

Low frequencies --- -10.3552 -0.9775 -0.0007 -0.0004 -0.0001

Zero-point correction= 0.463104 (Hartree/Particle)

Thermal correction to Energy= 0.489386

Thermal correction to Enthalpy= 0.490330

Thermal correction to Gibbs Free Energy= 0.403983

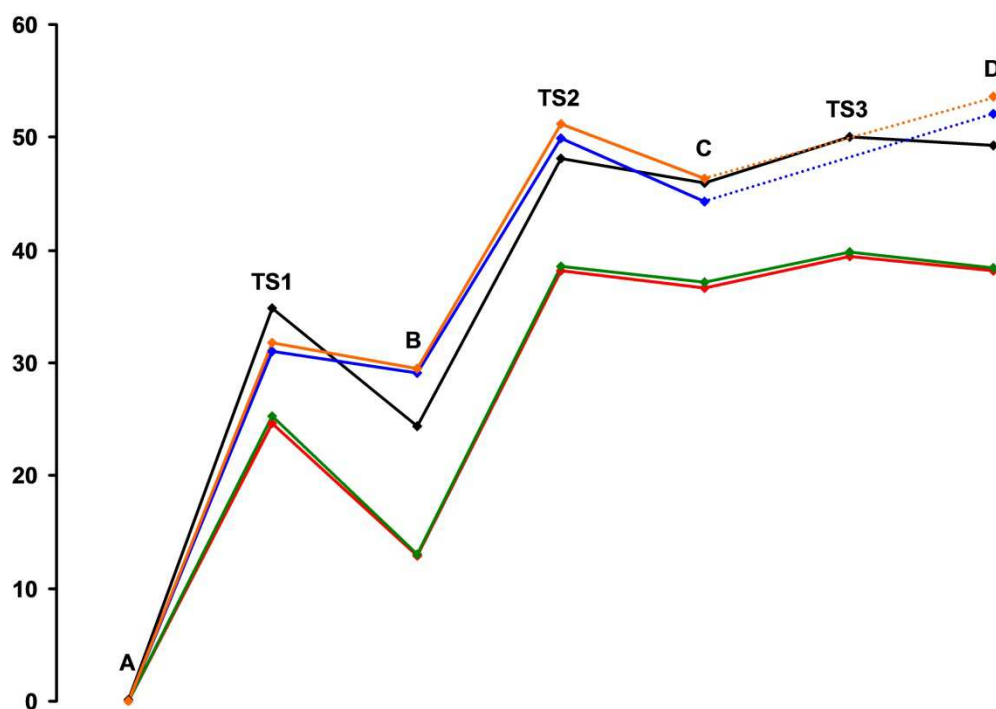
Sum of electronic and zero-point Energies= -1206.023738

Sum of electronic and thermal Energies= -1205.997456

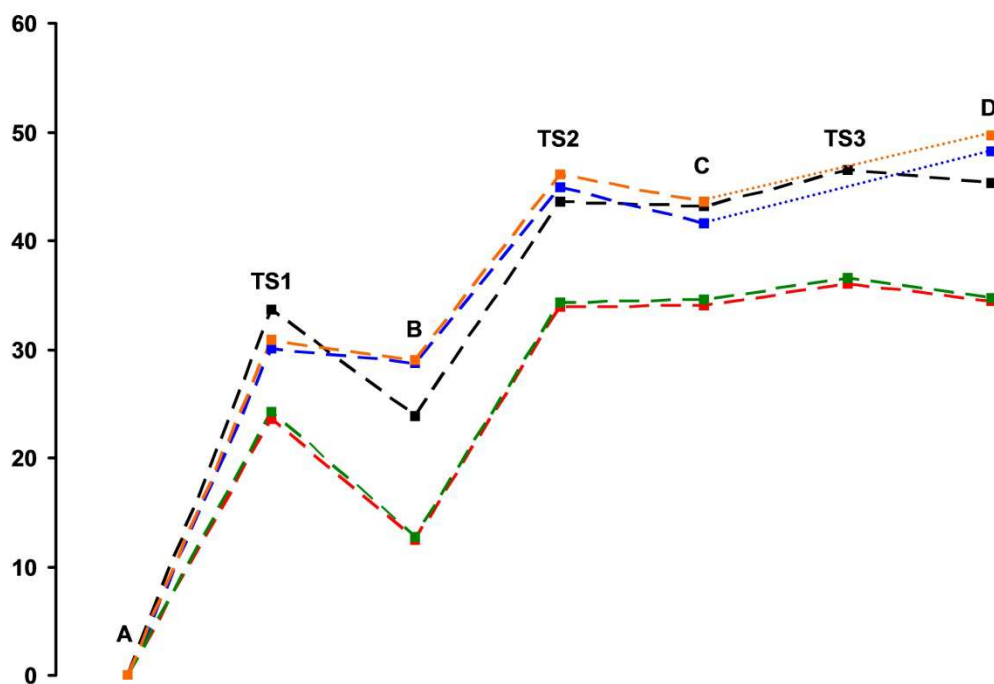
Sum of electronic and thermal Enthalpies= -1205.996512

Sum of electronic and thermal Free Energies= -1206.082860

7.2.5 Heats of formation

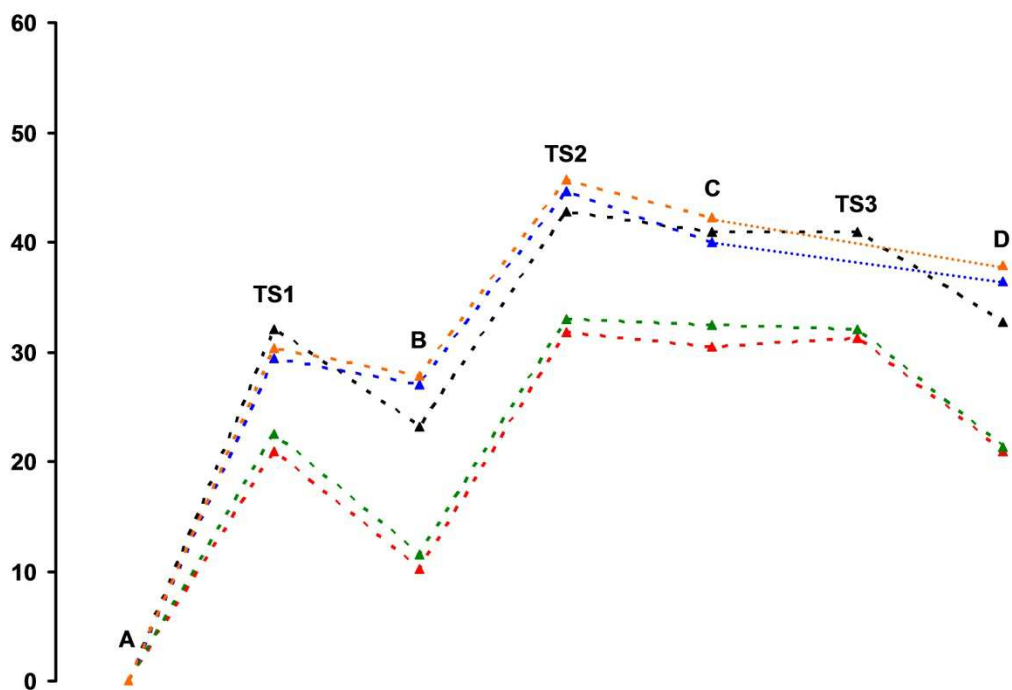


Calculated heats of formation (ΔH_f) of the geometries leading to the elimination of HCl from the cations **36a**⁺ (black), **36j**⁺ (red), **36g**⁺ (green), $[(\eta^6\text{-cymene})\text{Ru}(\text{Cl})(4\text{-phenylpyrimidine})]^+$ (blue) and $[(\eta^6\text{-cymene})\text{Ru}(\text{Cl})(\text{bipy})]^+$ (orange).



Calculated reaction enthalpies (ΔH_r) of the geometries leading to the elimination of HCl from the cations **36a**⁺ (black), **36j**⁺ (red), **36g**⁺ (green), $[(\eta^6\text{-cymene})\text{Ru}(\text{Cl})(4\text{-phenylpyrimidine})]^+$ (blue) and $[(\eta^6\text{-cymene})\text{Ru}(\text{Cl})(\text{bipy})]^+$ (orange).

Index



Calculated Gibbs enthalpies (ΔG^\ddagger) of the geometries leading to the elimination of HCl from the cations $36a^+$ (black), $36j^+$ (red), $36g^+$ (green), $[(\eta^6\text{-cymene})\text{Ru}(\text{Cl})(4\text{-phenylpyrimidine})]^+$ (blue) and $[(\eta^6\text{-cymene})\text{Ru}(\text{Cl})(\text{bipy})]^+$ (orange).

7.3 Statutory Explanation

Hiermit bestätige ich, dass ich die vorliegende Arbeit gemas der Promotionsordnung des Fachbereichs Chemie der Technischen Universitat Kaiserslautern selbstständig und nur unter Verwendung der angegebenen Quellen und Hilfsmittel angefertigt habe.

Kaiserslautern, April, 2012

Leila Taghizadeh Ghoochany

7.4 Acknowledgement

First of all I would like to thank warmly my supervisor Prof. Werner R. Thiel for giving me the opportunity to work in his group on this very interesting topic openly. His constant and invaluable support with abundant knowledge and his extreme patience with positive attitude helped me a lot throughout my work. Also, I will never forget his well-timed helps and strong support, from the first day I applied for my scholarship and then as I arrived here which continued throughout all these years. I would like to take this opportunity to express my deepest respect and most intense thanks to him.

I am also very grateful to Prof. Dr. Gereon Niedner-Schatteburg and Fabian Menges for ESI-MS measurements and their helpful discussions and our successful cooperation.

Special thanks to Dr. Yu Sun for X-ray crystallography measurements. Many thanks is also given to Ms Christiane Müller for her efficient measurements of large numbers of my NMR samples. Thanks to Dr. Harald Kelm for teaching me how to measure NMR.

I would also like to thank Merve Cayir for her help in the synthesis of the guanidinium salts. I also acknowledge Andy, Christoph, Lisa, Eva, Katrin, Kevin and Jessica for their help during the AC Praktikum. Many thanks to Tomas who had been in the same lab with me since the beginning of my work and given me a lot of help, especially I respect his tolerance with my German language. I am also very thankful to Shylesh, Dirk and Agnes who joined us in our lab later. Many thanks to Daniel and Max for their unassuming supports in all aspect of my life in Germany. I thank previous coworkers, Andreas Reis, Annett, Claudia, Susi and Frank, who helped me to have a good start in Germany. Thanks to Kifa for his useful tips and readiness to help.

Also, many thanks to my research trainees, Shi and Alexander who assisted me in laboratory.

I would like to give my faithful thanks to everyone in this group for the friendly working atmosphere and the happy hours of hiking, BBQ, dinner, cakes and so on.

Last but not least, especial thanks to my husband, Saeid, who consecutive encouraged and supported me in these years not only in private life but also in my scientific life. I am forever indebted to my parents, my brothers and sisters for their understanding and supports. Their love is always motivating me to go on and on.

Index

7.5 Curriculum Vitae

Personal Information

Name: Leila Taghizadeh Ghoochany

Date of birth: 21.09.1982

Place of birth: Mashhad, Iran

Status of marriage: Married

Education

12/2007–06/2012 Technische Universitat Kaiserslautern, Kaiserslautern, Germany

Ph.D. study in Inorganic Chemistry.

09/2004–09/2006 Sharif University of Technology, Tehran, Iran

M. Sc. study in Inorganic Chemistry

09/2000–06/2004 Tehran University, Tehran, Iran

B. Sc. study in pure chemistry

Publications

1. Novel *N,N,N*-Donors Giving Highly Active Ruthenium Catalysts for Transfer Hydrogenation at Room Temperature, L. Taghizadeh Ghoochany, S. Farsadpour, Y. Sun, W. R. Thiel, *Eur. J. Inorg. Chem.* **2011**, 23, 3431.
2. Small substituents make large differences: aminopyrimidinyl phosphines undergoing C-H activation, S. Farsadpour, L. Taghizadeh Ghoochany, Y. Sun, W. R. Thiel, *Eur. J. Inorg. Chem.*, **2011**, 29, 4603.
3. Intramolecular C-H Activation at a ruthenium(II) complex: A key step for base free catalytic transfer hydrogenation, L. Taghizadeh Ghoochany, S. Farsadpour, F. Menges, G. Niedner-Schatteburg, W.R. Thiel to be submitted to *Chemistry*.

4. A Covalently Supported Pyrimidinylphosphane Palladacycle as a Heterogenized Catalyst for the Suzuki–Miyaura Cross Coupling, S. Farsadpour, L. Taghizadeh Ghoochany, S. Shylesh, S. Ernst, W. R. Thiel, *Chem. Cat.Chem.* **2012**, *4*, 401.
5. Pyridylpyrimidine Derivatives as N,N-Ligands for the Palladium-catalyzed Suzuki-Miyaura Reaction, L. Taghizadeh Ghoochany, S. Farsadpour, W.R. Thiel, in hand.
6. Synthesis of Polydentate Ligands for Bimetallic Complexes with Electron-rich and Electron-poor Transition Metals, L. Taghizadeh Ghoochany, A. Ganß, S. Farsadpour, M. Amirnasr, W.R. Thiel, in hand.

Seminars

1. Catalyst Self-activation by C-H Bond Cleavage in the Ligand Sphere, 45. Jahrestreffen Deutscher Katalytiker, Weimar, Germany, Mar. 2012.
2. Developing New N,N and N,N,N Ligands and Their Application in Catalytic Reactions, Aachen, July, 2011.
3. Novel Ruthenium Catalysts for Transfer Hydrogenation, 9th Ferrocene Colloquium, Chemnitz, Germany, Feb. 2011.
4. Synthesis and Characterization of Complexes of Tridentate Bis(pyrazolyl)pyridine Ligands , Benz Stiftung, Dec. 2007.
5. Carbon nanotubes as Support in Catalytic Reactions, TU Sharif, Iran, Oct. 2005.
6. Usage of Microwaves in Organic Reaction, University of Tehran, Iran, Aug. 2004.

Posters:

1. Intramolecular CH-Activation at a ruthenium(II) complex: A key step for base free catalytic transfer hydrogenation, First EuCheMS Inorganic Chemistry Conference, Manchester, United Kingdom, Apr. 2011.

Index

2. Novel N,N,N-Donors for Ruthenium Catalyzed Hydrogenation, 44. Jahrestreffen Deutscher Katalytiker mit Jahrestreffen Reaktionstechnik, Weimar, Germany, Mar. 2011.
3. Unexpected Structures of Palladacycles derived from N,N-Ligands, 7. Koordinationschemie-Treffen, Stuttgart, Germany, Feb. 2011.
4. Novel N,N-Donors for Ruthenium Catalyzed Hydrogenation, 3rd EuCheMS Chemistry Congress, Nürnberg, Germany, Aug. 2010.
5. Synthesis of Multidentate Ligands and their Corresponding Bimetallic Complexes with Electron-rich and Electron-poor Transition Metals, 8th Ferrocene Colloquium, Ruhr-Universität Bochum, Germany, Feb. 2010.